UNIVERSIDADE ESTADUAL DE CAMPINAS
FACULDADE DE ENGENHARIA QUÍMICA

ARTHUR DA SILVA VASCONCELOS DE ALMEIDA

SÍNTESE DE NANOMATERIAIS MAGNÉTICOS BASEADOS EM ÓXIDO DE GRAFENO/QUITOSANA/ARGILA ORGANOFÍLICA PARA ADSORÇÃO DE CONTAMINANTES EMERGENTES EM ÁGUA

SYNTHESIS OF MAGNETIC NANOMATERIALS BASED ON GRAPHENE OXIDE/CHITOSAN/ORGANOCLAY FOR ADSORPTION OF EMERGING CONTAMINANTS IN WATER

Campinas - SP
2022

ARTHUR DA SILVA VASCONCELOS DE ALMEIDA

SÍNTESE DE NANOMATERIAIS MAGNÉTICOS BASEADOS EM ÓXIDO DE GRAFENO/QUITOSANA/ARGILA ORGANOFÍLICA PARA ADSORÇÃO DE CONTAMINANTES EMERGENTES EM ÁGUA

SYNTHESIS OF MAGNETIC NANOMATERIALS BASED ON GRAPHENE OXIDE/CHITOSAN/ORGANOCLAY FOR ADSORPTION OF EMERGING CONTAMINANTS IN WATER

Dissertação de Mestrado apresentada à Faculdade de Engenharia Química da Universidade Estadual de Campinas como parte dos requisitos para a obtenção do título de Mestre em Engenharia Química.

Dissertation presented to the Faculty of Chemical Engineering of the University of Campinas as part of the requirements for the degree of Master in Chemical Engineering.

Orientadora: Profª. Drª. Melissa Gurgel Adeodato Vieira

Coorientadora: Profª. Drª. Patrícia Prediger

ESTE TRABALHO CORRESPONDE À VERSÃO FINAL DA DISSERTAÇÃO DEFENDIDA PELO ALUNO ARTHUR ALMEIDA, E ORIENTADO PELA PROFª DRª MELISSA VIEIRA.

Campinas - SP

2022

FICHA CATALOGRÁFICA

Ficha catalográfica
Universidade Estadual de Campinas
Biblioteca da Área de Engenharia e Arquitetura
Rose Meire da Silva - CRB 8/5974

AL64s

Almeida, Arthur da Silva Vasconcelos de, 1997-
Síntese de nanomateriais magnéticos baseados em óxido de grafeno/quitosana/argila organofílica para adsorção de contaminantes emergentes em água / Arthur da Silva Vasconcelos de Almeida. – Campinas, SP : [s.n.], 2022.

Orientador: Melissa Gurgel Adeodato Vieira.
Coorientador: Patrícia Prediger.
Dissertação (mestrado) – Universidade Estadual de Campinas, Faculdade de Engenharia Química.

1. Contaminantes emergentes. 2. Etinilestradiol. 3. Nanocompósitos (Materiais). 4. Adsorção. I. Vieira, Melissa Gurgel Adeodato, 1979-. II. Prediger, Patrícia, 1984-. III. Universidade Estadual de Campinas. Faculdade de Engenharia Química. IV. Título.

Informações para Biblioteca Digital

Título em outro idioma: Synthesis of magnetic nanomaterials based on graphene oxide/chitosan/organoclay for adsorption of emerging contaminants in water
Palavras-chave em inglês:
Emerging contaminants
Ethinylestradiol
Nanocomposites (Materials)
Adsorption
Área de concentração: Engenharia Química
Titulação: Mestre em Engenharia Química
Banca examinadora:
Melissa Gurgel Adeodato Vieira [Orientador]
Adriano Luiz Tonetti
Maria Regina Wolf Maciel
Data de defesa: 23-02-2022
Programa de Pós-Graduação: Engenharia Química

Identificação e informações acadêmicas do(a) aluno(a)
- ORCID do autor: https://orcid.org/0000-0001-9199-946x
- Currículo Lattes do autor: http://lattes.cnpq.br/8631083755526681

FOLHA DE APROVAÇÃO

Dissertação de Mestrado defendida por Arthur da Silva Vasconcelos de Almeida e aprovada em 24 de FEVEREIRO de 2022 pela banca examinadora constituída pelos doutores:

Profª. Drª. Melissa Gurgel Adeodato Vieira – Presidente e Orientadora

Faculdade de Engenharia Química – FEQ/UNICAMP
Videoconferência

Prof. Dr. Adriano Luiz Tonetti
Faculdade de Engenharia Civil, Arquitetura e Urbanismo – FEC/UNICAMP
Videoconferência

Profª. Drª. Maria Regina Wolf Maciel

Faculdade de Engenharia Química – FEQ/UNICAMP
Videoconferência

A Ata da defesa com as respectivas assinaturas dos membros encontra-se no SIGA/Sistema de Fluxo de Dissertação/Tese e na Secretaria do Programa da Unidade.

AGRADECIMENTOS

Agradeço primeiramente à minha família por todo suporte e amor oferecido no decorrer da minha caminhada. Um agradecimento especial aos meus pais, Gilmara, Rodrigo, Julio e Danielle, que sempre apoiaram e acreditaram no meu potencial para a conclusão deste ciclo. Gostaria de agradecer à minha companheira, Renata, por todo apoio e amor incondicional que foi essencial para a conclusão desta etapa. Gostaria de agradecer também a vida pela oportunidade de acordar com saúde todos os dias e cruzar o caminho de pessoas incríveis que foram muito importantes no meu desenvolvimento pessoal e profissional.

Agradeço às Profª. Drª. Melissa Gurgel Adeodato Vieira, Profª. Drª. Patrícia Prediger e Profª. Drª. Meuris Gurgel Carlos da Silva pelo aceite de orientação, suporte e auxílio em todas as etapas de execução desse projeto.

Aos técnicos do Laboratório de Caracterização de Biomassa, Recursos Analíticos e de Calibração (LRAC) da FEQ/UNICAMP, pela grande contribuição com as análises de caracterização.

Aos psicólogos do Serviço de Assistência Psicológica e Psiquátrica do Estudante (SAPPE) da UNICAMP, pelo apoio e suporte que me permitiram concluir esta etapa de forma mais leve e tranquila.

Agradeço ao programa de pós-graduação em Engenharia Química da FEQ/UNICAMP pela infraestrutura e equipe excepcionais.

Um agradecimento aos colegas/amigos do LEA/LEPA da FEQ/UNICAMP, em especial ao Talles, Thiago, Wedja e Maria Vitoria que sempre contribuíram com suas experiências e deram todo suporte necessário para o meu desenvolvimento.

Agradeço também as amizades que Campinas me proporcionou, mas também aos meus grandes amigos de Maceió que por onde quer que eu vá estarão sempre comigo, contribuindo para que me torne um ser humano melhor.

Ao apoio da Coordenação de Aperfeiçoamento de Pessoal de Nível Superior – Brasil (CAPES) – Código de Financiamento 001 [33003017034P-8], Conselho Nacional de Desenvolvimento Científico e Tecnológico (CNPq) [Proc. 406193/2018-5 e 308046/2019-6] e Fundação de Amparo à Pesquisa do Estado de São Paulo – Brasil (FAPESP) [Proc. 2020/16004-9, 2019/07822-2 e 2019/25228-0] pelo suporte financeiro. Agradeço à empresa SpectroChem pela doação da argila organofílica Spectrogel®

utilizada neste estudo e ao CENAPAD SP pela licença de uso dos programas empregados na simulação molecular.

A todos, que mesmo aqui não citados, cruzaram meu caminho nessa passagem, e torcem pelo meu sucesso pessoal e profissional.

Meus sinceros agradecimentos.

RESUMO

Os contaminantes emergentes vêm atraindo atenção da comunidade científica face ao seu grande impacto no ecossistema, mesmo em concentrações baixas, e devido à intensificação de sua ocorrência ao redor do mundo. O bisfenol A (BPA), o 17α–etinilestradiol (EE2) e o triclosan (TCS) são exemplos de contaminantes emergentes encontrados em diferentes matrizes aquáticas e que são muito danosos à biota aquática e à saúde humana. Em decorrência na ineficácia de tratamentos convencionais na remoção dessa classe de contaminante presente em matrizes aquosas, diversas tecnologias avançadas vêm sendo amplamente avaliadas para este fim. Esta dissertação de mestrado teve como objetivo desenvolver um nanocompósito adsorvente magnético baseado em óxido de grafeno, quitosana magnética e argila organofílica para remoção de contaminantes emergentes de matrizes aquáticas. O nanoadsorvente desenvolvido foi caracterizado por técnicas analíticas de FTIR, DRX, MEV, EDS, VSM, Raman, potencial zeta, BET, TGA, e XPS, buscando investigar suas características estruturais, morfológicas, assim como sua estabilidade térmica e os mecanismos envolvidos na adsorção dos contaminantes. A afinidade do nanocompósito foi avaliada para o BPA, EE2 e TCS e o sistema GO/mCS/OC – EE2 foi considerado o mais promissor. Seu processo de adsorção foi investigado, avaliando-se o efeito de parâmetros operacionais, além de estudos cinético, de equilíbrio e termodinâmico e de seletividade. A dosagem de 0,1 mg mL^{-1}, o pH natural da água ultrapura e a não aplicação do banho de ultrassom foram estabelecidos como condições ótimas e utilizados nos experimentos posteriores. O estudo cinético alcançou o equilíbrio com 120 min e os dados foram melhor descritos pelo modelo de pseudossegunda ordem. A etapa de transferência de massa em filme externo foi considerada a limitante do processo. A capacidade máxima adsortiva do material foi de 0.25 mmol g^{-1} (73.3 mg g^{-1}) a 50 °C e os modelos de Freundlich e BET foram os que melhor representaram os dados de equilíbrio. A avaliação dos parâmetros dos modelos de equilíbrio indicou característica superficial heterogênea do nanocompósito e a presença de interações físicas e químicas entre o adsorbato e adsorvente, entretanto com predominância da fisissorção em multicamadas. O estudo termodinâmico indicou que o processo é endotérmico, espontâneo e com a predominância da fisissorção. O nanocompósito foi submetido a cinco ciclos de regeneração, demonstrando sua capacidade de reuso. O nanocompósito apresentou bons resultados nos ensaios de seletividade, mostrando remoção significativa do EE2 e do BPA em diferentes condições e boa seletividade para o EE2.

Palavras-chave: Contaminantes Emergentes; 17α–etinilestradiol; Nanocompósito; Adsorção.

ABSTRACT

Emerging contaminants have attracted the attention of scientific community due to their great impact on the ecosystem, even at low concentrations, and due to the intensification of their occurrence around the world. Bisphenol A (BPA), 17α–ethinylestradiol (EE2) and triclosan (TCS) are examples of emerging contaminants found in different aquatic matrices that are very harmful to aquatic biota and human health. Several advanced technologies have been widely evaluated for this purpose, due to the ineffectiveness of conventional treatments in removing this class of contaminant present in aqueous matrices. This master's dissertation aimed to develop a magnetic adsorbent nanocomposite based on graphene oxide, magnetic chitosan and organoclay for the removal of contaminants emerging from aquatic matrices. The developed nanoadsorbent was characterized by analytical techniques of FTIR, XRD, SEM, EDS, VSM, Raman, zeta potential, BET, TGA, and XPS, seeking to investigate its structural and morphological characteristics, as well as its thermal stability and the mechanisms involved in the adsorption of contaminants. The affinity of the nanocomposite was evaluated for BPA, EE2 and TCS and the GO/mCS/OC – EE2 system was considered the most promising. Its adsorption process was investigated, evaluating the effect of operational parameters, in addition to kinetic, equilibrium, thermodynamic and selectivity studies. The dosage of 0.1 mg mL^{-1}, the natural pH of the ultrapure water and the non-application of the ultrasonic bath were established as optimal conditions and used in subsequent experiments. The kinetic study reached equilibrium within 120 min and the data were better described by pseudo-second order model. The external film mass transfer step was considered the process limiting step. The maximum adsorption capacity of the nanomaterial was 0.25 mmol g^{-1} (73.3 mg g^{-1}) at 50 °C and Freundlich and BET models were the ones that best represented the equilibrium data. The evaluation of equilibrium models' parameters indicated a heterogeneous surface characteristic of the nanocomposite and the presence of physical and chemical interactions between adsorbate and adsorbent, however with a predominance of multilayer physisorption. The thermodynamic study indicated that the process is endothermic, spontaneous and with a predominance of physisorption. The nanocomposite underwent five adsorption/desorption cycles, demonstrating its ability to reuse. The nanocomposite showed good results in selectivity tests, showing significant removal of EE2 and BPA under different conditions and good selectivity for EE2.

Key Words: Emerging Contaminants; 17α–ethinylestradiol; Nanocomposite; Adsorption.

LISTA DE FIGURAS

LISTA DE TABELAS

SUMÁRIO

CAPÍTULO 1. INTRODUÇÃO E OBJETIVOS

1.1 Motivação e Relevância

Os processos de industrialização e urbanização contribuem para o surgimento de novos contaminantes nas matrizes aquáticas. A falta de uma regulação que acompanha a dinâmica dos poluentes contidos nos rejeitos, seja industrial ou doméstico, também contribui para o acúmulo no meio ambiente. São classificados como poluentes emergentes novos compostos cujos impactos não foram completamente compreendidos, além daqueles que foram amplamente estudados, que entretanto surgem novas informações sobre os seus danos ao ser humano e ao meio ambiente (Varsha et al., 2022). Dentre os contaminantes emergentes estão os hormônios sintéticos, plastificantes, produtos de higiene pessoal, fármacos, drogas ilícitas, nanomateriais, que vem sendo reportado em diversas matrizes aquáticas ao redor do mundo (Parida et al., 2021a; Wells et al., 2009). Esses poluentes têm um grande impacto a longo prazo no ecossistema, os tratamentos convencionais não são capazes de remover completamente e por estas razões a proposição de tecnologias visando à sua remoção de águas e efluentes são extremamente relevantes (Varsha et al., 2022; Yang et al., 2013).

Dentre as alternativas viáveis, a adsorção se destaca devido à sua facilidade de operação, seu baixo custo e sua vasta diversidade de materiais adsorventes disponíveis. A variedade de características estruturais e químicas dos materiais adsorventes possibilita diferentes tipos de interações que podem favorecer a remoção de uma classe de contaminante de interesse. Nesse contexto, a utilização de nanoadsorventes apresenta diversas vantagens como sua grande área superficial, além da concentração da maioria dos átomos com alta atividade química e capacidade de adsorção em sua superfície (Kyzas e Matis, 2015).

Do grupo dos nanoadsorventes destacam-se os derivados de grafeno, que pode ser definido como uma monocamada plana de átomos de carbono, de espessura nanométrica, hibridizados em sp^2 com ligações covalentes, formando um filme com estrutura hexagonal densamente compactadas. A estrutura descrita implica em um material com elevada condutividade elétrica e térmica, boa elasticidade e estabilidade, além de extensa área superficial (Novoselov, 2011; Yang et al., 2011). A inserção de grupamentos coordenantes em sua estrutura é amplamente utilizada visando à potencialização das suas características, viabilizando-o como adsorvente para purificação de águas (Abdolmaleki

et al., 2017).

O óxido de grafeno (GO) é resultado da oxidação incompleta do grafite, onde são incorporados grupos hidroxilas e epóxi no plano basal, além de grupamentos carboxilas nos seus limites (Figura 1.1) (Chen et al., 2014). O processo de oxidação promove maiores interações eletrostáticas com íons metálicos e compostos orgânicos, facilitando sua remoção (Madadrang et al., 2012).

Figura 1.1 - Estrutura do GO.

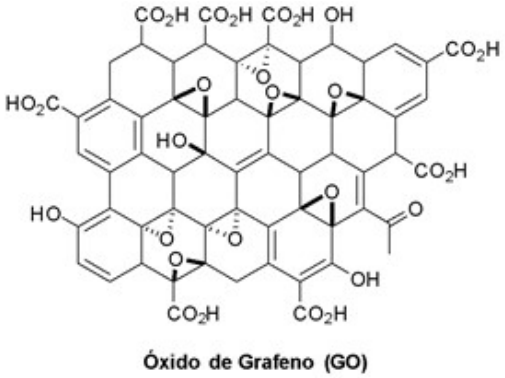

Fonte: Autor, 2020.

Nos últimos anos, diversas aplicações do GO foram investigadas, apresentando um enorme potencial no campo da engenharia ambiental, com destaque para a remoção de contaminantes da água (Xu et al., 2012).

Com o intuito de obter características singulares e aumentar a capacidade adsortiva do GO, a literatura reporta processos de mistura com outros compostos, sendo o material resultante denominado de compósito. A variedade de materiais para formação dos compósitos implica em propriedades adsorventes diversas.

A quitosana (CS) é amplamente incluída na preparação de compósitos e se destaca no campo da adsorção por ser um polissacarídeo natural, biodegradável, renovável, atóxico, de fácil manipulação, baixo custo e boa capacidade adsortiva (Gonsalves et al., 2011). Nanopartículas magnéticas são misturadas com a CS dando ao material um caráter magnético, facilitando técnicas de separação, um fator importante no processo de adsorção (Gregorio-Jauregui et al., 2012). Em função disso, a CS magnética vem sendo aplicada no tratamento de águas, promovendo a remoção de diversos contaminantes (Zhang et al., 2016; Zhou et al., 2019).

As argilas organofílicas também são utilizadas como compósitos e são definidas como argilas minerais em que foram inseridos compostos orgânicos em sua superfície a

fim de melhorar as interações com meios orgânicos (Silva e Ferreira, 2008). Esse material vem sendo amplamente empregado como adsorvente em tratamento de águas residuais devido a sua grande área superficial e alta capacidade de troca de cátions, além de ter um baixo custo e grande disponibilidade (Taylor et al., 2013).

Os contaminantes emergentes 17α–etinilestradiol (EE2), bisfenol A (BPA) e Triclosan (TCS) foram selecionados para representar as classes dos hormônios sintéticos, plastificantes e antissépticos e assim realizar uma avaliação do seu processo de remoção através de compósitos de GO.

Considerando o contexto exposto, esta Dissertação almejou o estudo do processo de remoção de poluentes emergentes, tais como o EE2, BPA e TCS via adsorção em nanocompósitos sintetizados baseados em óxido de grafeno, quitosana magnética e argila organofílica Spectrogel®. O desempenho do sistema adsorbato-adsorvente mais promissor foi avaliado em termos cinético, de equilíbrio e termodinâmica e seletividade. Estudos envolvendo o uso de compósitos de óxido de grafeno/quitosana magnética/argila organofílica na remoção de contaminantes emergentes em água não foram encontrados na literatura até o momento.

1.2 Objetivos

1.2.1 Objetivo Geral

O objetivo geral do presente trabalho foi sintetizar e avaliar a adsorção de nanocompósitos com óxido de grafeno, quitosana magnética e argila organofílica Spectrogel® para remoção de contaminantes emergentes, sendo representados pelo EE2, BPA e TCS. Para o sistema adsorvente-adsorbato mais promissor, estudar e otimizar o processo de adsorção em sistema de batelada.

1.2.2 Objetivos Específicos

Os objetivos específicos desta pesquisa envolveram o desenvolvimento das seguintes etapas de execução:

- Sintetizar o nanocompósito baseado no óxido de grafeno, quitosana magnética e argila organofílica;
- Realizar experimentos de afinidade adsortiva dos contaminantes emergentes EE2, BPA e TCS pelos adsorventes produzidos para se determinar o sistema mais promissor;

- Realizar cálculos baseados na teoria da densidade funcional (DFT) para obtenção de descritores químicos moleculares*;*
- Caracterizar o material adsorvente mais promissor;
- Otimizar os parâmetros do processo de adsorção avaliando o pH, o tempo de sonicação e a dose de adsorvente;
- Estudar a cinética de adsorção e descrever o modelo matemático para predizer o processo;
- Determinar as isotermas de adsorção em diferentes temperaturas, efetuar a modelagem de equilíbrio e avaliar a termodinâmica do processo;
- Avaliar o reuso do nanoadsorvente em ciclos de adsorção e dessorção;
- Avaliar a seletividade do adsorvente promissor em relação a diferentes contaminantes emergentes.

1.3 Apresentação da dissertação em capítulos

A dissertação de mestrado foi estruturada na forma de capítulos, os quais apresentam os resultados de cada uma das etapas da pesquisa realizada. Os resultados desta pesquisa de adsorção dos contaminantes emergentes são apresentados e discutidos por meio dos artigos científicos oriundos da dissertação. Estes artigos são apresentados no formato dos periódicos internacionais nos quais foram publicados/submetidos. Além da revisão bibliográfica contida no **Capítulo 2**, dois artigos foram desenvolvidos a partir desta dissertação trazendo uma contextualização e embasamento dos tópicos abordados.

O **Capítulo 3** apresenta a síntese do nanocompósito desenvolvido, assim como sua comparação com a sua argila precursora na remoção de três contaminantes emergentes a partir de ensaios de afinidade em batelada. O BPA, EE2 e TCS também foram avaliados a partir da teoria da densidade funcional (DFT) buscando investigar os seus descritores químicos moleculares e mapas de potencial eletrostático. Os resultados foram publicados no periódico internacional *Journal of Environmental Chemical Engineering*, intitulado "*Synthesis of a novel magnetic composite based on graphene oxide, chitosan and organoclay and its application in the removal of bisfenol A, 17α-ethinylestradiol and triclosan*".

No **Capítulo 4** é apresentado o artigo publicado no *Journal of Water Process Engineering* intitulado "*Adsorption of 17α-ethinylestradiol onto a novel nanocomposite based on graphene oxide, magnetic chitosan and organoclay (GO/mCS/OC): Kinetics,*

equilibrium, thermodynamics and selectivity studies". Esse capítulo investigou o desempenho do nanocompósito desenvolvido na adsorção de EE2. Diferentes parâmetros operacionais como pH, tempo de sonicação no ultrassom e dose de nanoadsorvente foram avaliados, bem como uma avaliação da cinética, do equilíbrio e da termodinâmica do processo. Um projeto simplificado em batelada e ensaios para avaliação da seletividade do nanocompósito em soluções binárias com EE2 e BPA foram efetuados. O GO/mCS/OC foi caracterizado antes e depois do processo de adsorção por diferentes técnicas analíticas. Os mecanismos de adsorção e grupos funcionais presentes no nanoadsorventes e envolvidos no processo de remoção também foram investigados.

O **Capítulo 5** apresenta uma discussão geral sobre os principais resultados obtidos nesta dissertação de mestrado. No **Capítulo 6** são apresentadas as conclusões gerais desse projeto, assim como as sugestões para trabalhos futuros utilizando o nanocompósito desenvolvido para a remoção de contaminantes emergentes. No **Capítulo 7** está descrita a produção científica gerada durante o mestrado.

CAPÍTULO 2. REVISÃO BIBLIOGRÁFICA

Este capítulo é composto por uma revisão da literatura sobre os tópicos discutidos neste projeto. É apresentada a problemática da contaminação de efluentes por contaminantes emergentes, abordando principalmente o EE2, o BPA e o TCS, reportando seus impactos no meio ambiente. São descritas técnicas de remoção de contaminantes emergentes em solução aquosa, aspectos gerais sobre a adsorção e adsorventes tradicionais, avançados e alternativos.

2.1 Contaminação de efluentes por contaminantes emergentes

Até o início do século 19, a qualidade da água era avaliada apenas por aspectos estéticos, como odor, cor e gosto, entretanto há relatos desde a Grécia antiga da utilização de técnicas de filtração e fervura para melhorar sua qualidade. Os gregos já apontavam empiricamente para a relação entre a água e enfermidades, mas foi só em 1880 que *Louis Pasteur* demonstrou que organismos microscópicos poderiam transmitir doenças por meio da água. No início do século 20, técnicas como a cloração e a ozonização já eram utilizadas para desinfecção da água em alguns países mesmo sem legislação regulando o limite das substâncias (Freitas e Freitas, 2005). Na atualidade, a Organização Mundial da Saúde (OMS) avalia os estudos toxicológicos publicados pela comunidade científica e informa as concentrações máximas sugeridas para diferentes corpos hídricos. Alguns países além de se basearem nas recomendações da OMS, também fomentam pesquisas toxicológicas que também fundamentam suas legislações e acabam servindo de referência para a organizações e para outros países. No Brasil, as normas de potabilidade seguem a maioria das sugestões da OMS descritas no *Guidelines for Drinking-Water Quality* (Racar et al., 2020; WHO, 1996).

Muitos compostos de alta toxicidade como fertilizantes e solventes, além de patógenos como bactérias e protozoários foram amplamente estudados pela comunidade científica. Entretanto, com o aumento do impacto da atividade antropogênica e industrial a presença de novos contaminantes nas matrizes aquáticas vem sendo reportada (Sauvé e Desrosiers, 2014a). Nos últimos anos, alguns poluentes foram identificados nos corpos hídricos em concentrações na ordem de microgramas, onde não existem muitas informações sobre sua ocorrência e ecotoxicidade. Nesse contexto, surge o termo contaminantes emergentes, que são os compostos cujo impacto na saúde humana e do

ecossistema não foi completamente compreendido e que englobam a categoria dos fármacos, pesticidas, plastificantes, hormônios, microplásticos, entre outras (Sophia e Lima, 2018).

Devido à falta de informação relacionado ao seu impacto, a concentração de ocorrência de muitos contaminantes orgânicos não é monitorada com frequência. A maioria dos países do mundo não possuem regulamentações específicas para poluentes emergentes, de forma que o procedimento convencional das estações de tratamento de esgoto (ETE) e de água (ETA) não remove com eficiência essa classe de compostos. Algumas etapas do tratamento como a cloração podem inclusive promover metabólitos mais danosos ao ecossistema, assim como a natureza polar de alguns compostos dificulta sua remoção pelo tratamento convencional. O aumento da sua ocorrência está associado a essa ineficiência de remoção e descarte nos corpos hídricos, que contribuem para o seu acúmulo no meio ambiente. Atualmente, diversas tecnologias são avaliadas por pesquisadores, buscando metodologias que removam com eficiência os contaminantes emergentes de meios aquosos (Antonelli et al., 2020b; Montagner et al., 2017; Resende et al., 2020).

2.2 Contaminação de efluentes por Etinilestradiol (EE2)

O etinilestradiol (17α-etinilestradiol), de fórmula $C_{20}H_{24}O_2$ (Figura 2.1) é um hormônio sintético derivado do estradiol (E2), amplamente utilizado na reposição de estrogênios. O fármaco é o principal componente estrogênico dos contraceptivos orais, além de ser aplicado no tratamento de osteoporose, menopausa e câncer de próstata. O composto é classificado como um disruptor endócrino (EDC) que compreende os compostos que têm a capacidade de desregular o funcionamento do sistema endócrino de seres humanos e animais (Liu et al., 2012). Estudos revelam que além da feminização anatômica da biota aquática, mesmo em baixas concentrações, o hormônio pode atrasar a maturidade sexual e provocar grandes alterações fisiológicas devido à desregulação endócrina (Aris et al., 2014; Bhandari et al., 2015). A Tabela 2.1 mostra algumas propriedades do EE2.

Figura 2.1 - Estrutura da molécula do EE2, de forma que o carbono, oxigênio e hidrogênio são representados pelas esferas cinzas, vermelhas e brancas, respectivamente.

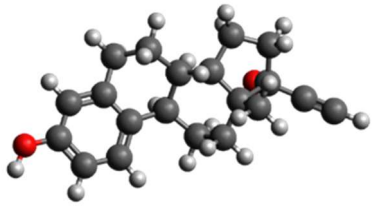

Fonte: Autor, 2020.

Tabela 2.1 – Principais propriedades do EE2.

17α-Etinilestradiol	
Fórmula molecular	$C_{20}H_{24}O_2$
Número CAS	57-63-6
Massa molar (g mol^{-1})	296,4
Ponto de fusão a 1 atm (ºC)	183
Solubilidade em água a 27 ºC e 1 atm (mg L^{-1})	11,3
pK_a (Ácido mais forte)	10,33
pK_a (Base mais forte)	-1,7

(Pubchem, 2020) - Adaptada

A fonte principal de depósito de fármacos e disruptores endócrinos é o lançamento de esgotos in natura e tratado no meio ambiente, além da própria indústria farmacêutica e agrícola que também contribuem para o descarte indevido (Crouse et al., 2012; de Aquino et al., 2013). A produção global de EE2 apenas para uso em contraceptivos orais já alcançava 0,3 toneladas por ano em 2006 (Poirier et al., 2006). O contaminante mostra resistência aos procedimentos convencionais utilizados nas estações de tratamento de água e efluentes, onde a biodegradação, principal etapa de remoção de estrogênios, não mostra eficiência para remoção do EE2, contribuindo para o seu acúmulo nas matrizes aquáticas. O EE2 é o mais resistente dentre os estrogênios, possui baixa solubilidade em água, tem baixa taxa de fotodegradação e tempo de meia vida de aproximadamente 17 dias em água (Yang et al., 2017). A Tabela 2.2 mostra a faixa de concentração de ocorrência desse contaminante em matrizes aquáticas do mundo.

Tabela 2.2 – Concentrações de ocorrência de EE2 no mundo.

País	**Faixa de concentração (ng L^{-1})**	**Referência**
França	1,1 – 2,9	(Cargouët et al., 2004)
USA	3 – 4,7	(Zuo et al., 2006)
Turquia	11,7 – 14	(Aydin and Talinli, 2013)
Austrália	0 – 0,5	(Ying et al., 2009)
Brasil*	0 – 25	(Sodré et al., 2010)
Alemanha	0,3 – 0,7	(Bögi et al., 2003)
Taiwan	7,5 – 27,4	(Chen et al., 2007)
China	7 – 24	(Zhou et al., 2011)

*O estudo foi realizado no estado de São Paulo/Brasil.

(Aris et al., 2014) - Adaptada

No Brasil é observada grande ocorrência do contaminante, além de um dos maiores valores de concentração, só estando abaixo de Taiwan. Essa comparação indica uma ineficiência dos procedimentos de tratamentos convencionais de efluentes que chegam, além da possibilidade de descartes irregulares e sem tratamento diretamente nas matrizes aquáticas. A presença desses contaminantes indica a ocorrência de outros microcontaminantes também decorrentes da ação antrópica e o aumento de suas concentrações é preocupante devido a falta do domínio amplo de suas consequências no ecossistema. A ocorrência do EE2 foi investigada por Tang e colaboradores em 282 estações de tratamento de esgoto em 29 países, apresentando uma faixa de concentração da entrada desde o não detectável até 7890 ng L^{-1}. Um fator destacado como preocupante foi a concentração de descarte média ser muito superior a concentração de exposição crônica a biota aquática, levantando a necessidade de desenvolvimento de tecnologias de remoção eficientes (Tang et al., 2021c).

O impacto da acumulação de compostos estrogênicos, incluindo o EE2, foi avaliado em lagoa na China por Zhang e colaboradores. As concentrações dos hormônios foram avaliadas na água, sedimentos e organismos aquáticos, assim como sua estrogenicidade. O estudo relatou que os contaminantes apresentaram preferência em se depositar nos sedimentos, assim como a concentração em amostras mais profundas foram superiores as da superfície. A avaliação anterior foi relacionada com as concentrações encontradas nos organismos, onde o mais contaminado foi um molusco que seu habitat é

justamente o sedimento contaminado. Algumas espécies de peixes foram avaliadas onde os carnívoros superiores na cadeia alimentar mostraram maior ocorrência dos estrogênios sugerindo perpetuação dos compostos através das relações alimentares do ecossistema. O autor defende a correlação entre o nível do poluente no organismo com o seu ambiente, sua habilidade metabólica e a capacidade de biodegradação nos sedimentos (Zhang et al., 2011).

2.3 Contaminação de efluentes por Bisfenol A (BPA)

O bisfenol A (4,4'-dihidroxi-2,2-difenilpropano) (Figura 2.3) é um composto orgânico sintético utilizado para produção diversos produtos de consumo, embalagens materiais e insumos industriais. Compõe a matéria prima para produção de plásticos, resinas e retardantes de chamas para aplicações diversas no cotidiano. O volume de produção industrial de BPA no mundo vem crescendo, acompanhando principalmente o aumento da demanda por policarbonatos e resinas epóxi, onde já em 2020 a produção alcançou cerca de 6 milhões de toneladas por ano (Mordor Intelligence, 2021). Organizações como a *European Food Safety Autority* avaliam desde 2008 os riscos da exposição dessa substância a humanos, entretanto só em 2010 o governo americano reconheceu um possível potencial negativo a organismos aquáticos e houve uma mudança na classificação da *US Food and Drug Administration* do BPA, passando de "substância considerada segura" para "substância com efeitos potenciais" (Flint et al., 2012). O composto também é classificado como disruptor endócrino, e interfere diretamente no funcionamento hormonal dos seres vivos. A exposição desse composto a humanos e animais está também relacionada a doenças cardiovasculares, anomalias no cérebro, disfunção na tireoide e infertilidade, o que contribuiu para o banimento do uso desse composto em alguns produtos específicos como nas mamadeiras (Amjad et al., 2020; Erler and Novak, 2010; Liu et al., 2009). A Tabela 2.3 ilustra algumas propriedades do BPA.

Figura 2.3 - Estrutura da molécula do BPA, de forma que o carbono, oxigênio e hidrogênio são representados pelas esferas cinzas, vermelhas e brancas, respectivamente.

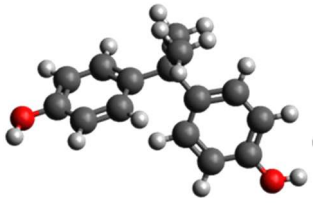

Fonte: Autor, 2020.

Tabela 2.3 – Principais propriedades do BPA.

Bisfenol A	
Fórmula molecular	$C_{15}H_{16}O_2$
Número CAS	80-05-7
Massa molar (g mol^{-1})	228,29
Ponto de fusão a 1 atm (ºC)	160
Ponto de ebulição a 1 atm (ºC)	360,5
Solubilidade em água a 25 ºC e 1 atm (mg L^{-1})	120
Densidade a 25 ºC	1,195

(Pubchem, 2020) - Adaptada

O BPA chega ao ambiente, resultado de sua alta produção global e consumo dos seus derivados. As fontes principais de deposição do contaminante são o descarte de efluentes das fábricas que utilizam o BPA e o descarte pós-consumo que inclui a descarga de efluentes das estações de tratamento (Guerra et al., 2015; Tsai, 2006). Apesar da sua baixa persistência no ambiente, com uma meia vida menor que 7 dias em rio na faixa de temperatura de 20–30 ºC, o descarte elevado pelas fontes apresentadas contribui para o seu acúmulo (Kang e Kondo, 2002). A Tabela 2.4 mostra a faixa de concentração de ocorrência desse contaminante em matrizes aquáticas do mundo.

Tabela 2.4 – Concentrações de ocorrência de BPA no mundo.

País	**Faixa de concentração (ng L^{-1})**	**Referência**
Espanha	10 – 2500	(Zafra et al., 2003)
USA	281 – 3642	(Drewes et al., 2012)
Brasil*	5 – 1760	(Sodré et al., 2007)
Holanda	10 – 330	(Belfroid et al., 2002)
Alemanha	8,9 – 776	(Stachel et al., 2003)
Japão	500 – 900	(Kang and Kondo, 2006)
Singapura	40 – 190	(Basheer and Lee, 2004)
Taiwan	50 – 3000	(Ding and Wu, 2000)
China	43,5 – 639	(Gong et al., 2009)

*O estudo foi realizado no estado de São Paulo/Brasil.

(Huang et al., 2012) - Adaptada

Uma grande variabilidade é encontrada na concentração de ocorrência do BPA entre diversos países. No Brasil, foram observadas altas concentrações, além de grande variação, assim como em outros países industrializados do mundo. Países mais industrializados apresentaram a tendência de concentrações maiores nas matrizes hídricas. A ocorrência desse contaminante também foi avaliada em algumas estações de tratamento de esgoto do mundo, apresentando nível de concentração na faixa entre 109 – 615 ng L^{-1} em Hong Kong, nível similar em países europeus e concentrações 10 vezes maiores na China (Wu et al., 2017).

Uma avaliação do impacto de diversos disruptores endócrinos, incluindo o BPA, foi investigado em lagoa em Veneza, Itália. A região avaliada é um ecossistema costeiro amplamente urbanizado que recebe efluentes de águas residuais industriais e municipais. As concentrações encontradas foram superiores nos sedimentos em relação à água e aos organismos aquáticos. Dentre os disruptores encontrados na água e nos sedimentos, o BPA foi a substância detectada em maiores concentrações. Foram avaliadas as concentrações desses contaminantes em espécies de mexilhões e outros organismos filtrantes, que apresentou a tendência de bioacumulação de micropoluentes (Pojana et al., 2007).

2.4 Contaminação de efluentes por Triclosan (TCS)

O triclosan (5-cloro-2-(2,4-diclorofenoxi)-fenol) (Figura 2.4) é um agente microbiano encontrado em shampoos, sabonetes, desodorantes, cremes dentais, cosméticos e em alguns produtos comerciais, como plásticos e tecidos, visando evitar o crescimento microbiano. O composto é classificado como um fármaco e produto de cuidados pessoal, do inglês *pharmaceutical and personal care products* (PPCPs), e sua presença é frequente no cotidiano social. A produção anual de TCS alcançou cerca de 1500 toneladas em 2019 (Milanovic et al., 2021). Seu uso generalizado vem se mostrando uma problemática ao ecossistema, levantando preocupações devido a sua relação com o desenvolvimento de câncer e ao impacto na contração muscular. Nesse contexto diversos países propuseram regulamentações limitando seu uso em produtos de higiene e cosméticos, como o Canadá e a África do Sul onde sua percentagem limite, em massa, é de 0,3% (Bedoux et al., 2012; Cherednichenko et al., 2012; Dinwiddie et al., 2014; Ramaswamy et al., 2011). A Tabela 2.5 traz as principais propriedades do TCS.

Tabela 2.5 – Principais propriedades do TCS.

Triclosan	
Fórmula molecular	$C_{12}H_7Cl_3O_2$
Número CAS	3380-34-5
Massa molar (g mol^{-1})	289,5
Ponto de ebulição a 1 atm (ºC)	120
Ponto de fusão a 1 atm (ºC)	57
Solubilidade em água a 20 ºC e 1 atm (mg L^{-1})	10
pK_a	7,9

(Pubchem, 2020) - Adaptada

Figura 2.4 - Estrutura da molécula do TCS, de forma que o carbono, oxigênio, hidrogênio e cloro são representados pelas esferas cinzas, vermelhas, brancas e verdes, respectivamente.

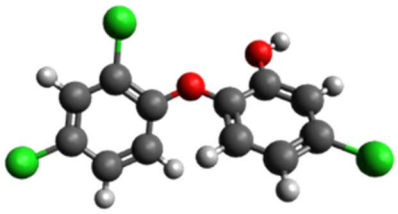

Fonte: Autor, 2020.

Devido à sua presença em produtos amplamente utilizados no cotidiano há uma tendência de contaminação dos resíduos residenciais, apesar da sua baixa solubilidade em água. Diversos estudos além de reportarem o poluente nas estações de tratamento de efluentes, verificaram sua presença na urina, plasma e até no leite materno humano. O estudo de (Adolfsson-Erici et al., 2002) reportou altos níveis do poluente em 60% das amostras de leite materno, assim como a *National Health and Nutrition Examination Survey* (NHANES) encontrou em 75% das amostras de urina de adultos e crianças, indicando um potencial de absorção no corpo. Os processos convencionais das estações de tratamento de esgoto removem cerca de 90% do TCS, que por seu caráter hidrofóbico tem a tendência de se aglomerar com o resíduo sólido. O composto apresenta biodegradação moderada sob condições aeróbicas quando aplicado em solos (18 dias), entretanto uma resistência muito alta a biodegradação sob condições anaeróbicas, que não se inicia antes de 70 dias. Portanto, há duas fontes principais de descarte do TCS no meio ambiente, sendo elas a parcela não removida das estações de tratamento e a aplicação no

solo dos biosólidos contaminados resultantes do processo. Apesar da redução global do seu uso devido aos seus potenciais danos, a sua alta resistência à degradação, resulta no seu frequente acúmulo no ecossistema (Dhillon et al., 2015; Fuchsman et al., 2010; C. Zhao et al., 2016). A Tabela 2.6 mostra a faixa de concentração de ocorrência desse poluente em matrizes aquáticas do mundo.

Tabela 2.6 – Concentrações de ocorrência de TCS no mundo.

País	**Faixa de concentração ($ng\ L^{-1}$)**	**Referência**
Suíça	11 – 98	(Singer et al., 2002)
USA	104 – 431	(Morrall et al., 2004)
Brasil*	2,2 - 66	(Montagner et al., 2014)
Austrália	< 3 – 75	(Ying and Kookana, 2007)
Alemanha	3 – 10	(Bester, 2005)
Japão	11 – 31	(Nishi et al., 2008)
Canadá	4 – 8	(Hua et al., 2005)
Espanha	58 – 138	(Villaverde-De-Sáa et al., 2010)
China	11 – 478	(Zhao et al., 2010)

*O estudo foi realizado no estado de São Paulo/Brasil.

(Bedoux et al., 2012; Dhillon et al., 2015) - Adaptada

É possível identificar uma variabilidade na concentração de ocorrência do TCS em águas superficiais de rios e lagos pelo mundo. No Brasil, foi observada faixa de concentração similar a dos outros países. Um estudo de caso foi realizado em alguns rios da China para avaliação da ocorrência e dos riscos do TCS no seu corpo hídrico. O composto foi encontrado em altas concentrações em um dos rios e moderada nos outros dois, representando um grande e moderado risco aos organismos aquáticos respectivamente. Devido ao caráter lipofílico o contaminante demonstrou tendência em se acumular em organismos animais. Quando presente nos corpos hídricos o contaminante também demonstrou tendência em se depositar nos sedimentos, devido ao seu caráter hidrofóbico, resultando em concentrações até 6 vezes superior que na água superficial. Essa grande diferença se torna mais uma problemática visto que além de concentrar o contaminante, ele se torna uma fonte de recontaminação das águas

superficiais (Zhao et al., 2010). A ocorrência desse contaminante também foi avaliada em algumas estações de tratamento de esgoto do mundo, apresentando nível de concentração média de 295 ng L^{-1} na China, 213 ng L^{-1} na Suíça e 25 ng L^{-1} nos Estados Unidos. Assim como em águas superficiais, o TCS também apresentou tendência de acúmulo na fase sólida das estações de tratamento (Lodo Ativado) (Wang e Liang, 2021; Zhang et al., 2021).

2.5 Métodos de remoção de contaminantes emergentes em efluentes

As estações de tratamento de água e esgoto foram planejadas para a remoção de certos tipos de contaminantes convencionais, entretanto com a presença de novos compostos nas matrizes aquáticas, com ocorrência na ordem de microgramas e até nanogramas por litro, surge uma problemática. Tratamentos convencionais como a coagulação e floculação na maioria das vezes não remove contaminantes emergentes com eficiência, e têm resultados distintos devido à ampla diferença das propriedades químicas dessa classe de poluentes. Outra etapa comum nas estações de tratamento de água é a desinfecção através da cloração, que é diretamente afetada pela presença de compostos orgânicos, resultando em alguns casos de metabólitos mais tóxicos que seus precursores. Tratamentos biológicos como a aplicação de lodo ativado também apresentam capacidade limitada de remoção de poluentes emergentes, além de inibir a atividade de microorganismos, contribuindo para o seu acúmulo no ecossistema (Bolong et al., 2009; Rivera-Utrilla et al., 2013; Sophia e Lima, 2018).

Devido à ineficiência dos tratamentos convencionais para remoção de contaminantes emergentes, muitos pesquisadores reconhecem a importância de desenvolver processos eficientes para resolução da problemática. Os processos mais citados na literatura são os processos oxidativos avançados (POAs), a separação por membranas e os métodos de sorção.

Os processos oxidativos avançados utilizam radicais livres oxigenados, como a hidroxila (·OH), o ânion superóxido ($\cdot O^{2-}$), o hidroperoxil ($\cdot O_2H$) e o alcoxil (·OR), para promover a degradação de contaminantes. A presença de catalizadores no processo pode aumentar o potencial de degradação de alguns tipos de POAs acelerando a taxa de degradação de muitos contaminantes emergentes. São exemplos de POAs os processos de fotólise, fotocatálise, radiação ultravioleta, irradiação ultrassônica, sonólise, sonocatálise, onde a maioria apresenta boa eficiência de remoção (Rodriguez-Narvaez et

al., 2017; Yap et al., 2019a). A remoção de diversos contaminantes emergentes foi investigada através de POAs com UV/H_2O_2 e alcançaram eficiências de remoção de 95,4, 95 e 82,2 % para o BPA, TCS e EE2 (Huang et al., 2018; Rosenfeldt et al., 2007; Sharma et al., 2016). Apesar do tratamento remover com eficiência diversos microcontaminantes, seu alto custo e a possibilidade de geração de subprodutos mais danosos ao ecossistema são fatores que desestimulam sua aplicação (Andrade et al., 2020a).

Processos de filtração por membrana incluem a osmose reversa, a ultrafiltração e a nanofiltração. Apesar de apresentar bons desempenhos de remoção, algumas desvantagens também são reportadas na literatura como o alto custo relacionado ao consumo de energia para a osmose reversa, a ocorrência de incrustações e a dependência do desempenho com as propriedades físico-químicas do efluente, propriedades da membrana e com as condições operacionais do processo (Bolong et al., 2009; Kim et al., 2018). Marysková e colaboradores (2020) reportaram na literatura o uso de membranas de poliamida/polietilenimina para remover BPA, EE2 e TCS, apresentando percentuais de remoção de 27,9, 47,3 e 73,6 %, respectivamente.

A sorção é um fenômeno de transferência de massa em que as moléculas migram da fase fluida para uma fase sólida ou líquida, englobando a adsorção e a absorção. A diferença entre eles é que na absorção a molécula ultrapassa a interface do material e na adsorção ela fica aderida em sua superfície (Brandt, 2012).

2.6 Adsorção

Desde a antiguidade, populações egípcias, gregas e romanas utilizavam carvão, argila e areia para purificação e clarificação de fluidos, mas foi só por volta de 1773 que as propriedades adsortivas foram reconhecidas e que experimentos formais começaram a serem empregados. Apesar disso a aplicação desse processo na indústria se iniciou somente a partir do século XX, relacionado com a descoberta da remoção seletiva de materiais adsorventes devido a suas interações e afinidades moleculares (Dąbrowski, 2001).

2.6.1 Aspectos gerais da adsorção

O processo de adsorção é um método de transferência de massa da fase fluida para a superfície do material adsorvente, compreendendo a interação entre os sítios disponíveis da superfície e o adsorbato além de sua difusão através dos poros, como

ilustrado na Figura 2.5. Esse fenômeno apresenta grande importância e é aplicado na purificação de matérias primas, recuperação de compostos, liberação controlada de fármacos, além da remoção de contaminantes de efluentes. A adsorção é um método de separação promissor, de baixo custo e fácil operação, onde as interações do adsorbato com a superfície do material adsorvente são essenciais para um processo eficiente, assim como uma estrutura porosa e de elevada área superficial (Dąbrowski et al., 2005).

Figura 2.5 – Ilustração do processo de adsorção.

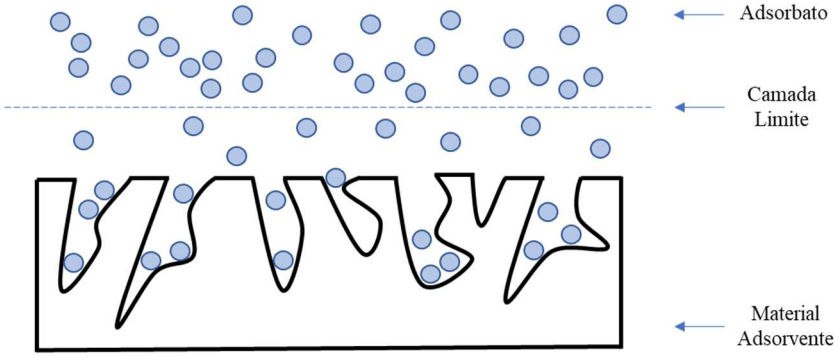

Fonte: Autor, 2020.

A adsorção é classificada de acordo com as interações predominantes do processo em fisissorção e quimissorção. Na adsorção física, as forças intrínsecas ao processo, como interações de van der Waals e eletrostáticas, são fracas e não ocorrem ligações químicas entre adsorbato e adsorvente. Na maioria das vezes, a adsorção física ocorre em baixas temperaturas, é rápida, reversível e exotérmica, onde é promovida a formação de diversas camadas de moléculas adsorvidas (Keller e Staudt, 2005; Karge, 2008; Rouqueirol, 2013; Ruthven, 1984).

Na adsorção química, as interações são mais fortes, compreendem a transferência e o compartilhamento de elétrons, que acarretam em ligações químicas entre adsorvente e adsorbato e promovem a irreversibilidade do processo. Esse tipo de adsorção geralmente é favorecido pela temperatura e apresenta grande variação de sua velocidade, podendo ser muito lenta. Em condições favoráveis, ambos processos podem ocorrer simultaneamente ou alternadamente. Entretanto, devido às características de ambos os tipos, a fisissorção é mais aplicado em processos de separação, já que facilita o processo de dessorção devido as baixas interações citadas, e a quimissorção é amplamente empregada na remoção de contaminantes em baixas concentrações, que necessitam de

interações mais fortes para serem removidas (Dąbrowski *et al.*, 2005; Karge, 2008; Keller e Staudt, 2005; Ruthven, 1984).

2.6.2 Características do sistema que influenciam na adsorção

As características físico-químicas do material adsorvente, do adsorbato de interesse, além da presença de todos os componentes no efluente em questão detém grande influência no processo. Outros fatores operacionais como temperatura, pH e velocidade de agitação afetam diretamente a eficiência do processo de adsorção (Ruthven, 1984).

- Temperatura

A influência da temperatura nas taxas de adsorção pode ser positiva ou negativa e isto está relacionado com a energia do sistema e com a natureza do processo. Em sistemas em que ocorrem interações eletrostáticas, geralmente de natureza química, há uma contribuição adicional exotérmica a entalpia de adsorção. O efeito da temperatura no equilíbrio de adsorção se apresenta então como um indicador da força da sorção. Para sistemas compostos por ligações de menor energia, geralmente de natureza física, uma baixa influência da temperatura é esperada devido à baixa entalpia de adsorção no equilíbrio. O sistema pode compreender tanto a natureza física quanto a química, onde em baixas temperaturas ocorre da fisissorção ser o processo dominante e a quimissorção não ser significativa. Essas condições implicam na diminuição da capacidade adsorvente com o aumento da temperatura. No entanto, em certa faixa de temperatura o seu aumento pode favorecer a ocorrência da quimissorção, inferindo em um aumento da capacidade de adsorção (Ten Hulscher e Cornelissen, 1996).

Um aumento na temperatura implica ainda em um aumento da taxa de difusão do adsorbato pela camada limite e através dos poros do adsorvente, devido a diminuição na viscosidade da solução (Doğan et al., 2006).

- pH

O valor do pH tem grande influência na adsorção visto que esse parâmetro determina o grau de distribuição das espécies químicas em que a molécula de interesse vai estar disposta no meio, além de modificar as cargas da superfície do adsorvente. Os

íons hidrogênio (H^+) e hidróxido (OH^-) podem ainda serem adsorvidos, ocupando um sítio ativo e concorrendo com o adsorbato de interesse (Appel et al., 2003; Farrah e Pickering, 1979).

- Velocidade de agitação

Um aumento na velocidade de agitação promove uma melhor dispersão do soluto, contribuindo para a homogeneização do sistema. Esse aumento pode ainda implicar no aumento da difusão pela camada limite, devido a diminuição da sua espessura e ao aumento da turbulência, colaborando para melhores taxas de transferência de massa. Em contrapartida, esse efeito positivo tem uma limitação, visto que agitações muito elevadas não permitem o tempo de contato suficiente para que a adsorção ocorra (Anwar et al., 2010; Kuśmierek e Wiatkowski, 2015).

2.6.3 Características do adsorvente que influenciam na adsorção

- Diâmetro de partícula

O tamanho da partícula do adsorvente é uma característica importante na adsorção afetando diretamente a resistência a transferência de massa do processo. O coeficiente de transferência de massa externa e de difusão intrapartícula, parâmetros importantes tanto na adsorção em batelada quanto em leito fixo, variam em função do diâmetro. Partículas com menor diâmetro levam a um aumento da capacidade de penetração do adsorbato, relacionado a diminuição do caminho a percorrer na difusão dentro da partícula adsorvente (Karau et al., 1997; Mathews e Zayas, 1989).

- Tamanho dos poros

A distribuição do tamanho de poros é uma das propriedades do adsorvente mais importantes no processo de adsorção. Essa característica engloba também o volume total disponível no adsorvente que pode ser ocupado pelo adsorbato. A organização *International Union of Pure and Applied Chemistry* (IUPAC) classifica o tamanho dos poros de acordo com a sua largura. Os poros com diâmetro maior que 50 nm são classificados como macroporos, já os poros com largura entre 2 e 50 nm são denominados mesoporos, e por fim os microporos que tem largura menor que 2 nm (McCusker et al., 2001; Pelekani e Snoeyink, 1999).

Do ponto de vista da energia livre do sistema, os adsorbatos são preferencialmente adsorvidos em poros de tamanho similar por causa do seu maior contato mútuo. As forças potenciais criadas pelas paredes opostas separadas por um tamanho levemente superior ao da molécula de interesse, são responsáveis por um incremento nas forças de adsorção nos microporos. Já nos mesoporos e macroporos, as moléculas que adentram não sofrem com os efeitos do campo de força exercida pela superfície. Em geral, os macroporos apresentam baixa área superficial em relação ao volume do poro e não são efetivos para remoção de adsorbatos e não contribuem para o processo de adsorção (Pelekani e Snoeyink, 1999; Schirmer, 2007).

- Área superficial específica

A área superficial específica é um fator importante para melhorar a qualidade de um material adsorvente, já que a adsorção é um fenômeno de superfície e quanto maior a área disponível para o contato, mais sítios ativos estarão disponíveis. Vale ressaltar ainda que para partículas menores há um incremento na área superficial específica, além de uma diminuição da resistência difusional ao transporte de massa pela camada limite, facilitando para que a superfície interna seja aproveitada (Sekar et al., 2004).

2.6.4 Materiais adsorventes

Diversos materiais sólidos detém as características necessárias para um material adsorvente promissor e são constantemente investigados pela literatura, dentre eles, estão em destaque:

- Carvão ativado

O carvão ativado é um dos adsorventes mais utilizados e apresenta uma elevada área superficial e porosidade, além de uma superfície reativa. O material carbonáceo em solução aquosa gera cargas elétricas devido a dissociação dos seus grupos funcionais na superfície, além disso a alta reatividade da mesma influencia na capacidade de doar e receber elétrons, favorecendo sua interação com íons. Apesar do carvão ativado comercial apresentar alto custo de produção, diversos materiais de baixo custo vem sendo desenvolvido com rejeitos e biomateriais visando a remoção de contaminantes da água (Dias et al., 2007).

- Nanotubos de carbono

Os nanotubos de carbono são adsorventes da família dos materiais carbonáceos, que formam cilindros ocos de proporções nanométricas. Esse material é considerado promissor em pesquisas devido as suas boas propriedades mecânicas, térmicas e elétricas, que dependem do seu diâmetro, comprimento, morfologia e nanoestrutura. Sua superfície hidrofóbica e os grupos funcionais presentes na mesma proporcionam fortes interações tanto com íons metálicos quanto compostos orgânicos. Em comparação com outros materiais carbonáceos, os nanotubos além de apresentarem alta área superficial, detém estrutura bem definida e uniformidade na distribuição de poros e de energia de adsorção. Apesar das propriedades de destaque do material, sua tecnologia apresenta um alto custo e necessita de mais estudos visando à aplicação em maiores escalas (Ren et al., 2011).

- Zeólitas

As zeólitas são materiais aluminossilicatos cristalinos, compostos por estruturas tetraédricas de óxidos de silício ou alumínio (SiO_4 ou AlO_4). Sua estrutura apresenta grande porosidade uniforme, o que torna o seu uso para adsorção vantajoso quando comparado a alguns adsorventes. Além disso outras vantagens como as boas propriedades mecânicas e térmicas, seu baixo custo, grande disponibilidade e sua alta capacidade de adsorção com a habilidade de se ajustar ao pH são evidenciadas pela literatura. Sua aplicação no meio ambiente com o intuito de remover poluentes se baseia principalmente na sua capacidade de troca de íons. Algumas modificações na estrutura do material são propostas com intuito de melhorar suas propriedades adsortivas (Misaelides, 2011).

- Argilas organofílicas

As argilas são aluminossilicatos de baixa cristalinidade com estrutura similar às zeólitas, onde a principal diferença são as estruturas heterogêneas dos materiais argilosos. As argilas são constituídas por folhas tetraédricas de sílica e octaédricas de alumina alternadas, além de outros materiais como ferro e magnésio. Esses argilominerais são classificados de acordo com a proporção de sílica e alumina, em conjunto com propriedades como troca catiônica, distância interatômica e capacidade de hidratação e expansão (Ruthven, 1984; Santos, 1975).

A estrutura da maior parte das argilas naturais proporciona características hidrofílicas ao material, o que dificulta o seu uso em meios hidrofóbicos e orgânicos. Entretanto um processo de funcionalização das argilas, com a troca de alguns íons da estrutura acaba proporcionando uma melhor interação com esses meios. Assim, as argilas que passam a ter moléculas orgânicas intercaladas em sua estrutura, são denominadas de argilas organofílicas. Esse material vem sendo amplamente investigado para uma ampla variedade de aplicações ambientais, devido à sua boa capacidade de adsorção, com destaque para a sua efetividade na remoção de poluentes orgânicos e metais pesados (He et al., 2014; Maia et al., 2019a; Park et al., 2011).

- Quitosana

A quitosana é um dos biopolímeros naturais mais baratos e abundantes com propriedades adsortivas do mundo. Sua matéria prima principal, a quitina, é o segundo polissacarídeo mais abundante do mundo e é extraído de diversas espécies de fungos e do exoesqueleto animal. Com a desacetilação da quitina, a quitosana é produzida a partir da transformação dos grupos acetil em grupos amina, gerando um material atóxico, heterogêneo, biodegradável e de satisfatória capacidade adsortiva (Kyzas et al., 2017; Vakili et al., 2014).

O biopolímero é insolúvel em água, solventes orgânicos e soluções alcalinas devido a suas ligações de hidrogênio, e em razão destas propriedades tem grande afinidade para adsorver metais e corantes, devido aos seus grupos funcionais. Além de não ter uma boa solubilidade, sua baixa área superficial limita seu desempenho no processo de adsorção, promovendo uma tendência de estudo na investigação de tecnologias para superar suas desvantagens e aproveitar o seu potencial de interação. Devido à importância no desenvolvimento de um material adsorvente que seja de fácil remoção, diversos estudos propõem a inserção do óxido de ferro (Fe_3O_4) na estrutura da quitosana (Kyzas et al., 2017; Vakili et al., 2014; Wang et al., 2014).

- Grafeno

O grafeno é uma estrutura bidimensional que consiste em um filme em monocamada de carbonos hibridizados em sp^2, que vem se mostrando uma tecnologia promissora devido às suas propriedades. O material apresenta uma alta área específica superficial, boas propriedades eletrônicas e térmicas, além de uma capacidade alta de

modificação. Esse material vem sendo reconhecido como boa alternativa para remoção de diversos poluentes da água. Diversas vantagens em relação a outros materiais baseados em carbono são evidenciadas como sua síntese utilizar oxidantes comuns e de baixo custo e grafite, que é abundante. Por outro lado, sua estrutura lamelar proporciona uma alta área específica e uma boa capacidade de carregar outras nanopartículas para desenvolver seu potencial adsortivo (Cao e Li, 2014).

- Óxido de grafeno

O óxido de grafeno (GO) é um nanomaterial obtido via processos de oxidação incompleta do grafite visando inserir grupos funcionais, como o epóxi (C–O–C) e a hidroxila (–OH), que se aderem ao plano basal, e ácidos carboxílicos (–COOH) que se ligam aos limites. A estrutura desenvolvida nos limites do GO confere característica hidrofílica ao material, que o auxilia na sua dispersão em concentrações maiores. Entretanto, a estrutura no plano basal contribui para a hidrofobicidade da região, promovendo ao material um caráter anfifílico. Esses grupos funcionais aderidos facilitam a interação com íons metálicos e compostos orgânicos por meio de coordenações e interações eletrostáticas. O GO é considerado um dos materiais adsorventes mais promissores dentre os usuais devido à sua grande área superficial específica, característica anfifílica e alta densidade de cargas negativas, além de ser facilmente sintetizado e sua matéria prima principal (grafite) ser abundante (Alam et al., 2017; Chabot et al., 2014; Madadrang et al., 2012; Peng et al., 2017).

Apesar da grande eficiência do GO como adsorvente, diversas técnicas de funcionalização do material vêm sendo pesquisadas buscando a melhoria do seu potencial. Uma das técnicas estudadas é chamada de grafitização, onde espécies reativas com características diferentes da cadeia principal são conectadas ao plano basal, conferindo ao material uma estrutura tridimensional e melhorando a capacidade de adsorção (Figueiredo Neves et al., 2020b).

A mistura do GO com outros compostos é outra técnica de potencialização utilizada, onde o material é chamado de compósito, e que usualmente promovem outras características distintas dos seus constituintes de base.

2.6.5 Adsorventes utilizados na remoção de contaminantes emergentes da água

Ao longo dos anos, os contaminantes emergentes vêm sendo encontrado com maior frequência nas águas superficiais do mundo. A avaliação de novos materiais para remoção eficiente desse grupo de contaminantes é constantemente reportada na literatura. A Tabela 2.7 reúne o desempenho de diversos materiais adsorventes na remoção de EE2, BPA e TCS:

Tabela 2.7 – Desempenho na adsorção de contaminantes emergentes.

Material Adsorvente	**Contaminante**	**Concentração Inicial**	**Percentual de Adsorção**	**Tempo de Equilíbrio**	**Referência**
Turfa	EE2	0,1 mg L^{-1}	55 %	36 h	(Fernandes et al., 2011)
Sulfeto de Cobre	EE2	5 mg L^{-1}	89 %	3 h	(Zhang et al., 2020)
Lodo de Esgoto	EE2	5 mg L^{-1}	88 %	15 min	(Feng et al., 2010)
Argila Organofílica	BPA	100 mg L^{-1}	99 %	12 h	(Park et al., 2014)
Quitosana Comercial	BPA	0,25 mg L^{-1}	75 %	2 h	(Dehghani et al., 2016)
Biochar Ativado	BPA	7 mg L^{-1}	92 %	1,5 h	(Chang et al., 2012)
Zeólita Modificada	TCS	40 mg L^{-1}	96 %	1 h	(Lei et al., 2013)
Sílica Modificada	TCS	1 mg L^{-1}	97%	2 h	(Caon et al., 2020)
Biochar	TCS	300 µg L^{-1}	70%	24 h	(Tong et al., 2016)

Fonte: Autor, 2021.

Por meio da avaliação de alguns estudos, observa-se percentuais satisfatórios de remoção com uso de diversos materiais adsorventes, incluindo materiais carbonáceos, biomateriais e argilas. Na Tabela 2.7, nota-se também uma variação considerável no tempo de equilíbrio para cada material, que é resultado do uso de diferentes concentrações iniciais em cada estudo e intensificada pelas diferentes capacidades adsortivas intrínsecas de cada material. As capacidades de adsorção de alguns contaminantes emergentes em diferentes materiais são apresentadas na Tabela 2.8:

Tabela 2.8 – Capacidade de adsorção no equilíbrio para contaminantes emergentes.

Material Adsorvente	**Contaminante**	**Concentração Inicial**	**Capacidade de adsorção no equilíbrio**	**Referência**
Sulfeto de Cobre	EE2	1 – 9 mg L^{-1}	147 mg g^{-1}	(Zhang et al., 2020)
Poliamida Alifática	EE2	0,15 – 6 mg L^{-1}	36 mg g^{-1}	(Han et al., 2012)
Lodo de Esgoto	EE2	0,5 – 5 mg L^{-1}	2,43 mg g^{-1}	(Feng et al., 2010)
Carvão Ativado	EE2	5 – 200 µg L^{-1}	1667 µmol g^{-1}	(Hemidouche et al., 2017)
Óxido de Magnésio	EE2	10 – 15 µg L^{-1}	2 µg g^{-1}	(Rudder et al., 2004)
Argila Organofílica	BPA	5 – 500 mg L^{-1}	256 mg g^{-1}	(Park et al., 2014)
Quitosana Comercial	BPA	60 – 100 mg L^{-1}	27 mg g^{-1}	(Dehghani et al., 2016)
Óxido de Grafite	BPA	10 – 500 mg L^{-1}	17 mg g^{-1}	(Bele et al., 2016)
Carvão Ativado	BPA	5 – 200 µg L^{-1}	1521 µmol g^{-1}	(Hemidouche et al., 2017)
Carbono Magnetizado	BPA	75 – 400 mg L^{-1}	347 mg g^{-1}	(Tang et al., 2016)
Biochar	TCS	5 – 200 µg L^{-1}	518 µg g^{-1}	(Tong et al., 2016)
Carbono Magnetizado	TCS	10 – 50 mg L^{-1}	892 mg g^{-1}	(Zhu et al., 2014)

Nanotubos de Carbono	TCS	1 – 12 mg L^{-1}	166 mg g^{-1}	(Zhou et al., 2013)
Zeólita Modificada	TCS	1 – 50 mg L^{-1}	47 mg g^{-1}	(Lei et al., 2013)
Argila Modificada	TCS	2 – 10 mg L^{-1}	1750 mg g^{-1}	(Phuekphong et al., 2020)

Fonte: Autor, 2021.

A capacidade adsortiva de diversos materiais apresentaram potencial satisfatório, com destaque para argila modificada que obteve capacidade adsortiva no equilíbrio de 1750 mg g^{-1}, quando avaliado na faixa de concentração inicial de TCS entre 2 e 10 mg L^{-1}. Outro material que sua capacidade de adsorção se destacou para a remoção do BPA foi um compósito de carbono mesoporoso e partículas de ferro (Fe) preparado por Tang e colaboradores (2016). O material carbonáceo magnetizado apresentou capacidade adsortiva de 347 mg g^{-1} em avaliação com faixa de concentração entre 75 e 400 mg L^{-1}.

2.6.6 Uso de compósitos para remoção de contaminantes da água

O termo compósito se refere a um sistema material que é composto de duas ou mais fases em escala macroscópica, onde a mistura proporciona melhorias em seu desempenho mecânico e em suas propriedades adsorventes em relação a seus constituintes. As propriedades dos materiais compósitos dependem das propriedades dos seus constituintes, assim como da sua distribuição entre as fases e de sua geometria (Daniel e Ishai, 2006).

A síntese de materiais compósitos para serem utilizados em processos adsortivos mostram uma grande melhora em alguns fatores que afetam a remoção de contaminantes, incluindo aumentos da área superficial específica e número de sítios ativos, melhoria na distribuição dos poros e seu volume, assim como a facilitação da remoção do adsorvente pós processo (Tan et al., 2016).

Com a finalidade de melhorar a capacidade adsortiva e facilitar a separação da água, o GO é muitas vezes misturado com outros materiais para síntese de material compósito. A funcionalização do GO já foi investigada com diversos materiais, incluindo o ácido etilenodiamino tetra-acético (EDTA), sal de diazônio aromático, etilenodiamina, ácido sulfanílico, óxido de magnésio, quitosana, entre outros (Peng et al., 2017).

Kyzas e colaboradores (2014) investigaram o uso de compósitos de GO junto à quitosana modificada com grupamentos de ácido acrílico para a remoção, via adsorção, do fármaco dorzolamida utilizado para problemas de pressão ocular. Devido à natureza catiônica do contaminante foram incorporados grupos aniônicos na quitosana para o desenvolvimento das suas capacidades adsortivas. O estudo do equilíbrio comprovou que a promoção do material compósito melhorou a capacidade máxima de adsorção em relação ao GO separadamente, de 175 para 334 mg/g, justificada pelas suas interações mais intensas com o poluente. Foi observado um efeito positivo da temperatura na eficiência de remoção, que foi mais expressivo no material compósito.

Esmaeili e Tamjidi (2020) também estudaram a síntese de compósitos baseados no óxido de grafeno junto com nanopartículas de óxido de ferro (Fe_3O_4) e argila natural para a remoção de cromo (Cr^{VI}). O material compósito apresentou excelentes propriedades magnéticas, além de uma boa estrutura mesoporosa. Os ensaios no equilíbrio conferiram ao compósito que incluía os três materiais a melhor capacidade adsortiva, alcançando a marca de 71 mg/g para a remoção do íon.

Levando em consideração a problemática apresentada, o presente trabalho busca a proposição de um nanocompósito utilizando o GO, a argila organofílica e a quitosana magnética, que remova com eficiência a classe dos contaminante emergente, além de almejar a sua otimização. Até o presente momento não foi encontrado nenhum estudo na literatura propondo o uso dessa combinação de materiais, destacando o caráter inovador do estudo.

2.7 Avaliação do processo adsortivo

2.7.1 Cinética de adsorção e modelos cinéticos

A cinética de adsorção é a representação da taxa de remoção do adsorbato da fase fluida em relação ao tempo. A avaliação da cinética compreende diferentes processos como a transferência de massa externa, a difusão no poro e a difusão na superfície do material. A transferência de massa externa é a fase que compreende a ida das moléculas da fase fluida para a superfície externa da partícula, que é envolta por uma camada de fluido. Em sequência as moléculas são difundidas para o interior dos poros da partícula, e a etapa é denominada difusão no poro. A etapa final é quando as moléculas adsorvidas são difundidas ao longo da superfície do poro, onde a etapa é chamada de difusão na superfície (Nascimento et al., 2014). As etapas descritas estão ilustradas na Figura 2.6.

Figura 2.6 – Etapas da cinética de adsorção.

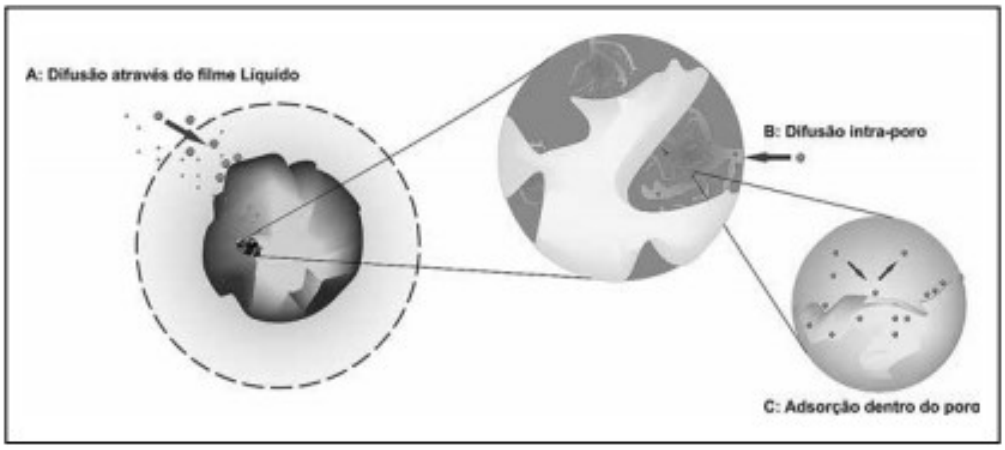

Fonte: Nascimento *et al*., 2014.

O estudo cinético de um processo de adsorção investiga os mecanismos de sorção e as etapas descritas da adsorção de certo composto. Os ensaios realizados em banho finito, não variando o volume de solução, a quantidade de soluto adsorvida pode ser calculada através da Equação 2.1:

$$q(t) = \left(C_0 - C(t)\right) * \frac{V}{m} \tag{2.1}$$

Em que:

q(t) – Quantidade de soluto adsorvido em um tempo *t* (mmol g^{-1});

t – Tempo (min);

C_0 – Concentração inicial de soluto em solução (mmol L^{-1});

C(t) – Concentração de soluto em solução em um tempo *t* (mmol L^{-1});

V – Volume de solução (L);

m – Massa de adsorvente (g).

Para a investigação do mecanismo de adsorção, os dados experimentais são avaliados a partir de modelos matemáticos que descrevem as cinéticas de adsorção.

- Modelo de pseudoprimeira ordem

O modelo proposto por Lagergren, em 1898, foi o primeiro a descrever a adsorção em sistemas líquido-sólidos com base na capacidade de adsorção do sólido, e é muito importante na descrição de sistemas em solução aquosa. O modelo cinético de pseudoprimeira ordem é apresentado na Equação 2.2:

$$\frac{\partial q(t)}{\partial t} = K_1 * \left(q_e - q(t)\right) \tag{2.2}$$

Sendo:
q(t) – Quantidade de soluto adsorvido em um tempo *t* (mmol g^{-1});
t – Tempo (min);
K_1 – Constate da taxa de adsorção de pseudoprimeira ordem (min^{-1});
q(e) – Quantidade de soluto adsorvido por massa de adsorvente no equilíbrio (mmol g^{-1}).

Aplicando na Equação 2.2 as condições de contorno levando em consideração que no tempo inicial nada foi adsorvido, foi proposta a Equação 2.3 (Lagergren, 1898):

$$q(t) = q_e * (1 - e^{-K_1 t}) \tag{2.3}$$

O modelo de pseudoprimeira ordem não ajusta com precisão os dados referentes a processos longos, onde nesses casos a determinação da constante da taxa de adsorção fica comprometida (K_1) (Ho e McKay, 1998).

- Modelo de pseudosegunda ordem

O modelo de pseudosegunda ordem leva em consideração que a etapa determinante da cinética de adsorção é a de difusão externa, assumindo que a quimissorção representa majoritariamente o processo (HO e MCKAY, 1999). O modelo cinético de pseudosegunda ordem é descrito pela Equação 2.4:

$$\frac{\partial q(t)}{\partial t} = K_2 * \left(q_e - q(t)\right)^2 \quad (2.4)$$

Em que:

q(t) – Quantidade de soluto adsorvido em um tempo t (mmol g^{-1});

t – Tempo (min);

K_2 – Constate da taxa de adsorção de pseudosegunda ordem ($g.mmol^{-1}.min^{-1}$);

q(e) – Quantidade de soluto adsorvido no equilíbrio (mmol g^{-1}).

Aplicando na Equação 4 as condições de contorno levando em consideração que no tempo inicial nada foi adsorvido, foi proposta a Equação 2.5 (Ho e McKay, 2000):

$$q(t) = \frac{K_2 {q_e}^2 t}{1 + K_2 q_e t} \quad (2.5)$$

- Modelo de difusão intrapartícula

O modelo de difusão intrapartícula considera o processo de transporte no poro ou na superfície, a etapa mais lenta e significativa, sendo descrito pela Equação 2.6 (Weber e Morris, 1963):

$$q(t) = K_i t^{\frac{1}{2}} + C \quad (2.6)$$

Em que:

q(t) – Quantidade de soluto adsorvido em um tempo *t* (mmol g^{-1});

t – Tempo (min);

K_i – Constate da taxa de difusão intrapartícula (mmol g^{-1} $min^{-0,5}$);

C – Coeficiente linear do modelo (mmol g^{-1}).

Através da análise gráfica de *q(t)* por $t^{0,5}$ é possível verificar a tendência a apresentar multilinearidade, divididas em três regiões. A primeira região representa a etapa de transferência de massa externa, compreendendo a difusão do seio do fluido até a camada limite. A etapa de difusão intrapartícula é representada pela segunda região, e é dela onde se encontra as constantes K_i e *C* referente ao modelo. Caso o modelo apresente valor de *C* igual a zero, o processo é dependente da difusão intrapartícula, sendo esta, a etapa determinante da adsorção. Entretanto quando o processo é limitado por outras

etapas além da difusão intrapartícula o coeficiente linear apresenta valor positivo, onde sua dimensão está também relacionada com a espessura da camada limite. A última região é referente ao equilíbrio e a saturação do material (Wu et al., 2009).

- Modelo de Boyd

O modelo proposto por Boyd descreve todo o processo de transferência de massa e é capaz de distinguir, através do coeficiente de difusividade efetiva do adsorbato no adsorvente (D_{ef}), se o processo é limitado pela etapa de difusão na camada externa ou de difusão intrapartícula. O seu estudo propõe que a fração de soluto adsorvido até um instante *t* (Equação 2.7), possa também ser calculada pela Equação 2.8 (Boyd et al., 1947):

$$F(t) = \frac{q(t)}{q_e} \tag{2.7}$$

$$F(t) = 1 - \frac{6}{\pi^2} \sum_{n=1}^{\infty} \frac{1}{n^2} * \exp(-n^2 Bt) \tag{2.8}$$

O parâmetro B é proposto como na Equação 2.9:

$$B = \frac{D_{ef}\pi^2}{r^2} \tag{2.9}$$

Em que:
$q(t)$ – Quantidade de soluto adsorvido em um tempo *t* (mmol g^{-1});
q_e – Quantidade de soluto adsorvido no equilíbrio (mmol g^{-1});
t – Tempo (min);
D_{ef} – Coeficiente de difusividade efetiva do adsorbato no adsorvente (m^2 min^{-1});
r – Tamanho médio da partícula (m).

A partir da técnica da transformada de Fourier e de integrações numéricas, a Equação 2.9 foi simplificada matematicamente nas Equações 2.10 e 2.11 (Reichenberg, 1953):

Se o valor de *F* for maior que 0,85:

$$Bt = -\ln\left(\frac{\pi^2(1-F)}{6}\right) \quad (2.10)$$

Se o valor de *F* for menor ou igual a 0,85:

$$Bt = 2\pi - \frac{\pi^2 F}{3} - 2\pi\sqrt{1-\frac{\pi F}{3}} \quad (2.11)$$

A partir da construção gráfica com os valores experimentais de *Bt* em relação a *t*, é possível observar a etapa controladora do processo, de forma que se os dados obtidos formarem uma linha reta passando pela origem, a difusão intrapartícula será a etapa de maior relevância. Caso a reta não passe pela origem, é um indicativo que a difusão pela camada limite até a superfície do material é a etapa controladora (Reichenberg, 1953; Viegas et al., 2014).

2.7.2 Isotermas de adsorção e modelos de equilíbrio

A adsorção é um fenômeno universal onde existe uma mobilidade das substâncias em meio aquoso que se transferem para a superfície de uma fase sólida. As isotermas de adsorção descrevem a capacidade de retenção de uma substância em um material adsorvente, sendo uma ferramenta importante para compreender a mobilidade da mesma no meio ambiente. A remoção do soluto para a fase sólida é investigada de forma que a concentração resultante da solução é comparada com a capacidade de adsorção do material adsorvente (Equação 2.12). O estudo das isotermas requer a avaliação da adsorção para diversas concentrações iniciais até a condição de equilíbrio, mantendo todas as condições físico-químicas constantes (Limousin et al., 2007).

$$q_e = \frac{V}{m} * (C_0 - C_e) \quad (2.12)$$

Em que:

q_e – Quantidade de soluto adsorvido no equilíbrio (mmol g^{-1});

V – Volume de solução (L);

m – Massa de adsorvente (g);

C_0 – Concentração inicial de soluto em solução no tempo t (mmol L^{-1});
C_e – Concentração de soluto em solução no equilíbrio (mmol L^{-1}).

O estudo do equilíbrio levanta informações sobre a distribuição de poros e termodinâmica do processo, além trazer uma compreensão sobre a favorabilidade do mesmo. A IUPAC (*International Union of Pure and Applied Chemistry*), buscando classificar os comportamentos e as particularidades das isotermas, publicou diretrizes no ano de 1985, revisadas em 2015, que estão ilustradas na Figura 2.7 (Limousin et al., 2007; Thommes et al., 2015).

Figura 2.7 – Classificação da IUPAC referente as isotermas.

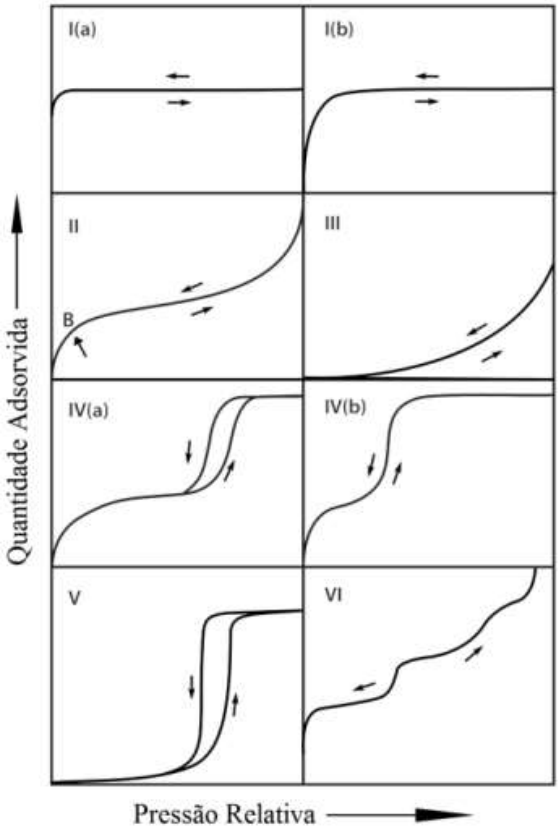

Fonte: THOMMES *et al*., 2015 (Adaptado).

As isotermas do tipo I são reversíveis e característica de materiais microporosos de baixa área superficial. A diferença entre o tipo I (a) e (b) está relacionado a distribuição de poros, de forma que na versão (b) há um indício da presença de pequenos mesoporos, além dos microporos também encontrados na versão (a). As isotermas do tipo II são reversíveis estão relacionadas a fisissorção de gases em materiais não porosos ou macroporosos. O ponto B, descrito na Figura 2.7, está relacionado ao preenchimento

completo da adsorção em monocamada, passando para a adsorção em multicamada. Uma curva até esse ponto de forma gradual contribui para a e discrição do mesmo, sendo um indicativo de uma grande quantidade adsorvida em monocamada.

Nas isotermas do tipo III a faixa de adsorção em monocamada não é identificável, as interações entre adsorbato e adsorvente são fracas, e diferentemente do tipo II, sua capacidade adsorvente é limitada. As isotermas do tipo IV estão relacionadas a materiais mesoporosos, onde seu comportamento é determinado pelas interações entre adsorbato e adsorvente e é comum apresentar um platô no final relacionado a saturação. A diferença relacionada ao tipo IV (a) e (b) se deve à presença da histerese, de forma que o tipo (a) apresenta essa diferença na dessorção.

O fenômeno da histerese está associado à largura dos poros, onde para cada condição de sistema e temperatura existe uma largura crítica de forma que se apresentar valor superior, sua curva de dessorção não coincidirá com a de adsorção, se assemelhando com o tipo IV (a).

As isotermas do tipo V são inicialmente similares as do tipo III, devido também a baixa interação entre adsorbato e adsorvente. Sob pressões relativas maiores, esses sistemas apresentam um agrupamento molecular maior, seguido do preenchimento dos poros. Esse tipo de isoterma é comum na adsorção em fase aquosa em materiais mesoporoso e microporosos hidrofóbicos.

As isotermas do tipo VI são reversíveis e representam uma adsorção multicamada em superfície não porosa uniforme. É possível observar na Figura 2.7 a formação de diversos degraus, de forma que cada um representa a formação de uma camada e sua altura indica a capacidade de adsorção relacionada a mesma (Thommes et al., 2015).

Alguns modelos matemáticos foram propostos visando descrever equações para representação do comportamento do adsorbato no processo de adsorção, ajudando na compreensão do mesmo.

- Modelo de Langmuir

O modelo matemático de Langmuir foi o primeiro proposto que representou o processo de adsorção em uma superfície e ainda é bastante utilizado para esse propósito. Esse modelo se baseia em algumas premissas para sua construção, como a consideração que a superfície adsorvente é homogênea, assim como a energia de cada sítio de adsorção,

que só acomoda uma molécula e não interage com sítios vizinhos (Langmuir, 1918). O modelo é representado pela Equação 2.13:

$$q_e = \frac{q_{max} K_L C_e}{1 + K_L C_e} \tag{2.13}$$

Em que:
q_e – Quantidade de soluto adsorvido no equilíbrio (mmol g^{-1});
q_{max} – Capacidade máxima de adsorção de Langmuir (mmol g^{-1});
K_L – Constante de equilíbrio de adsorção de Langmuir (L $mmol^{-1}$);
C_e – Concentração de soluto em solução no equilíbrio (mmol L^{-1}).

- Modelo de Freundlich

O modelo desenvolvido por Freundlich é um modelo de isotermas empírico que consegue descrever a reversibilidade e a não idealidade da adsorção. O modelo considera uma superfície heterogênea com distribuição exponencial de sítios ativos e consegue também representar a adsorção em multicamada, diferentemente do modelo de Langmuir. Apesar disso esse modelo não compreende a saturação do material adsorvente, de forma que com o aumento da concentração do sistema, a quantidade adsorvida tende ao infinito. Sistemas compostos por materiais de superfície heterogênea e espécies com grande interatividade, como carvão ativado e compostos orgânicos, são bem representados pelo modelo descrito na Equação 2.14 (Al-Ghouti e Da'ana, 2020).

$$q_e = K_F C_e^{1/n} \tag{2.14}$$

Sendo:
q_e – Quantidade de soluto adsorvido por massa de adsorvente no equilíbrio (mmol g^{-1});
K_F – Constante de equilíbrio de adsorção de Freundlich [(mmol g^{-1}) (L $mmol^{-1})^{1/n}$];
C_e – Concentração de soluto em solução no equilíbrio (mmol L^{-1});
n – Constante empírica adimensional.

Os parâmetros K_F e n, apesar do modelo ser empírico, ambos apresentam dependência com a temperatura, resultando em uma relação linear entre o $ln(K_F)$ e $1/n$ para cada temperatura. A constante n mensura a intensidade da adsorção e indicam o tipo

de adsorção envolvida. Em geral, valores de n entre 2 e 10 é considerada uma boa capacidade de adsorção, entre 1 e 2, uma capacidade moderada, em 1, demonstra a irreversibilidade do sistema, e abaixo de 1, indica um processo de adsorção desfavorável (Al-Ghouti and Da'ana, 2020; Treybal, 1980).

2.7.3 Termodinâmica do processo adsortivo

O estudo termodinâmico da adsorção é importante para o entendimento da energia do sistema, da natureza e dos mecanismos do processo. A partir da avaliação dos parâmetros termodinâmicos, como a variação da entalpia (ΔH), da entropia (ΔS) e da energia livre de Gibbs (ΔG), uma melhor compreensão da espontaneidade do sistema é facilitada, assim como da sua relação com a temperatura. A constante de Langmuir (K_L), se apresenta bons ajustes, pode ser utilizada para determinar o ΔG a partir da Equação 2.15 (Kuo et al., 2008; Milonjić, 2007a):

$$ln(K_L) = \frac{\Delta G}{RT} \tag{2.15}$$

Em que:
K_L – Constante de equilíbrio de adsorção de Langmuir (L mol^{-1});
ΔG – Energia livre de Gibbs (kJ mol^{-1});
R – Constante universal dos gases (kJ mol K^{-1});
T – Temperatura (K).

Pela combinação da Equação 2.15 com a equação de Gibbs, é possível obter uma relação capaz de deduzir, através de uma regressão linear, a entalpia e a entropia do sistema para cada temperatura. Essa relação é descrita na Equação 2.16:

$$ln(K_L) = \frac{\Delta S}{R} - \frac{\Delta H}{RT} \tag{2.16}$$

Sendo:
K_L – Constante de equilíbrio de adsorção de Langmuir (L mol^{-1});
ΔS – Variação de entropia do sistema (kJ mol^{-1} K^{-1});
ΔH – Variação de entalpia do sistema (kJ mol^{-1});

R – Constante universal dos gases (kJ mol K^{-1});
T – Temperatura (K);

Os valores de ΔG evidenciam, a favorabilidade termodinâmica, de forma que quanto mais negativo for o seu valor, mais espontâneo será o processo, implicando em um aumento da capacidade de adsorção do material. A variação da entalpia com a temperatura confirma a natureza do processo, se é endotérmico ou exotérmico. Em geral, na fisissorção os valores de ΔG são inferiores, estando por volta de -20 e 0 kJ mol^{-1}, enquanto na quimissorção entre -80 e -400 kJ mol^{-1}. A magnitude do parâmetro de entalpia do sistema, que está relacionado à força das ligações, também é um indicativo do mecanismo de adsorção envolvido, de forma que valores de ΔH menores que 84 kJ mol^{-1} indicam ligações relacionadas à fisissorção, enquanto quando entre 84 e 420 kJ mol^{-1}, à quimissorção (Kuo et al., 2008).

2.7.4 Avaliação dos descritores químicos moleculares pela Teoria da Densidade Funcional (DFT)

A DFT colabora com uma ampla base teórica para a predição dos descritores químicos moleculares, como dureza química, eletrofilicidade e potencial químico, e agrega para a compreensão da reatividade química do sistema em um nível molecular. Os descritores químicos moleculares são utilizados em diversas áreas de pesquisa, como na área farmacêutica, na química agrícola, na corrosão, e inclusive na adsorção, que proporciona um melhor entendimento da reatividade e da estrutura eletrônica do sistema (Honório e Silva, 2003; Nayara et al., 2018; Regti et al., 2016; Rotaru et al., 2014).

O estudo proporciona a determinação da energia do orbital molecular ocupado mais energético (HOMO) e do orbital molecular desocupado de menor energia (LUMO), que permite um melhor entendimento das transferências de cargas em um nível molecular. A energia associada ao orbital HOMO está relacionada com a habilidade de doar elétrons em nível molecular, enquanto o LUMO, com a habilidade de aceitar elétrons. A diferença de energia entre HOMO e LUMO é um indicativo de estabilidade molecular, de forma que *gaps* de energia maiores corrobora com moléculas mais estáveis (Andrade et al., 2020; Nayara et al., 2018).

Os descritores químicos que são comumente avaliados pela teoria DFT são a dureza química global (η), o potencial químico (μ) e o índice de eletrofilicidade (ω), que

em conjunto esclarece sobre a reatividade química molecular. O descritor η está relacionado com a resistência da molécula em redistribuir seus elétrons, já o descritor μ está ligado a força que um elétron tem quando conectado em um átomo, adicionalmente, o valor descritor ω determina a habilidade da molécula em aceitar elétrons. Os valores do gap de energia e os descritores químicos moleculares estão abordados nas Equações 2.17, 2.18, 2.19 e 2.20 (Almeida et al., 2021a; Nayara et al., 2018):

$$GAP_E = E_H - E_L \tag{2.17}$$

$$\eta = \frac{E_L - E_H}{2} \tag{2.18}$$

$$\mu = \frac{-(E_H + E_L)}{2} \tag{2.19}$$

$$\omega = \frac{\mu^2}{2\eta} \tag{2.20}$$

2.8 Contribuições científicas e impacto do trabalho

O contexto apresentado mostra a grande importância no estudo de remoção de contaminantes emergentes de matrizes aquáticas. A quantidade de novos contaminantes emergentes, o aumento de suas concentrações no meio ambiente e a falta de compreensão de todos os seus danos no ecossistema torna essa problemática uma preocupação global e atual. As tecnologias convencionais não removem completamente a maioria dos contaminantes emergentes, alguns apresentam alta persistência e por isso surge a necessidade do desenvolvimento de tecnologias que removam com eficiência essa classe de contaminantes (Antonelli et al., 2020b; Montagner et al., 2017; Resende et al., 2020; Sauvé e Desrosiers, 2014a).

Diversas são as tecnologias avaliadas para o desenvolvimento procedimento do tratamento de águas, esgotos e efluentes, entretanto, a adsorção se destaca pelo baixo custo e facilidade de operação. Outro fator positivo da adsorção é a diversidade de materiais e de propriedades que podem ser avaliadas no processo. O desenvolvimento de materiais compósitos surge buscando obter misturas com propriedades melhores e distintas dos seus constituintes base (Dąbrowski et al., 2005).

O óxido de grafeno vem sendo cada vez mais reportado na literatura para remoção de contaminantes via adsorção devido a sua grande área superficial e capacidade promover interações eletrostáticas. Alguns trabalhos da literatura aplicam compósitos com esse material buscando melhoria nas propriedades mecânicas e adsortivas do adsorvente (Alam et al., 2017; Chabot et al., 2014; Madadrang et al., 2012; Peng et al., 2017).

A quitosana e a argila organofílica são materiais, apresentados previamente, que são amplamente aplicados como adsorventes, e já foram utilizados no grupo de pesquisa com a finalidade de remover contaminantes emergentes (Andrade et al., 2020; Antonelli et al., 2020a; Almeida et al., 2022; Souza et al., 2019).

Neste trabalho sintetizou-se nanocompósitos baseados em óxido de grafeno, quitosana magnética e argila organofílica para avaliação da remoção de contaminantes emergentes presentes em fase aquosa. Até o presente, não foram encontrados estudos na literatura que utilizassem os compósitos propostos por este trabalho.

CAPÍTULO 3. SÍNTESE DE NANOCOMPÓSITO MAGNÉTICO BASEADO E APLICAÇÃO NA REMOÇÃO DE CONTAMINANTES EMERGENTES

Synthesis of a novel magnetic composite based on graphene oxide, chitosan and organoclay and its application in the removal of bisphenol A, 17α-ethinylestradiol and triclosan[1]

Arthur da Silva Vasconcelos de Almeida[a], Tauany de Figueiredo Neves[b], Meuris Gurgel Carlos da Silva[a], Patricia Prediger[b], Melissa Gurgel Adeodato Vieira[a]

[a]Chemical Engineering Faculty, University of Campinas, 13083-852, Campinas, São Paulo, Brazil.
[b]School of Technology, University of Campinas, 13484-332, Limeira, São Paulo, Brazil.

ABSTRACT

A new nanocomposite was synthesized from graphene oxide, magnetic chitosan and organoclay (GO/mCS/OC). Its application as an adsorbent was investigated for the removal of emerging contaminants such as bisphenol A (BPA), 17α-ethinylestradiol (EE2) and triclosan (TCS). These contaminants, even at low concentrations, cause damage to aquatic biota and have been attracting the attention of researchers around the world. The synthesis of nanocomposite comprised the preparation of GO through hummers method, followed by the aggregation of magnetic chitosan and organoclay particles. These adsorbent materials were characterized using FTIR, XRD, SEM, EDS, TGA, VSM and zeta potential. Furthermore, their adsorptive capacities were evaluated in batch system. The synthesized nanocomposite exhibited satisfactory performance and similar to that of the precursor organophilic clay under the conditions evaluated. TCS was easier to be removed, followed by EE2 and BPA, with removal percentages of about 98, 72 and 58% and adsorptive capacities of about 40, 30 and 20 mg g^{-1}, respectively, when using the nanocomposite. In order to unveil the chemical reactivity of the approached contaminants at a molecular level, density functional theory (DFT) was evaluated by calculating molecular chemical descriptors and evaluating the electrostatic potential maps. The chemical reactivity corroborates the affinity assays, showing a more effective

[1] Manuscript published in *Journal of Environmental Chemical Engineering* 10 (2022) 107071. DOI: https://doi.org/10.1016/j.jece.2021.107071. Reprinted with permission from *Journal of Environmental Chemical Engineering*. Copyright 2022 (Anexo A).

adsorption of the most reactive molecule, which was the TCS. The synthesized nanocomposite performed well in removing emerging contaminants and proved to be a good alternative in the treatment of contaminated effluents.

Key Words: Graphene oxide; Chitosan; Organoclay; Emerging contaminants; Adsorption; Density functional theory.

1. INTRODUCTION

Emerging contaminants are being detected more and more frequently in different aquatic matrices around the world. The lack of regulation that follows the dynamics of contaminants emerging from effluents contributes to the deterioration of the ecosystem (Sauvé and Desrosiers, 2014a). Despite being found in low concentrations, emerging contaminants are related to serious damage to the ecosystem and human health (Sauvé and Desrosiers, 2014a; Sophia A. and Lima, 2018). This class of contaminants includes hormones, plasticizers, pharmaceuticals, illicit drugs, nanomaterials, personal care products, pesticides, among others that end up polluting aquatic matrices (Sophia A. and Lima, 2018; Wells et al., 2009). Examples of emerging contaminants are bisphenol A (BPA), 17α-ethynylestradiol (EE2) and triclosan (TCS) which, with the increase in anthropic and industrial activity, have been found more easily.

EE2 is a synthetic hormone derived from estradiol, found in most oral contraceptives and used in the treatment of osteoporosis, menopause and prostate cancer (Aris et al., 2014). Studies relate water contamination with EE2 to anatomical feminization of aquatic biota, delayed sexual maturity and endocrine disruption (Bhandari et al., 2015). TCS is a synthetic antimicrobial widely used in personal care products such as shampoos, soaps, deodorants, as well as in plastics and fabrics. (Ramaswamy et al., 2011). Its widespread use has raised concerns due to its relationship with the development of cancer and impact on muscle contraction (Cherednichenko et al., 2012; Dinwiddie et al., 2014). BPA, like EE2, is considered an endocrine disruptor, and its use is related to the industrial production of plastic, epoxy resins and flame retardant materials (Guerra et al., 2015). The exposure of this compound to living beings is associated with cardiovascular diseases, brain abnormalities, thyroid dysfunction and infertility, contributing to the ban on specific products such as baby bottles (Amjad et al., 2020; Erler and Novak, 2010; Liu et al., 2009).

The main sources of contamination by emerging contaminants are residential, hospital, agricultural and industrial effluents, which are not completely removed by conventional treatments (Parida et al., 2021b; Sivaranjanee and Kumar, 2021). The inefficiency of wastewater treatment is the main aggravating factor of the issue, causing these different emerging pollutants to occur simultaneously in the environment (Langdon et al., 2011; Lin et al., 2020; Wang et al., 2011; Williams et al., 2019). Disposal without treatment or partial treatment is a major risk to aquatic ecosystem, due to the impact of these contaminants even at low concentrations (in the order of micrograms and nanograms per liter) (Parida et al., 2021b). A wide variability in removal of emerging contaminants occurs in conventional wastewater treatment due to the large difference in chemical properties of this class of contaminant (Bolong et al., 2009; Rivera-utrilla et al., 2013). The steps of disinfection by chlorinated agents or ozonization are directly affected by the presence of organic compounds, which can result in more harmful and persistent metabolites than their precursors (*Transformation Products of Emerging Contaminants in the Environment*, 2014).

Due to the tendency of increasing anthropic and industrial activity, in addition to the inefficiency of conventional treatments, the interest in the development of efficient processes and effective materials in the removal of emerging contaminants is evident. Advanced oxidation processes (AOPs) (Starling et al., 2019; Yap et al., 2019b), bioremediation (Delgado-Moreno et al., 2019; Rempel et al., 2021), membrane (Bhattacharya et al., 2021; M. Racar et al., 2020) and adsorption (Cheng et al., 2021; Rathi and Kumar, 2021) are some of the alternatives evaluated to solve this question. Among these techniques, adsorption stands out for its simple operation, high efficiency and low cost, as well as being able to use different adsorbent materials with high affinity and selectivity for different adsorbates of economic and environmental interest (Cheng et al., 2021; Rathi and Kumar, 2021).

The great diversity of materials provides different adsorptive properties and contaminant removal mechanisms, which is another advantage of the process (Cheng et al., 2021). The removal performance of many emerging contaminants has been evaluated on numerous materials, such as biochars (Kozyatnyk et al., 2021; Wurzer and Mašek, 2021), clays (Antonelli et al., 2020b; Cristina do Nascimento et al., 2021), zeolites (Goyal et al., 2018; Liu and Carr, 2013), bioadsorbents (Cardoso and Vitali, 2021; Xiong et al., 2021), seeking to increase the efficiency of the adsorptive process from the understanding

of the nature of the process, the mechanisms involved and the interactions between adsorbate and adsorbent.

Nanoadsorbents are nanoscale adsorbents, which have several advantages such as their large surface area and a concentration of atoms of high chemical activity on their surface. (Kyzas and Matis, 2015). Graphene oxide (GO) is a nanoadsorbent with a high density of negative charges structured in a monolayer (Guerra et al., 2021). The presence of hydroxyl, epoxy groups and double bonds in its basal plane, in addition to carboxyl groups in its edges, promote an amphiphilic characteristic, and also good interactions with metallic ions and organic compounds (Chen et al., 2014; Guerra et al., 2021; Song et al., 2021). Organoclays (OC) are mineral clays that have undergone a treatment to insert organic chains on their surface in order to intensify their interactions with organic environments (Zhuang et al., 2019). Chitosan (CS) is a natural, low cost, biodegradable polysaccharide, obtained mainly from chitin and which has good adsorption capacity due to the abundance of hydroxyl (OH) and amine (NH_2) groups (Jawad et al., 2020a; Zhou et al., 2019). Fe_3O_4 magnetic nanoparticles are usually mixed with CS, generating materials with magnetic properties (mCS), thus facilitating the separation process after adsorption. (Jawad et al., 2020a; Zhou et al., 2019). The synthesis of nanocomposites comprises mixing techniques between different compounds with no chemical reaction between them, aiming to increase the adsorptive capacity and the development of unique characteristics in relation to their constituents (Agboola et al., 2021; Leudjo Taka et al., 2021).

The insertion of chitosan in the nanocomposite considerably increases the number of functional groups, and contributes with cationic and hydrophilic characteristics, increasing heterogeneity and reactivity (Karimi-Maleh et al., 2021). The mixture of chitosan with clay materials is also related to the increase in the basal plane and interlayers, favoring a better adsorption capacity (Karimi-Maleh et al., 2021). The long chains present in organoclays cause an increase in interlayers and contribute to more intense hydrophobic interactions with organic contaminants (Shen and Gao, 2019). Despite having several advantages, chitosan does not have a large surface area, unlike GO, which contributes to the increase of this characteristic due to its planar sheet-like morphology (Karimi-Maleh et al., 2021; Thakur and Kandasubramanian, 2019).

In this work a new magnetic nanocomposite (GO/mCS/OC) was prepared, and its performance was compared with OC in the removal of different emerging contaminants, such as BPA, EE2 and TCS. The materials were characterized using several analytical

techniques, such as Fourier-transform infrared spectroscopy (FTIR), X-ray diffraction (XRD), zeta potential, scanning electron microscopy (SEM), energy dispersive spectroscopy (EDS), thermogravimetry (TGA) and vibrating sample magnetometer (VSM). Calculations based on the density functional theory (DFT) were used to obtain HOMO and LUMO energy values of the investigated emerging contaminants. The electronic density and global chemical descriptors were also evaluated, such as global chemical hardness (η), chemical potential (μ) and electrophilicity index (ω), seeking to better understand the interactions on a molecular scale. As far as is known, there is no study in the literature reporting the use of GO, mCS and OC nanocomposites in the removal of these contaminants.

2. METHODOLOGY

2.1 Materials

The emerging contaminants investigated were BPA, EE2 and TCS, acquired through Sigma-Aldrich. Among the materials used in the synthesis of adsorbents are mineral graphite and Spectrogel® – Type C organoclay, supplied by the companies Nacional Grafite LTDA and Spectrochem®, in addition to chitosan and iron chlorides (II) and (III), from the companies Sigma-Aldrich, Dynamics and Vetec, respectively. Spectrogel® – Type C is a commercial Brazilian bentonite clay modified with dialkyl dimethylammonium (DMA) cations seeking to improve its organophilic properties. Among the chemical reagents used are potassium permanganate ($KMnO_4$), sodium nitrate ($NaNO_3$), ammonium hydroxide (NH_4OH), sodium hydroxide (NaOH), acetic acid and paraffin oil purchased from Synth; potassium persulfate (K_2SO_4), glutaraldehyde (5%), N,N'-dicyclohexylcarbodiimide (DCC), N,N-dimethylformamide (DMF, 99.8%), 4-(dimethylamino)pyridine (DMAP, 98%) and phosphorus pentoxide (P_2O_5, 99%) purchased from Sigma-Aldrich; hydrogen peroxide, ethanol (C_2H_5OH, 99%) and petroleum ether purchased from Vetec; hydrochloric acid (HCl) and concentrated sulfuric acid (H_2SO_4, 98%) were obtained from CRQ Química.

2.2 Synthesis of GO/mCS/OC nanocomposite

The synthesis of the nanocomposite started with preparation of GO through modified Hummers method (Hummers and Offeman, 1958). This process was initiated by pre-oxidation of graphite. In the process, under ambient air, ice bath and magnetic

stirring, 120 mL of H_2SO_4, 10 g of K_2SO_4 and 10 g of P_2O_5 were added to 20 g of mineral graphite. After reaching room temperature, the mixture was heated to 80 °C for 6 h. Then, ultrapure water was added to the system and the mixture was filtered on Buchner funnel until it reached neutral pH. Pre-oxidized graphite was collected and added to 500 mL of H_2SO_4, under ambient air, magnetic stirring and ice bath. Subsequently, 10 g of $NaNO_3$ and 60 g of $KMnO_4$ were slowly added to the system, keeping the temperature strictly below 20 °C. The reaction product was kept under mechanical stirring at 0 °C for 1 h, and then kept under vigorous stirring for another 10 days at room temperature. The system was again cooled in an ice bath, adding 2 L of ultrapure water and 100 mL of H_2O_2 solution (3%). The system was then heated to 100 °C and kept in reaction for 30 min. The solution at room temperature was centrifuged for 5 minutes under agitation at 8000 rpm. At the end of each process cycle, the supernatant was discarded and solution was added to wash the material. For this purpose, 10 L of H_2SO_4 (3%) and H_2O_2 (0.5%) solutions, 5 L of HCl (10%) solution and ultrapure water were used until pH 5 was reached. The GO obtained was placed in dialysis bags and immersed in ultrapure water, aiming to remove the salts present. The GO was placed in amber glass bottles and submitted to an ultrasonic bath for 1h.

The synthesis of the new nanocomposite (GO/mCS/OC) began with the generation of magnetic iron nanoparticles. Based on the methodology proposed by Silva *et* al. (Silva et al., 2013), 200 mL of ultrapure water, 1.5 g of $FeCl_2$, 5.9 g of $FeCl_3$, 1 mL of oleic acid and NH_4OH (27%) were added dropwise into a flask, until the mixture reached the pH value 11. Subsequently, the mixture was heated at 85 °C for 30 minutes, filtered on a Buchner funnel and washed with ultrapure water. Magnetic iron nanoparticles were obtained, removed by a high vacuum pump and stored in a glass flask at room temperature.

The mCS synthesis was based on the methodology proposed by Wang *et* al. (Wang et al., 2016). In a reaction flask, 3 g of commercial chitosan and 300 mL of acetic acid solution (2%) were added and the system was kept under vigorous agitation for 2 h. Then, 6 g of magnetic nanoparticles were added and the mixture was subjected to an ultrasonic bath and mechanical agitation. In the homogeneous mixture obtained, 200 mL of paraffin oil, 30 mL of glutaraldehyde and 300 mL of NaOH solution (1M) was slowly added and the system was kept under mechanical agitation for 1 hour. The product was washed in a Buchner funnel with petroleum ether, ethanol and ultrapure water, and between each

solvent, the system was subjected to an ultrasonic bath for 5 min. After reaching neutral pH, the mCS was dried and stored in a glass flask at room temperature.

Aiming at the incorporation of mCS in the GO structure and based on the study proposed by Maleki and Paydar (Maleki and Paydar, 2015), 2.5 g of GO, 5.8 g of mCS and 584 mL of dry N,N-dimethylformamide (DMF) were added in a flamed flask. The system was kept under nitrogen atmosphere, strong magnetic stirring and submitted to an ultrasonic bath. Subsequently, 22.5 g of N,N'-dicyclohexylcarbodiimide (DCC) and 15 g of 4-(dimethylamino)pyridine (DMAP) were added and the system was kept under magnetic stirring for 48 h in a nitrogen atmosphere. The resulting material was centrifuged and washed in a Buchner funnel with acetic acid solution (2%) to remove the mCS that did not adhere to the surface of the GO. The product was subjected to ultrasonic bath and then washed with methanol, acetone and ultrapure water. GO/mCS was dispersed in ultrapure water, stored in a glass flask and kept under cooling.

The formation of nanocomposites was obtained from the addition of the organoclay Spectrogel® – Type C (OC) in the suspension of the synthesized GO/mCS under vigorous agitation. The OC, before being added, was classified to obtain particles with a particle size between 200-400 mesh. The mass of OC added was proportional to the mass of GO/mCS in solution, resulting in a nanocomposite composed of 50% of each base material. The GO/mCS/OC synthesis was summarized in flowcharts in the Supplementary Material (see Figures S1, S2 and S3).

2.3 Characterization of OC and GO/mCS/OC

The surface functional groups were identified by FTIR spectroscopy using the KBr tablet method and the Nicolet 6700 equipment (Thermo Scientific, Madison, USA) with an amplitude between 500 and 4000 cm^{-1}. The crystal structure of the materials was evaluated by X-ray diffraction (XRD) using the X'Pert-MPD equipment (Philips Analytical X Ray, Almelo, Netherlands), with a voltage of 40kV, current of 40 mA and copper radiation with amplitude of 1.54 Å. The surface morphology of the materials and the elements present were investigated by SEM with an EDS, model VEGA 3 (Tescan, Brun, Czech Republic) and XFlash 630m (Bruker, Massachusetts, USA). Surface electrical charges and the influence of pH on the adsorbent were evaluated by zeta potential analysis. The procedure was evaluated in the presence of the emerging contaminants studied, in triplicate, at four different pH values (4, 6, 8 and 10), with an

adsorbent concentration of 0.01 mg L^{-1}. The analysis was performed on the Zetasizer Nano ZS ZEN3600 instrument (Malvern Panalytical, Malvern, UK). The thermal stability of the materials was verified by TGA using the DTG-60H equipment (Shimadzu, Kyoto, Japan). The analysis was performed with a heating rate of 10 °C min^{-1}, from 25 to 1000 °C, in an inert nitrogen atmosphere. The magnetic capacity of the nanocomposite was determined using a vibrating sample magnetometer (VSM) model 7400 (Lake Shore, Westerville, USA) at room temperature.

2.4 Adsorptive affinity assays

The removal percentage and the adsorption capacity of the adsorbent materials in relation to BPA, EE2 and TCS were evaluated through batch tests. The experiments were carried out in triplicate, with stirring at 200 rpm, temperature at 30 °C and initial adsorbate concentration of 0.03 mmol L^{-1} (6.8, 8.9 and 8.7 mg L^{-1}, respectively). The samples were stirred for 24 hours and then most of GO/mCS/OC was removed by magnetic separation. Both materials were centrifuged under agitation at 6000 rpm for 15 min and complete removal of particulate material was confirmed by applying syringe filters (0.45 μm, PTFE) to the supernatant. Concentrations were measured using a high-performance liquid chromatography (HPLC) system (Shimadzu, Kyoto, Japan) coupled with a CTO-10ASVP heating oven, SPD-10AV UV-Vis detector, LC-10AD gradient pump and CBM-10A connection module. The system also contained a 25 μL manual injector, a C18 column (5 μ, 150 x 4.6 mm) (Phenomenex, Torrance, USA) and the data was processed using LC Solution Software. The methods for BPA and EE2 were validated using acetonitrile and deionized water (50:50), column flow rate of 1.5 mL min^{-1}, UV detector at 230 nm and temperature at 30 °C. The method validated for TCS used methanol and deionized water (80:20), column flow rate of 1.2 mL min^{-1} and UV detector at 220 nm. More information regarding method validation is described in the Supplementary Material (see Table 3.S1).

The adsorption capacity (q_t) (mg g^{-1}) and removal percentage (R_t) at each time t were calculated from Equations 3.1 and 3.2:

$$q_t = \frac{V}{m}\,(C_i - C_t) \tag{3.1}$$

$$R_t\,(\%) = \frac{100\,(C_i - C_t)}{C_i} \tag{3.2}$$

Thus, V (L) represents the solution volume, m (mg) the mass of nanoadsorbent, C_i and C_t (mg L^{-1}) the initial concentration and at a time interval t.

2.5 Study of molecular chemical descriptors

Density Functional Theory (DFT) was used as the basis for the study of geometric and electronic properties of the studied microcontaminants. DFT calculations helped to determine the electrostatic potential and chemical descriptors on a molecular scale. Among the molecular chemical descriptors discussed are the highest occupied molecular orbital (HOMO, E_H), the lowest unoccupied molecular orbital (LUMO, E_L) and the energy gap (E_L - E_H). Through these parameters it is possible to evaluate reactivity descriptors such as chemical potential (μ), global chemical hardness (η) and global electrophilicity index (ω), using Equations 3.3 to 3.5 (Souza et al., 2018):

$$\mu = \frac{-(E_H + E_L)}{2} \quad (3.3)$$

$$\eta = \frac{(-E_H + E_L)}{2} \quad (3.4)$$

$$\omega = \frac{\mu^2}{2\eta} \quad (3.5)$$

Avogadro 1.1.0 and GaussView 6 softwares were used to simulate the three-dimensional geometry and obtain the molecular electrostatic potential of microcontaminants BPA, EE2 and TCS (Frisch et al., 2016; Hanwell et al., 2012). Gaussian software was used to perform the DFT calculations and model the lower energy and higher stability conformations (Frisch et al., 2009). The implemented modeling used a hybrid of Beck's three parameters and the Lee-Yang-Parr functional correlation (B3LYP), recommended for intermediate size molecules (Becke, 1993; Frisch et al., 1984). Two variations of the 6-31G base were tested seeking conformation of molecules with lower energy (Becke, 1993; Frisch et al., 1984).

3. RESULTS

3.1 Characterization of OC and GO/mCS/OC

The FTIR spectra of OC and GO/mCS/OC are shown in Figure 3.1. The spectrum of organophilic clay showed an expressive band close to 3627 cm^{-1} which is related to Al-rich montmorillonites, as well as an indicative of –OH elongations of the structural water

(Andrade et al., 2020; Maia et al., 2019b). The bands found at 3433 and 1634 cm^{-1} suggest H–O–H elongations that refer to interlayer water (Maia et al., 2019b). The prominent peaks near 2921 and 2850 cm^{-1} are related to asymmetrical and symmetrical C–H elongations, respectively, which represent the alkylammonium cations present in the clay, which infer the organophilic profile of the materials (Andrade et al., 2020; Maia et al., 2019b). The N–H and C–H bonds can represent ammonia groups and are indicated in bands close to 1634 and 1469 cm^{-1} (Maia et al., 2019b). The presence of Si–O stretch is indicated by peak at 1044 cm^{-1} and the range between 600 and 400 cm^{-1}, which also represents the Al–O stretch (Andrade et al., 2020; Maia et al., 2019b). The prominent peaks between 950 and 800 cm^{-1} represent –OH stretches, which are characteristic of 2:1 minerals (Andrade et al., 2020; Maia et al., 2019b).

Some bands that were present in the OC spectrum remained in evidence in GO/mCS/OC, as well as others that emerged or intensified, corroborating the synthesis of the nanocomposite. The –NH and –OH stretches were identified by peaks 3620 and 3371 cm^{-1} representing characteristic groups of chitosan and GO (Erim et al., 2021; Jawad et al., 2020b). The increase in intensity and the broadening of the peak at 3371 cm^{-1} may represent a greater presence of –OH stretches on the surface with the synthesis of the material. The presence of functional groups amide 1 and amide 2 of chitosan were observed by bands 1642 and 1567 cm^{-1}, representing C=O stretch, which is also present on the surface of GO, and the N–H stretch, respectively. (Erim et al., 2021; Olewnik-Kruszkowska et al., 2019). The bands that appeared at 1377 and 1307 cm^{-1} may represent the C–N bonds, which constitute chitosan surface (Erim et al., 2021; Jawad et al., 2020b). The band close to 521 cm^{-1} is also related to Fe–O bonds that arise with magnetization of chitosan (Jawad et al., 2020b; Malwal and Gopinath, 2017).

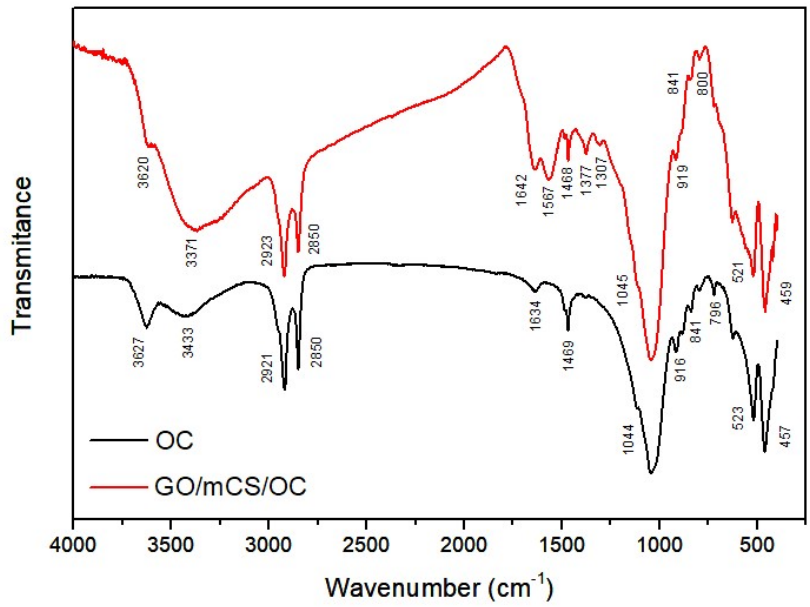

Figure 3.1 – OC and GO/mCS/OC FTIR spectra.

The zeta potential versus pH describes the behavior of the surface electrical charge of OC and GO/mCS/OC when dispersed in water or in solutions contaminated with BPA, EE2 and TCS (Figure 3.2).

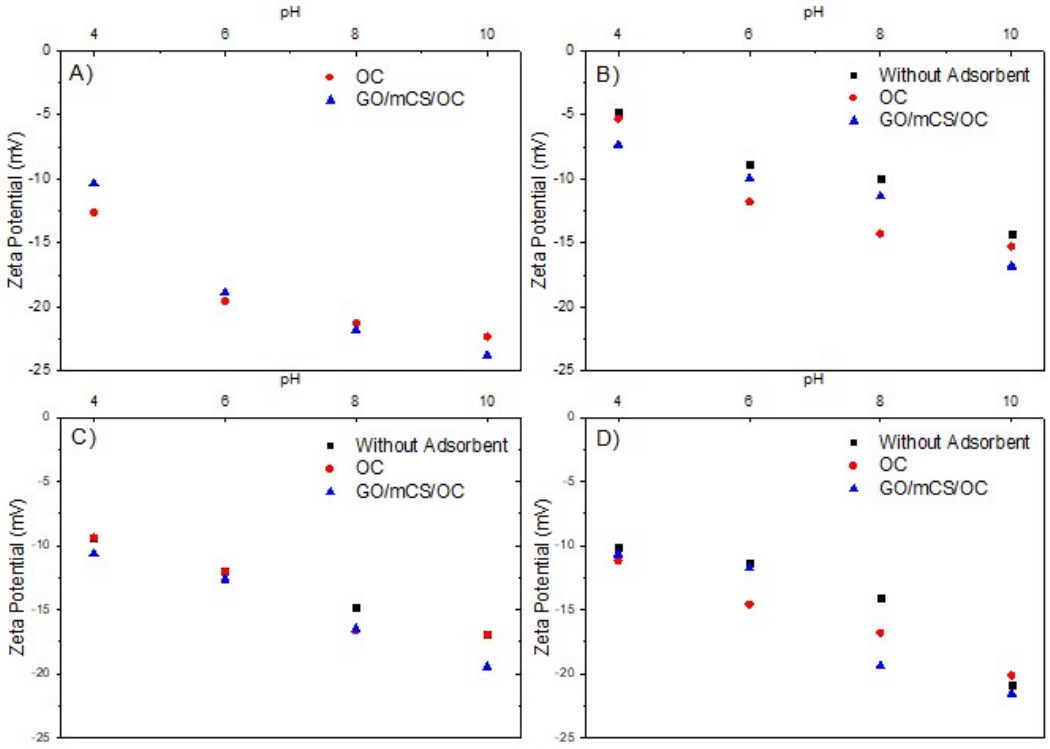

Figure 3.2 – Zeta Potential of OC and GO/mCS/OC dispersed in water (A), BPA solution (B), EE2 solution (C) and TCS solution (D).

Both adsorbents showed electronegative surfaces in the evaluated pH range (4 – 10), as well as a tendency for an increase in electronegativity with an increase in pH. The materials did not show a zero-charge point (pH_{ZPC}) in the pH range evaluated for any solution. The ASTM standard for stability of colloidal suspensions says that a zeta potential between 30 and 40 mV, whether positive or negative, implies stable dispersions due to electrostatic repulsion (ASTM D4187-92) (ASTM, 1985). Taking this parameter into account, the dispersions do not reach stability in the evaluated pH range but tend to do in a very alkaline medium. The decrease in electronegativity and stability in nanocomposite under acidic conditions can be explained by the presence of amine groups on the surface of magnetic chitosan and carboxyl and hydroxyl groups on the surface of GO. These groups tend to protonate under acidic conditions, justifying the decrease in electronegativity (Cheminski et al., 2019; Loganathan et al., 2013).

Comparison of zeta potential between the different solutions shows that the surface of the adsorbents is a little less negatively charged when in contact with the contaminants, indicating the neutralization of part of the surface charges with the adsorbed contaminants. It is possible to observe in Figure 3.2b that GO/mCS/OC was less electronegative than OC in the presence of BPA, indicating better electrostatic interactions between adsorbate and nanocomposite at pH between 4 and 6. The zeta potential of EE2 solutions (Figure 3.2c) did not show relevant differences between adsorbents, indicating similar interactions between them and this contaminant. Comparing the behavior of the surface charges of adsorbents in contact with BPA and EE2, it is possible to observe that the electrostatic interactions with BPA are more evident, especially in relation to GO/mCS/OC. At pH 10, OC interacted better with both BPA and EE2. The speciation of adsorbates (Figure 3.3) showed a tendency of deprotonation of its phenolic groups, which disfavor electrostatic interactions with the negative surfaces of the materials, however it favors complexation of these groups with metals cations, mainly of OC (Forder e Jones, 2015). These metals are more present on the clay surface and may justify it better interactions with adsorbates at higher pH due to the complexations (Ahmat et al., 2019; Forder e Jones, 2015). TCS speciation showed that its deprotonation occurs at a lower pH (7.7) than the others compounds evaluated, implying a more intense interaction with OC already at pH 8. The electrostatic interactions between TCS and GO/mCS/OC proved to be more intense up to pH 6, but after the deprotonation of the phenolic groups, OC interacted better as occurred with BPA and EE2 (Figure 3.2d).

Adsorbate speciation (Figure 3.3) elucidates the formation of cations or anions in contaminants as a function of pH value. Pollutant charges together with adsorbate charges can favor or hinder adsorption process due to electrostatic attraction or repulsion. The negative surface charge of both materials does not favor electrostatic interactions with anionic molecules. It is possible to observe that BPA, EE2 and TCS, from pH 9.6, 10.4 and 7.7, their anionic versions start to represent most of the system due to hydrogen loss. Electrostatic interactions are harmed with the increase of the solution pH due to the surface of the adsorbents becoming more electronegative, as observed in the zeta potential analysis, and the anion formation tendency of the molecules. BPA and TCS showed, from acidic to neutral pH range, a tendency to remain without ionizing. The EE2 in extremely acidic conditions (0 – 2) can protonate and present a cationic profile, however, with the decrease of the pH value, the negative charges of the adsorbents also tend to decrease according to the zeta potential analysis.

The speciation of adsorbates shows that BPA and EE2 are available in their neutral condition in almost every pH range evaluated in the zeta potential analysis, while TCS at pH 8 and 10 show a considerable amount of their anionic condition. In the evaluated pH range, because a large part of the molecules are in neutral form, pi – pi interactions can play an important role in the adsorption mechanism, corroborating with aromatic ‘networks of the adsorbates and the adsorbent (Martins et al., 2021).

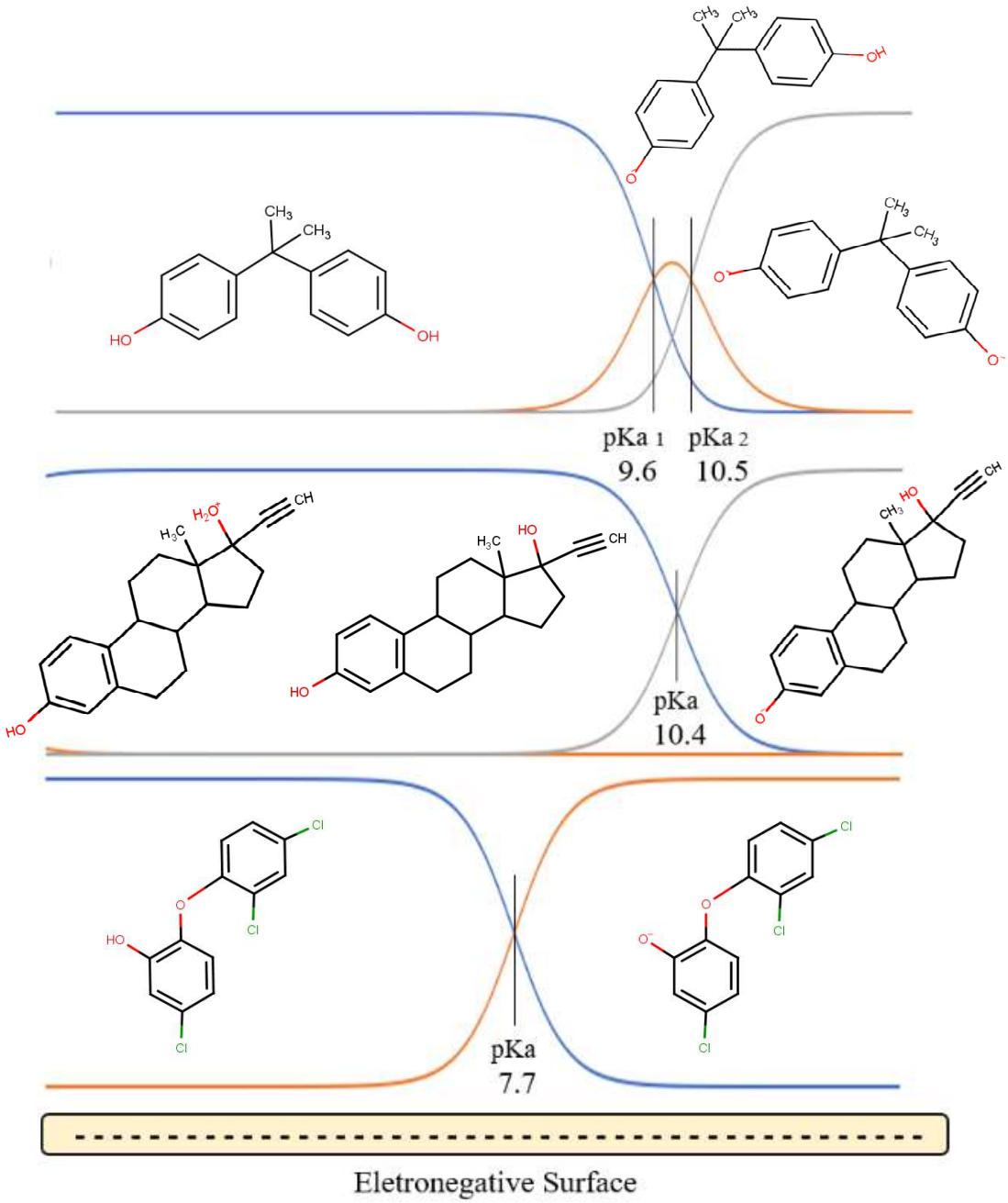

Figure 3.3 – Speciation of BPA, EE2 and TCS as a function of pH.

The X-ray patterns of GO, OC and GO/mCS/OC are illustrated in Figure 3.4. The GO is represented by a single peak at 11.24°, which is characteristic of the material and indicates the presence of hydroxyl, epoxy and carboxyl groups between layers (Cheminski et al., 2019; Prediger et al., 2018). The peak corresponding to (001) plane indicated an interlayer space of 0.79 nm, according to Bragg's law (Almeida et al., 2021b), being related to the repulsion of the mentioned functional groups (Cheminski et al., 2019). The OC pattern presented a profile similar to works reported in literature for

the same Spectrogel Clay – Type C (De Andrade et al., 2020; Maia et al., 2019c; Speridião et al., 2014). The prominent peaks were found at 6.9, 9.5, 19.8, 26.6, 28, 31.7, 34.8, 45.5, 56.5, 62.7 and 73.2°, and through its (001) plane an interlayer distance of 1.27 nm was observed, this value being close to expected for bentonite clays (1.5 nm) (De Andrade et al., 2020; Lagaly et al., 2006). This parameter is a way to evaluate the modification related to the intercalation of organic compounds in its structure, which causes a decrease in interlayer size (Lagaly et al., 2006). The peaks represented at 0.33, 0.31 and 0.25 nm are indicative of quartz, while the peaks at 0.28 and 0.19 nm suggest the presence of mica (Maia et al., 2019c; Speridião et al., 2014). The peak at 0.36 indicates the orientation similar to kaolinite, which together with other peaks corroborate with clay characteristics. (Nowak et al., 2018). In addition to OC profile, other peaks observed in GO/mCS/OC, such as those found in 30.2, 35.6, 43.4, 54, 57.2 and 62.8° may be associated with the insertion of mCS in nanocomposite synthesis (Jawad et al., 2020a). These peaks are cited as indicative of Fe_3O_4 nanoparticles, proving the successful binding with chitosan (Motahharifar et al., 2020). The highlighted peaks correspond to Bragg's reflection planes (220), (311), (400), (422), (511) and (440) confirming the cubic conformation of Fe_3O_4 nanoparticles (de Figueiredo Neves et al., 2020b). Nanocomposite pattern showed similar peaks to its precursors, however, it presented a decrease in its intensity and a broader profile, being related to the decrease of the crystalline profile of OC with nanocomposite synthesis (Taher et al., 2018).

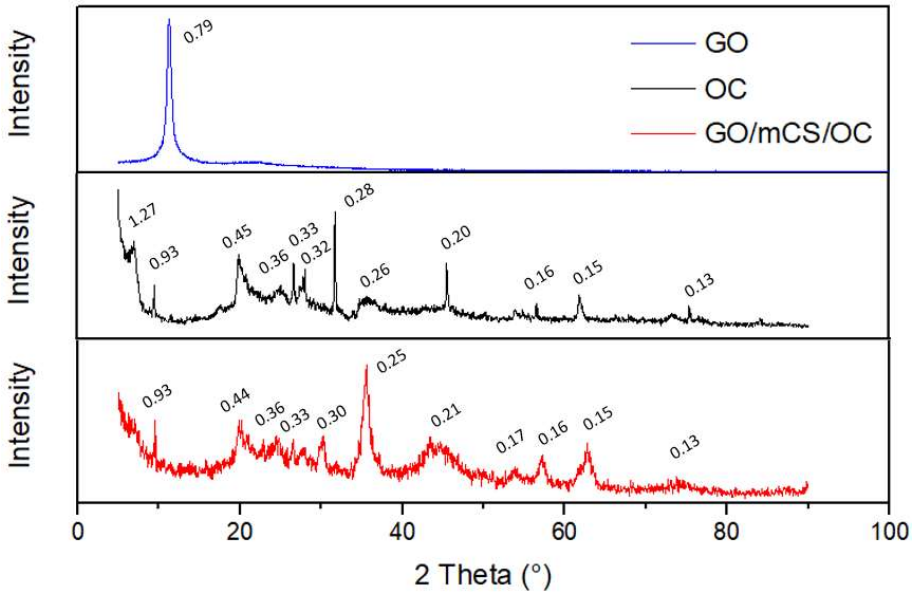

Figure 3.4 – X-ray diffractograms of GO, OC and GO/mCS/OC.

The structures of pristine and contaminated adsorbents are represented by the micrographs of OC and GO/mCS/OC (Figure 3.5). Both materials presented a heterogeneous surface profile. The adsorption process did not change the surface structure, confirming the stability of the adsorbents. However, it was possible to verify in the clay its layering and, for the nanocomposite, the presence of the graphene oxide lamellar structure intercalated with the clay layer.

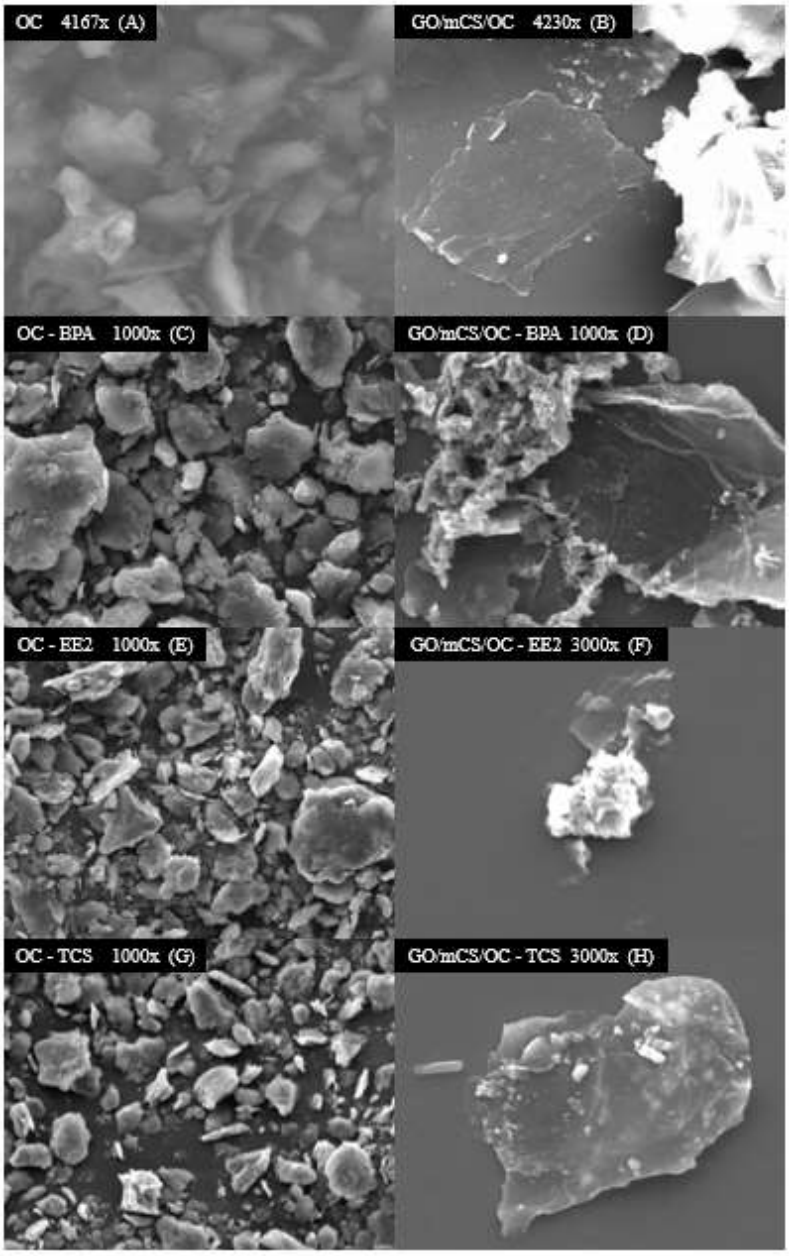

Figure 3.5 – SEM images of OC (A), GO/mCS/OC (B), OC contaminated with BPA (C), GO/mCS/OC contaminated with BPA (D), OC contaminated with EE2 (E), GO/mCS/OC contaminated with EE2 (F), OC contaminated with TCS (G) and GO/mCS/OC contaminated with TCS (H).

The elements that make up the materials were evaluated on a mass basis from EDS analysis, which was highlighted in Table 3.1. The analysis suggested in OC the presence of atoms such as Si, Fe, Na, Cl, and Al, referring to its mineral structure, as well as C and O, which also make up the organophilic chains connected in its structure. The nanocomposite synthesis resulted in a significant increase in carbon and iron percentages, as well as a decrease in some elements related to the mineral portion. It is important to emphasize the semi-quantitative characteristic of EDS analysis, as it is not adequate to precisely quantify the elements.

Table 3.1 – Mass percentage of OC and GO/mCS/OC elements.

Sample	C (%)	O (%)	Si (%)	Fe (%)	Na (%)	Cl (%)	Al (%)	Mg (%)
OC	24.7	46	16.2	2.4	2.1	0.9	6.5	1.3
GO/mCS/OC	34.5	32.4	18.5	4.5	0	0	8.4	1.4

The GO/mCS/OC magnetization curve (Figure 3.6) was obtained by vibrating sample magnetometer (VSM) and confirmed the magnetic properties of synthesized nanocomposite as illustrated in the Figure 3.7. The magnetization saturation value of the nanocomposite was 0.06 emu g^{-1}, showing a significant reduction compared to the iron nanoparticles used in its synthesis (Neves et al., 2020b). The decrease in its magnetic capacity is related to the increase in iron nanoparticles size and the change in anisotropy (Ge et al., 2009).

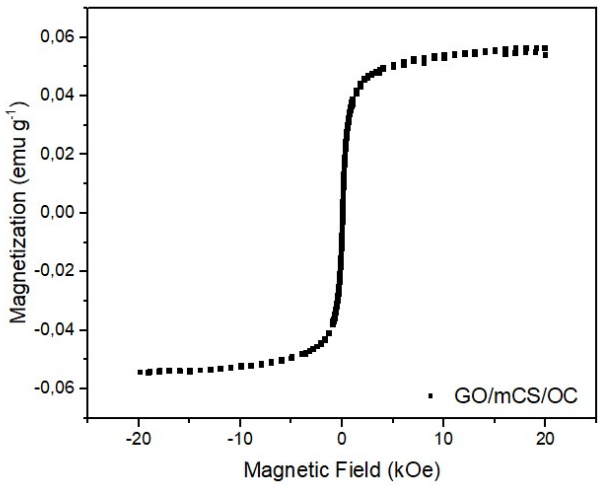

Figure 3.6 – GO/mCS/OC magnetization curve.

Figure 3.7 – GO/mCS/OC separation with magnet.

The thermal stability of OC and GO/mCS/OC was evaluated from 25 to 1000 °C, quantifying the degraded mass and its rate, which are highlighted in Figure 3.8. A decrease related to water loss up to about 130 °C was observed in both materials, being a little more evident in nanocomposite, indicating a lower presence of free water on OC surface due to its hydrophobic characteristic. The degradation of organoclays commonly presents stages of water desorption, dehydration, surfactant decomposition and surface dehydroxylation. After 200 °C, the OC starts its most intense degradation process, obtaining its highest rate at around 300 °C. This range is related to degradation process of the organic material that makes up its intercalated structure, represented by DMA surfactant cation. It is possible to identify a significant increase in the rate with increasing temperature, reaching the apex at 620 °C, representing the loss of hydroxyl surface groups that leads to the collapse of layered structure (De Andrade et al., 2020; Mallakpour and Dinari, 2011; McLauchlin and Thomas, 2009).

The degradation nanocomposites containing materials such as GO, chitosan and iron oxide exhibit similar behaviors to those found in GO/mCS/OC. After dehydration phase, the most intense range of degradation of the nanocomposite begins at around 150 °C, reaching its peak at 300 °C as well, but with greater intensity than the OC. The degradation of oxygenated groups present in GO was related in literature with a temperature range of 177 – 227 °C, as well as the elimination of the glycosidic units of chitosan between 175 – 300 °C (Mohseni Kafshgari and Tahermansouri, 2017; Salahuddin et al., 2018). The dehydroxylation of iron nanoparticles causes their degradation, which occurs in the temperature range of 250 and 290 °C (Oliveira et al., 2003a). The degradation range of mentioned compounds corroborates with the more

evident degradation peak of the nanocomposite, which progressively decreases until the end of the analysis.

The mixture of OC with GO and mCS did not significantly change the degradation regions of the material in relation to the nanocomposite, however it proved to be a little less resistant to temperature. At the end of the analysis, a final degradation of 36% for OC and 51% for GO/mCS/OC was observed. This higher value of nanocomposite may be related to the increase in organic content due to the insertion of GO and mCS.

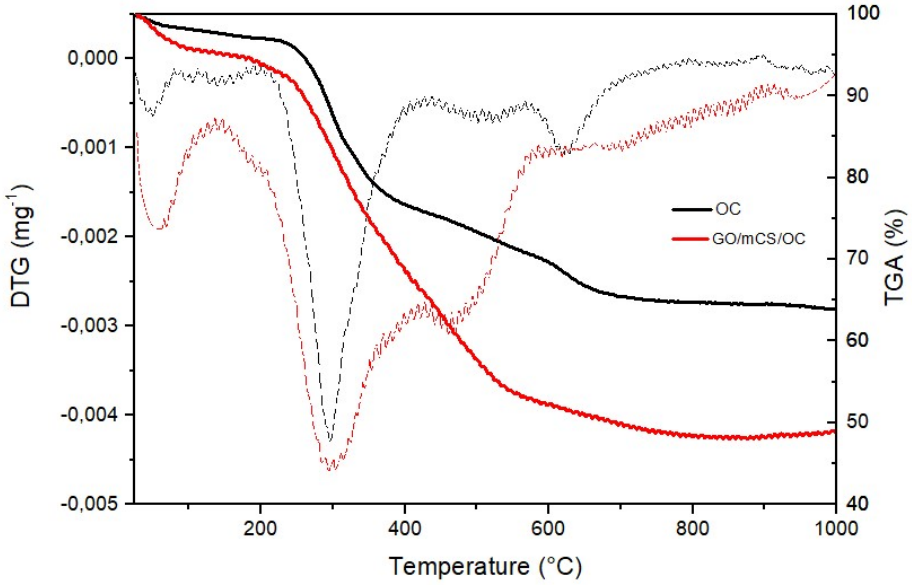

Figure 3.8 – Thermogravimetric curves of OC and GO/mCS/OC.

3.4 Adsorptive affinity assays

Affinity assays shown in Figure 3.9 evaluated the removal percentage and adsorption capacity for BPA, EE2 and TCS. The performance of OC was superior to GO/mCS/OC for BPA and EE2 and similar in the removal of TCS under the operating conditions employed. The OC removed 76.2 and 80.1% of BPA and EE2, respectively, reaching an adsorption capacity of 27 and 32.7 mg g^{-1} (0.118 and 0.110 mmol g^{-1}), while GO/mCS/OC removed 57.5 and 72%, respectively, presenting an adsorption capacity of 19.7 and 30 mg g^{-1} (0.086 and 0.101 mmol g^{-1}). Among the evaluated adsorbate–adsorbent systems, GO/mCS/OC in the presence of TCS obtained the best performance, removing 98.3% and with adsorption capacity of 40.7 mg g^{-1} (0.140 mmol g^{-1}). OC showed similar performance for this contaminant, with 98.6% removal and adsorption capacity of 39.2 mg g^{-1} (0.135 mmol g^{-1}). The removal of TCS proved to be the most effective among the contaminants evaluated. BPA and EE2 showed similar performance in the materials

evaluated, considering the number of adsorbed molecules (unit in mmol g^{-1}) and the standard deviation of the tests. The similar results between BPA and EE2, despite the evaluation of DFT and zeta potential showing more intense electrostatic interactions for BPA, may indicate that other interactions are contributing to the removal of EE2, such as pi – pi and hydrophobic interactions.

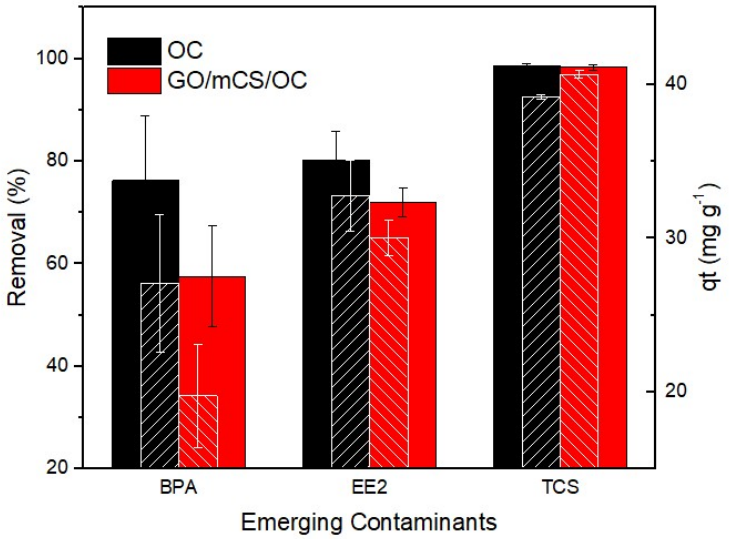

Figure 3.9 – Adsorptive affinity assay for BPA, EE2 and TCS. Adsorbent dosage of 0.2 mg ml^{-1}, initial concentration of 0.03 mmol L^{-1}, contact time of 24 h, stirring of 200 rpm and temperature of 30 °C. Solid bars indicate percent removal (%) and hatched bars refer to adsorption capacity (q_t).

Both materials showed good performance removing emerging contaminants, presenting high removal percentages compared to other conventional or complex adsorbents. The adsorptive affinity assay of OC and GO/mCS/OC, even with non-optimized operating conditions, showed similar adsorption capacity to other materials based on GO and carbon nanotubes in removing BPA (Catherine et al., 2018; Delhiraja et al., 2019; Wang et al., 2021). The performance of the materials in terms of adsorption capacity was better than several alternative or conventional adsorbents in the removal of EE2 and TCS, such as, inactivated sewage sludge (Feng et al., 2010), modified activated carbon (Alizadeh Fard e Barkdoll, 2019; Prokić et al., 2020), commercial activated carbon (Behera et al., 2010; Han et al., 2013), polyamide particles (Han et al., 2013), aliphatic polyamides (Han et al., 2012), microplastics (Lu et al., 2020), polymers (X. Wang et al.,

2018), bioadsorbents (Kozyatnyk et al., 2021; Menk et al., 2019) and GO (Delhiraja et al., 2019).

3.5 Study of molecular chemical descriptors

DFT calculations were applied focusing on electronic and molecular properties of adsorbates, seeking to better understand the behavior of molecules on adsorbent surfaces. The geometric optimization used the B3LYP method and the molecules were evaluated by 6-31G(d) and 6-31G(d,p) molecular bases, and the second base presented lower molecular energy. The lower molecular energy implies conformations with greater structural stability and for this reason it was used in this work. The molecular chemical descriptors and energy of the HOMO and LUMO orbitals are described in Table 3.2.

Table 3.2 – Molecular chemical descriptors, HOMO and LUMO energy for BPA, EE2 and TCS.

Molecular Chemical Descriptors	BPA	EE2	TCS
HOMO (E_H, eV)	-5.59711	-5.66106	-6.26298
LUMO (E_L, eV)	-0.07456	0.14857	-0.81172
Energy Gap (ΔE, eV)	5.5226	5.80963	5.45126
Chemical Potencial (μ, eV)	2.8358	2.7562	3.5373
Global Chemical Hardness (η, eV)	2.7613	2.9048	2.7256
Electrophilicity Index (ω, eV)	1.4562	1.3076	2.2954

The energy of HOMO and LUMO molecular orbitals are important for understanding chemical reactivity on an atomic level and is directly related to charge transfer within the molecule. A higher energy HOMO orbital implies a greater ability to donate electrons, while a lower energy LUMO orbital indicates a greater ability to receive electrons. Energy GAP, on the other hand, represents molecular stability, making charge transfer interactions and its reactivity more significant as this GAP decreases (Sheela et al., 2014). Among the contaminants evaluated, BPA had a greater capacity to donate electrons, while TCS had a greater capacity to receive electrons and reactivity.

Boundary molecular orbitals, as HOMO and LUMO orbitals may also be called, are depicted in Figure 3.10 and may elucidate the way these molecules interact with other species (Fazilath Basha A et al., 2021; Mumit et al., 2020). The HOMO orbitals, which

represent rich electronic sites, are distributed throughout the entire BPA and TCS molecule, while in EE2 it concentrates on the aromatic ring and the oxygen atom attached to it. The LUMO orbitals of contaminants, which represent deficient electronic sites, are distributed practically throughout the entire TCS molecule, while in the case of BPA and EE2 they are concentrated in aromatic rings.

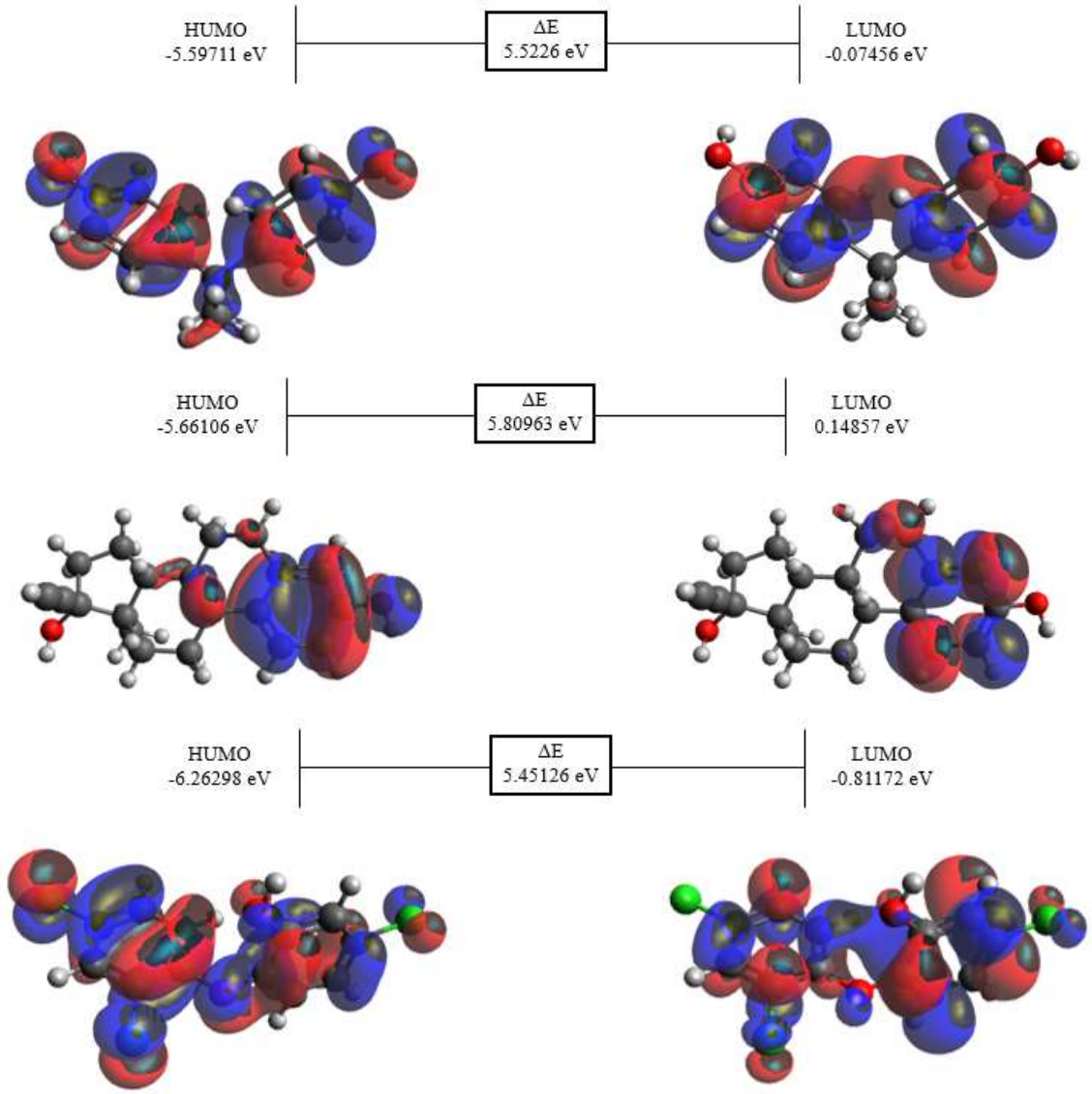

Figure 3.10 –BPA, EE2 e TCS boundary molecular orbitals.

The chemical descriptors were obtained from the energy of highlighted orbitals, including global chemical hardness (η), chemical potential (μ) and electrophilicity index (ω). Global chemical hardness represents molecule's resistance to deformation, so that the lower its value, the lower the energy required for electron transition through HOMO and LUMO orbitals, and the greater contaminant's reactivity. The chemical potential

represents the opposite of electronegativity, so the higher its value, the easier it is for electrons to escape. The electrophilicity index represents acceptance of electrons by the molecule, taking into account the energy reduction of the ligand due to electron acceptance, so that the smaller the parameter, the lesser the tendency to receive electrons (Júlia Resende de Andrade et al., 2020; Vigneresse, 2018). Considering the parameter of global chemical hardness, TCS obtained the lowest value, followed by BPA and EE2, demonstrating that it is easier to modify its electronic density among the evaluated molecules, also corroborating with the lowest energy GAP. The chemical potential and electrophilicity index evaluations demonstrated a lower electron retention capacity, as well as a greater tendency to receive electrons for the TCS molecule, followed by BPA and EE2.

Taking into account the number of adsorbed molecules and observing adsorption capacity in mmol g^{-1}, it is possible to infer that the modeling corroborates the results of adsorptive affinity tests. TCS molecule, which showed the highest reactivity and the easiest electron density deformation, was the most adsorbed adsorbate among those evaluated in the study. Although BPA has greater reactivity than EE2, the molecules had a similar performance with the adsorbents, being an indication of the presence of other significant factors besides electrostatic interactions, pi – pi bonds and hydrogen bonds. It is important to mention that the interpretation of molecular chemical descriptors aims to help understand the adsorption process and does not exclude the evaluation of other parameters such as molecular dimension and conformation of the adsorbent. These parameters may be associated with steric impediment, promoting a decrease in removal (Dordio et al., 2017; Lu et al., 2014).

The molecular electrostatic potential and the optimized dimension, available in Figure 3.11, was determined by DFT calculations and helps to understand regions with the highest probability of interaction of adsorbates. Electrostatic density indicates regions with excess and deficiency of electrons, being represented by red color the region with the highest electrostatic density, followed by yellow color to green color, which represents neutrality. The green color to blue color on scale represents regions with electron deficiency, being this more evident in the dark blue regions.

The negatively charged surface region is related to electrophilic attacks, while positive region is related to nucleophilic reactivity (Sheela et al., 2014). BPA molecule was shown to have a higher electron concentration close to oxygen atoms and a higher deficiency close to hydrogen atoms in the same region. EE2 molecule also had a higher

concentration of electrons close to oxygen atoms, as well as in the aromatic ring attached to this atom. The deficient zone of EE2 was located in the hydrogens near the oxygen atoms and triple bond. The TCS molecule, on the other hand, showed a slight concentration of negative charges between the oxygen atoms as well as the chlorine atoms. The electron–deficient region of the molecule was found near the hydrogen bonded to the oxygen atom.

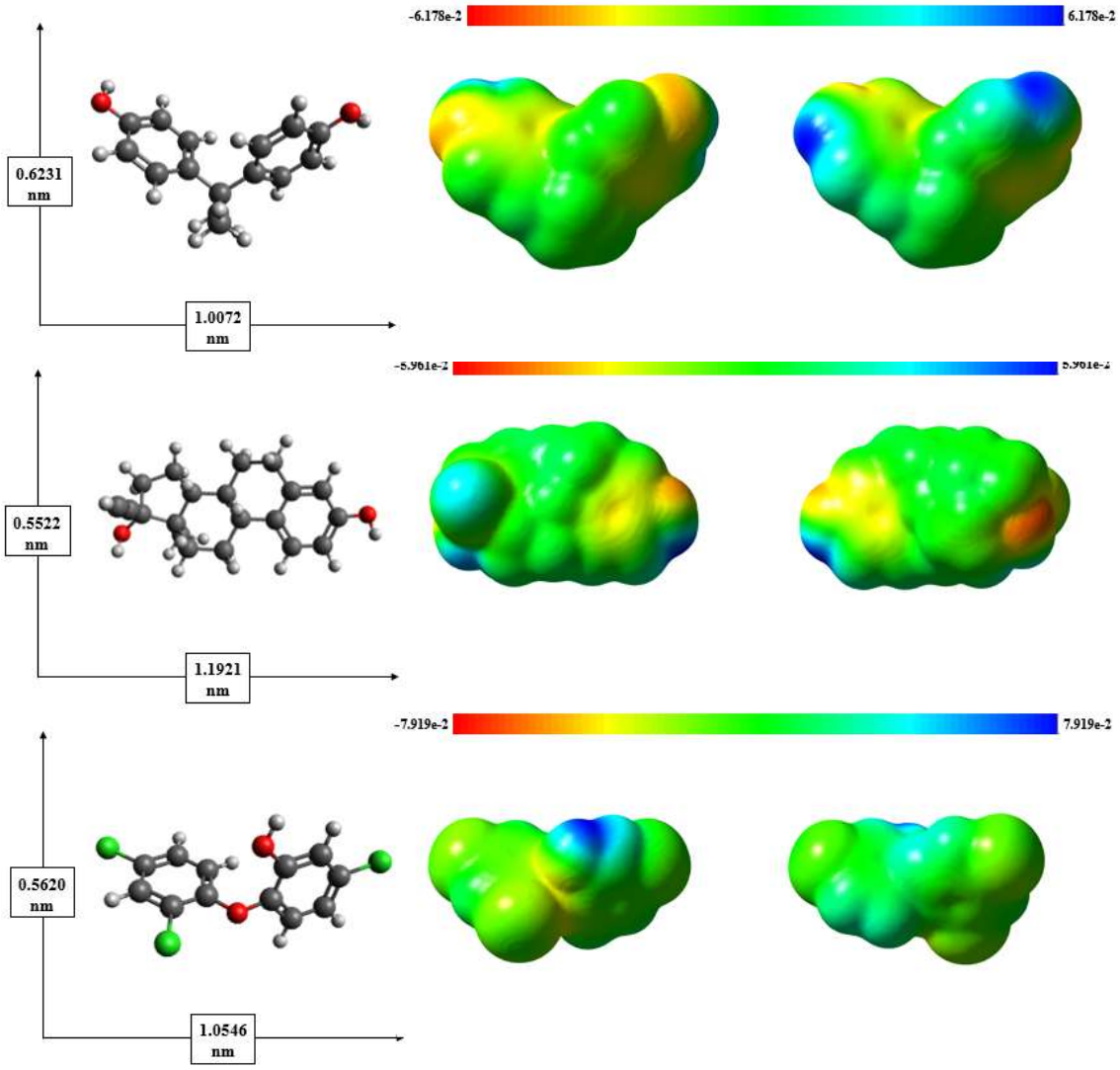

Figure 3.11 – Optimized structure and molecular electrostatic potential for BPA, EE2 and TCS.

4. CONCLUSIONS

In this study a new magnetic nanocomposite based on GO, mCS and OC was synthesized and applied to emerging contaminants adsorption (BPA, EE2 and TCS). The characterization confirmed nanocomposite synthesis success, as well as revealed

important information regarding its magnetic capacity and thermal stability. SEM micrographs and XRD patterns confirmed the heterogeneous structure and the morphology of the nanocomposite. Zeta potential analysis evaluated the behavior of surface electrical charge and confirmed the tendency of an increase in electronegativity with increasing pH. EDS analysis and FTIR spectra showed composition and presence of functional groups relevant to adsorption process. In adsorption tests, it was found an affinity order of the adsorbent materials (TCS > EE2 > BPA) with a performance superior to other reported adsorbents. The removal percentage ranged from 57.5 – 98.6% for the evaluated contaminants with similar performance among the evaluated adsorbents. The adsorption capacity ranged from 19.7 – 40.7 mg g^{-1}. BPA, EE2 and TCS were evaluated at molecular level based on DFT theory, determining information about their molecular chemical descriptors and electron density, which corroborated with adsorptive assays. The results showed that the evaluated adsorbents are promising for emerging contaminant adsorption, even appearing in low concentrations, and encourage a more detailed study of the adsorption process, evaluating more complex aqueous matrices as multicomponent systems.

5. ACKNOWLEDGEMENTS

The authors are grateful for the funding for this research provided by Research Supporting Foundation of the State of São Paulo (FAPESP, grants no. 2020/16004-9, 2019/07822-2 and 2019/25228-0), the Brazilian National Research Council (CNPq, grants no. 406193/2018-5 and 308046/2019-6), and the Coordination for the Improvement of Higher Education Personnel (CAPES, financial code – 001). This research was supported by LNBR – Brazilian Biorenewables National Laboratory (CNPEM/MCTIC) during the use of the characterization of macromolecules (MAC). We also thank the SpectroChem Company for donating the organoclay and to CENAPAD SP for the support.

APPENDIX 3.A. SUPPLEMENTARY DATA

Summary. This file contains 3 figures and 1 table.

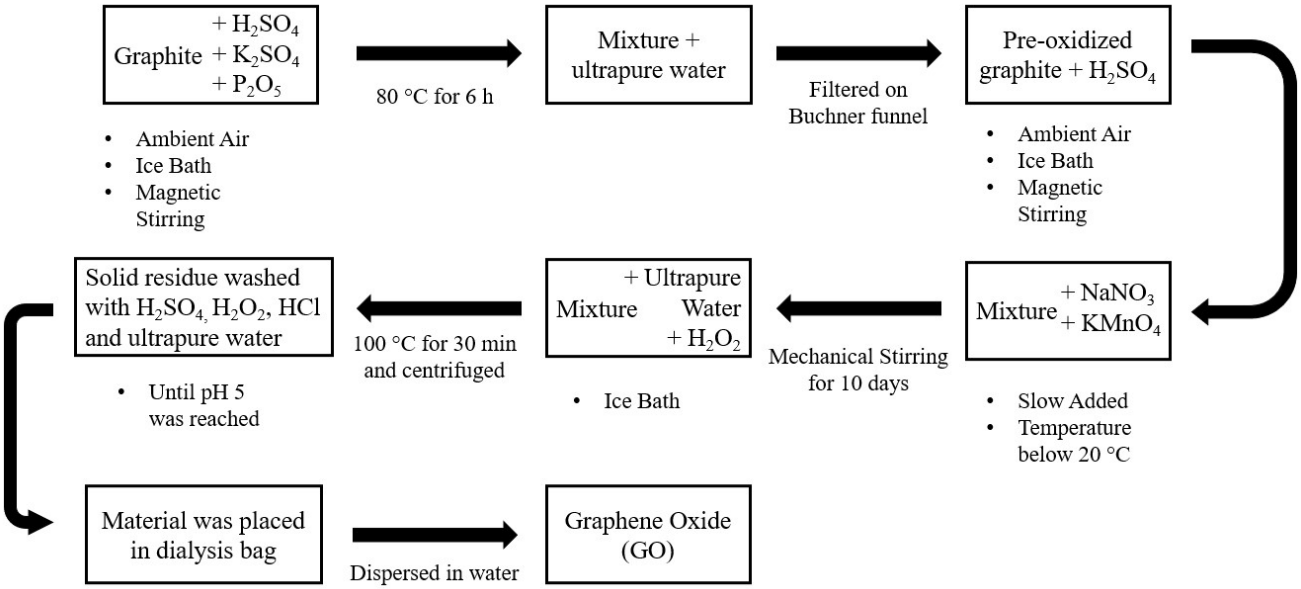

Figure 3.S1 – Graphene oxide synthesis scheme.

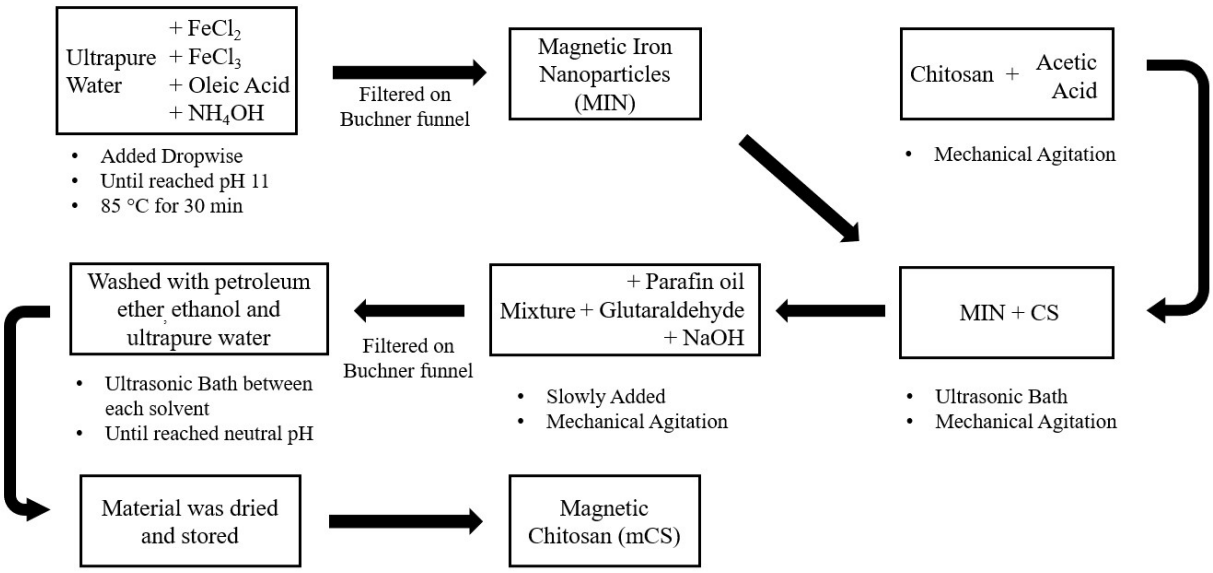

Figure 3.S2 – Magnetic chitosan synthesis scheme.

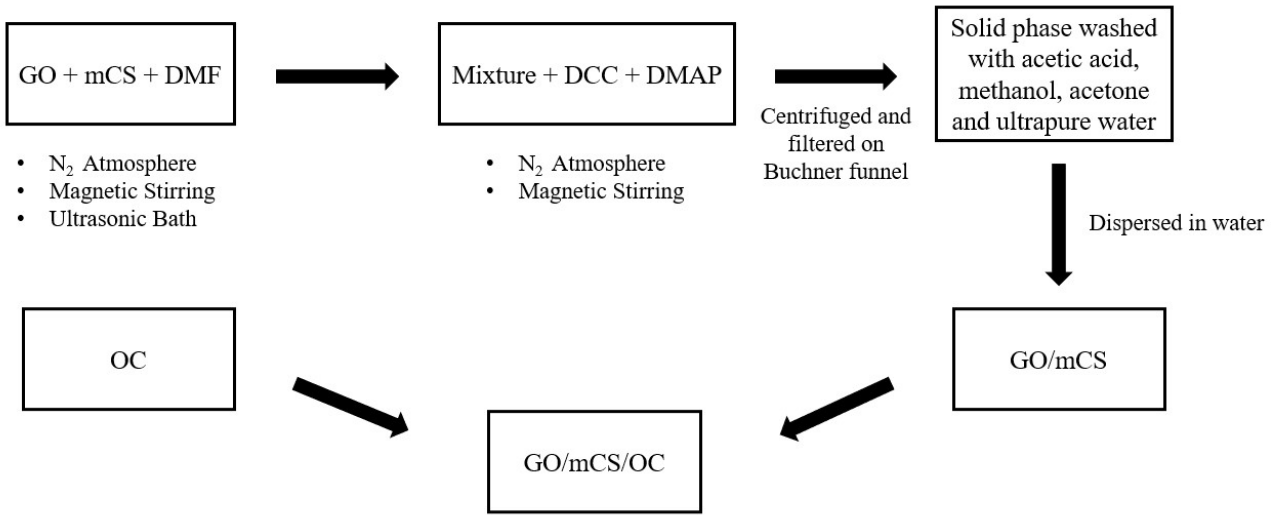

Figure 3.S3 – GO/mCS/OC synthesis scheme.

The analytical method for quantifying emerging contaminants was developed and validated based on RDC 166 resolution, evaluating the criteria of linearity, precision, selectivity, robustness, as well as the limits of detection (LoD) and quantitation (LoQ). The question of linearity was evaluated in independent triplicates in 6 different concentrations for BPA and EE2, and in 5 for TCS. The concentration range evaluated was from 0.001 to 0.033 mmol L^{-1}. The directly proportional profile was observed for all methods, obtaining correlation coefficients above 0.990, as required by the resolution, and even for their adjusted versions (R^2_{Adj}) as shown in Table 3.S1.

Precision was evaluated in triplicate for three different concentrations (low, medium and high) within the range proposed by method. The tests observed the repeatability of analytical method and was evidenced by the low relative standard deviation (RSD) values (< 3.3 %).

Samples with three contaminants together, as well as their standards, were evaluated in both methods conditions, seeking to evaluate the selectivity parameter and observe possible interferences in peaks. The operating conditions of BPA and EE2 method did not show interference in their peaks and, therefore, a satisfactory selectivity factor (α > 1.5), making its appearance evident at around 3.5 and 5 minutes, respectively.

The occurrence of TCS peak in BPA and EE2 method, as well as the presence of BPA and EE2 peak in TCS method was not observed. The combined solution showed no interference in TCS peak, which was evident around 8 minutes. Variations in solvent

percentage and column temperature were evaluated in order to verify the robustness of the method. Acetonitrile percentage ranged from 50 – 60%, in relation to BPA and EE2, with a non-significant change being observed for BPA and a little higher for EE2, taking into account RDSs shown in Table S1. Methanol percentage ranged from 75 to 85%, in relation to the TCS, not observing a significant change in the signal.

The robustness regarding column temperature was evaluated in each analytical method, varying the temperature from 25 – 35 °C, not showing significant changes in peaks. The detection and quantitation limits were evaluated in relation to the analytical curve parameters, obtaining values shown in Table S1 and enabling the quantification of removal percentages of 98, 97.7 and 98 % for BPA, EE2 and TCS, respectively. The peaks found below the quantification limits were considered due to the proximity of the limit and its evident profile against baseline noise.

Table 3.S1 – Information about analytical method validation for BPA, EE2 and TCS.

	BPA	EE2	TCS
Linearity (R^2_{Adj})	0.997	0.998	0.999
Precision – Higher Concentration ($RDS_{\%}$)	1.35	3.30	1.27
Precision – Intermediate Concentration ($RDS_{\%}$)	0.54	1.86	0.92
Precision – Lower Concentration ($RDS_{\%}$)	1.72	2.33	3.04
Robustness – Temperature ($RDS_{\%}$)	0.19	1.59	2.67
Robustness – Solvent ($RDS_{\%}$)	1.98	7.80	1.68
LoD (mmol L^{-1})	0.00021	0.00023	0.00021
LoQ (mmol L^{-1})	0.00062	0.00071	0.00062

REFERENCES

Abdolmaleki, A., Mallakpour, S., Karshenas, A., 2017. Synthesis and characterization of new nanocomposites films using alanine-Cu-functionalized graphene oxide as nanofiller and PVA as polymeric matrix for improving of their properties. Journal of Solid State Chemistry 253, 398–405. https://doi.org/10.1016/j.jssc.2017.06.014

Adolfsson-Erici, M., Pettersson, M., Parkkonen, J., Sturve, J., 2002. Triclosan, a commonly used bactericide found in human milk and in the aquatic environment in Sweden. Chemosphere 46, 1485–1489. https://doi.org/10.1016/S0045-6535(01)00255-7

Agboola, O., Fayomi, O.S.I., Ayodeji, A., Ayeni, A.O., Alagbe, E.E., Sanni, S.E., Okoro, E.E., Moropeng, L., Sadiku, R., Kupolati, K.W., Oni, B.A., 2021. A review on polymer nanocomposites and their effective applications in membranes and adsorbents for water treatment and gas separation. Membranes 11, 1–33. https://doi.org/10.3390/membranes11020139

Ahmat, A.M., Thiebault, T., Guégan, R., 2019. Phenolic acids interactions with clay minerals: A spotlight on the adsorption mechanisms of Gallic Acid onto montmorillonite. Applied Clay Science. https://doi.org/10.1016/j.clay.2019.105188

Alam, S.N., Sharma, N., Kumar, L., 2017. Synthesis of Graphene Oxide (GO) by Modified Hummers Method and Its Thermal Reduction to Obtain Reduced Graphene Oxide (rGO)*. Graphene 06, 1–18. https://doi.org/10.4236/graphene.2017.61001

Al-Gaashani, R., Najjar, A., Zakaria, Y., Mansour, S., Atieh, M.A., 2019. XPS and structural studies of high quality graphene oxide and reduced graphene oxide prepared by different chemical oxidation methods. Ceramics International 45, 14439–14448. https://doi.org/10.1016/j.ceramint.2019.04.165

Al-Ghouti, M.A., Da'ana, D.A., 2020. Guidelines for the use and interpretation of adsorption isotherm models: A review. Journal of Hazardous Materials 393, 122383. https://doi.org/10.1016/j.jhazmat.2020.122383

Alizadeh Fard, M., Barkdoll, B., 2019. Magnetic activated carbon as a sustainable solution for removal of micropollutants from water. International Journal of Environmental Science and Technology 16, 1625–1636. https://doi.org/10.1007/s13762-018-1809-5

Al-Khateeb, L.A., Obaid, A.Y., Asiri, N.A., Abdel Salam, M., 2014. Adsorption behavior of estrogenic compounds on carbon nanotubes from aqueous solutions: Kinetic and

thermodynamic studies. Journal of Industrial and Engineering Chemistry 20, 916–924. https://doi.org/10.1016/j.jiec.2013.06.023

Almeida, A.S. V, Vieira, W.T., Bispo, M.D., Melo, S.F., Silva, T.L., Balliano, T.L., Vieira, M.G.A., Soletti, J.I., 2021a. Journal of Environmental Chemical Engineering Caffeine removal using activated biochar from açaí seed (Euterpe oleracea Mart): Experimental study and description of adsorbate properties using Density Functional Theory (DFT). Journal of Environmental Chemical Engineering 9, 104891. https://doi.org/10.1016/j.jece.2020.104891

Almeida, A.S. V, Vieira, W.T., Bispo, M.D., Melo, S.F., Silva, T.L., Balliano, T.L., Vieira, M.G.A., Soletti, J.I., 2021b. Caffeine removal using activated biochar from açaí seed (Euterpe oleracea Mart): Experimental study and description of adsorbate properties using Density Functional Theory (DFT). Journal of Environmental Chemical Engineering 9.

Álvarez-Torrellas, S., Sotelo, J.L., Rodríguez, A., Ovejero, G., García, J., 2017. Influence of the natural organic matter in the removal of caffeine from water by fixed-bed column adsorption. International Journal of Environmental Science and Technology 14, 833–840. https://doi.org/10.1007/s13762-016-1189-7

Amjad, S., Rahman, M.S., Pang, M.G., 2020. Role of antioxidants in alleviating bisphenol a toxicity. Biomolecules 10, 1–26. https://doi.org/10.3390/biom10081105

Andrade, Júlia Resende, Oliveira, M.F., Canevesi, R.L.S., Landers, R., da Silva, M.G.C., Vieira, M.G.A., 2020. Comparative adsorption of diclofenac sodium and losartan potassium in organophilic clay-packed fixed-bed: X-ray photoelectron spectroscopy characterization, experimental tests and theoretical study on DFT-based chemical descriptors. Journal of Molecular Liquids 312. https://doi.org/10.1016/j.molliq.2020.113427

Andrade, J R, Oliveira, M.F., Canevesi, R.L.S., Landers, R., Silva, M.G.C., Vieira, M.G.A., 2020. Comparative adsorption of diclofenac sodium and losartan potassium in organophilic clay-packed fi xed-bed : X-ray photoelectron spectroscopy characterization , experimental tests and theoretical study on DFT-based chemical descriptors. Journal of Molecular Liquids 312, 113427. https://doi.org/10.1016/j.molliq.2020.113427

Antonelli, R., Malpass, G.R.P., da Silva, M.G.C., Vieira, M.G.A., 2021. Fixed-bed adsorption of ciprofloxacin onto bentonite clay: Characterization, mathematical

modeling, and DFT-based calculations. Industrial and Engineering Chemistry Research 60, 4030–4040. https://doi.org/10.1021/acs.iecr.0c05700

Antonelli, R., Malpass, G.R.P., da Silva, M.G.C., Vieira, M.G.A., 2020a. Adsorption of ciprofloxacin onto thermally modified bentonite clay: Experimental design, characterization, and adsorbent regeneration. Journal of Environmental Chemical Engineering 8. https://doi.org/10.1016/j.jece.2020.104553

Antonelli, R., Martins, F.R., Malpass, G.R.P., da Silva, M.G.C., Vieira, M.G.A., 2020b. Ofloxacin adsorption by calcined Verde-lodo bentonite clay: Batch and fixed bed system evaluation. Journal of Molecular Liquids 315, 113718. https://doi.org/10.1016/j.molliq.2020.113718

Anwar, J., Shafique, U., Waheed-uz-Zaman, Salman, M., Dar, A., Anwar, S., 2010. Removal of Pb(II) and Cd(II) from water by adsorption on peels of banana. Bioresource Technology 101, 1752–1755. https://doi.org/10.1016/j.biortech.2009.10.021

Appel, C., Ma, L.Q., Rhue, R.D., Kennelley, E., 2003. Point of zero charge determination in soils and minerals via traditional methods and detection of electroacoustic mobility. Geoderma 113, 77–93. https://doi.org/10.1016/S0016-7061(02)00316-6

Aris, A.Z., Shamsuddin, A.S., Praveena, S.M., 2014. Occurrence of 17α-ethynylestradiol (EE2) in the environment and effect on exposed biota: A review. Environment International 69, 104–119. https://doi.org/10.1016/j.envint.2014.04.011

ASTM, 1985. Zeta potential of colloids in water and waste water. ASTM Standard D 4187–82.

Astrahan, P., Korzen, L., Khanin, M., Sharoni, Y., Israel, Á., 2021. Seaweeds fast EDC bioremediation: Supporting evidence of EE2 and BPA degradation by the red seaweed Gracilaria sp., and a proposed model for the remedy of marine-borne phenol pollutants. Environmental Pollution 278. https://doi.org/10.1016/j.envpol.2021.116853

Aydin, E., Talinli, I., 2013. Analysis, occurrence and fate of commonly used pharmaceuticals and hormones in the Buyukcekmece Watershed, Turkey. Chemosphere 90, 2004–2012. https://doi.org/10.1016/j.chemosphere.2012.10.074

Basheer, C., Lee, H.K., 2004. Analysis of endocrine disrupting alkylphenols, chlorophenols and bisphenol-A using hollow fiber-protected liquid-phase microextraction coupled with injection port-derivatization gas chromatography-

mass spectrometry. Journal of Chromatography A 1057, 163–169. https://doi.org/10.1016/j.chroma.2004.09.083

Bavasso, I., Poggi, C., Petrucci, E., 2020. Enhanced degradation of paracetamol by combining UV with electrogenerated hydrogen peroxide and ozone. Journal of Water Process Engineering 34. https://doi.org/10.1016/j.jwpe.2019.101102

Becke, A.D., 1993. Density-functional thermochemistry. III. The role of exact exchange. The Journal of Chemical Physics 98, 5648–5652. https://doi.org/10.1063/1.464913

Bediako, J.K., Lin, S., Sarkar, A.K., Zhao, Y., Choi, J.W., Song, M.H., Cho, C.W., Yun, Y.S., 2019. Evaluation of orange peel-derived activated carbons for treatment of dye-contaminated wastewater tailings. Environmental Science and Pollution Research 27, 1053–1068. https://doi.org/10.1007/s11356-019-07031-8

Bedoux, G., Roig, B., Thomas, O., Dupont, V., Le Bot, B., 2012. Occurrence and toxicity of antimicrobial triclosan and by-products in the environment. Environmental Science and Pollution Research 19, 1044–1065. https://doi.org/10.1007/s11356-011-0632-z

Behera, S.K., Oh, S.Y., Park, H.S., 2010. Sorption of triclosan onto activated carbon, kaolinite and montmorillonite: Effects of pH, ionic strength, and humic acid. Journal of Hazardous Materials 179, 684–691. https://doi.org/10.1016/j.jhazmat.2010.03.056

Bele, S., Samanidou, V., Deliyanni, E., 2016. Effect of the reduction degree of graphene oxide on the adsorption of Bisphenol A. Chemical Engineering Research and Design. https://doi.org/10.1016/j.cherd.2016.03.002

Belfroid, A., Van Velzen, M., Van der Horst, B., Vethaak, D., 2002. Occurrence of bisphenol A in surface water and uptake in fish: Evaluation of field measurements. Chemosphere 49, 97–103. https://doi.org/10.1016/S0045-6535(02)00157-1

Bester, K., 2005. Fate of triclosan and triclosan-methyl in sewage treatment plants and surface waters. Archives of Environmental Contamination and Toxicology 49, 9–17. https://doi.org/10.1007/s00244-004-0155-4

Bhandari, R.K., Deem, S.L., Holliday, D.K., Jandegian, C.M., Kassotis, C.D., Nagel, S.C., Tillitt, D.E., vom Saal, F.S., Rosenfeld, C.S., 2015. Effects of the environmental estrogenic contaminants bisphenol A and 17α-ethinyl estradiol on sexual development and adult behaviors in aquatic wildlife species. General and Comparative Endocrinology 214, 195–219. https://doi.org/10.1016/j.ygcen.2014.09.014

Bhattacharya, P., Mukherjee, D., Deb, N., Swarnakar, S., Banerjee, S., 2021. Indigenously developed CuO/TiO2 coated ceramic ultrafiltration membrane for removal of emerging contaminantes like phtalates and parabens: Toxicity evaluation in PA-1 cell line. Materials Chemistry and Physics.

Bögi, C., Schwaiger, J., Ferling, H., Mallow, U., Steineck, C., Sinowatz, F., Kalbfus, W., Negele, R.D., Lutz, I., Kloas, W., 2003. Endocrine effects of environmental pollution on Xenopus laevis and Rana temporaria. Environmental Research 93, 195–201. https://doi.org/10.1016/S0013-9351(03)00082-3

Bolong, N., Ismail, A.F., Salim, M.R., Matsuura, T., 2009. A review of the effects of emerging contaminants in wastewater and options for their removal. Desalination 239, 229–246. https://doi.org/10.1016/j.desal.2008.03.020

Bonate, P.L., 2011. Pharmacokinetic-Pharmacodynamic Modeling and Simulation, 2nd ed. Springer.

Boyd, G.E., Adamson, A.W., Myers Jr, L.S., 1947. The Exchange Adsorption of Ions from Aqueous Solutions by Organic Zeolites. II. Kinetics.

Brandt, E.M.F., 2012. Avaliação da remoção de fármacos e desreguladores endócrinos em sistemas simplificados de tratamento de esgoto (reatores uasb seguidos de pós-tratamento). Dissertação de Mestrado em Saneamento do Programa de Pós-Graduação em Saneamento, Meio Ambiente e Recursos Hídricos da Universidade Federal de Minas Gerais.

Brazovskaya, E.Y., Golubeva, O.Y., 2020. Development of Magnetic Nanocomposites Based on Beta Zeolites and Study of Their Sorption Properties. Petroleum Chemistry 60, 957–963. https://doi.org/10.1134/S0965544120080046

Cao, Y., Li, X., 2014. Adsorption of graphene for the removal of inorganic pollutants in water purification: A review. Adsorption 20, 713–727. https://doi.org/10.1007/s10450-014-9615-y

Caon, N.B., Cardoso, C., Faita, F.L., Vitali, L., Parize, A.L., 2020. Magnetic solid-phase extraction of triclosan from water using n -octadecyl modi fi ed silica-coated magnetic nanoparticles. Journal of Environmental Chemical Engineering 8. https://doi.org/10.1016/j.jece.2020.104003

Cargouët, M., Perdiz, D., Mouatassim-Souali, A., Tamisier-Karolak, S., Levi, Y., 2004. Assessment of river contamination by estrogenic compounds in Paris area (France). Science of the Total Environment 324, 55–66. https://doi.org/10.1016/j.scitotenv.2003.10.035

Catherine, H.N., Ou, M.H., Manu, B., Shih, Y. hsin, 2018. Adsorption mechanism of emerging and conventional phenolic compounds on graphene oxide nanoflakes in water. Science of the Total Environment. https://doi.org/10.1016/j.scitotenv.2018.03.389

Chabot, V., Higgins, D., Yu, A., Xiao, X., Chen, Z., Zhang, J., 2014. A review of graphene and graphene oxide sponge: Material synthesis and applications to energy and the environment. Energy and Environmental Science 7, 1564–1596. https://doi.org/10.1039/c3ee43385d

Chang, K., Hsieh, J., Ou, B., Chang, M., Hseih, W., Lin, J.-H., Huang, P.-J., Wong, K.-F., Chen, S.-T., 2012. Adsorption Studies on the Removal of an Endocrine-Disrupting Compound (Bisphenol A) using Activated Carbon from Rice Straw Agricultural Waste Adsorption Studies on the Removal of an Endocrine-Disrupting Compound (Bisphenol A) using Activated Carbon f. Separation Science and Technology 37–41. https://doi.org/10.1080/01496395.2011.647212

Cheminski, T., De Figueiredo Neves, T., Silva, P.M., Guimarães, C.H., Prediger, P., 2019. Insertion of phenyl ethyleneglycol units on graphene oxide as stabilizers and its application for surfactant removal. Journal of Environmental Chemical Engineering 7, 102976. https://doi.org/10.1016/j.jece.2019.102976

Chen, C.Y., Wen, T.Y., Wang, G.S., Cheng, H.W., Lin, Y.H., Lien, G.W., 2007. Determining estrogenic steroids in Taipei waters and removal in drinking water treatment using high-flow solid-phase extraction and liquid chromatography/tandem mass spectrometry. Science of the Total Environment 378, 352–365. https://doi.org/10.1016/j.scitotenv.2007.02.038

Chen, J., Wang, X., Dai, C., Chen, S., Tu, Y., 2014. Adsorption of GA module onto graphene and graphene oxide: A molecular dynamics simulation study. Physica E: Low-Dimensional Systems and Nanostructures 62, 59–63. https://doi.org/10.1016/j.physe.2014.04.021

Cheng, N., Wang, B., Wu, P., Lee, X., Xing, Y., Chen, M., Gao, B., 2021. Adsorption of emerging contaminants from water and wastewater by modified biochar: A review. Environmental Pollution. https://doi.org/10.1016/j.envpol.2021.116448

Cherednichenko, G., Zhang, R., Bannister, R.A., Timofeyev, V., Li, N., Fritsch, E.B., Feng, W., Barrientos, G.C., Schebb, N.H., Hammock, B.D., Beam, K.G., Chiamvimonvat, N., Pessah, I.N., 2012. Triclosan impairs excitation-contraction coupling and Ca2+ dynamics in striated muscle (Proceedings of the National

Academy of Sciences of the United States of America (2012) 109, 35, (14158 - 14163) DOI:10.1073/pnas. 1211314109). Proceedings of the National Academy of Sciences of the United States of America 109, 16393. https://doi.org/10.1073/pnas.1215071109

Cobos, M., González, B., Fernández, M.J., Fernández, M.D., 2018. Study on the effect of graphene and glycerol plasticizer on the properties of chitosan-graphene nanocomposites via in situ green chemical reduction of graphene oxide. International Journal of Biological Macromolecules 114, 599–613. https://doi.org/10.1016/j.ijbiomac.2018.03.129

Coelho, C.M., de Andrade, J.R., da Silva, M.G.C., Vieira, M.G.A., 2020. Removal of propranolol hydrochloride by batch biosorption using remaining biomass of alginate extraction from Sargassum filipendula algae. Environmental Science and Pollution Research 27, 16599–16611. https://doi.org/10.1007/s11356-020-08109-4

Cristina do Nascimento, D., Gurgel Carlos da Silva, M., Gurgel Adeodato Vieira, M., 2021. Adsorption of propranolol hydrochloride from aqueous solutions onto thermally treated bentonite clay: A complete batch system evaluation. Journal of Molecular Liquids 337. https://doi.org/10.1016/j.molliq.2021.116442

Crouse, B.A., Ghoshdastidar, A.J., Tong, A.Z., 2012. The presence of acidic and neutral drugs in treated sewage effluents and receiving waters in the Cornwallis and Annapolis River watersheds and the Mill CoveSewage Treatment Plant in Nova Scotia, Canada. Environmental Research 112, 92–99. https://doi.org/10.1016/j.envres.2011.11.011

Cychosz, K.A., Guillet-Nicolas, R., García-Martínez, J., Thommes, M., 2017. Recent advances in the textural characterization of hierarchically structured nanoporous materials. Chemical Society Reviews. https://doi.org/10.1039/c6cs00391e

Dąbrowski, A., 2001. Adsorption - From theory to practice. Advances in Colloid and Interface Science 93, 135–224. https://doi.org/10.1016/S0001-8686(00)00082-8

Dąbrowski, A., Podkościelny, P., Hubicki, Z., Barczak, M., 2005. Adsorption of phenolic compounds by activated carbon - A critical review. Chemosphere 58, 1049–1070. https://doi.org/10.1016/j.chemosphere.2004.09.067

Dai, J., Meng, X., Zhang, Y., Huang, Y., 2020. Effects of modification and magnetization of rice straw derived biochar on adsorption of tetracycline from water. Bioresource Technology 311. https://doi.org/10.1016/j.biortech.2020.123455

Daniel, I.M., Ishai, O., 2006. Engineering mechanics of composite materials, Oxford University Press. https://doi.org/10.1016/s0261-3069(97)87195-6

de Almeida, A. da S.V., de Figueiredo Neves, T., da Silva, M.G.C., Prediger, P., Vieira, M.G.A., 2022. Synthesis of a novel magnetic composite based on graphene oxide, chitosan and organoclay and its application in the removal of bisphenol A, 17α-ethinylestradiol and triclosan. Journal of Environmental Chemical Engineering 10, 107071. https://doi.org/10.1016/j.jece.2021.107071

de Andrade, J. R., da Silva, M.G.C., Gimenes, M.L., Vieira, M.G.A., 2020. Performance of organoclay in adsorptive uptake of antihypertensive losartan potassium: A comparative batch study using micro-grain activated carbon. Journal of Environmental Chemical Engineering 8, 103562. https://doi.org/10.1016/j.jece.2019.103562

De Andrade, J.R., Da Silva, M.G.C., Gimenes, M.L., Vieira, M.G.A., 2020. Performance of organoclay in adsorptive uptake of antihypertensive losartan potassium: A comparative batch study using micro-grain activated carbon. Journal of Environmental Chemical Engineering 8, 103562. https://doi.org/10.1016/j.jece.2019.103562

de Andrade, Júlia Resende, Oliveira, M.F., Canevesi, R.L.S., Landers, R., da Silva, M.G.C., Vieira, M.G.A., 2020. Comparative adsorption of diclofenac sodium and losartan potassium in organophilic clay-packed fixed-bed: X-ray photoelectron spectroscopy characterization, experimental tests and theoretical study on DFT-based chemical descriptors. Journal of Molecular Liquids 312, 113427. https://doi.org/10.1016/j.molliq.2020.113427

de Aquino, S.F., Brandt, E.M.F., Chernicharo, C.A. de L., 2013. Remoção de fármacos e desreguladores endócrinos em estações de tratamento de esgoto: Revisão da literatura. Engenharia Sanitaria e Ambiental 18, 187–204. https://doi.org/10.1590/S1413-41522013000300002

De Assis Gonsalves, A., Araujo, C.R.M., Soares, N.A., Goulart, M.O.F., De Abreu, F.C., 2011. Diferentes Estrategias Para A Reticulaqao De Quitosana. Quimica Nova 34, 1215–1223. https://doi.org/10.1590/S0100-40422011000700021

de Farias, M.B., Spaolonzi, M.P., Silva, M.G.C., Vieira, M.G.A., 2021. Fixed-bed adsorption of bisphenol A onto organoclay: Characterisation, mathematical modelling and theoretical calculation of DFT-based chemical descriptors. Journal of Environmental Chemical Engineering 9. https://doi.org/10.1016/j.jece.2021.106103

de Figueiredo Neves, T., Barticiotto Dalarme, N., da Silva, P.M.M., Landers, R., Siqueira Franco Picone, C., Prediger, P., 2020a. Novel magnetic chitosan/quaternary ammonium salt graphene oxide composite applied to dye removal. Journal of Environmental Chemical Engineering 8, 103820. https://doi.org/10.1016/j.jece.2020.103820

de Figueiredo Neves, T., Barticiotto Dalarme, N., da Silva, P.M.M., Landers, R., Siqueira Franco Picone, C., Prediger, P., 2020b. Novel magnetic chitosan/quaternary ammonium salt graphene oxide composite applied to dye removal. Journal of Environmental Chemical Engineering 8, 103820. https://doi.org/10.1016/j.jece.2020.103820

de Souza, F.M., dos Santos, O.A.A., Vieira, M.G.A., 2019. Adsorption of herbicide 2,4-D from aqueous solution using organo-modified bentonite clay. Environmental Science and Pollution Research 26, 18329–18342. https://doi.org/10.1007/s11356-019-05196-w

de Souza, T.N.V., de Carvalho, S.M.L., Vieira, M.G.A., da Silva, M.G.C., Brasil, D. do S.B., 2018. Adsorption of basic dyes onto activated carbon: Experimental and theoretical investigation of chemical reactivity of basic dyes using DFT-based descriptors. Applied Surface Science 448, 662–670. https://doi.org/10.1016/j.apsusc.2018.04.087

Dehghani, M.H., Ghadermazi, M., Bhatnagar, A., Sadighara, P., Jahed-khaniki, G., Heibati, B., Mckay, G., 2016. Adsorptive removal of endocrine disrupting bisphenol A from aqueous solution using chitosan. Biochemical Pharmacology. https://doi.org/10.1016/j.jece.2016.05.011

Delgado-Moreno, L., Bazhari, S., Nogales, R., Romero, E., 2019. Innovative application of biobed bioremediation systems to remove emerging contaminants: Adsorption, degradation and bioaccesibility. Science of the Total Environment 651, 990–997. https://doi.org/10.1016/j.scitotenv.2018.09.268

Delhiraja, K., Vellingiri, K., Boukhvalov, D.W., Philip, L., 2019. Development of Highly Water Stable Graphene Oxide-Based Composites for the Removal of Pharmaceuticals and Personal Care Products. Industrial and Engineering Chemistry Research 58, 2899–2913. https://doi.org/10.1021/acs.iecr.8b02668

Dhillon, G.S., Kaur, S., Pulicharla, R., Brar, S.K., Cledón, M., Verma, M., Surampalli, R.Y., 2015. Triclosan: Current status, occurrence, environmental risks and

bioaccumulation potential. International Journal of Environmental Research and Public Health 12, 5657–5684. https://doi.org/10.3390/ijerph120505657

Dias, J.M., Alvim-Ferraz, M.C.M., Almeida, M.F., Rivera-Utrilla, J., Sánchez-Polo, M., 2007. Waste materials for activated carbon preparation and its use in aqueous-phase treatment: A review. Journal of Environmental Management 85, 833–846. https://doi.org/10.1016/j.jenvman.2007.07.031

Ding, W.H., Wu, C.Y., 2000. Determination of estrogenic nonylphenol and bisphenol A in river water by solid-phase extraction and gas chromatography-mass spectrometry. Journal of the Chinese Chemical Society 47, 1155–1160. https://doi.org/10.1002/jccs.200000155

Dinwiddie, M.T., Terry, P.D., Chen, J., 2014. Recent evidence regarding triclosan and cancer risk. International Journal of Environmental Research and Public Health 11, 2209–2217. https://doi.org/10.3390/ijerph110202209

Doğan, M., Alkan, M., Demirbaş, Ö., Özdemir, Y., Özmetin, C., 2006. Adsorption kinetics of maxilon blue GRL onto sepiolite from aqueous solutions. Chemical Engineering Journal 124, 89–101. https://doi.org/10.1016/j.cej.2006.08.016

Dordio, A. V., Miranda, S., Prates Ramalho, J.P., Carvalho, A.J.P., 2017. Mechanisms of removal of three widespread pharmaceuticals by two clay materials. Journal of Hazardous Materials 323, 575–583. https://doi.org/10.1016/j.jhazmat.2016.05.091

dos Santos Cardoso, C., Vitali, L., 2021. Chitosan Versus Chitosan-Vanillin Modified: An Evaluation of the Competitive Adsorption of Five Emerging Contaminants. Water, Air, and Soil Pollution 232. https://doi.org/10.1007/s11270-021-05118-y

Drewes, J.E., Hemming, J., Ladenburger, S.J., Schauer, J., Sonzogni, W., 2012. an Assessment of Endocrine Disrupting Activity Changes in Water Reclamation Systems Through the Use of Bioassays and Chemical Measurements. Proceedings of the Water Environment Federation 2004, 47–65. https://doi.org/10.2175/193864704784147476

Ebadi, A., Soltan Mohammadzadeh, J.S., Khudiev, A., 2009. What is the correct form of BET isotherm for modeling liquid phase adsorption? Adsorption 15, 65–73. https://doi.org/10.1007/s10450-009-9151-3

Ederer, J., Janos, P., Ecorchard, P., Tolasz, J., Stengl, V., Benes, H., Perchacz, M., Pop-Georgievski, O., 2017. Determination of amino groups on functionalized graphene oxide for polyurethane nanomaterial. RSC Advances.

Egea-Corbacho, A., Gutiérrez Ruiz, S., Quiroga Alonso, J.M., 2019. Removal of emerging contaminants from wastewater using nanofiltration for its subsequent reuse: Full–scale pilot plant. Journal of Cleaner Production 214, 514–523. https://doi.org/10.1016/j.jclepro.2018.12.297

Erim, B., Ciğeroğlu, Z., Bayramoğlu, M., 2021. Green synthesis of TiO2/GO/chitosan by using leaf extract of Olea europaea as a highly efficient photocatalyst for the degradation of cefixime trihydrate under UV-A radiation exposure: An optimization study with D-optimal design. Journal of Molecular Structure 1234. https://doi.org/10.1016/j.molstruc.2021.130194

Erler, C., Novak, J., 2010. Bisphenol a exposure: Human risk and health policy. Journal of Pediatric Nursing 25, 400–407. https://doi.org/10.1016/j.pedn.2009.05.006

Esmaeili, H., Tamjidi, S., 2020. Ultrasonic-assisted synthesis of natural clay/Fe3O4/graphene oxide for enhance removal of Cr (VI) from aqueous media. Environmental Science and Pollution Research 27, 31652–31664. https://doi.org/10.1007/s11356-020-09448-y

Fagerlund, G., 1973. Determination of specific surface by the BET method. Matériaux et Construction 239–245.

Farias, M.B. de, Silva, M.G.C., Vieira, M.G.A., 2022. Adsorption of bisphenol A from aqueous solution onto organoclay: Experimental design, kinetic, equilibrium and thermodynamic study. Powder Technology 395, 695–707. https://doi.org/10.1016/j.powtec.2021.10.021

Farrah, H., Pickering, W.F., 1979. pH effects in the adsorption of heavy metal ions by clays. Chemical Geology 25, 317–326. https://doi.org/10.1016/0009-2541(79)90063-9

Fazilath Basha A, Liakath Ali Khan, F., Muthu, S., Raja, M., 2021. Computational evaluation on molecular structure (Monomer, Dimer), RDG, ELF, electronic (HOMO-LUMO, MEP) properties, and spectroscopic profiling of 8-Quinolinesulfonamide with molecular docking studies. Computational and Theoretical Chemistry 1198, 113169. https://doi.org/10.1016/j.comptc.2021.113169

Feng, Y., Zhang, Z., Gao, P., Su, H., Yu, Y., Ren, N., 2010. Adsorption behavior of EE2 (17α-ethinylestradiol) onto the inactivated sewage sludge: Kinetics, thermodynamics and influence factors. Journal of Hazardous Materials 175, 970–976. https://doi.org/10.1016/j.jhazmat.2009.10.105

Fernandes, A.N., Giovanela, M., Esteves, V.I., Grassi, M.T., Almeida, C.A., Sierra, M.M.D., 2011. Remoção dos hormônios E2 e EE2 de soluções aquosas empregando turfa decomposta como material adsorvente 34, 1526–1533.

Flint, S., Markle, T., Thompson, S., Wallace, E., 2012. Bisphenol A exposure, effects, and policy: A wildlife perspective. Journal of Environmental Management 104, 19–34. https://doi.org/10.1016/j.jenvman.2012.03.021

Forder, T.R., Jones, M.D., 2015. Synthesis and characterisation of aluminium(III) imine bis(phenolate) complexes with application for the polymerisation of rac-LA. New Journal of Chemistry 39, 1974–1978. https://doi.org/10.1039/c4nj02228a

Freitas, M.B., Freitas, C.M. de, 2005. A vigilância da qualidade da água para consumo humano: desafios e perspectivas para o Sistema Único de Saúde. Ciência & Saúde Coletiva 10, 993–1004. https://doi.org/10.1590/s1413-81232005000400022

Freundlich, H., 1906. Über die Adsorption in Lösungen (Concerning adsorption in solutions). Chemie–Stochiometrie, Zeitschrift Fur Physikalische.

Frisch, Æ., Hratchian, H.P., Dennington, R.D., Keith, T.A., Millam, J., 2016. Gaussview 6.

Frisch, M.J., Pople, J.A., Binkley, J.S., 1984. Self-consistent molecular orbital methods 25. Supplementary functions for Gaussian basis sets. The Journal of Chemical Physics 80, 3265–3269. https://doi.org/10.1063/1.447079

Frisch, M.J., Trucks, G.W., Schlegel, H.B., Scuseria, G.E., Robb, M.A., Cheeseman, J.R., Scalmani, G., Barone, V., Mennucci, B., Petersson, G.A., Nakatsuji, H., Caricato, M., Li, X., Hratchian, H.P., Izmaylov, A.F., Bloino, J., Zheng, G., Sonnenberg, J.L., Hada, M., Ehar, M., Fox, D.J., 2009. Gaussian 09. Gaussian, Inc., Wallingford.

Fuchsman, P., Lyndall, J., Bock, M., Lauren, D., Barber, T., Leigh, K., Perruchon, E., Capdevielle, M., 2010. Terrestrial ecological risk evaluation for triclosan in land-applied biosolids. Integrated Environmental Assessment and Management 6, 405–418. https://doi.org/10.1897/ieam_2009-071.1

Ge, Y., Zhang, Y., Xia, J., Ma, M., He, S., Nie, F., Gu, N., 2009. Effect of surface charge and agglomerate degree of magnetic iron oxide nanoparticles on KB cellular uptake in vitro. Colloids and Surfaces B: Biointerfaces 73, 294–301. https://doi.org/10.1016/j.colsurfb.2009.05.031

Ghosh, A., Ghosh, S., Seshadhri, G.M., Ramaprabhu, S., 2019. Green synthesis of nitrogen-doped self-assembled porous carbon-metal oxide composite towards

energy and environmental applications. Scientific Reports 9. https://doi.org/10.1038/s41598-019-41700-5

Gong, J., Ran, Y., Chen, D., Yang, Y., Ma, X., 2009. Occurrence and environmental risk of endocrine-disrupting chemicals in surface waters of the Pearl River, South China. Environmental Monitoring and Assessment 156, 199–210. https://doi.org/10.1007/s10661-008-0474-4

Gong, Y., Yu, Y., Kang, H., Chen, X., Liu, H., Zhang, Y., Sun, Y., Song, H., 2019. Synthesis and Characterization of Graphene Oxide Chitosan Composite Aerogels. Polymers.

Goyal, N., Bulasara, V.K., Barman, S., 2018. Removal of emerging contaminants daidzein and coumestrol from water by nanozeolite beta modified with tetrasubstituted ammonium cation. Journal of Hazardous Materials 344, 417–430. https://doi.org/10.1016/j.jhazmat.2017.10.051

Gregorio-Jauregui, K.M., Pineda, M.G., Rivera-Salinas, J.E., Hurtado, G., Saade, H., Martinez, J.L., Ilyina, A., López, R.G., 2012. One-step method for preparation of magnetic nanoparticles coated with chitosan. Journal of Nanomaterials 2012. https://doi.org/10.1155/2012/813958

Guerra, A.C.S., de Andrade, M.B., Tonial dos Santos, T.R., Bergamasco, R., 2021. Adsorption of sodium diclofenac in aqueous medium using graphene oxide nanosheets. Environmental Technology (United Kingdom) 42, 2599–2609. https://doi.org/10.1080/09593330.2019.1707882

Guerra, P., Kim, M., Teslic, S., Alaee, M., Smyth, S.A., 2015. Bisphenol-A removal in various wastewater treatment processes: Operational conditions, mass balance, and optimization. Journal of Environmental Management 152, 192–200. https://doi.org/10.1016/j.jenvman.2015.01.044

Han, J., Qiu, W., Cao, Z., Hu, J., Gao, W., 2013. Adsorption of ethinylestradiol (EE2) on polyamide 612: Molecular modeling and effects of water chemistry. Water Research 47, 2273–2284. https://doi.org/10.1016/j.watres.2013.01.046

Han, J., Qiu, W., Meng, S., Gao, W., 2012. Removal of ethinylestradiol (EE2) from water via adsorption on aliphatic polyamides. Water Research 46, 5715–5724. https://doi.org/10.1016/j.watres.2012.08.001

Hanwell, M.D., Curtis, D.E., Lonie, D.C., Vandermeerschd, T., Zurek, E., Hutchison, G.R., 2012. Avogadro: An advanced semantic chemical editor, visualization, and

analysis platform. Journal of Cheminformatics 4. https://doi.org/10.1186/1758-2946-4-17

He, H., Ma, L., Zhu, J., Frost, R.L., Theng, B.K.G., Bergaya, F., 2014. Synthesis of organoclays: A critical review and some unresolved issues. Applied Clay Science 100, 22–28. https://doi.org/10.1016/j.clay.2014.02.008

Hemidouche, S., Assoumani, A., Favier, L., Simion, A.I., Grigoras, C.G., Wolbert, D., Gavrila, L., Nationale, E., Chimie, S. De, 2017. Removal of some Endocrine Disruptors via Adsorption on Activated Carbon 410–413.

Ho, Y.S., McKay, G., 2000. The kinetics of sorption of divalent metal ions onto sphagnum moss peat. Water Research 34, 735–742. https://doi.org/10.1016/S0043-1354(99)00232-8

HO, Y.S., MCKAY, G., 1999. Pseudo-second order model for sorption processes. Process Biochemistry 34, 451–465. https://doi.org/10.1021/acs.oprd.7b00090

Ho, Y.S., McKay, G., 1998. A Comparison of chemisorption kinetic models applied to pollutant removal on various sorbents. Process Safety and Environmental Protection 76, 332–340. https://doi.org/10.1205/095758298529696

Honório, K.M., Silva, A.B.F., 2003. An AM1 Study on the Electron-Donating and Electron-Accepting Character of Biomolecules 95, 126–132. https://doi.org/10.1002/qua.10661

Hosseini, Y., Najafi, M., Khalili, S., Jahanshahi, M., Peyravi, M., 2021. Assembly of amine-functionalized graphene oxide for efficient and selective adsorption of CO2. Materials Chemistry and Physics 270. https://doi.org/10.1016/j.matchemphys.2021.124788

Hu, D., Lian, Z., Xian, H., Jiang, R., Wang, N., Weng, Y., Peng, X., Wang, S., Ouyang, X. –K, 2020. Adsorption of Pb(II) from aqueous solution by polyacrylic acid grafted magnetic chitosan nanocomposite. International Journal of Biological Macromolecules 154, 1537–1547. https://doi.org/10.1016/j.ijbiomac.2019.11.038

Hu, Y., Zhu, Y., Zhang, Y., Lin, T., Zeng, G., Zhang, S., Wang, Y., He, W., Zhang, M., Long, H., 2019. An efficient adsorbent: Simultaneous activated and magnetic ZnO doped biochar derived from camphor leaves for ciprofloxacin adsorption. Bioresource Technology 288. https://doi.org/10.1016/j.biortech.2019.121511

Hua, W., Bennett, E.R., Letcher, R.J., 2005. Triclosan in waste and surface waters from the upper Detroit River by liquid chromatography-electrospray-tandem quadrupole

mass spectrometry. Environment International 31, 621–630. https://doi.org/10.1016/j.envint.2004.10.019

Huang, Y., Liu, Y., Kong, M., Xu, E.G., Coffin, S., Schlenk, D., Dionysiou, D.D., 2018. Efficient degradation of cytotoxic contaminants of emerging concern by UV/H2O2. Environmental Science: Water Research and Technology 4, 1272–1281. https://doi.org/10.1039/c8ew00290h

Huang, Y.Q., Wong, C.K.C., Zheng, J.S., Bouwman, H., Barra, R., Wahlström, B., Neretin, L., Wong, M.H., 2012. Bisphenol A (BPA) in China: A review of sources, environmental levels, and potential human health impacts. Environment International 42, 91–99. https://doi.org/10.1016/j.envint.2011.04.010

Huang, Z., Li, Z., Zheng, L., Zhou, L., Chai, Z., Wang, X., Shi, W., 2017. Interaction mechanism of uranium(VI) with three-dimensional graphene oxide-chitosan composite: Insights from batch experiments, IR, XPS, and EXAFS spectroscopy. Chemical Engineering Journal 328, 1066–1074. https://doi.org/10.1016/j.cej.2017.07.067

Hummers, W.S., Offeman, R.E., 1958. Preparation of Graphitic Oxide. Journal of the American Chemical Society 80, 1339. https://doi.org/10.1021/ja01539a017

Ifelebuegu, A.O., Ezenwa, C.P., 2011. Removal of endocrine disrupting chemicals in wastewater treatment by fenton-like oxidation. Water, Air, and Soil Pollution 217, 213–220. https://doi.org/10.1007/s11270-010-0580-0

Im, J.S., Park, S.J., Lee, Y.S., 2007. Preparation and characteristics of electrospun activated carbon materials having meso- and macropores. Journal of Colloid and Interface Science 314, 32–37. https://doi.org/10.1016/j.jcis.2007.05.033

Jawad, A.H., Malek, N.N.A., Abdulhameed, A.S., Razuan, R., 2020a. Synthesis of Magnetic Chitosan-Fly Ash/Fe3O4 Composite for Adsorption of Reactive Orange 16 Dye: Optimization by Box–Behnken Design. Journal of Polymers and the Environment 28, 1068–1082. https://doi.org/10.1007/s10924-020-01669-z

Jawad, A.H., Malek, N.N.A., Abdulhameed, A.S., Razuan, R., 2020b. Synthesis of Magnetic Chitosan-Fly Ash/Fe3O4 Composite for Adsorption of Reactive Orange 16 Dye: Optimization by Box–Behnken Design. Journal of Polymers and the Environment 28, 1068–1082. https://doi.org/10.1007/s10924-020-01669-z

Jiang, N., Shang, R., Heijman, S.G.J., Rietveld, L.C., 2020. Adsorption of triclosan, trichlorophenol and phenol by high-silica zeolites: Adsorption efficiencies and

mechanisms. Separation and Purification Technology 235. https://doi.org/10.1016/j.seppur.2019.116152

Jun, B.M., Hwang, H.S., Heo, J., Han, J., Jang, M., Sohn, J., Park, C.M., Yoon, Y., 2019. Removal of selected endocrine-disrupting compounds using Al-based metal organic framework: Performance and mechanism of competitive adsorption. Journal of Industrial and Engineering Chemistry 79, 345–352. https://doi.org/10.1016/j.jiec.2019.07.009

Kang, J.H., Kondo, F., 2006. Bisphenol A in the surface water and freshwater snail collected from rivers around a secure landfill. Bulletin of Environmental Contamination and Toxicology 76, 113–118. https://doi.org/10.1007/s00128-005-0896-4

Kang, J.H., Kondo, F., 2002. Effects of bacterial counts and temperature on the biodegradation of bisphenol A in river water. Chemosphere 49, 493–498. https://doi.org/10.1016/S0045-6535(02)00315-6

Karau, A., Benken, C., Thömmes, J., Kula, M.R., 1997. The influence of particle size distribution and operating conditions on the adsorption performance in fluidized beds. Biotechnology and Bioengineering 55, 54–64. https://doi.org/10.1002/(SICI)1097-0290(19970705)55:1<54::AID-BIT7>3.0.CO;2-W

Karimi, F., Ayati, A., Tanhaei, B., Sanati, A.L., Afshar, S., Kardan, A., Dabirifar, Z., Karaman, C., 2022. Removal of metal ions using a new magnetic chitosan nano-bio-adsorbent; A powerful approach in water treatment. Environmental Research 203. https://doi.org/10.1016/j.envres.2021.111753

Karimi-Maleh, H., Ayati, A., Davoodi, R., Tanhaei, B., Karimi, F., Malekmohammadi, S., Orooji, Y., Fu, L., Sillanpää, M., 2021. Recent advances in using of chitosan-based adsorbents for removal of pharmaceutical contaminants: A review. Journal of Cleaner Production 291. https://doi.org/10.1016/j.jclepro.2021.125880

Kim, S., Chu, K.H., Al-Hamadani, Y.A.J., Park, C.M., Jang, M., Kim, D.H., Yu, M., Heo, J., Yoon, Y., 2018. Removal of contaminants of emerging concern by membranes in water and wastewater: A review. Chemical Engineering Journal 335, 896–914. https://doi.org/10.1016/j.cej.2017.11.044

Kong, Q., Shi, X., Ma, W., Zhang, F., Yu, T., Zhao, F., Zhao, D., Wei, C., 2021. Strategies to improve the adsorption properties of graphene-based adsorbent towards heavy

metal ions and their compound pollutants: A review. Journal of Hazardous Materials. https://doi.org/10.1016/j.jhazmat.2021.125690

Kozyatnyk, I., Oesterle, P., Wurzer, C., Mašek, O., Jansson, S., 2021. Removal of contaminants of emerging concern from multicomponent systems using carbon dioxide activated biochar from lignocellulosic feedstocks. Bioresource Technology 340, 125561. https://doi.org/10.1016/j.biortech.2021.125561

Kuo, C.Y., Wu, C.H., Wu, J.Y., 2008. Adsorption of direct dyes from aqueous solutions by carbon nanotubes: Determination of equilibrium, kinetics and thermodynamics parameters. Journal of Colloid and Interface Science 327, 308–315. https://doi.org/10.1016/j.jcis.2008.08.038

Kuśmierek, K., Świątkowski, A., 2015. The influence of different agitation techniques on the adsorption kinetics of 4-chlorophenol on granular activated carbon. Reaction Kinetics, Mechanisms and Catalysis 116, 261–271. https://doi.org/10.1007/s11144-015-0889-1

Kyzas, G.Z., Bikiaris, D.N., Mitropoulos, A.C., 2017. Chitosan adsorbents for dye removal: a review. Polymer International 66, 1800–1811. https://doi.org/10.1002/pi.5467

Kyzas, G.Z., Bikiaris, D.N., Seredych, M., Bandosz, T.J., Deliyanni, E.A., 2014. Removal of dorzolamide from biomedical wastewaters with adsorption onto graphite oxide/poly(acrylic acid) grafted chitosan nanocomposite. Bioresource Technology 152, 399–406. https://doi.org/10.1016/j.biortech.2013.11.046

Kyzas, G.Z., Matis, K.A., 2015. Nanoadsorbents for pollutants removal: A review. Journal of Molecular Liquids 203, 159–168. https://doi.org/10.1016/j.molliq.2015.01.004

Ladavos, A.K., Katsoulidis, A.P., Iosifidis, A., Triantafyllidis, K.S., Pinnavaia, T.J., Pomonis, P.J., 2012. The BET equation, the inflection points of N 2 adsorption isotherms and the estimation of specific surface area of porous solids. Microporous and Mesoporous Materials 151, 126–133. https://doi.org/10.1016/j.micromeso.2011.11.005

Lagaly, G., Ogawa, M., Dékány, I., 2006. Chapter 7.3 Clay Mineral Organic Interactions. Developments in Clay Science 1, 309–377. https://doi.org/10.1016/S1572-4352(05)01010-X

Lagergren, S., 1898. Zur theorie Der Sogenannten adsorption geloster stoffe, Kungliga Svenska Vetenskapsakademiens.

Lai, C., He, H., Xie, W., Fan, S., Huang, H., Wang, Y., Huang, B., Pan, X., 2022. Adsorption and photochemical capacity on 17α-ethinylestradiol by char produced in the thermo treatment process of plastic waste. Journal of Hazardous Materials 423. https://doi.org/10.1016/j.jhazmat.2021.127066

Langdon, K.A., Warne, M.S.J., Smernik, R.J., Shareef, A., Kookana, R.S., 2011. Selected personal care products and endocrine disruptors in biosolids: An Australia-wide survey. Science of the Total Environment 409, 1075–1081. https://doi.org/10.1016/j.scitotenv.2010.12.013

Langmuir, I, 1918. The Adsorption of Gases on Plane Surfaces of Glass, Mica and Platinum. Journal of the American Chemical Society 40, 1361–1403. https://doi.org/10.1021/ja01269a066

Langmuir, Irving, 1918. The adsorption of gases on plane surfaces of glass, mica and platinum. Journal of the American Chemical Society 40, 1361–1403. https://doi.org/10.1021/ja02242a004

Lawrie, G., Keen, I., Drew, B., Chandler-Temple, A., Rintoul, L., Fredericks, P., Grøndahl, L., 2007. Interactions between alginate and chitosan biopolymers characterized using FTIR and XPS. Biomacromolecules 8, 2533–2541. https://doi.org/10.1021/bm070014y

Lei, C., Hu, Y., He, M., 2013. Adsorption characteristics of triclosan from aqueous solution onto cetylpyridinium bromide (CPB) modified zeolites. CHEMICAL ENGINEERING JOURNAL 219, 361–370. https://doi.org/10.1016/j.cej.2012.12.099

Leudjo Taka, A., Klink, M.J., Yangkou Mbianda, X., Naidoo, E.B., 2021. Chitosan nanocomposites for water treatment by fixed-bed continuous flow column adsorption: A review. Carbohydrate Polymers 255, 117398. https://doi.org/10.1016/j.carbpol.2020.117398

Li, Y., Umer, R., Samad, Y.A., Zheng, L., Liao, K., 2013. The effect of the ultrasonication pre-treatment of graphene oxide (GO) on the mechanical properties of GO/polyvinyl alcohol composites. Carbon 55, 321–327. https://doi.org/10.1016/j.carbon.2012.12.071

Limousin, G., Gaudet, J.P., Charlet, L., Szenknect, S., Barthès, V., Krimissa, M., 2007. Sorption isotherms: A review on physical bases, modeling and measurement. Applied Geochemistry 22, 249–275. https://doi.org/10.1016/j.apgeochem.2006.09.010

Lin, X., Xu, J., Keller, A.A., He, L., Gu, Y., Zheng, W., Sun, D., Lu, Z., Huang, J., Huang, X., Li, G., 2020. Occurrence and risk assessment of emerging contaminants in a water reclamation and ecological reuse project. Science of the Total Environment 744. https://doi.org/10.1016/j.scitotenv.2020.140977

Lin, Z., Waller, G.H., Liu, Y., Liu, M., Wong, C.P., 2013. Simple preparation of nanoporous few-layer nitrogen-doped graphene for use as an efficient electrocatalyst for oxygen reduction and oxygen evolution reactions. Carbon 53, 130–136. https://doi.org/10.1016/j.carbon.2012.10.039

Liu, F.F., Zhao, J., Wang, S., Du, P., Xing, B., 2014. Effects of solution chemistry on adsorption of selected pharmaceuticals and personal care products (PPCPs) by graphenes and carbon nanotubes. Environmental Science and Technology 48, 13197–13206. https://doi.org/10.1021/es5034684

Liu, G., Ma, J., Li, X., Qin, Q., 2009. Adsorption of bisphenol A from aqueous solution onto activated carbons with different modification treatments. Journal of Hazardous Materials 164, 1275–1280. https://doi.org/10.1016/j.jhazmat.2008.09.038

Liu, J., Carr, S.A., 2013. Removal of Estrogenic Compounds from Aqueous Solutions Using Zeolites. Water Environment Research 85, 2157–2163. https://doi.org/10.2175/106143013x13736496909356

Liu, J., Wang, R., Huang, B., Lin, C., Zhou, J., Pan, X., 2012. Biological effects and bioaccumulation of steroidal and phenolic endocrine disrupting chemicals in high-back crucian carp exposed to wastewater treatment plant effluents. Environmental Pollution 162, 325–331. https://doi.org/10.1016/j.envpol.2011.11.036

Liu, S.H., Tang, W.T., 2020. Photodecomposition of ibuprofen over g-C3N4/Bi2WO6/rGO heterostructured composites under visible/solar light. Science of the Total Environment 731. https://doi.org/10.1016/j.scitotenv.2020.139172

Liu, T., Han, X., Wang, Y., Yan, L., Du, B., Wei, Q., Wei, D., 2017. Magnetic chitosan/anaerobic granular sludge composite: Synthesis, characterization and application in heavy metal ions removal. Journal of Colloid and Interface Science 508, 405–414. https://doi.org/10.1016/j.jcis.2017.08.067

Liu, X., Cao, Z., Yuan, Z., Zhang, J., Guo, X., Yang, Y., He, F., Zhao, Y., Xu, J., 2018. Insight into the kinetics and mechanism of removal of aqueous chlorinated nitroaromatic antibiotic chloramphenicol by nanoscale zero-valent iron. Chemical Engineering Journal 334, 508–518. https://doi.org/10.1016/j.cej.2017.10.060

Loganathan, P., Vigneswaran, S., Kandasamy, J., 2013. Enhanced removal of nitrate from water using surface modification of adsorbents - A review. Journal of Environmental Management 131, 363–374. https://doi.org/10.1016/j.jenvman.2013.09.034

López-Velázquez, K., Guzmán-Mar, J.L., Saldarriaga-Noreña, H.A., Murillo-Tovar, M.A., Hinojosa-Reyes, L., Villanueva-Rodríguez, M., 2021. Occurrence and seasonal distribution of five selected endocrine-disrupting compounds in wastewater treatment plants of the Metropolitan Area of Monterrey, Mexico: The role of water quality parameters. Environmental Pollution 269. https://doi.org/10.1016/j.envpol.2020.116223

Lu, J., Wu, Jie, Wu, Jun, Zhang, C., Luo, Y., 2020. Adsorption and Desorption of Steroid Hormones by Microplastics in Seawater. Bulletin of Environmental Contamination and Toxicology. https://doi.org/10.1007/s00128-020-02784-2

Lu, Y., Jiang, M., Wang, C., Wang, Y., Yang, W., 2014. Impact of molecular size on two antibiotics adsorption by porous resins. Journal of the Taiwan Institute of Chemical Engineers 45, 955–961. https://doi.org/10.1016/j.jtice.2013.09.009

Lu, Y., Zhang, S., Yin, J., Bai, C., Zhang, J., Li, Y., Yang, Y., Ge, Z., Zhang, M., Wei, L., Ma, M., Ma, Y., Chen, Y., 2017. Mesoporous activated carbon materials with ultrahigh mesopore volume and effective specific surface area for high performance supercapacitors. Carbon 124, 64–71. https://doi.org/10.1016/j.carbon.2017.08.044

Luo, Z., Li, H., Yang, Y., Lin, H., Yang, Z., 2017. Adsorption of 17α-ethinylestradiol from aqueous solution onto a reduced graphene oxide-magnetic composite. Journal of the Taiwan Institute of Chemical Engineers 80, 797–804. https://doi.org/10.1016/j.jtice.2017.09.028

Ly, Q.V., Maqbool, T., Zhang, Z., van Le, Q., An, X., Hu, Y., Cho, J., Li, J., Hur, J., 2021. Characterization of dissolved organic matter for understanding the adsorption on nanomaterials in aquatic environment: A review. Chemosphere. https://doi.org/10.1016/j.chemosphere.2020.128690

Ma, J.W., Lee, W.J., Bae, J.M., Jeong, K.S., Oh, S.H., Kim, J.H., Kim, S.H., Seo, J.H., Ahn, J.P., Kim, H., Cho, M.H., 2015. Carrier Mobility Enhancement of Tensile Strained Si and SiGe Nanowires via Surface Defect Engineering. Nano Letters 15, 7204–7210. https://doi.org/10.1021/acs.nanolett.5b01634

Madadrang, C.J., Kim, H.Y., Gao, G., Wang, N., Zhu, J., Feng, H., Gorring, M., Kasner, M.L., Hou, S., 2012. Adsorption behavior of EDTA-graphene oxide for Pb (II)

removal. ACS Applied Materials and Interfaces 4, 1186–1193. https://doi.org/10.1021/am201645g

Maia, G.S., de Andrade, J.R., da Silva, M.G.C., Vieira, M.G.A., 2019a. Adsorption of diclofenac sodium onto commercial organoclay: Kinetic, equilibrium and thermodynamic study. Powder Technology 345, 140–150. https://doi.org/10.1016/j.powtec.2018.12.097

Maia, G.S., de Andrade, J.R., da Silva, M.G.C., Vieira, M.G.A., 2019b. Adsorption of diclofenac sodium onto commercial organoclay: Kinetic, equilibrium and thermodynamic study. Powder Technology 345, 140–150. https://doi.org/10.1016/j.powtec.2018.12.097

Maia, G.S., de Andrade, J.R., da Silva, M.G.C., Vieira, M.G.A., 2019c. Adsorption of diclofenac sodium onto commercial organoclay: Kinetic, equilibrium and thermodynamic study. Powder Technology 345, 140–150. https://doi.org/10.1016/j.powtec.2018.12.097

Maleki, A., Paydar, R., 2015. Graphene oxide-chitosan bionanocomposite: a highly efficient nanocatalyst for the one-pot three-component synthesis of trisubstituted imidazoles under solvent-free conditions. RSC Advances 5, 33177–33184. https://doi.org/10.1039/c5ra03355a

Mallakpour, S., Dinari, M., 2011. Preparation and characterization of new organoclays using natural amino acids and Cloisite Na+. Applied Clay Science 51, 353–359. https://doi.org/10.1016/j.clay.2010.12.028

Malwal, D., Gopinath, P., 2017. Silica Stabilized Magnetic-Chitosan Beads for Removal of Arsenic from Water. Colloids and Interface Science Communications 19, 14–19. https://doi.org/10.1016/j.colcom.2017.06.003

Mansouriieh, N., Sohrabi, M.R., Khosravi, M., 2016. Adsorption kinetics and thermodynamics of organophosphorus profenofos pesticide onto Fe/Ni bimetallic nanoparticles. International Journal of Environmental Science and Technology 13, 1393–1404. https://doi.org/10.1007/s13762-016-0960-0

Martins, J.T., Guimarães, C.H., Silva, P.M., Oliveira, R.L., Prediger, P., 2021. Enhanced removal of basic dye using carbon nitride/graphene oxide nanocomposites as adsorbents: high performance, recycling, and mechanism. Environmental Science and Pollution Research 28, 3386–3405. https://doi.org/10.1007/s11356-020-10779-z

Marysková, M., Schaabová, M., Tománková, H., Novotny, V., Rysová, M., 2020. Wastewater Treatment by Novel Polyamide/Polyethylenimine Nanofibers with Immobilized Laccase. Water 12, 588.

Mathews, B.A.P., Zayas, I., 1989. Particle s i z e and shape e f f e c t s on adsorption r a t e parameters 115, 41–55.

McCusker, L.B., Liebau, F., Engelhardt, G., 2001. Nomenclature of structural and compositional characteristics of ordered microporous and mesoporous materials with inorganic hosts: (IUPAC recommendations 2001). Pure and Applied Chemistry 73, 381–394. https://doi.org/10.1351/pac200173020381

McLauchlin, A.R., Thomas, N.L., 2009. Preparation and thermal characterisation of poly(lactic acid) nanocomposites prepared from organoclays based on an amphoteric surfactant. Polymer Degradation and Stability 94, 868–872. https://doi.org/10.1016/j.polymdegradstab.2009.01.012

Menk, J. de J., do Nascimento, A.I.S., Leite, F.G., de Oliveira, R.A., Jozala, A.F., de Oliveira Junior, J.M., Chaud, M.V., Grotto, D., 2019. Biosorption of pharmaceutical products by mushroom stem waste. Chemosphere 237. https://doi.org/10.1016/j.chemosphere.2019.124515

Milanovic, M., Duric, L., Milosevic, N., Milic, N., 2021. Comprehensive insight into triclosan—from widespread occurrence to health outcomes occurrence. Environmental Science and Pollution Research.

Milonjić, S.K., 2007a. A consideration of the correct calculation of thermodynamic parameters of adsorption. Journal of the Serbian Chemical Society 72, 1363–1367. https://doi.org/10.2298/JSC0712363M

Milonjić, S.K., 2007b. A consideration of the correct calculation of thermodynamic parameters of adsorption. Journal of the Serbian Chemical Society 72, 1363–1367. https://doi.org/10.2298/JSC0712363M

Misaelides, P., 2011. Application of natural zeolites in environmental remediation: A short review. Microporous and Mesoporous Materials 144, 15–18. https://doi.org/10.1016/j.micromeso.2011.03.024

Mohseni Kafshgari, M., Tahermansouri, H., 2017. Development of a graphene oxide/chitosan nanocomposite for the removal of picric acid from aqueous solutions: Study of sorption parameters. Colloids and Surfaces B: Biointerfaces 160, 671–681. https://doi.org/10.1016/j.colsurfb.2017.10.019

Montagner, C.C., Jardim, W.F., Von der Ohe, P.C., Umbuzeiro, G.A., 2014. Occurrence and potential risk of triclosan in freshwaters of São Paulo, Brazil-the need for regulatory actions. Environmental Science and Pollution Research 21, 1850–1858. https://doi.org/10.1007/s11356-013-2063-5

Montagner, C.C., Vidal, C., Acayaba, R.D., 2017. Contaminantes emergentes em matrizes aquáticas do Brasil: Cenário atual e aspectos analíticos, ecotoxicológicos e regulatórios. Quimica Nova 40, 1094–1110. https://doi.org/10.21577/0100-4042.20170091

Mordor Intelligence, 2021. BISPHENOL A (BPA) MARKET - GROWTH, TRENDS, COVID-19 IMPACT, AND FORECASTS (2022 - 2027).

Morrall, D., McAvoy, D., Schatowitz, B., Inauen, J., Jacob, M., Hauk, A., Eckhoff, W., 2004. A field study of triclosan loss rates in river water (Cibolo Creek, TX). Chemosphere 54, 653–660. https://doi.org/10.1016/j.chemosphere.2003.08.002

Motahharifar, N., Nasrollahzadeh, M., Taheri-Kafrani, A., Varma, R.S., Shokouhimehr, M., 2020. Magnetic chitosan-copper nanocomposite: A plant assembled catalyst for the synthesis of amino- and N-sulfonyl tetrazoles in eco-friendly media. Carbohydrate Polymers 232, 115819. https://doi.org/10.1016/j.carbpol.2019.115819

Mumit, M.A., Pal, T.K., Alam, M.A., Islam, M.A.A.A.A., Paul, S., Sheikh, M.C., 2020. DFT studies on vibrational and electronic spectra, HOMO–LUMO, MEP, HOMA, NBO and molecular docking analysis of benzyl-3-N-(2,4,5-trimethoxyphenylmethylene)hydrazinecarbodithioate. Journal of Molecular Structure 1220, 128715. https://doi.org/10.1016/j.molstruc.2020.128715

Narayanan, D.P., Gopalakrishnan, A., Yaakob, Z., Sugunan, S., Narayanan, B.N., 2020. A facile synthesis of clay – graphene oxide nanocomposite catalysts for solvent free multicomponent Biginelli reaction. Arabian Journal of Chemistry 13, 318–334. https://doi.org/10.1016/j.arabjc.2017.04.011

Nascimento, R.F., Melo, D.Q., Lima, A.C.A., Barros, A.L., Vidal, C.B., Raulino, G.S.C., 2014. Adsorção: Aspectos teóricos e aplicações ambientais, Adsorção aspescyos teóricos e aplicações ambientais.

Nasri, A., Mezni, A., Lafon, P.-A., Wahbi, A., Cubedo, N., Clair, P., Harrath, A.H., Beyrem, H., Rossel, M., Perrier, V., 2021. Ethinylestradiol (EE2) residues from birth control pills impair nervoussystem development and swimming behavior of zebrafish larvae. Science of the Total Environment.

Nayara, T., Souza, V. De, Maria, S., Carvalho, L. De, Gurgel, Melissa, Vieira, A., Gurgel, Meuris, Barros, S., 2018. Applied Surface Science Adsorption of basic dyes onto activated carbon : Experimental and theoretical investigation of chemical reactivity of basic dyes using DFT-based descriptors. Applied Surface Science 448, 662–670. https://doi.org/10.1016/j.apsusc.2018.04.087

Nazraz, M., Yamini, Y., Asiabi, H., 2019. Chitosan-based sorbent for efficient removal and extraction of ciprofloxacin and norfloxacin from aqueous solutions. Microchimica Acta 186. https://doi.org/10.1007/s00604-019-3563-x

Neves, T. de F., Assano, P.K., Sabino, L.R., Nunes, W.B., Prediger, P., 2020. Influence of Adsorbent/Adsorbate Interactions on the Removal of Cationic Surfactants from Water by Graphene Oxide. Water, Air, and Soil Pollution 231. https://doi.org/10.1007/s11270-020-04669-w

Nishi, I., Kawakami, T., Onodera, S., 2008. Monitoring of triclosan in the surface water of the Tone Canal, Japan. Bulletin of Environmental Contamination and Toxicology 80, 163–166. https://doi.org/10.1007/s00128-007-9338-9

Novoselov, K.S., 2011. Nobel Lecture: Graphene: Materials in the Flatland. Reviews of Modern Physics 83, 837–849. https://doi.org/10.1103/RevModPhys.83.837

Nowak, S., Lafon, S., Caquineau, S., Journet, E., Laurent, B., 2018. Quantitative study of the mineralogical composition of mineral dust aerosols by X-ray diffraction. Talanta 186, 133–139. https://doi.org/10.1016/j.talanta.2018.03.059

Olewnik-Kruszkowska, E., Gierszewska, M., Jakubowska, E., Tarach, I., Sedlarik, V., Pummerova, M., 2019. Antibacterial films based on PVA and PVA-chitosan modified with poly(hexamethylene guanidine). Polymers 11. https://doi.org/10.3390/polym11122093

Oliveira, L.C.A., Rios, R.V.R.A., Fabris, J.D., Sapag, K., Garg, V.K., Lago, R.M., 2003a. Clay-iron oxide magnetic composites for the adsorption of contaminants in water. Applied Clay Science 22, 169–177. https://doi.org/10.1016/S0169-1317(02)00156-4

Oliveira, L.C.A., Rios, R.V.R.A., Fabris, J.D., Sapag, K., Garg, V.K., Lago, R.M., 2003b. Clay-iron oxide magnetic composites for the adsorption of contaminants in water. Applied Clay Science 22, 169–177. https://doi.org/10.1016/S0169-1317(02)00156-4

Oliveira, M.F., da Silva, M.G.C., Vieira, M.G.A., 2019. Equilibrium and kinetic studies of caffeine adsorption from aqueous solutions on thermally modified Verde-lodo

bentonite. Applied Clay Science 168, 366–373. https://doi.org/10.1016/j.clay.2018.12.011

Parida, V.K., Saidulu, D., Majumder, A., Srivastava, A., Gupta, B., Gupta, A.K., 2021a. Emerging contaminants in wastewater: A critical review on occurrence, existing legislations, risk assessment, and sustainable treatment alternatives. Journal of Environmental Chemical Engineering. https://doi.org/10.1016/j.jece.2021.105966

Parida, V.K., Saidulu, D., Majumder, A., Srivastava, A., Gupta, B., Gupta, A.K., 2021b. Emerging contaminants in wastewater: A critical review on occurrence, existing legislations, risk assessment, and sustainable treatment alternatives. Journal of Environmental Chemical Engineering 9, 105966. https://doi.org/10.1016/j.jece.2021.105966

Park, Y., Ayoko, G.A., Frost, R.L., 2011. Application of organoclays for the adsorption of recalcitrant organic molecules from aqueous media. Journal of Colloid and Interface Science 354, 292–305. https://doi.org/10.1016/j.jcis.2010.09.068

Park, Y., Sun, Z., Ayoko, G.A., Frost, R.L., 2014. Bisphenol A sorption by organo-montmorillonite: Implications for the removal of organic contaminants from water 107, 249–256.

Parladé, E., Hom-Diaz, A., Blánquez, P., Martínez-Alonso, M., Vicent, T., Gaju, N., 2018. Effect of cultivation conditions on B-estradiol removal in laboratory and pilot-plant photobioreactors by an algal-bacterial consortium treating urban wastewater. Water Research 137, 86–96. https://doi.org/10.1016/j.watres.2018.02.060

Pelekani, C., Snoeyink, V.L., 1999. Competitive adsorption in natural water: Role of activated carbon pore size. Water Research 33, 1209–1219. https://doi.org/10.1016/S0043-1354(98)00329-7

Peng, W., Li, H., Liu, Y., Song, S., 2017. A review on heavy metal ions adsorption from water by graphene oxide and its composites. Journal of Molecular Liquids 230, 496–504. https://doi.org/10.1016/j.molliq.2017.01.064

Pérez-Guardiola, A., Pérez-Jiménez, A.J., Sancho-García, J.C., 2017. Studying physisorption processes and molecular friction of cycloparaphenylene molecules on graphene nano-sized flakes: Role of π···π and CH···π interactions. Molecular Systems Design and Engineering 2, 253–262. https://doi.org/10.1039/c7me00024c

Phuekphong, A.F., Imwiset, K.J., Ogawa, M., 2020. Organically modified bentonite as an efficient and reusable adsorbent for triclosan removal from water. Langmuir. https://doi.org/10.1021/acs.langmuir.0c00407

Piccin, J.S., Cadaval, T.R.S.A., de Pinto, L.A.A., Dotto, G.L., 2017. Adsorption isotherms in liquid phase: Experimental, modeling, and interpretations, in: Adsorption Processes for Water Treatment and Purification. Springer International Publishing, pp. 19–51. https://doi.org/10.1007/978-3-319-58136-1_2

Poirier, J.C., Cahoreau, C., Combarnous, Y., 2006. Cross-Inhibitions of Human Chorionic Gonadotropin (hCG) and Ethynyl-Estradiol (EE2) at Pico-Molar Concentrations on Mouse Leydig Tumor Cells (mLTC) Progesterone Secretion. Epidemiology 17, 376.

Pojana, G., Gomiero, A., Jonkers, N., Marcomini, A., 2007. Natural and synthetic endocrine disrupting compounds (EDCs) in water, sediment and biota of a coastal lagoon. Environment International 33, 929–936. https://doi.org/10.1016/j.envint.2007.05.003

Prediger, P., Cheminski, T., de Figueiredo Neves, T., Nunes, W.B., Sabino, L., Picone, C.S.F., Oliveira, R.L., Correia, C.R.D., 2018. Graphene oxide nanomaterials for the removal of non-ionic surfactant from water. Journal of Environmental Chemical Engineering 6, 1536–1545. https://doi.org/10.1016/j.jece.2018.01.072

Prokić, D., Vukčević, M., Kalijadis, A., Maletić, M., Babić, B., Đurkić, T., 2020. Removal of Estrone, 17β-Estradiol, and 17α-Ethinylestradiol from Water by Adsorption onto Chemically Modified Activated Carbon Cloths. Fibers and Polymers 21, 2263–2274. https://doi.org/10.1007/s12221-020-9758-2

Racar, M, Dolar, D., Karadadic, K., Cavarovic, N., Glumac, N., Asperger, D., Kosutic, K., 2020. Challenges of municipal wastewater reclamation for irrigation by MBR and NF/RO: Physico-chemical and microbiological parameters, and emerging contaminantsirrigation. Science of the Total Environment 722, 137959.

Racar, M., Dolar, D., Karadakić, K., Čavarović, N., Glumac, N., Ašperger, D., Košutić, K., 2020. Challenges of municipal wastewater reclamation for irrigation by MBR and NF/RO: Physico-chemical and microbiological parameters, and emerging contaminants. Science of the Total Environment 722. https://doi.org/10.1016/j.scitotenv.2020.137959

Rad, L.R., Anbia, M., 2021. Zeolite-based composites for the adsorption of toxic matters from water: A review. Journal of Environmental Chemical Engineering 9. https://doi.org/10.1016/j.jece.2021.106088

Ramaswamy, B.R., Shanmugam, G., Velu, G., Rengarajan, B., Larsson, D.G.J., 2011. GC-MS analysis and ecotoxicological risk assessment of triclosan, carbamazepine

and parabens in Indian rivers. Journal of Hazardous Materials 186, 1586–1593. https://doi.org/10.1016/j.jhazmat.2010.12.037

Rathi, B.S., Kumar, P.S., 2021. Application of adsorption process for effective removal of emerging contaminants from water and wastewater. Environmental Pollution 280, 116995. https://doi.org/10.1016/j.envpol.2021.116995

Regti, A., Ben, H., Ayouchia, E., Rachid, M., Eddine, S., Anane, H., El, M., 2016. Applied Surface Science Experimental and theoretical study using DFT method for the competitive adsorption of two cationic dyes from wastewaters. Applied Surface Science 390, 311–319. https://doi.org/10.1016/j.apsusc.2016.08.059

Reichenberg, D., 1953. Properties of Ion-Exchange Resins in Relation to their Structure. III. Kinetics of Exchange. Journal of the American Chemical Society 75, 589–597. https://doi.org/10.1021/ja01099a022

Rempel, A., Gutkoski, J.P., Nazari, M.T., Biolchi, G.N., Cavanhi, V.A.F., Treichel, H., Colla, L.M., 2021. Current advances in microalgae-based bioremediation and other technologies for emerging contaminants treatment. Science of the Total Environment 772, 144918. https://doi.org/10.1016/j.scitotenv.2020.144918

Ren, X., Chen, C., Nagatsu, M., Wang, X., 2011. Carbon nanotubes as adsorbents in environmental pollution management: A review. Chemical Engineering Journal 170, 395–410. https://doi.org/10.1016/j.cej.2010.08.045

Resende, J., Andrade, D., Gurgel, Melissa, Vieira, A., Gurgel, Meuris, 2020. Oxidative degradation of pharmaceutical losartan potassium with N-doped hierarchical porous carbon and peroxymonosulfate. Chemical Engineering Journal 382, 122971. https://doi.org/10.1016/j.cej.2019.122971

Rivera-Utrilla, J., Sánchez-Polo, M., Ferro-García, M.Á., Prados-Joya, G., Ocampo-Pérez, R., 2013. Pharmaceuticals as emerging contaminants and their removal from water. A review. Chemosphere 93, 1268–1287. https://doi.org/10.1016/j.chemosphere.2013.07.059

Rivera-utrilla, J., Sánchez-polo, M., Ferro-garcía, M.Á., Prados-joya, G., Ocampo-Pérez, R., 2013. Pharmaceuticals as emerging contaminants and their removal from water . A review. Chemosphere 93, 1268–1287.

Rodriguez-Narvaez, O.M., Peralta-Hernandez, J.M., Goonetilleke, A., Bandala, E.R., 2017. Treatment technologies for emerging contaminants in water: A review. Chemical Engineering Journal 323, 361–380. https://doi.org/10.1016/j.cej.2017.04.106

Rojas, S., Navarro, J.A.R., Horcajada, P., 2021. Metal-organic frameworks for the removal of the emerging contaminant atenolol under real conditions. Dalton Transactions 50, 2493–2500. https://doi.org/10.1039/d0dt03637d

Rosenfeldt, E.J., Chen, P.J., Kullman, S., Linden, K.G., 2007. Destruction of estrogenic activity in water using UV advanced oxidation. Science of the Total Environment 377, 105–113. https://doi.org/10.1016/j.scitotenv.2007.01.096

Rotaru, I., Varvara, S., Gaina, L., Maria, L., 2014. Applied Surface Science Antibacterial drugs as corrosion inhibitors for bronze surfaces in acidic solutions. Applied Surface Science 321, 188–196. https://doi.org/10.1016/j.apsusc.2014.09.201

Rudder, J. De, Wiele, T. Van De, Dhooge, W., Comhaire, F., Verstraete, W., 2004. Advanced water treatment with manganese oxide for the removal of 17 a - ethynylestradiol (EE2) 38, 184–192. https://doi.org/10.1016/j.watres.2003.09.018

Ruiz, B., Cabrita, I., Mestre, A.S., Parra, J.B., Pires, J., Carvalho, A.P., Ania, C.O., 2010. Surface heterogeneity effects of activated carbons on the kinetics of paracetamol removal from aqueous solution. Applied Surface Science 256, 5171–5175. https://doi.org/10.1016/j.apsusc.2009.12.086

Sáaedi, A., Yousefi, R., Jamali-Sheini, F., Zak, A.K., Cheraghizade, M., Mahmoudian, M.R., Baghchesara, M.A., Dezaki, A.S., 2016. XPS studies and photocurrent applications of alkali-metals-doped ZnO nanoparticles under visible illumination conditions. Physica E: Low-Dimensional Systems and Nanostructures 79, 113–118. https://doi.org/10.1016/j.physe.2015.12.002

Saha, P., Chowdhury, S., 2011. Insight Into Adsorption Thermodynamics, in: Thermodynamics. pp. 349–363.

Saheed, I.O., Oh, W. da, Suah, F.B.M., 2021. Chitosan modifications for adsorption of pollutants – A review. Journal of Hazardous Materials. https://doi.org/10.1016/j.jhazmat.2020.124889

Sahoo, G., Sarkar, N., Swain, S.K., 2018. The effect of reduced graphene oxide intercalated hybrid organoclay on the dielectric properties of polyvinylidene fluoride nanocomposite films. Applied Clay Science 162, 69–82. https://doi.org/10.1016/j.clay.2018.05.008

Sahu, S., Pahi, S., Tripathy, S., Singh, S.K., Behera, A., Sahu, U.K., Patel, R.K., 2020. Adsorption of methylene blue on chemically modified lychee seed biochar: Dynamic, equilibrium, and thermodynamic study. Journal of Molecular Liquids 315. https://doi.org/10.1016/j.molliq.2020.113743

Salahuddin, N.A., EL-Daly, H.A., el Sharkawy, R.G., Nasr, B.T., 2018. Synthesis and efficacy of PPy/CS/GO nanocomposites for adsorption of ponceau 4R dye, Polymer. Elsevier Ltd. https://doi.org/10.1016/j.polymer.2018.04.053

Sauvé, S., Desrosiers, M., 2014a. A review of what is an emerging contaminant. Chemistry Central Journal 8, 1–7. https://doi.org/10.1186/1752-153X-8-15

Sauvé, S., Desrosiers, M., 2014b. A review of what is an emerging contaminant, Chemistry Central Journal.

Schirmer, W.N., 2007. Avaliação do desempenho de nanotubos de carbono "cup-stacked" na remoção de compostos orgânicos voláteis (COV) de correntes gasosas 91.

Sekar, M., Sakthi, V., Rengaraj, S., 2004. Kinetics and equilibrium adsorption study of lead(II) onto activated carbon prepared from coconut shell. Journal of Colloid and Interface Science 279, 307–313. https://doi.org/10.1016/j.jcis.2004.06.042

Sekulic, M.T., Boskovic, N., Slavkovic, A., Garunovic, J., Kolakovic, S., Pap, S., 2019. Surface functionalised adsorbent for emerging pharmaceutical removal: Adsorption performance and mechanisms. Process Safety and Environmental Protection 125, 50–63. https://doi.org/10.1016/j.psep.2019.03.007

Shahid, M.K., Kashif, A., Fuwad, A., Choi, Y., 2021. Current advances in treatment technologies for removal of emerging contaminants from water – A critical review. Coordination Chemistry Reviews. https://doi.org/10.1016/j.ccr.2021.213993

Shang, J., Guo, Y., He, D., Qu, W., Tang, Y., Zhou, L., Zhu, R., 2021. A novel graphene oxide-dicationic ionic liquid composite for Cr(VI) adsorption from aqueous solutions. Journal of Hazardous Materials 416. https://doi.org/10.1016/j.jhazmat.2021.125706

Sharma, J., Mishra, I.M., Kumar, V., 2016. Mechanistic study of photo-oxidation of Bisphenol-A (BPA) with hydrogen peroxide (H2O2) and sodium persulfate (SPS). Journal of Environmental Management 166, 12–22. https://doi.org/10.1016/j.jenvman.2015.09.043

Sheela, N.R., Muthu, S., Sampathkrishnan, S., 2014. Molecular orbital studies (hardness, chemical potential and electrophilicity), vibrational investigation and theoretical NBO analysis of 4-4′-(1H-1,2,4-triazol-1-yl methylene) dibenzonitrile based on abinitio and DFT methods. Spectrochimica Acta - Part A: Molecular and Biomolecular Spectroscopy 120, 237–251. https://doi.org/10.1016/j.saa.2013.10.007

Shen, T., Gao, M., 2019. Gemini surfactant modified organo-clays for removal of organic pollutants from water: A review. Chemical Engineering Journal 375, 121910. https://doi.org/10.1016/j.cej.2019.121910

Silva, T.L. da, Silva, M.G.C. da, Vieira, M.G.A., 2021. Palladium adsorption on natural polymeric sericin-alginate particles crosslinked by polyethylene glycol diglycidyl ether. Journal of Environmental Chemical Engineering 9. https://doi.org/10.1016/j.jece.2021.105617

Silva, A.R. V, Ferreira, H.C., 2008. Esmectitas organofílicas: conceitos, estruturas, propriedades, síntese, usos industriais e produtores/fornecedores nacionais e internacionais. Revista Eletrônica de Materiais e Processos 33, 1–11.

Silva, V.A.J., Andrade, P.L., Silva, M.P.C., Bustamante, A.D., de Los Santos Valladares, L., Albino Aguiar, J., 2013. Synthesis and characterization of Fe3O4 nanoparticles coated with fucan polysaccharides. Journal of Magnetism and Magnetic Materials 343, 138–143. https://doi.org/10.1016/j.jmmm.2013.04.062

Singer, H., Müller, S., Tixier, C., Pillonel, L., 2002. Triclosan: Occurrence and fate of a widely used biocide in the aquatic environment: Field measurements in wastewater treatment plants, surface waters, and lake sediments. Environmental Science and Technology 36, 4998–5004. https://doi.org/10.1021/es025750i

Site, A.D., 2001. Factors Affecting Sorption of Organic Compounds in Natural Sorbent/Water Systems and Sorption Coefficients for Selected Pollutants. A Review. Journal of Physical and Chemical Reference Data 187.

Sivaranjanee, R., Kumar, P.S., 2021. A review on remedial measures for effective separation of emerging contaminants from wastewater. Environmental Technology and Innovation. https://doi.org/10.1016/j.eti.2021.101741

Sobhanardakani, S., Zandipak, R., 2018. Cerium dioxide nanoparticles decorated on CuFe2O4 nanofibers as an effective adsorbent for removal of estrogenic contaminants (bisphenol A and 17-α ethinylestradiol) from water. Separation Science and Technology (Philadelphia) 53, 2339–2351. https://doi.org/10.1080/01496395.2018.1457053

Soboleva, T., Zhao, X., Malek, K., Xie, Z., Navessin, T., Holdcroft, S., 2010. On the micro-, meso-, and macroporous structures of polymer electrolyte membrane fuel cell catalyst layers. ACS Applied Materials and Interfaces 2, 375–384. https://doi.org/10.1021/am900600y

Sodré, F.F., Montagner, C.C., Locatelli, M.A.F., Jardim, W.F., 2007. Ocorrência de Interferentes Endócrinos e Produtos Farmacêuticos em Águas Superficiais da Região de Campinas (SP, Brasil). Journal of the Brazilian Society of Ecotoxicology 2, 187–196. https://doi.org/10.5132/jbse.2007.02.012

Sodré, F.F., Pescara, I.C., Montagner, C.C., Jardim, W.F., 2010. Assessing selected estrogens and xenoestrogens in Brazilian surface waters by liquid chromatography-tandem mass spectrometry. Microchemical Journal 96, 92–98. https://doi.org/10.1016/j.microc.2010.02.012

Song, T., Tian, W., Qiao, K., Zhao, J., Chu, M., Du, Z., Wang, L., Xie, W., 2021. Adsorption Behaviors of Polycyclic Aromatic Hydrocarbons and Oxygen Derivatives in Wastewater on N-Doped Reduced Graphene Oxide. Separation and Purification Technology 254, 117565. https://doi.org/10.1016/j.seppur.2020.117565

Song, X., Zhang, Y., Yan, C., Jiang, W., Chang, C., 2013. The Langmuir monolayer adsorption model of organic matter into effective pores in activated carbon. Journal of Colloid and Interface Science 389, 213–219. https://doi.org/10.1016/j.jcis.2012.08.060

Sophia A., C., Lima, E.C., 2018. Removal of emerging contaminants from the environment by adsorption. Ecotoxicology and Environmental Safety 150, 1–17. https://doi.org/10.1016/j.ecoenv.2017.12.026

Sophia, C.A., Lima, E.C., 2018. Removal of emerging contaminants from the environment by adsorption. Ecotoxicology and Environmental Safety 150, 1–17.

Speridião, D.D.C.A., dos Santos, O.A.A., de Almeida Neto, A.F., Vieira, M.G.A., 2014. Characterization of spectrogel organoclay used to adsorption of petroleum derivatives. Materials Science Forum 798–799, 558–563. https://doi.org/10.4028/www.scientific.net/MSF.798-799.558

Stachel, B., Ehrhorn, U., Heemken, O.P., Lepom, P., Reincke, H., Sawal, G., Theobald, N., 2003. Xenoestrogens in the River Elbe and its tributaries. Environmental Pollution 124, 497–507. https://doi.org/10.1016/S0269-7491(02)00483-9

Starling, M.C.V.M., Souza, P.P., Le Person, A., Amorim, C.C., Criquet, J., 2019. Intensification of UV-C treatment to remove emerging contaminants by UV-C/H2O2 and UV-C/S2O82−: Susceptibility to photolysis and investigation of acute toxicity. Chemical Engineering Journal 376, 120856. https://doi.org/10.1016/j.cej.2019.01.135

Taher, F.A., Kamal, F.H., Badawy, N.A., Shrshr, A.E., 2018. Hierarchical magnetic chitosan graphene oxide 3D nanostructure as highly effective adsorbent. Materials Research Bulletin 97, 361–368.

Tan, X. fei, Liu, Y. guo, Gu, Y. ling, Xu, Y., Zeng, G. ming, Hu, X. jiang, Liu, Shao bo, Wang, X., Liu, Si mian, Li, J., 2016. Biochar-based nano-composites for the decontamination of wastewater: A review. Bioresource Technology 212, 318–333. https://doi.org/10.1016/j.biortech.2016.04.093

Tang, L., Xie, Z., Dong, H., Fan, C., Zhou, Y., Wang, J., Zeng, G., Deng, Y., Wang, J., Wei, X., 2016. Removal of bisphenol A by iron nanoparticles doped magnetic ordered mesoporous carbon. https://doi.org/10.1039/C5RA27710H

Tang, Z., Liu, Z. hua, Wang, H., Dang, Z., Liu, Y., 2021a. Occurrence and removal of 17α-ethynylestradiol (EE2) in municipal wastewater treatment plants: Current status and challenges. Chemosphere. https://doi.org/10.1016/j.chemosphere.2021.129551

Tang, Z., Liu, Z. hua, Wang, H., Dang, Z., Liu, Y., 2021b. A review of 17α-ethynylestradiol (EE2) in surface water across 32 countries: Sources, concentrations, and potential estrogenic effects. Journal of Environmental Management 292. https://doi.org/10.1016/j.jenvman.2021.112804

Tang, Z., Liu, Z., Wang, H., Dang, Z., Liu, Y., 2021c. Occurrence and removal of 17a-ethynylestradiol (EE2) in municipal wastewater treatment plants: Current status and challenges. Chemosphere 271.

Taylor, P., Ganguly, S., Dana, K., Mukhopadhyay, T.K., Parya, T.K., Ghatak, S., Ganguly, S., Dana, K., Mukhopadhyay, T.K., Parya, T.K., Ghatak, S., 2013. Organophilic Nano Clay : A Comprehensive Review Organophilic Nano Clay : A Comprehensive Review. Transactions of the Indian Ceramic Society 37–41.

Ten Hulscher, T.E.M., Cornelissen, G., 1996. Effect of temperature on sorption equilibrium and sorption kinetics of organic micropollutants - A review. Chemosphere 32, 609–626. https://doi.org/10.1016/0045-6535(95)00345-2

Thakur, K., Kandasubramanian, B., 2019. Graphene and Graphene Oxide-Based Composites for Removal of Organic Pollutants: A Review. Journal of Chemical and Engineering Data 64, 833–867. https://doi.org/10.1021/acs.jced.8b01057

Thommes, M., Kaneko, K., Neimark, A. V., Olivier, J.P., Rodriguez-Reinoso, F., Rouquerol, J., Sing, K.S.W., 2015. Physisorption of gases, with special reference to the evaluation of surface area and pore size distribution (IUPAC Technical Report). Pure and Applied Chemistry 87, 1051–1069. https://doi.org/10.1515/pac-2014-1117

Tong, Y., Mayer, B.K., McNamara, P.J., 2016. Triclosan adsorption using wastewater biosolids-derived biochar. Environmental Science: Water Research & Technology 761–768. https://doi.org/10.1039/C6EW00127K

Tran, H.N., You, S.J., Chao, H.P., 2016. Thermodynamic parameters of cadmium adsorption onto orange peel calculated from various methods: A comparison study. Journal of Environmental Chemical Engineering 4, 2671–2682. https://doi.org/10.1016/j.jece.2016.05.009

Transformation Products of Emerging Contaminants in the Environment, 2014. , Transformation Products of Emerging Contaminants in the Environment.

Treybal, R.E., 1980. Mass - Transfer Operations.

Tsai, W.T., 2006. Human health risk on environmental exposure to bisphenol-A: A review. Journal of Environmental Science and Health - Part C Environmental Carcinogenesis and Ecotoxicology Reviews 24, 225–255. https://doi.org/10.1080/10590500600936482

Vakili, M., Rafatullah, M., Salamatinia, B., Abdullah, A.Z., Ibrahim, M.H., Tan, K.B., Gholami, Z., Amouzgar, P., 2014. Application of chitosan and its derivatives as adsorbents for dye removal from water and wastewater: A review. Carbohydrate Polymers 113, 115–130. https://doi.org/10.1016/j.carbpol.2014.07.007

Varsha, M., Kumar, P.S., Rathi, B.S., 2022. A review on recent trends in the removal of emerging contaminants from aquatic environment using low-cost adsorbents. Chemosphere 287.

Viegas, R.M.C., Campinas, M., Costa, H., Rosa, M.J., 2014. How do the HSDM and Boyd's model compare for estimating intraparticle diffusion coefficients in adsorption processes. Adsorption 20, 737–746. https://doi.org/10.1007/s10450-014-9617-9

Vieira, W.T., Bispo, M.D., de Melo Farias, S., de Almeida, A.D.S.V., da Silva, T.L., Vieira, M.G.A., Soletti, J.I., Balliano, T.L., 2021. Activated carbon from macauba endocarp (Acrocomia aculeate) for removal of atrazine: Experimental and theoretical investigation using descriptors based on DFT. Journal of Environmental Chemical Engineering 9. https://doi.org/10.1016/j.jece.2021.105155

Vigneresse, J.L., 2018. Variations in chemical descriptors during reactions. Chemical Physics Letters 706, 577–585. https://doi.org/10.1016/j.cplett.2018.05.032

Villaverde-De-Sáa, E., González-Mariño, I., Quintana, J.B., Rodil, R., Rodríguez, I., Cela, R., 2010. In-sample acetylation-non-porous membrane-assisted liquid-liquid

extraction for the determination of parabens and triclosan in water samples. Analytical and Bioanalytical Chemistry 397, 2559–2568. https://doi.org/10.1007/s00216-010-3789-2

Wang, F., Zhang, Q., Sha, W., Wang, X., Miao, M., Wang, Z.L., Li, Y., 2021. The adsorption of endocrine-disrupting compounds (EDCs) on carbon nanotubes: effects of algal extracellular organic matter (EOM). Journal of Nanoparticle Research 23. https://doi.org/10.1007/s11051-021-05215-3

Wang, L., Ying, G.G., Zhao, J.L., Liu, S., Yang, B., Zhou, L.J., Tao, R., Su, H.C., 2011. Assessing estrogenic activity in surface water and sediment of the Liao River system in northeast China using combined chemical and biological tools. Environmental Pollution 159, 148–156. https://doi.org/10.1016/j.envpol.2010.09.017

Wang, S., Zhai, Y.Y., Gao, Q., Luo, W.J., Xia, H., Zhou, C.G., 2014. Highly efficient removal of acid red 18 from aqueous solution by magnetically retrievable chitosan/carbon nanotube: Batch study, isotherms, kinetics, and thermodynamics. Journal of Chemical and Engineering Data 59, 39–51. https://doi.org/10.1021/je400700c

Wang, W., Zhu, Z., Zhang, M., Wang, S., Qu, C., 2020. Synthesis of a novel magnetic multi-amine decorated resin for the adsorption of tetracycline and copper. Journal of the Taiwan Institute of Chemical Engineers 106, 130–137. https://doi.org/10.1016/j.jtice.2019.10.017

Wang, X., Huang, P., Ma, X., Du, X., Lu, X., 2018. Magnetic Mesoporous Molecularly Imprinted Polymers Based on Surface Precipitation Polymerization for Selective Enrichment of Triclosan and Triclocarban. Journal ofChromatography A.

Wang, X., Song, L., Yang, H., Xing, W., Kandola, B., Hu, Y., 2012. Simultaneous reduction and surface functionalization of graphene oxide with POSS for reducing fire hazards in epoxy composites. Journal of Materials Chemistry 22, 22037–22043. https://doi.org/10.1039/c2jm35479a

Wang, Y., Li, L.L., Luo, C., Wang, X., Duan, H., 2016. Removal of Pb2+ from water environment using a novel magnetic chitosan/graphene oxide imprinted Pb2+. International Journal of Biological Macromolecules 86, 505–511. https://doi.org/10.1016/j.ijbiomac.2016.01.035

Wang, Y., Liang, W., 2021. Occurrence, Toxicity, and Removal Methods of Triclosan: a Timely Review. Current Pollution Reports. https://doi.org/10.1007/s40726-021-00173-9/Published

Wang, Y., Yang, Q., Dong, J., Huang, H., 2018. Competitive adsorption of PPCP and humic substances by carbon nanotube membranes: Effects of coagulation and PPCP properties. Science of the Total Environment 619–620, 352–359. https://doi.org/10.1016/j.scitotenv.2017.11.117

Weber, W., Morris, J., 1963. Kinetics of adsorption on carbon from solution. Journal of the Sanitary Engineering Division 89, 31–60.

Wells, M.J.M., Morse, A., Bell, K.Y., Pellegrin, M.-L., Fono, L.J., 2009. Emerging Pollutants, Water Environment Research. https://doi.org/10.2175/106143009x12445568400854

Westrup, J.L., Bertoldi, C., Cercena, R., Dal-Bó, A.G., Soares, R.M.D., Fernandes, A.N., 2021. Adsorption of endocrine disrupting compounds from aqueous solution in poly(butyleneadipate-co-terephthalate) electrospun microfibers. Colloids and Surfaces A: Physicochemical and Engineering Aspects 611. https://doi.org/10.1016/j.colsurfa.2020.125800

Williams, M., Kookana, R.S., Mehta, A., Yadav, S.K., Tailor, B.L., Maheshwari, B., 2019. Emerging contaminants in a river receiving untreated wastewater from an Indian urban centre. Science of the Total Environment 647, 1256–1265. https://doi.org/10.1016/j.scitotenv.2018.08.084

Wong, S., Lim, Y., Ngadi, N., Mat, R., Hassan, O., Inuwa, I.M., Mohamed, N.B., Low, J.H., 2018. Removal of acetaminophen by activated carbon synthesized from spent tea leaves: equilibrium, kinetics and thermodynamics studies. Powder Technology 338, 878–886. https://doi.org/10.1016/j.powtec.2018.07.075

Wu, F.C., Tseng, R.L., Juang, R.S., 2009. Initial behavior of intraparticle diffusion model used in the description of adsorption kinetics. Chemical Engineering Journal 153, 1–8. https://doi.org/10.1016/j.cej.2009.04.042

Wu, Q., Lam, J.C.W., Kwok, K.Y., Tsui, M.M.P., Lam, P.K.S., 2017. Occurrence and fate of endogenous steroid hormones, alkylphenol ethoxylates, bisphenol A and phthalates in municipal sewage treatment systems. Journal of Environmental Sciences 61, 49–58.

Wu, S.-T., 1975. A Rigorous Justification of the Point B Method for Determination of Monolayer Capacity from a Type II Adsorption Isotherm, Progress of Theoretical Physics.

Wurzer, C., Mašek, O., 2021. Feedstock doping using iron rich waste increases the pyrolysis gas yield and adsorption performance of magnetic biochar for emerging

contaminants. Bioresource Technology 321. https://doi.org/10.1016/j.biortech.2020.124473

Xiong, J.Q., Kurade, M.B., Patil, D. v., Jang, M., Paeng, K.J., Jeon, B.H., 2017. Biodegradation and metabolic fate of levofloxacin via a freshwater green alga, Scenedesmus obliquus in synthetic saline wastewater. Algal Research 25, 54–61. https://doi.org/10.1016/j.algal.2017.04.012

Xiong, Q., Hu, L.X., Liu, Y.S., Zhao, J.L., He, L.Y., Ying, G.G., 2021. Microalgae-based technology for antibiotics removal: From mechanisms to application of innovational hybrid systems. Environment International 155, 106594. https://doi.org/10.1016/j.envint.2021.106594

Xu, J., Wang, L., Zhu, Y., 2012. Decontamination of bisphenol A from aqueous solution by graphene adsorption. Langmuir 28, 8418–8425. https://doi.org/10.1021/la301476p

Xu, L., Teng, J., Li, L., Huang, H.D., Xu, J.Z., Li, Y., Ren, P.G., Zhong, G.J., Li, Z.M., 2019. Hydrophobic Graphene Oxide as a Promising Barrier of Water Vapor for Regenerated Cellulose Nanocomposite Films. ACS Omega 4, 509–517. https://doi.org/10.1021/acsomega.8b02866

Yang, S., Feng, X., Müllen, K., 2011. Sandwich-like, graphene-based titania nanosheets with high surface area for fast lithium storage. Advanced Materials 23, 3575–3579. https://doi.org/10.1002/adma.201101599

Yang, S., Hai, F.I., Nghiem, L.D., Roddick, F., Price, W.E., 2013. Removal of trace organic contaminants by nitrifying activated sludge and whole-cell and crude enzyme extract of Trametes versicolor. Water Science and Technology 67, 1216–1223. https://doi.org/10.2166/wst.2013.684

Yang, W., Pan, M., Huang, C., Zhao, Z., Wang, J., Zeng, H., 2021. Graphene oxide-based noble-metal nanoparticles composites for environmental application. Composites Communications 24. https://doi.org/10.1016/j.coco.2021.100645

Yang, Y., Li, J., Lu, K., Shi, H., Gao, S., 2017. Transformation of 17A-ethinylestradiol by simultaneous photo-enzymatic process in Humic water. Chemosphere 178, 432–438. https://doi.org/10.1016/j.chemosphere.2017.03.077

Yankovych, H., Melnyk, I., Václavíková, M., 2021. Understanding of mechanisms of organohalogens removal onto mesoporous granular activated carbon with acid-base properties. Microporous and Mesoporous Materials 317. https://doi.org/10.1016/j.micromeso.2021.110974

Yap, H.C., Pang, Y.L., Lim, S., Abdullah, A.Z., Ong, H.C., Wu, C.H., 2019a. A comprehensive review on state-of-the-art photo-, sono-, and sonophotocatalytic treatments to degrade emerging contaminants. International Journal of Environmental Science and Technology 16, 601–628. https://doi.org/10.1007/s13762-018-1961-y

Yap, H.C., Pang, Y.L., Lim, S., Abdullah, A.Z., Ong, H.C., Wu, C.H., 2019b. A comprehensive review on state-of-the-art photo-, sono-, and sonophotocatalytic treatments to degrade emerging contaminants. International Journal of Environmental Science and Technology 16, 601–628. https://doi.org/10.1007/s13762-018-1961-y

Ying, G.G., Kookana, R.S., 2007. Triclosan in wastewaters and biosolids from Australian wastewater treatment plants. Environment International 33, 199–205. https://doi.org/10.1016/j.envint.2006.09.008

Ying, G.G., Kookana, R.S., Kumar, A., Mortimer, M., 2009. Occurrence and implications of estrogens and xenoestrogens in sewage effluents and receiving waters from South East Queensland. Science of the Total Environment 407, 5147–5155. https://doi.org/10.1016/j.scitotenv.2009.06.002

Zafra, A., Del Olmo, M., Suárez, B., Hontoria, E., Navalón, A., Vílchez, J.L., 2003. Gas chromatographic-mass spectrometric method for the determination of bisphenol A and its chlorinated derivatives in urban wastewater. Water Research 37, 735–742. https://doi.org/10.1016/S0043-1354(02)00413-X

Zambianchi, M., Durso, M., Liscio, A., Treossi, E., Bettini, C., Capobianco, M.L., Aluigi, A., Kovtun, A., Ruani, G., Corticelli, F., Brucale, M., Palermo, V., Navacchia, M.L., Melucci, M., 2017. Graphene oxide doped polysulfone membrane adsorbers for the removal of organic contaminants from water. Chemical Engineering Journal 326, 130–140. https://doi.org/10.1016/j.cej.2017.05.143

Zhang, L., Zhang, B., Wu, T., Sun, D., Li, Y., 2015. Adsorption behavior and mechanism of chlorophenols onto organoclays in aqueous solution. Colloids and Surfaces A: Physicochemical and Engineering Aspects 484, 118–129. https://doi.org/10.1016/j.colsurfa.2015.07.055

Zhang, S., Dong, Y., Yang, Z., Yang, W., Wu, J., Dong, C., 2016. Adsorption of pharmaceuticals on chitosan-based magnetic composite particles with core-brush topology. Chemical Engineering Journal 304, 325–334. https://doi.org/10.1016/j.cej.2016.06.087

Zhang, S., Meng, W., Wang, L., Li, L., Long, Y., Hei, Y., Zhou, L., Wu, S., 2020. Preparation of Nano-Copper Sulfide and Its Adsorption Properties for 17 α -Ethynyl Estradiol.

Zhang, X., Gao, Y., Li, Q., Li, G., Guo, Q., Yan, C., 2011. Estrogenic compounds and estrogenicity in surface water, sediments, and organisms from Yundang Lagoon in Xiamen, China. Archives of Environmental Contamination and Toxicology 61, 93–100. https://doi.org/10.1007/s00244-010-9588-0

Zhang, Z.F., Wang, L., Zhang, Xianming, Zhang, Xue, Li, Y.F., Nikolaev, A., Li, W.L., 2021. Fate processes of Parabens, Triclocarban and Triclosan during wastewater treatment: assessment via field measurements and model simulations. Environmental Science and Pollution Research 28, 50602–50610. https://doi.org/10.1007/s11356-021-14141-9

Zhao, B., Ji, Y., Wang, F., Lei, H., Gu, Z., 2016. Adsorption of tetracycline onto alumina: experimental research and molecular dynamics simulation. Desalination and Water Treatment 57, 5174–5182. https://doi.org/10.1080/19443994.2015.1004595

Zhao, C., Xie, H.J., Xu, J., Zhang, J., Liang, S., Hao, J., Ngo, H.H., Guo, W., Xu, X., Wang, Q., Wang, J., 2016. Removal mechanisms and plant species selection by bioaccumulative factors in surface flow constructed wetlands (CWs): In the case of triclosan. Science of the Total Environment 547, 9–16. https://doi.org/10.1016/j.scitotenv.2015.12.119

Zhao, J.L., Ying, G.G., Liu, Y.S., Chen, F., Yang, J.F., Wang, L., 2010. Occurrence and risks of triclosan and triclocarban in the Pearl River system, South China: From source to the receiving environment. Journal of Hazardous Materials 179, 215–222. https://doi.org/10.1016/j.jhazmat.2010.02.082

Zhongbo, Z., Hu, J., 2008. Selective removal of estrogenic compoundsby molecular imprinted polymer. Water Research 42, 4101–4108.

Zhou, A., Chen, W., Liao, L., Xie, P., Zhang, T.C., Wu, X., Feng, X., 2019. Comparative adsorption of emerging contaminants in water by functional designed magnetic poly(N-isopropylacrylamide)/chitosan hydrogels. Science of the Total Environment 671, 377–387. https://doi.org/10.1016/j.scitotenv.2019.03.183

Zhou, S., Shao, Y., Gao, N., Deng, J., Tan, C., Reuse, R., Reuse, R., 2013. Equilibrium , Kinetic , and Thermodynamic Studies on the Adsorption of Triclosan onto Multi-Walled Carbon Nanotubes 41, 539–547. https://doi.org/10.1002/clen.201200082

Zhou, X., Lian, Z., Wang, J., Tan, L., Zhao, Z., 2011. Distribution of estrogens along Licun River in Qingdao, China. Procedia Environmental Sciences 10, 1876–1880. https://doi.org/10.1016/j.proenv.2011.09.293

Zhu, X., Liu, Y., Luo, G., Qian, F., Zhang, S., Chen, J., 2014. Facile Fabrication of Magnetic Carbon Composites from Hydrochar via Simultaneous Activation and Magnetization for Triclosan Adsorption.

Zhuang, G., Zhang, Z., Jaber, M., 2019. Organoclays used as colloidal and rheological additives in oil-based drilling fluids: An overview. Applied Clay Science 177, 63–81. https://doi.org/10.1016/j.clay.2019.05.006

Zhuang, S., Wang, J., 2021. Adsorptive removal of pharmaceutical pollutants by defective metal organic framework UiO-66: Insight into the contribution of defects. Chemosphere 281. https://doi.org/10.1016/j.chemosphere.2021.130997

Zuo, Y., Zhang, K., Deng, Y., 2006. Occurrence and photochemical degradation of 17α-ethinylestradiol in Acushnet River Estuary. Chemosphere 63, 1583–1590. https://doi.org/10.1016/j.chemosphere.2005.08.063

CAPÍTULO 4. ADSORÇÃO DO 17α-ETINILESTRADIOL EM NANOCOMPÓSITO DESENVOLVIDO: CINÉTICA, EQUILÍBRIO, TERMODINÂMICA E ESTUDO DE SELETIVIDADE

Adsorption of 17α-ethinylestradiol onto a novel nanocomposite based on graphene oxide, magnetic chitosan and organoclay (GO/mCS/OC): Kinetics, equilibrium, thermodynamics and selectivity studies[2]

Arthur da Silva Vasconcelos de Almeida[a], Valmor Roberto Mastelaro[b], Meuris Gurgel Carlos da Silva[a], Patricia Prediger[c] and Melissa Gurgel Adeodato Vieira[a]

[a] Chemical Engineering Faculty, University of Campinas, 13083-852, Campinas, São Paulo, Brazil.

[b] São Carlos Institute of Physics, University of São Paulo, 13566-590, São Carlos, Brazil.

[c] School of Technology, University of Campinas, 13484-332, Limeira, São Paulo, Brazil.

ABSTRACT

17α-ethinylestradiol (EE2) is a synthetic estrogen present in contraceptive pills, being considered an emerging contaminant. In this work, EE2 adsorption process in a nanocomposite of graphene oxide, magnetic chitosan and organophilic clay (GO/mCS/OC) was evaluated. The nanocomposite was characterized by nitrogen physisorption, thermogravimetry, X-ray diffraction, X-ray photoelectric spectroscopy, Fourier transform infrared spectroscopy, Raman spectroscopy and scanning electron microscopy. The effects of dosage, sonication time and pH on the process were assessed. Kinetics, equilibrium, thermodynamics and reusability tests of EE2 adsorption onto GO/mCS/OC were investigated. The adsorptive kinetics of EE2 followed a pseudo-second order model, while the equilibrium was better represented by the BET model, with a characteristic profile of multilayer physisorption. Thermodynamics suggested that the process was spontaneous and endothermic. Adsorption mechanisms were assessed, indicating an important role of oxygenated and nitrogenated functional groups, as well as the aromatic structure of the GO/mCS/OC, promoting H-bonds and π–π interactions. The nanoadsorbent had a maximum experimental capacity of 50.5 mg g^{-1} (30 °C). The selectivity of the nanocomposite in binary solutions with bisphenol A (BPA) revealed

[2] Manuscript published in *Journal of Water Process and Engineering* 47 (2022) 102729. DOI: https://doi.org/10.1016/j.jwpe.2022.102729. Reprinted with permission from *Journal of Water Process and Engineering*. Copyright 2022 (Anexo A).

satisfactory removal efficiency, good selectivity and material stability. The GO/OC nanocomposite showed reuse potential for two consecutive cycles, decreasing its capacity until the fifth adsorptive cycle. Finally, the developed nanocomposite proved to be a promising alternative for removing emerging contaminants from aquatic matrices.

Key Words: Adsorption; 17α-ethinylestradiol, Nanocomposite; Graphene Oxide; Emerging Contaminant.

1. INTRODUCTION

Emerging contaminants belong to a category of pollutants that comprises new compounds that appear as well as known molecules, but whose impact is not fully understood (Sauvé and Desrosiers, 2014). Pharmaceuticals, personal care products, pesticides, industrial products, microplastics, surfactants, illicit drugs, disinfection products, among other organic contaminants can be classified as emerging contaminants (Cheng et al., 2021; Morin-Crini et al., 2022). This group of pollutants has been attracting the world's attention due to its great impact on human health and its risk to the ecosystem even at low concentrations (Shahid et al., 2021). A fact that heightens the concern with this problem nowadays is the absence of specific regulations for many of these contaminants, and quality standards that define their acceptable safe levels for society (Shahid et al., 2021). Another aggravating factor is that conventional effluent treatments often do not efficiently remove the various emerging contaminants that have very different chemical properties and make a unique and effective treatment difficult (Sivaranjanee and Kumar, 2021).

17α-ethinylestradiol (EE2) is an emerging contaminant classified as synthetic estrogen with high estrogen potential and for this reason it is present in most commercial oral contraceptives (Nasri et al., 2021). The rise in the use of this substance over the years results in increasingly concentrated anthropogenic waste arriving at wastewater treatment plants (Tang et al., 2021a). Incomplete removal of EE2 by conventional treatments contributes to its accumulation in the environment and causes serious environmental damages (Ifelebuegu and Ezenwa, 2011). Its lipophilic characteristic shows a tendency of accumulation in animal fats that causes damages such as feminization, reduced fertility and increased fish mortality, in addition to endocrine dysfunction in humans (Astrahan et al., 2021; Nasri et al., 2021). Despite the difficult monitoring of emerging contaminants,

EE2 has already been identified in surface waters of more than 32 countries with great variability in its concentrations, but with a tendency to occur more frequently in underdeveloped countries (Tang et al., 2021b). Even with all the concern related to this drug, existing regulations are only related to its occurrence levels in drinking water, such as the Japanese Drinking Water Quality Standard and the Environmental Quality Standard promoted by Japan and the European Union, respectively (Tang et al., 2021b). The lack of monitoring and regulation for this class of contaminants also contributes to the fact that more expensive and efficient treatments do not replace conventional treatments.

Several procedures are investigated in order to efficiently remove emerging contaminants from water, among them are bioremediation (Parladé et al., 2018; Xiong et al., 2017), advanced oxidative processes (Bavasso et al., 2020; Liu and Tang, 2020; Vieira et al., 2021), membrane (Egea-Corbacho et al., 2019; Racar et al., 2020), photocatalysis (Hasijaa et al., 2019; Sonu et al., 2019) and adsorption (Álvarez-Torrellas et al., 2017; Liu et al., 2018). Membrane and oxidation treatments present high efficiency, however with high cost and problems of fouling and release of toxic end products respectively (Sharma et al., 2019; Siebdrath et al., 2021; Vieira et al., 2020). Adsorption stands out among the alternatives due to its easy operation, low cost, high efficiency and mainly due to the great diversity of adsorbent materials (Freitas et. al., 2017; Naushada et al., 2019; Rad and Anbia, 2021). The structural variety available for adsorbent materials allows for different types of interactions that may favor the removal of a contaminant of interest. The removal of emerging contaminants via adsorption has been investigated in several materials such as modified biochar (Dai et al., 2020; Hu et al., 2019), activated biochar (Vieira et al., 2021; Wong et al., 2018), alumina (Zhao et al., 2016), zeolites (Jiang et al., 2020), clays (Antonelli et al., 2021; Nascimento et al., 2021), organoclays (Spaolonzi et al., 2022; Farias et al., 2021), metal organic frameworks (Rojas et al., 2021; Zhuang and Wang, 2021), etc. The adsorption process in each material presents particularities and differences that are related to different types of interactions obtained for different adsorbate-adsorbent systems.

Nanoadsorbents have been extensively investigated due to their particularities and advantages in environmental application. In general, nanoadsorbents have a large surface area and atoms with high reactivity are disposed on its surface (Ly et al., 2021). Several experimental works are presenting nanometric materials such as carbon nanotubes, graphene and graphene oxide (GO) to remove pharmaceuticals from water (Liu et al.,

2014; Wang et al., 2018; Zambianchi et al., 2017). Graphene oxide is a nanomaterial derived from graphene that has a large specific area and different oxygenated groups available on its surface (hydroxyl, carboxyl and epoxy) (Yang et al., 2021). Materials based on graphene oxide have been constantly developed through the formation of nanocomposites with different materials, such as organophilic clays and chitosan (Nazraz et al., 2019; Sahoo et al., 2018). The formation of the nanocomposite seeks to take advantage of the particular characteristics of precursor materials and improve their adsorption capacity (Kong et al., 2021; Meidanchi and Akhavan, 2014). Organoclays are materials that have undergone a modification process through the insertion of surfactant compounds that creates a hydrophobic surface on the clay, which easily interacts with organic contaminants (Zhang et al., 2015). Chitosan is a natural biopolymer abundant in the world that has low cost and good adsorption capacity for different types of adsorbates (Saheed et al., 2021). The amines and hydroxyls present on its surface are very important and have crucial contributions in the adsorption process (Saheed et al., 2021). There are several reports in the literature of chitosan modifications by the insertion of Fe_3O_4 nanoparticles, to obtain composites with magnetic properties that facilitate its reuse and its separation from the system (Karimi et al., 2022; Zhang et al., 2013).

In this work, the adsorption of EE2 by the nanocomposite synthesized from graphene oxide, chitosan and organophilic clay (GO/mCS/OC) was investigated. The adsorption study included the evaluation of operating parameters, kinetic, equilibrium and thermodynamic studies, as well as the design of a simplified batch system, reusability tests and an evaluation of the selectivity of the nanocomposite by EE2 in relation to BPA, another emerging contaminant. The pristine and contaminated nanocomposite was characterized by N_2 physisorption analysis at 77 K (BET), thermogravimetry (TGA), X-ray diffraction (XRD), X-ray photoelectric spectroscopy (XPS), Raman spectroscopy, Fourier transform infrared spectroscopy (FTIR) and scanning electron microscopy (SEM). Few studies reported the removal of EE2 from aquatic matrices and, much less, involving its removal by a nanocomposite with these characteristics.

2. METODOLOGY

2.1. Materials and Reagents

The mineral graphite and the organophilic clay Spectrogel® – Type C that were used to produce the nanocomposite were supplied by Nacional Grafite LTDA and

Spectrochem® companies. Chitosan and iron chlorides were purchased from Sigma-Aldrich and Dinâmica Química companies, respectively. The synthesis of the nanocomposite was briefly described in Supplementary Material. 17α-ethinylestradiol (EE2) and bisphenol A (BPA) with a high level of purity (> 99 %) were purchased from Sigma-Aldrich. The acetonitrile that was used as a solvent was acquired through Dinâmica Química. Hydrochloric acid (HCl) and sodium hydroxide (NaOH) that were used as pH regulators were obtained from the company ACS Científica.

2.2. Characterization of pristine and contaminated GO/mCS/OC

The adsorption and desorption isotherms of nitrogen were evaluated using the equipment ASAP 2010 (Micromeritics, Austin, USA) seeking to obtain structural information of pristine and contaminated material. The samples were pretreated for 6 h in vacuum and evaluated for 77 pressure points with an equilibrium time of 10 s. The degradation of pristine and contaminated nanocomposite was evaluated through thermogravimetric analysis (TGA) which was conducted in a DTG-60H equipment (Shimadzu, Kyoto, Japan). The materials were heated from 25 – 1000 °C with a heating rate of 20 °C min^{-1} and a nitrogen flow rate of 40 mL min^{-1}. The crystallinity of pristine and contaminated nanoadsorbent was analyzed by X-ray diffraction (XRD) using the X'Pert-MPD equipment (Philips Analytical X Ray, Almelo, Netherlands). The analysis was conducted with a current of 30 mA, voltage of 40 kV and copper radiation of 0.154 nm in amplitude. The interplanar distances were calculated based on Bragg's law (Lu et al., 2017). Raman spectra were measured on a Witec microscope (Witec, Ulm, Germany) with a laser excitation wavelength of 514 nm. Surface and chemical bonds were evaluated by X-ray photoelectric spectroscopy (XPS) using ESCA+ equipment (Scientia Omicron, Uppsala, Sweden). Monochromatic Al Kα radiation was used as an excitation source with an energy of 1486.6 eV. The XPS high-resolution spectra was recorded at constant pass energy of 20 eV with a 0.05 eV per step for the high-resolution spectra. The functional groups of the surface of pristine and contaminated nanocomposite were evaluated by Fourier transform infrared spectroscopy (FTIR) using Nicolet 6700 equipment (Thermo Scientific, Madison, USA). The analysis was based on the KBr tablet method and evaluated amplitudes between 450 and 4000 cm^{-1}. Surface micrographs of pristine and contaminated nanocomposite were obtained by scanning electron microscopy using VEGA 3 equipment (Tescan, Brun, Czech Republic).

2.3. Effects of nanoadsorbent dosage, pH and sonication time

The effects of important parameters such as dosage of GO/mCS/OC, pH and sonication time in the adsorption process were assessed. All tests were carried out in triplicate in 5 mL of 0.03 mmol L^{-1} (8.9 mg L^{-1}) solution. The experiments were performed under constant agitation at 200 rpm and 30 °C for 12 h. The dosage of GO/mCS/OC was evaluated in the range between 0.05 – 0.35 mg mL^{-1}. The initial pH values were adjusted with HCl and NaOH (0.1 mmol L^{-1}) and evaluated in the range between 3 - 8. The sonication time parameter was evaluated to 0 (no sonication treatment), 1, 5 and 30 min. After each test the samples were subjected to a magnetic field so that most of GO/mCS/OC was removed. The magnetic characteristics of the nanocomposite were previously described (Almeida et al., 2022). To ensure the complete removal of the nanocomposite, samples were centrifuged at 6000 rpm for 15 min and subjected to syringe filters (0.45 μm, PTFE). EE2 concentration at liquid phase was measured by high performance liquid chromatography (HPLC) (Shimadzu, Kyoto, Japan) with a UV-Vis detector and a C18 column (5 μ, 150 x 4.6 mm). EE2 analytical method was validated using a mobile phase with acetonitrile and deionized water (50/50), temperature of 30 °C, UV detector at 230 nm and column flow rate of 1.5 mL min^{-1}.

Removal percentage ($R_{\%}$) and adsorption capacity at an instant t (q_t) are described in Equations 1 and 2:

$$q_t = \frac{V}{m}\,(C_0 - C_t) \tag{1}$$

$$R_{\%} = \frac{(C_i - C_t)}{C_i} \tag{2}$$

Wherein, C_0 is the initial concentration of adsorbate (mg L^{-1}), C_t is the concentration at an instant t (mg L^{-1}), V is the volume of solution (L), and m is the nanoadsorbent mass (g).

2.4. Adsorption kinetics

Kinetic assays were performed for initial EE2 concentrations of 0.03, 0.02 and 0.01 mmol L^{-1} (8.9, 5.9 and 3 mg L^{-1}) keeping constant some parameters as GO/mCS/OC dosage (0.1 mg mL^{-1}), temperature (30 °C), stirring (200 rpm) and solution volume (5 mL). Several aliquots were removed over time and the system remained under agitation for 5 h. Aliquots were treated and their concentrations measured as previously described.

The experimental data were fitted to non-linear pseudo-first order (Lagergren, 1898), pseudo-second order (Ho and McKay, 1998), intraparticle diffusion (Weber and Morris, 1963) and Boyd models (Boyd et al., 1947). The models are described by Equations 3, 4, 5 and 6:

$$q_t = q_e(1 - e^{-K_1 t}) \quad (3)$$

$$q_t = \frac{K_2 q_e^2 t}{1 + K_2 q_e t} \quad (4)$$

$$q_t = K_I t^{\frac{1}{2}} + C \quad (5)$$

$$F = \frac{q_t}{q_e} = 1 - \frac{6}{\pi^2} \sum_{n=1}^{\infty} \frac{1}{n^2}\, e^{-Btn^2} \quad (6)$$

Wherein, q_e is the equilibrium adsorption capacity (mg g^{-1}), t is the time (min), K_1 is the pseudo-first order model constant (min^{-1}), K_2 is the pseudo-second order model constant (g mg^{-1} min^{-1}), K_I is the constant of intraparticle diffusion model (mg $g^{-0.5}$ $min^{-0.5}$), C is the constant related to boundary layer thickness (mg g^{-1}), F represents the equilibrium fraction and Bt are constants described by Equations 7 and 8 (Reichenberg, 1953):

If F > 0.85:

$$Bt = -0.4977 - ln(1 - F) \quad (7)$$

If F ≤ 0.85:

$$Bt = 2\pi - \frac{F\pi^2}{3} - 2\pi \left(1 - \frac{F\pi}{3}\right)^{\frac{1}{2}} \quad (8)$$

Boyd's model allows calculating the value of effective diffusivity coefficient through Equation 9:

$$B = \frac{D_{EF}\pi^2}{r^2} \quad (9)$$

Wherein, D_{EF} (mm^2 min^{-1}) is the effective diffusivity coefficient of EE2 in GO/mCS/OC and r is the estimated radius for the adsorbent particle (mm).

2.5. Adsorption isotherms

The equilibrium experiments were performed keeping the concentration at 0.03 mmol L^{-1} (8.9 mg L^{-1}) and with nanoadsorbent dosage ranging between 0.05 – 0.55 mg mL^{-1}. The tests were performed in beakers with 5 mL of contaminated solution that remained in the shaker stirring at 200 rpm for 150 min to ensure equilibrium. Isotherms were carried out at temperatures of 30, 40 and 50 °C and samples were treated and

evaluated as described previously. The equilibrium adsorption capacity (q_e) was calculated similarly to that described in Equation 1, however substituting the concentration at the instant t (C_t) for the equilibrium concentration (C_e).

The experimental data were fitted to nonlinear isotherm models of Langmuir (Langmuir, 1918), Freundlich (Freundlich, 1906) and BET (Ebadi et al., 2009), and are described in Equations 10, 11 and 12:

$$q_e = \frac{q_{Max} K_L C_e}{1+K_L C_e} \quad (10)$$

$$q_e = K_F C_e^{1/n} \quad (11)$$

$$q_e = \frac{q_B K_B C_e}{(1-K_U C_e)(1-K_U C_e+K_B C_e)} \quad (12)$$

Wherein, q_{Max} is the maximum monolayer adsorption capacity by Langmuir model (mg g^{-1}), K_L is the Langmuir model constant (L mg^{-1}), K_F is the Freundlich model constant [(mg g^{-1}).(L $mg^{-1})^{1/n}$], n is the exponent of Freundlich model, q_B is the maximum monolayer adsorption capacity by the BET model (mg g^{-1}), K_B is the monolayer adsorption constant of BET model (L mg^{-1}), K_U is the multilayer adsorption constant of BET model (L mg^{-1}).

The adjustment parameters were calculated taking into account the data predicted by the kinetic and isotherm models, seeking to evaluate its representativeness in relation to the experimental data. The parameters evaluated were the adjusted coefficient of determination (R^2_{Adj}), the reduced chi-squared (χ^2_{Red}) and the corrected Akaike information criterion (AIC_C). The decision of the most suitable model can be observed by the highest value of R^2_{Adj}, as well as by the lowest values for χ^2_{Red} e AIC_C (Bonate, 2011).

2.6. Adsorption thermodynamics

The equilibrium study for different temperatures allows calculating the thermodynamic parameters of the adsorption process. The equilibrium thermodynamic constant (K_D) was determined from Henry's law, which was applied in the infinite dilution region of each temperature (Equation 13). The modification proposed by Milonjić was applied to K_D seeking to make it dimensionless for application in the Van't Hoff equation (Equation 15) (Milonjić, 2007). The parameters of Gibbs energy variation (ΔG^0), enthalpy variation (ΔH^0), entropy variation (ΔS^0) and activation energy (E_a) were determined by Equations 14, 15 and 16:

$$q_e = K_D C_e \quad (13)$$

$$\Delta G^0 = -RTln(K_C) \quad (14)$$

$$ln(K_C) = \frac{\Delta S^0}{R} - \frac{\Delta H^0}{RT} \quad (15)$$

$$E_a = \Delta H^0 + RT \quad (16)$$

Wherein, K_C represents the dimensionless thermodynamic equilibrium constant, R the ideal gas constant and T (K) the experimental temperatures.

2.7. Designing a simplified batch adsorption system

A simplified batch system was designed to measure the amount of nanoadsorbent required to achieve different percentages of EE2 removal. The estimate was based on a mass balance for a batch system and is represented by Equation 17:

$$V(C_0 - C_1) = m(q_1 - q_0) \quad (17)$$

Some considerations were made to estimate the mass of GO/mCS/OC, such as considering the absence of EE2 initially in nanocomposite, considering the concentration in fluid phase equal to equilibrium, as well as considering the amount adsorbed on solid phase the amount adsorbed on equilibrium. In this way, Equation 17 becomes Equation 18:

$$V(C_0 - C_e) = mq_e \quad (18)$$

The nanocomposite mass required was evaluated for a solution volume range between 10 – 1000 L with an initial concentration of 0.03 mmol L^{-1} and removal percentages of 50, 70 and 90%. The data obtained at 30 °C, closer to room temperature, and the best fit model to the experimental data were considered for this system.

2.8. Isosteric heat of adsorption

Some characteristics about uniformity of the adsorbent surface can be evaluated through the isosteric heat of adsorption (ΔH_{Iso}). The adsorption heat is compared on a limited surface for different temperatures, so that energetic changes in the filling of the adsorbent material indicate heterogeneous surfaces. The parameter is evaluated from equilibrium data and Clausius-Clapeyron equation, that is exposed in Equation 19:

$$ln(C_e) = \frac{\Delta H_{Iso}}{R}\left(\frac{1}{T}\right) + Constant \quad (19)$$

Wherein, C_e is the equilibrium concentration (mg L^{-1}), ΔH_{Iso} represents the isosteric heat of adsorption (kJ mol^{-1}), R is the ideal gas constant and T is the experimental temperature (K).

2.9. Regeneration cycles in batch

GO/mCS/OC reuse tests for EE2 removal were evaluated for five adsorption/desorption cycles in a batch system. In each cycle, 25 mL of solution of initial concentration of 0.03 mmol L^{-1} were treated with 5 mg of GO/mCS/OC. After 180 min of agitation at 200 rpm in shaker equipment at 30 °C, the solid phase was separated through centrifugation and magnets and the concentration of the aliquots was measured as previously described. 3 mL of acetonitrile or ethanol were added to the solid phase and the system was subjected to a 3 min of ultrasonic bath. Acetonitrile and ethanol were selected as a desorption eluent due to its high solubility for organic contaminants. Subsequently, the solid phase was again separated and submitted to the adsorption/desorption cycle in a shaker equipment. The procedure described was repeated five times, evaluating the removal percentages and the adsorption capacities for five GO/mCS/OC reuses.

2.10. Selectivity evaluation

The selectivity parameter for GO/mCS/OC was evaluated through tests with binary solutions of EE2 and BPA. BPA is another emerging contaminant related to industrial activity but it can also be found in wastewater along with EE2 (López-Velázquez et al., 2021). The assays were carried out in triplicate, for systems with 5 mL of solution, nanoadsorbent dosage of 0.2 mg mL^{-1} and temperature of 30 °C. Initial concentrations of EE2 and BPA were adjusted and three different conditions were evaluated. The first condition showed a predominance of EE2 (0.016 and 0.009 mmol L^{-1}), the second showed a predominance of BPA (0.01 and 0.017 mmol L^{-1}), while the third was an equimolar solution (0.01 mmol L^{-1}). The samples were shaken for 300 min, then pre-treated and their concentration measured as described previously. The analytical method for evaluating BPA on HPLC was validated under the same conditions as EE2. The distribution coefficients (K_{EE2} e K_{BPA}) and selectivity coefficients ($K_{EE2/BPA}$) are described in Equations 20 and 21:

$$K = \frac{q_e}{C_e} \quad (20)$$

$$K_{EE2/BPA} = \frac{K_{EE2}}{K_{BPA}} \quad (21)$$

Wherein, K_{EE2} e K_{BPA} (L g^{-1}) represent the distribution coefficients of each emerging contaminant and $K_{EE2/BPA}$ represents the selectivity coefficient of the proposed system.

3. RESULTS AND DISCUSSION

3.1. Characterization of pristine and contaminated GO/mCS/OC

N_2 isotherms and pore distribution for pristine and contaminated GO/mCS/OC were evaluated using the BET and BJH method and shown in Figure 4.1. The isotherms obtained are classified as type II which are characteristics of non-porous and macroporous materials (Brião et al., 2022; Fagerlund, 1973; Wu, 1975). The transition from monolayer to multilayer adsorption was observed from the first inflection point and the beginning of the linear behavior (low relative pressure), corroborating the small amount of micropores (Fagerlund, 1973; Wu, 1975). Hysteresis phenomenon was observed in desorption, being classified as type H3 and typical of aggregates of plate-like particles and macroporous systems that are not completely filled (Cychosz et al., 2017). Table 4.1 summarizes the structural properties and pore volume information for pristine and contaminated material.

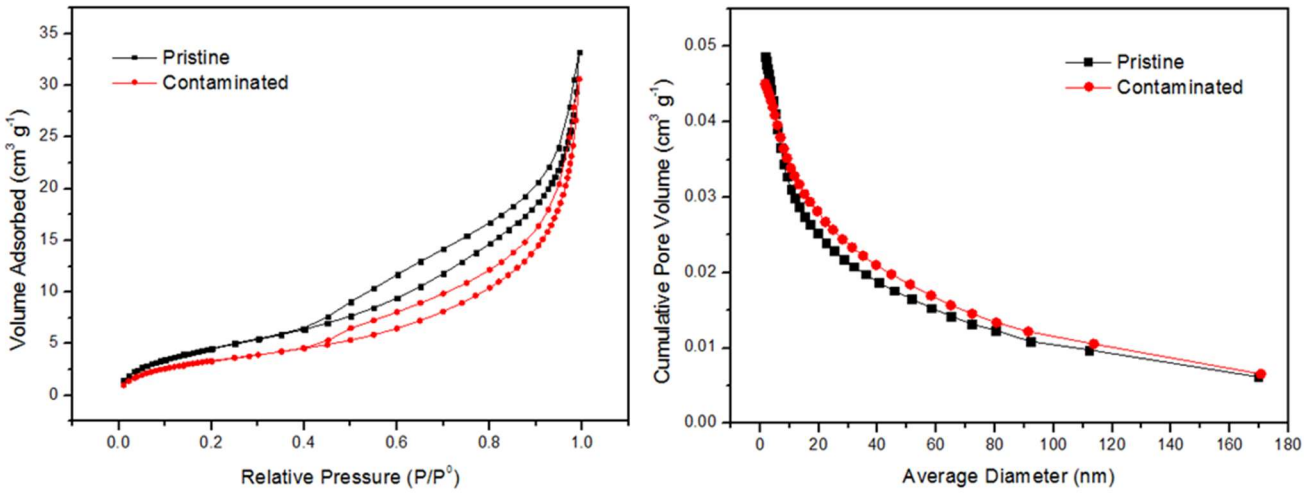

Figure 4.1 – N_2 physisorption isotherms and pore size distribution of pristine and contaminated GO/mCS/OC.

Table 4.1 – Specific area, average pore diameter and pore volume of pristine and contaminated GO/mCS/OC.

GO/mCS/OC Sample	Specific area ($m^2\ g^{-1}$)	Average pore diameter (nm)	$V_{Micropores}$ ($cm^3\ g^{-1}$)	$V_{Mesopores}$ ($cm^3\ g^{-1}$)	$V_{Macropores}$ ($cm^3\ g^{-1}$)
Pristine	17.8388	9.8241	4.5277	10.1914	18.4753
Contaminated	13.2101	13.2206	3.6560	6.0054	20.9578

Both samples showed an inflection point at relative pressure close to 0.2, having adsorbed 4.5 $cm^3\ g^{-1}$ of N_2 in pristine material and 3.7 $cm^3\ g^{-1}$ in contaminated material. This first range is related to the volume of micropores and suggests that, even in small quantities, some of them were occupied by EE2. After the inflection point, both curves have a slow linear growth until the relative pressure of 0.8, indicating the predominance of mesopores. After the relative pressure of 0.8, the curves showed a sharp increase, representing the presence of macropores in the material (Im et al., 2007; Ladavos et al., 2012; Soboleva et al., 2010).

The pore size distribution corroborated with the isotherm behavior, showing presence of micropores, however, presenting a larger range corresponding to mesopores and macropores. The increase in the volume adsorbed to larger pores of the contaminated material suggests surface changes with deposition of the contaminant. The average pore diameter of GO/mCS/OC was 9.8 nm, showing a slight increase (13.2 nm) with the contamination process. The surface area of the prepared nanocomposite was 17.8 $m^2\ g^{-1}$ and after contamination decreased to 13.2 $m^2\ g^{-1}$, indicating that part of the surface was occupied by the adsorbate.

Thermogravimetric curves of pristine and contaminated nanocomposite are illustrated in Figure 4.2. Both materials showed a decrease in the initial percentage related to water loss and, subsequently, there was a more evident loss of mass from 200 °C, which intensified as the temperature increased. The most intense mass loss occurred in the range between 200 - 500 °C and this is related to the degradation of oxygenated groups present in GO, glycosidic units of chitosan and iron nanoparticles (Kafshgari and Tahermansouri, 2017; Oliveira et al., 2003; Salahuddin et al., 2018). The samples lost mass with less intensity from this range, resulting in a final degradation (1000 °C) of 49.0 and 44.9% for pristine and contaminated samples, respectively. Despite the behavior of both samples being similar, the contaminated sample showed a slightly higher degradation than the non-contaminated sample, which may be associated with the increase of EE2 in the nanocomposite structure.

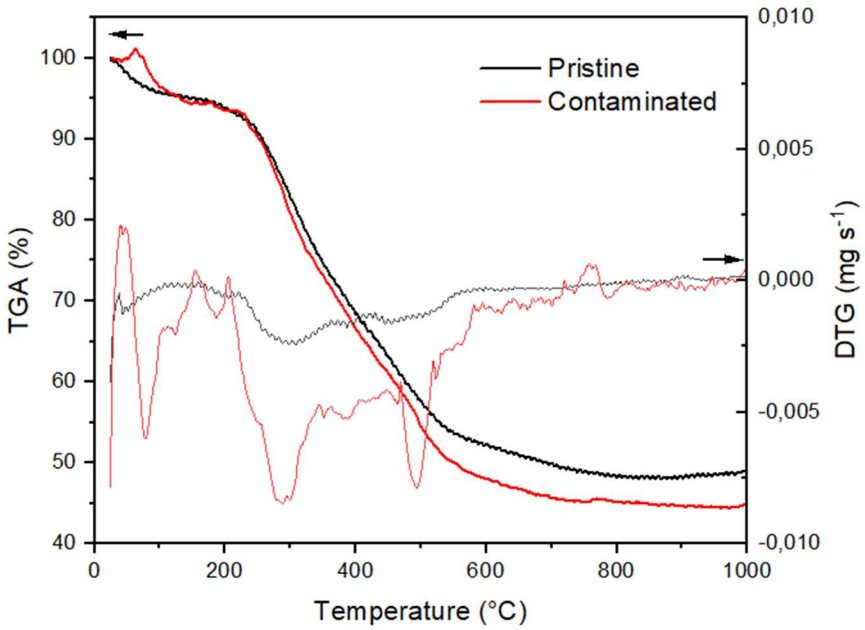

Figure 4.2 – Thermogravimetric analysis of pristine and contaminated GO/mCS/OC.

The crystallinity of pristine and contaminated GO/mCS/OC was evaluated from X-ray patterns shown in Figure 4.3. The materials presented amorphous characteristics, as well as the presence of some crystalline peaks similar to those presented for the organophilic clay Spectrogel®, which was used in nanocomposite synthesis (Andrade et al., 2020; Maia et al., 2019). The interplanar distances were evaluated using Bragg's law and showed that basal spaces of the material did not change significantly after EE2 adsorption. The interplanar distance found was 1.3 and 1.26 nm for pristine and contaminated nanocomposite, being a value close to that expected for bentonite clays (1.5 nm) (Andrade et al., 2020). The angles of 6.8°, 9.5°, 20°, 24.6°, 26.5°, 27.8°, 30.2°, 35.5°, 43.5°, 44.6°, 53.9°, 57.1°, 62.9° e 74.3° showed prominent peaks in pristine sample, being very close to peaks observed after contamination. Some peaks that were identified are characteristic of clayey materials such as montmorillonite (20 °/0.44 nm), kaolinite (24.6 °/0.36 nm), quartz (26.5 °, 27.8 ° and 35.5 °/0.33, 0.32 and 0.25 nm) and mica (44.6 °/0.20 nm) (Maia et al., 2019; Nowak et al., 2018; Speridião et al., 2014). The mineral morphology of dioctahedral conformation is related to the highlighted peak at 0.15 nm (Speridião et al., 2014). The diffractograms also showed some peaks that are characteristic of chitosan magnetized with Fe_3O_4 that stood out at 30.2 °, 35.5 °, 43.5 °, 53.9 °, 57.1 ° and 62.9 ° nm and represent the Bragg's diffraction planes (220), (311), (400), (422), (511) and (440) (Neves et al., 2020; Jawad et al., 2020). The peak that appears at 10° (0.94 nm) may be related to GO sheets intercalated within the clay interlayer and its decrease in contaminated sample is an indication of its reorganization and its participation in the adsorption process (Neves et al., 2020b; Sahoo et al., 2018).

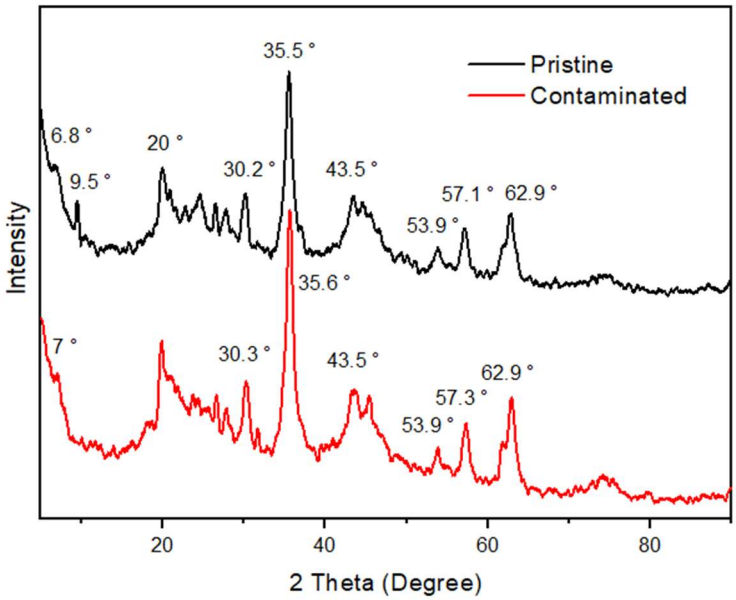

Figure 4.3 – X-ray diffractograms of pristine and contaminated GO/mCS/OC.

The structural changes of the GO, pristine and contaminated GO/mCS/OC was evaluated from Raman spectroscopy and their spectra are shown in Figure 4.4. The most common bands related to graphene oxide materials are the D and G bands. The D band represents imperfections in the aromatic structure of GO, being related to sp^3 hybridized carbon bonds such as hydroxyl and epoxy bonds in the basal plane. The G band represents the layer of sp^2-hybridized carbons, being related to the aromatic structure of GO (Akhavan, 2015; Li et al., 2015). The intensity ratio between the D and G bands (I_D/I_G) reflects the degree of imperfection of the GO graphitic layer (Jiang et al., 2015). The GO spectrum showed D and G bands located at 1343 and 1585 cm^{-1} and an I_D/I_G of 0.981. After the nanocomposite synthesis process, a loss of intensity of the D and G bands was observed, which may be related to the heterogeneous characteristic of the material, so that the presence of mineral portion impacts the intensity of the spectrum. The pristine GO/mCS/OC spectrum showed a red-shift in the D and G bands compared to GO, and were located at 1365 and 1590 cm^{-1}, however the I_D/I_G remained identical to GO. The identification of the D and G bands and the similarity of I_D/I_G in the nanocomposite spectrum suggests the presence of pristine GO in its structure and that the nanomaterial was not destroyed in the nanocomposite synthesis (Wu et al., 2020; Yang et al., 2016). The spectrum of contaminated GO/mCS/OC also revealed a red-shift of the D and G bands in relation to GO, being located at 1365 and 1590 cm^{-1}. The I_D/I_G of the contaminated nanocomposite was 1.004, which is superior to GO and pristine GO/mCS/OC, denoting a greater presence of imperfections in the aromatic structure after the adsorption process.

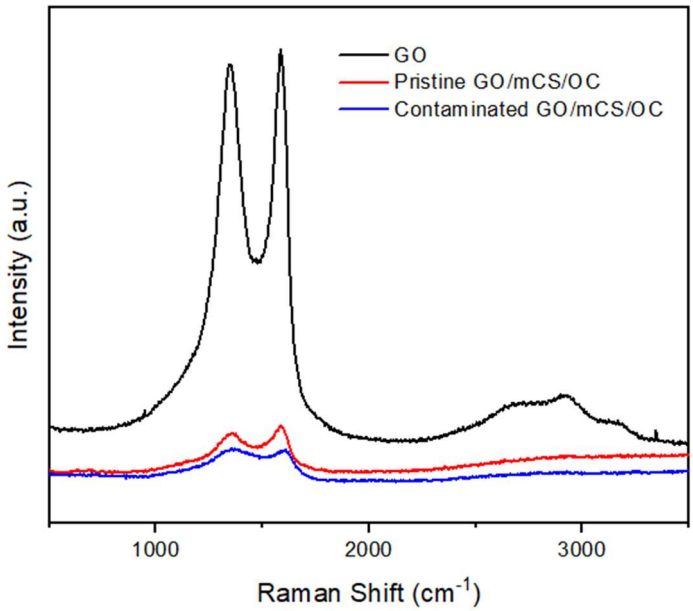

Figure 4.4 – Raman spectra of GO, pristine and contaminated GO/mCS/OC.

Pristine and contaminated GO/mCS/OC samples were verified by X-ray photoelectric spectroscopy (XPS) seeking to understand the chemical state of elements and measure the functional groups present in the samples. Survey spectra analysis of the pristine nanocomposite (Figure 4.5) showed the presence of carbon (70.1%) and oxygen (21.9%) in larger quantities, as well as small traces of silica (3.8%), aluminum (1.4%), nitrogen (1.3%), iron (1.2%) and sodium (0.2%). After contamination, the spectrum did not show significant changes in percentages.

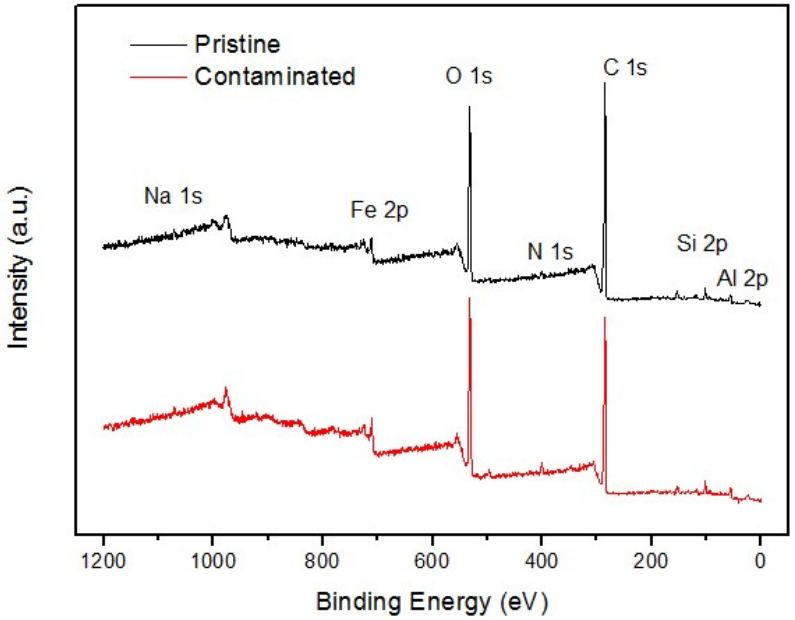

Figure 4.5 – XPS survey scans of pristine and contaminated GO/mCS/OC.

High resolution spectra of C 1s for pristine and contaminated GO/mCS/OC are shown in Figure 4.6 (A). The uncontaminated GO/mCS/OC spectrum revealed peaks at 284.7, 285.8, 286.8, 288.5 and 289.7 eV corresponding to the bonds C–C/C–H (55.5 %), C–N/C–OH (22 %), C–O/C–NH_2 (11 %), O–C=O (10.6 %) and π–π* interactions (0.9 %) between aromatic rings of GO, respectively (Al-Gaashani et al., 2019; Cobos et al., 2018; Ederer et al., 2017; Huang et al., 2017). After contamination with EE2 (Figure 4.6 (B)) the binding energies changed to 284.5, 285.5, 286.8 and 288.3 eV with different percentages for their representatives (50.5, 27.8, 15.7 and 6%, respectively). The peak related to π–π* interactions was not identified after contamination, suggesting that the nanocomposite interacts via π–π* interactions with the aromatic ring of EE2 (Bediako et al., 2019). The contaminated sample showed a shift of the peaks related to C–C/C–H, C–N/C–OH and O–C=O bonds to lower binding energies. This modification suggests an increase in electronic density due to the displacement of electrons on the nanocomposite

surface (Sahu et al., 2020). The decrease in these binding energies indicates that interactions via hydrogen bonding may be occurring between the hydroxyls present in EE2 and the C–N, C–OH and O–C=O groups of the nanocomposite (Wang et al., 2020).

High resolution spectra of O 1s for pristine and contaminated GO/mCS/OC are illustrated in Figure 4.6 (C) and Figure 4.6 (D). The uncontaminated GO/mCS/OC spectrum revealed peaks at 530.2, 531.7 and 533.2 eV corresponding to anionic oxygen of Fe_3O_4 (12.9%), C–O/O–C=O/Al–O binding (52.4%) and C–OH/Si–OH bond (34.7%), respectively (Al-Gaashani et al., 2019; Ghosh et al., 2019; Hu et al., 2020; Ma et al., 2015). After contamination, the spectrum showed peaks at the binding energies of 530.1, 531.5 and 532.8 eV with different percentages for their representatives (23.3, 45 and 31.7%, respectively). The discrete decrease in binding energies for O 1s indicates that oxygenated groups are involved in EE2 adsorption mechanisms (Sahu et al., 2020).

High resolution spectra of N 1s region for pristine and contaminated GO/mCS/OC are illustrated in Figure 4.6 (E) and Figure 4.6 (F). The crude sample showed peaks for binding energies of 399.8 and 402.1 eV that correspond to amines (primary and tertiary) and amides (53.3%) and to protonated amines (46.7%) (Gong et al., 2019; Lawrie et al., 2007), respectively. The contaminated sample presented peaks at binding energies of 399.7 and 401.9 eV with different percentages (71.5 and 28.5%). The variations in binding energy and percentages indicate that amines and protonated amines, present in nanocomposite through chitosan, act in EE2 adsorption process, possibly due to the reception and donation of hydrogen bonding (Wang et al., 2020). The hydroxyls present in the nanocomposite can also act as hydrogen bond donors like protonated amines. On the other hand, non-protonated amines and carboxylate groups can act as hydrogen bond receptors, supporting that this type of interaction is relevant between GO/mCS/OC and EE2.

High resolution spectra of Fe 2p showed for pristine and contaminated samples very similar peaks with binding energies of 710.2, 711.9, 723.7 and 725.4 eV. The first peak is related to the coexistence of Fe^{2+} and Fe^{3+} in the $2p^{3/2}$ oxidation state; the second is related to Fe^{3+} in the $2p^{3/2}$ oxidation state; the third is related to Fe^{2+} in the $2p^{1/2}$ oxidation state and the fourth indicates Fe^{3+} in the $2p^{1/2}$ oxidation state (Ghosh et al., 2019). This range of peaks is also related to the success in combining chitosan and Fe_3O_4 (Liu et al., 2017). High resolution spectra of Si 2p showed for pristine and contaminated samples identical peaks with binding energies of 101.8 and 102.8 eV that are related to Si^{3+} and Si^{4+}, respectively, which compose the clay layers (Ma et al., 2015). A peak close

to 1072 eV was identified in both samples and both are related to residual Na 1s that were not organophilized and that are ionized in the clay interlayer (Sáaedi et al., 2016). High resolution spectra of Al 2p showed for pristine and contaminated samples very close peaks with binding energies of 73.8 and 74.8 eV, which are related to octahedrally ordered aluminum in the clay layers (Narayanan et al., 2020). Similar peaks before and after adsorption demonstrate that iron, silicon, sodium and aluminum do not play an important role in interactions between GO/mCS/OC and EE2.

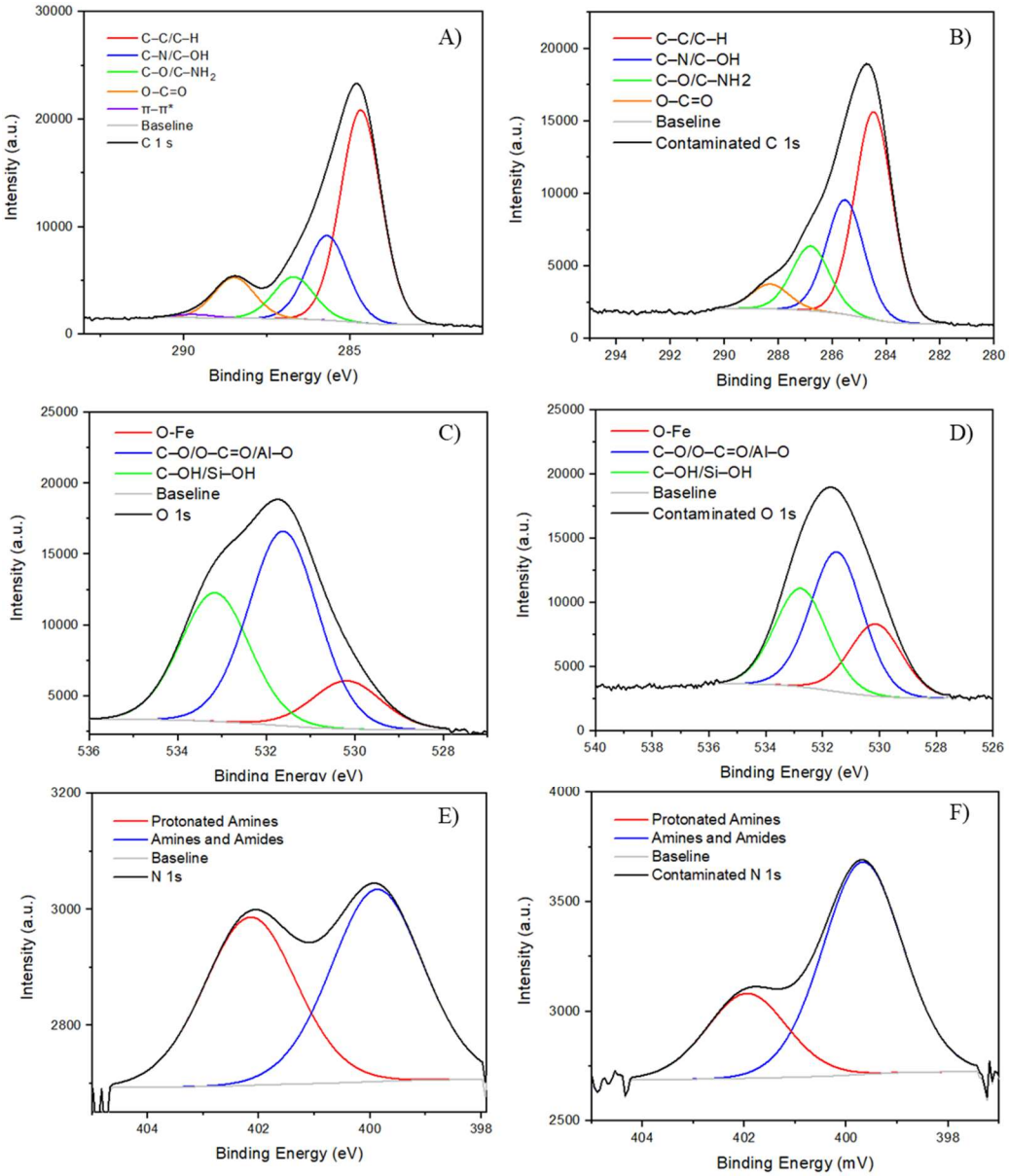

Figure 4.6 – XPS high resolution of pristine and contaminated GO/mCS/OC for C 1s (A and B), O 1s (C and D) and N 1s (E and F).

FTIR spectra of pristine and contaminated GO/mCS/OC are highlighted in Figure 4.7. Pristine nanocomposite showed several notable bands throughout the spectrum (4000

– 450 cm^{-1}). The bands that stood out at 3620 and 3371 cm^{-1} represent –NH and –OH elongations that come from the amines present in chitosan and from the hydroxyl group of carboxylic acids and the alcohol group that are mainly present in GO (Erim et al., 2021; Jawad et al., 2020). The bands found at 2923 and 2850 cm^{-1} represent asymmetric and symmetrical C–H elongations present in the aromatized groups of chitosan and GO, as well as in the alkylammonium cations that give the clay an organophilic character (Andrade et al., 2020; Hosseini et al., 2021). The highlighted bands at 1641 and 1567 cm^{-1} represent C=O and N–H elongations, respectively, being related to the GO carboxylates and to chitosan amines (Erim et al., 2021; Hosseini et al., 2021). The bands that stood out at 1468, 1377 and 1303 cm^{-1} are related to C–N elongations, representing amines that are on chitosan surface and can react with epoxy and carboxylate groups of GO to form amides, which are also related with this stretch (Jawad et al., 2020; Lin et al., 2013; Xu et al., 2019). The highlight band at 1045 cm^{-1} is related to Si–O stretches present in organoclay, as well as epoxy groups located in the basal plane of GO (Maia et al., 2019; Shang et al., 2021; Wang et al., 2012). The bands located between 950 and 800 cm^{-1} are related to –OH stretches in the mineral layer, as well as the bands of 600 – 450 cm^{-1} represent Si–O–Al and Si–O–Si bonds (de Andrade et al., 2020; Maia et al., 2019). The peak located at 521 cm^{-1} is also related to Fe–O bonds that represent chitosan magnetization (Jawad et al., 2020; Malwal and Gopinath, 2017).

The nanocomposite before adsorption showed similar bands to contaminated material, although in some cases displaced and less intense. The band related to –NH bond, which was already overshadowed by –OH band, was not evident after adsorption, even with the band related to the hydroxyl group being wider and displaced to 3410 cm^{-1}. The decrease in intensity and the red-shift of the hydroxyl-related peak indicates presence of hydrogen bonds. This functional group acts as hydrogen donor and possibly the aromatic ring and oxygens present in EE2 molecule act as hydrogen acceptors (Sekulic et al., 2019). The bands between 1650 and 1300 cm^{-1}, as well as the band at 1045 cm^{-1} showed significant loss of intensity corroborating the evidence that oxygenated groups (originated mainly from GO and chitosan) and nitrogen groups (from amines and possibly formed amides) participate in EE2 adsorption mechanisms. The analysis of XPS and FTIR spectra of pristine and contaminated sample showed that hydrogen bonds and $\pi - \pi$ interactions are present in EE2 adsorption process on GO/mCS/OC surface. The proposed interactions between the functional groups present on the nanocomposite surface and EE2 molecule are illustrated in Figure 4.8.

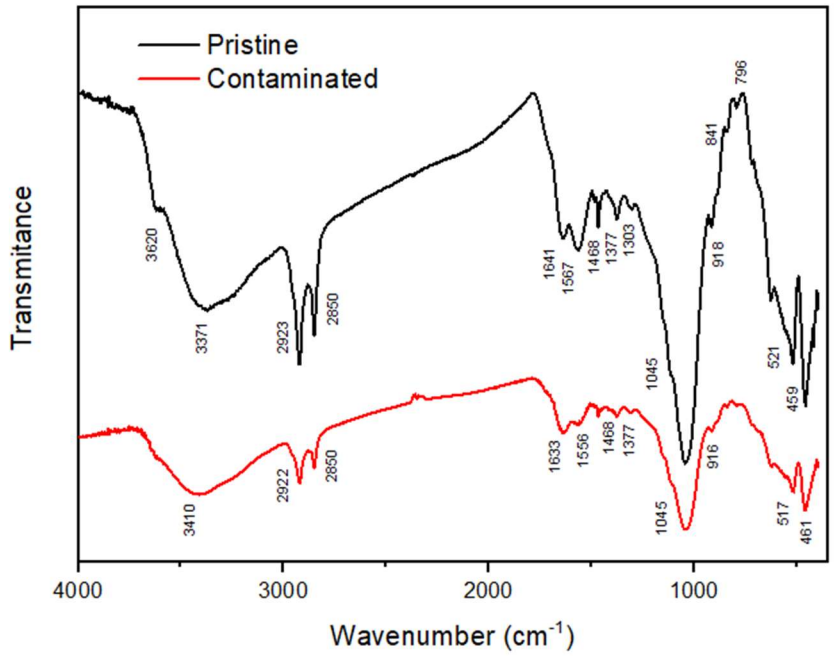

Figure 4.7 – FTIR spectra of pristine and contaminated GO/mCS/OC.

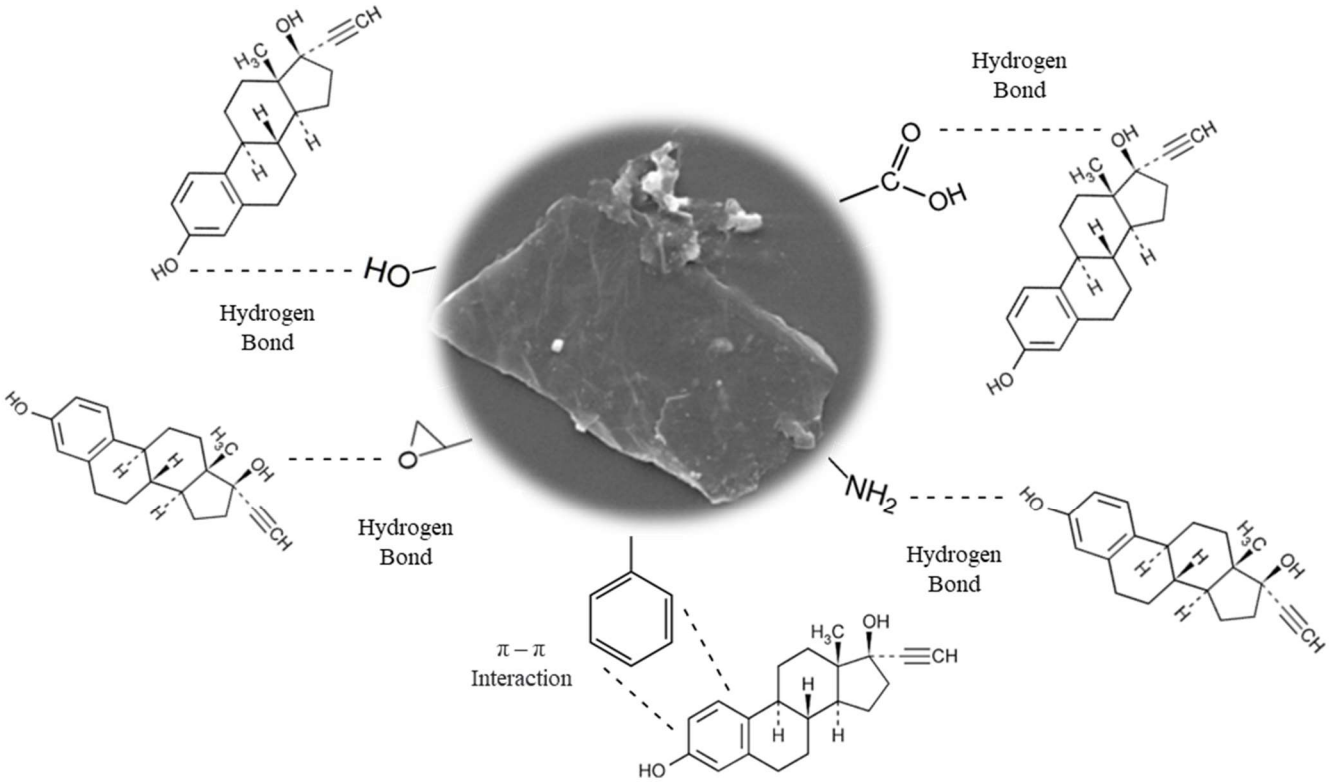

Figure 4.8 – Expected interactions between GO/mCS/OC functional groups and EE2.

SEM micrographs of pristine and contaminated GO/mCS/OC are shown in Figure 4.9. The micrographics from samples before and after the adsorption process were similar, indicating that the removal of EE2 did not change the material structure. The surface of GO/mCS/OC was heterogeneous, showing points of higher density that indicate the presence of clay, as well as intercalated lamellar structures confirming the presence of GO sheets.

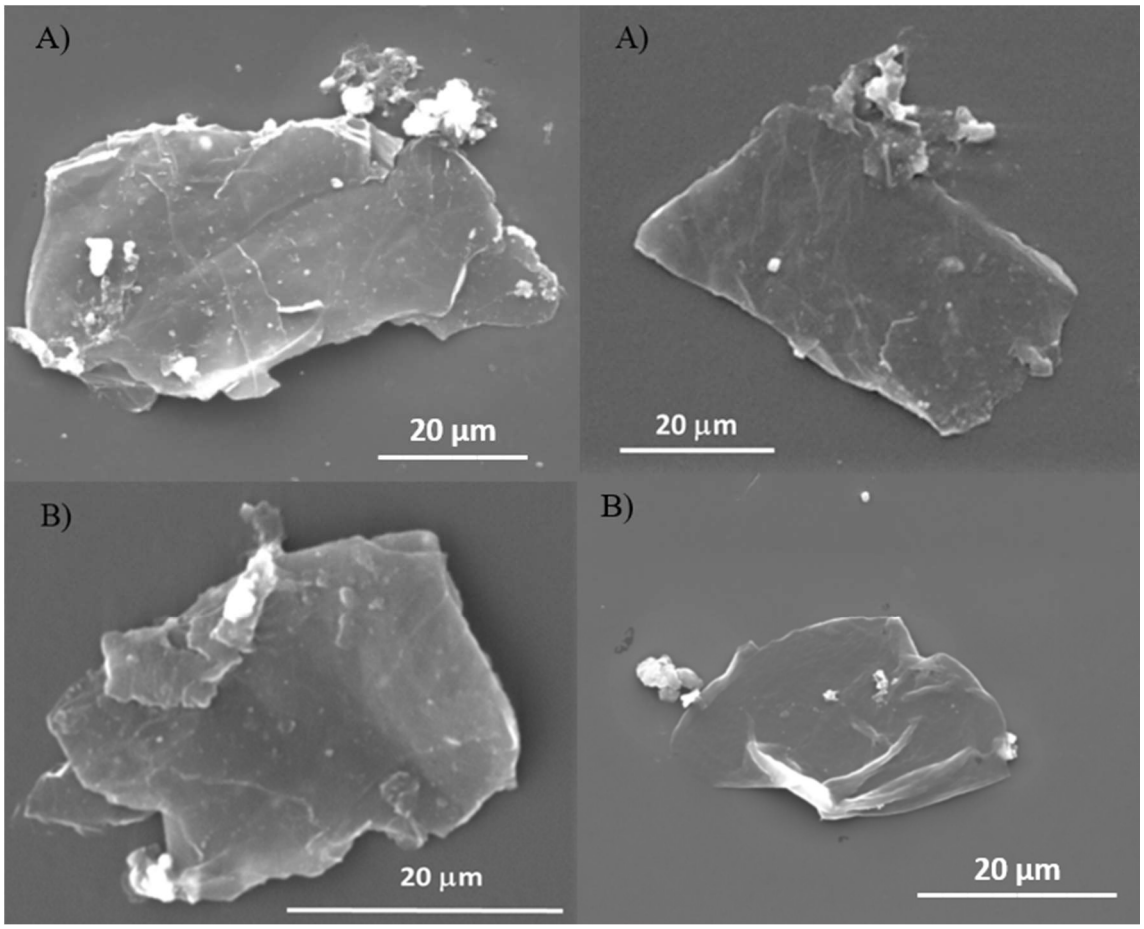

Figure 4.9 – SEM images of pristine (A) and contaminated (B) GO/mCS/OC.

3.2. Effects of nanoadsorbent dosage, pH and sonication time

The positive effect of nanoadsorbent dosage on EE2 removal was evident in Figure 4.10 (A), while the value of adsorption capacity decreases with the increase of the nanoadsorbent mass. Similar results on the effect of dosage in relation to adsorption capacity and percentage of removal were also observed for other nanoadsorbents (Alqadami et al., 2018, 2016). The system presented a maximum removal percentage of 89.8 % at a dosage of 0.35 mg mL^{-1} and a maximum adsorption capacity of 50.5 mg g^{-1} at a dosage of 0.05 mg mL^{-1}. The increase in dosage resulted in a significant increase in removal up to 0.25 mg mL^{-1}, so from that point on, the results were statistically similar

according to Turkey test with a 5 % significance level. Figure 4.10 (B) illustrates the effect of solution pH on EE2 adsorption process by GO/mCS/OC. The removal percentage had a decrease from pH 3 to pH 4 and a slight increase from pH 4 to pH 8. However, according to Turkey test, the results were statistically equivalent with a 5 % significance level, except between pH 4 and 8. Sonication time is a parameter widely evaluated in nanomaterial suspensions and implies the exfoliation of graphene materials, which can increase stability and surface area (Neves et al., 2020). The effect of sonication time of GO/mCS/OC suspensions on EE2 removal is illustrated in Figure 4.10 (C). The results indicated superior performance when the system was not submitted to ultrasonic bath and a decrease in efficiency with increasing sonication time. These results revealed that the nanocomposite sheets can suffer fragmentation with the procedure, compromising some interactions that help in adsorption process (Li et al., 2013). The evaluation of this parameter by Turkey test with a 5 % significance level demonstrated that the application of the ultrasonic bath resulted in statistically similar removal efficiencies.

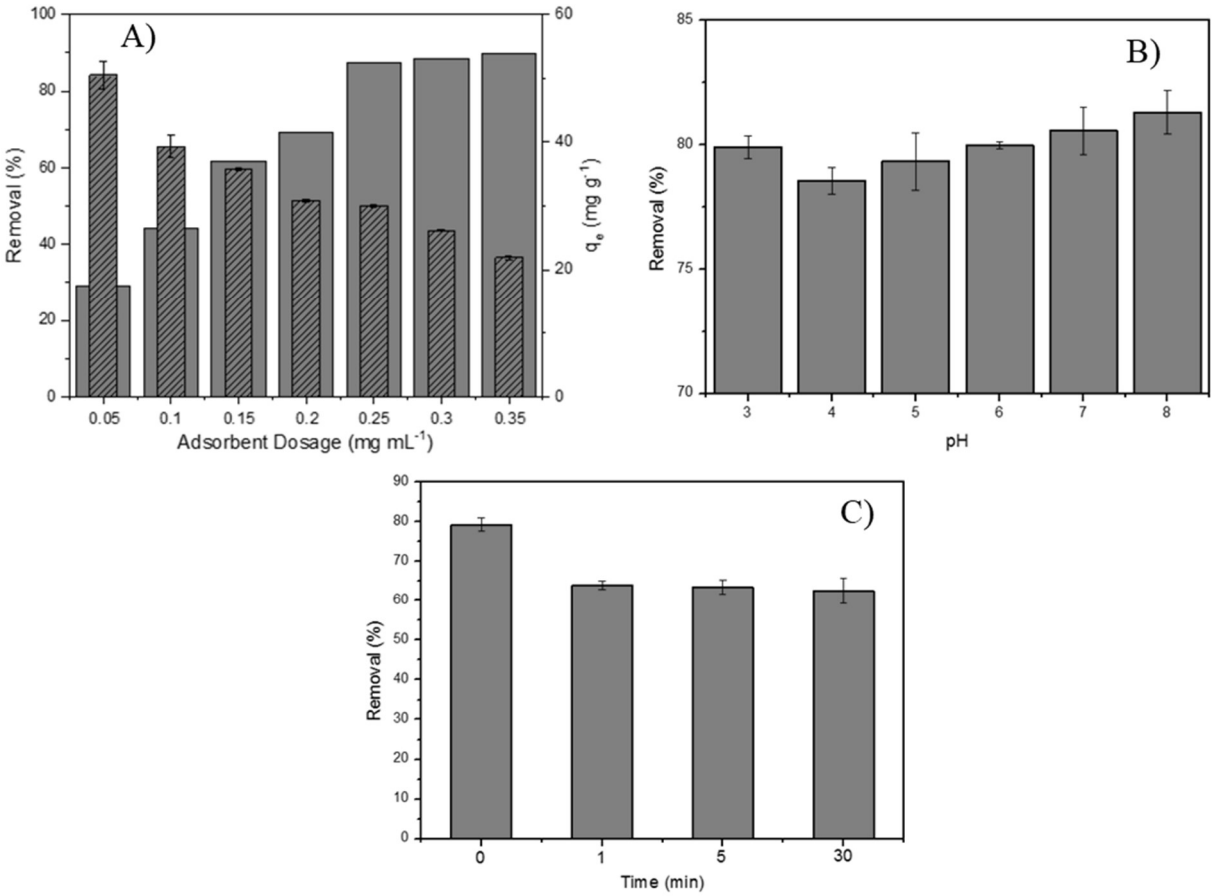

Figure 4.10 – Effects of nanoadsorbent dosage (A), solution pH (B) and sonication time (C). Solid bars indicate percent removal efficiency (%) and hatched bars refer to adsorption capacity (q_e)

3.3. Adsorption kinetics

The kinetic curves of EE2 adsorption by GO/mCS/OC for different initial concentrations of adsorbate are shown in Figure 4.11. The increase in adsorption capacity with the increase in initial concentration of EE2 is evidenced. EE2 was quickly removed in the first 30 min of the process, followed by slower removal kinetics until the equilibrium plateau, which was reached in about 120 min. The adsorption capacities at equilibrium were 0.131, 0.098 and 0.061 mmol g^{-1} (38.8, 29.2 and 18.2 mg g^{-1}) for initial concentrations of 0.03, 0.02 and 0.01 mmol L^{-1}, respectively.

Literature presents great variation in the equilibrium time for EE2 adsorption kinetic assays, depending on the type of adsorbent and the initial concentration evaluated. Han *et* al. (2013) reported equilibrium after 60 min in polyamides, whereas Lai *et* al. (2022) reported that equilibrium was reached after 10 h using heat-treated plastic waste (Han et al., 2013; Lai et al., 2022). Zhang *et* al. (2020) also reported a kinetic equilibrium around 120 min for a copper sulfide-based nanomaterial (Zhang et al., 2020). Thus, the developed nanocomposite showed relatively fast kinetics and is within the range found in the literature.

PFO and PSO kinetic models, as well as Boyd and IP diffusion models were applied to experimental data, seeking to describe adsorption mechanisms. The models and adjustment parameters are organized in Table 4.2.

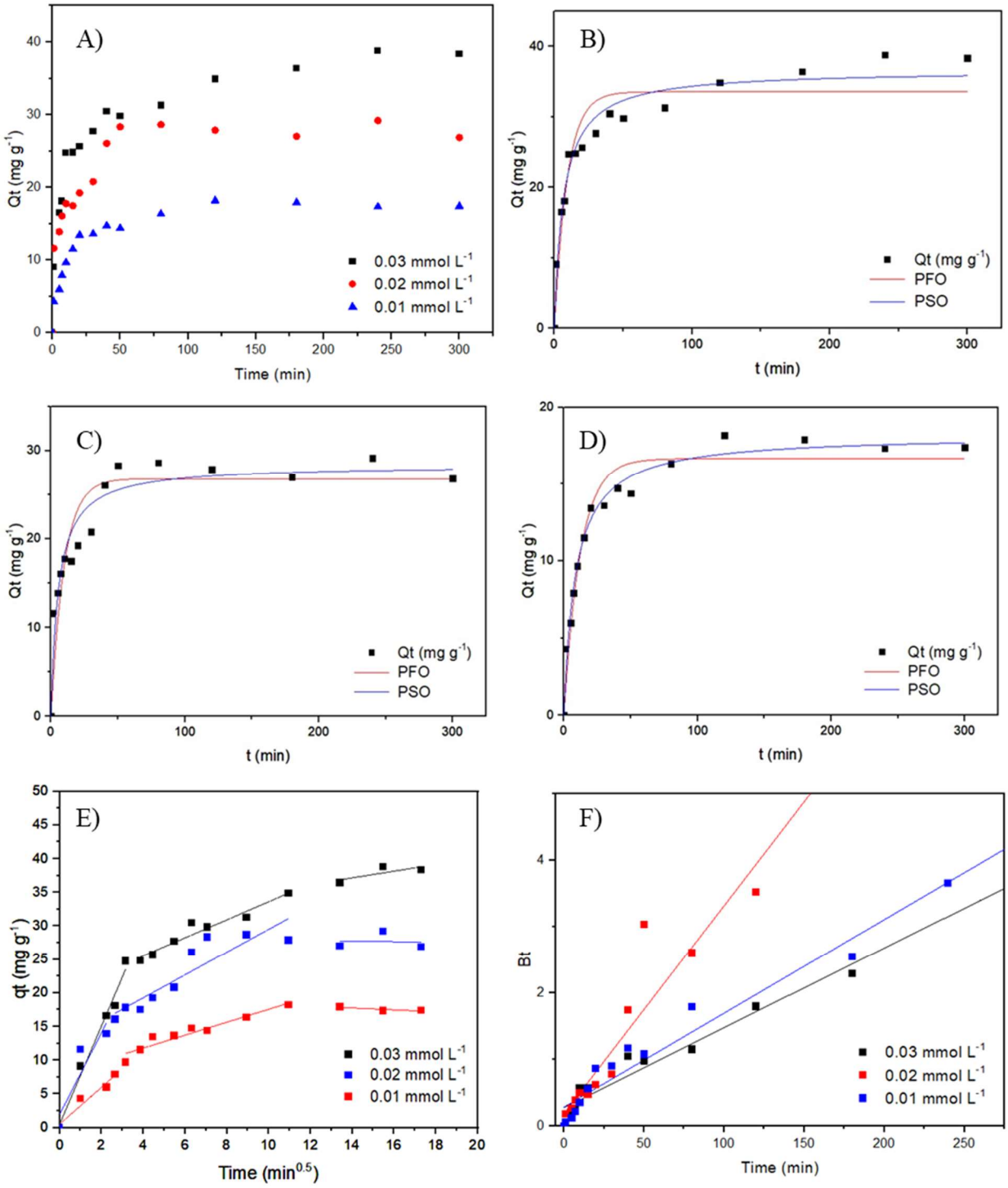

Figure 4.11 – Adsorption kinetics graph (A); Fitting of PFO and PSO models to the experimental data at 0.03 mmol L^{-1} (8.9 mg L^{-1}) (B), 0.02 mmol L^{-1} (5.9 mg L^{-1}) (C) and 0.01 mmol L^{-1} (3 mg L^{-1}) (D); Linear fit to intraparticle diffusion model (E) and to Boyd surface diffusion model (F).

Table 4.2 – Kinetic parameters of models fitted to the experimental data of EE2 adsorption onto GO/mCS/OC at different initial concentrations (0.03, 0.02 and 0.01 mmol L^{-1}).

Model	Parameter	Initial Concentration (mmol L^{-1})		
		0.03	**0.02**	**0.01**
Experimental	q_e (mmol g^{-1})	0.131	0.098	0.061
	q_e (mg g^{-1})	38.815	29.184	17.918
PFO	q_e (mmol g^{-1})	0.113	0.090	0.056
	q_e (mg g^{-1})	33.544	26.795	16.672
	K_1 (min^{-1})	0.107	0.102	0.081
	R^2_{Adj}	0.890	0.816	0.942
	χ^2_{Red}	13.269	12.486	1.775
	AIC_C	44.817	43.904	14.640
PSO	q_e (mmol g^{-1})	0.124	0.096	0.061
	q_e (mg g^{-1})	36.614	28.381	18.217
	K_2 (g mg^{-1} min^{-1})	0.00411	0.00634	0.00628
	R^2_{Adj}	0.957	0.887	0.974
	χ^2_{Red}	5.194	7.701	0.806
	AIC_C	30.748	36.660	2.803
IP	C (mmol g^{-1})	0.068	0.042	0.027
	C (mg g^{-1})	20.183	12.462	7.968
	K_I	1.343	1.704	0.959
	R^2_{Adj}	0.924	0.793	0.903
Boyd	D_{EF} (mm^2 min^{-1})	3.051×10^{-6}	7.948×10^{-6}	3.587×10^{-6}

	R^2_{Adj}	0.934	0.870	0.951

The pseudo-second order model exhibited q_e values closer to experimental ones and better represented the adsorption kinetic behavior for all concentrations. The upper value of adjusted coefficient of determination, as well as the lower value of reduced Chi-squared and corrected Akaike criterion, corroborated with a better fit of PSO model to experimental data. This fact indicates that chemisorption may be involved in adsorption mechanism of EE2 on GO/mCS/OC (Brazovskaya and Golubeva, 2020), as reported in the adsorption of this contaminant by other materials (Han et al., 2013; Jun et al., 2019; Lai et al., 2022). The presence of chemisorption corroborates the hydrogen bonds that were proposed by characterizations (Yankovych et al., 2021).

The intraparticle and Boyd diffusion models are based on the resistance to mass transfer and were applied to experimental data for a better understanding of the limiting step of the process. The IP model presented a multilinear profile separated into three stages for all concentrations evaluated. The three regions represent external mass transfer, intraparticle diffusion and equilibrium (Ruiz et al., 2010). The second region suggests the presence of intraparticle diffusion step, however the low adjustment and the constant C value greater than zero indicate that this is not the adsorption limiting step (Wu et al., 2009). The non-linear profile of endpoints presented by Boyd model and its straight line not crossing the origin corroborate the IP model hypothesis. The evaluation of diffusion models suggests the existence of a stage of resistance to mass transfer in external film (Boyd et al., 1947).

3.4. Adsorption isotherms

The equilibrium models of Langmuir, Freundlich and BET were fitted to experimental data of the equilibrium isotherms of EE2 adsorption by GO/mCS/OC obtained at 30, 40 and 50 °C (Figure 4.12). The positive effect of temperature is pronounced, revealing the endothermic character and that adsorption can occur via chemisorption or by a combination of chemisorption and physisorption (Tran et al., 2016). Similar behavior was also observed in EE2 removal by another reduced graphene oxide magnetic nanocomposite (Luo et al., 2017). The positive effect of temperature is pronounced for smaller dosages, however with increasing dosage (lower values of equilibrium concentration in fluid phase), this influence becomes less expressive in the

values of *q*. Table 4.3 grouped the parameters of Langmuir, Freundlich and BET models that were fitted to experimental data.

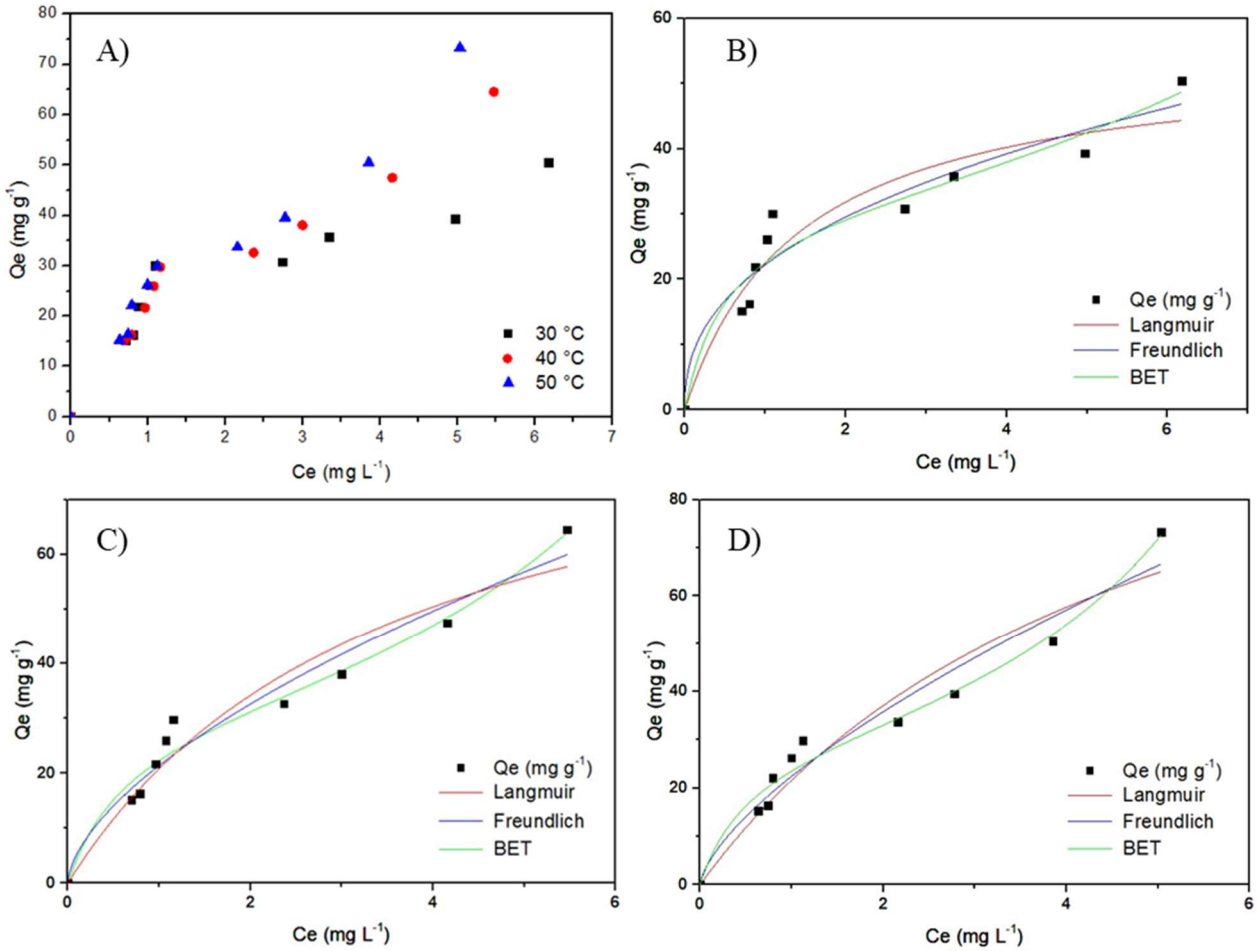

Figure 4.12 – Equilibrium isotherms of EE2 adsorption on GO/mCS/OC (A); Nonlinear fitting of Langmuir, Freundlich and BET models to the experimental data at temperatures of 30 (B), 40 (C) and 50 °C (D).

Table 4.3 – Parameters of equilibrium models applied to experimental data of EE2 adsorption on GO/mCS/OC at 30, 40 and 50 °C.

Model	Parameter	Temperature (°C)		
		30	**40**	**50**
Experimental	q_{Max} (mmol g^{-1})	0.170	0.218	0.247
	q_{Max} (mg g^{-1})	50.471	64.552	73.290
Langmuir	q_{Max} (mmol g^{-1})	0.184	0.324	0.437
	q_{Max} (mg g^{-1})	54.604	96.110	129.61
	K_L (L mg^{-1})	0.699	0.276	0.200
	R^2_{Adj}	0.905	0.932	0.923
	χ^2_{Red}	19.092	22.449	32.217
	AIC_C	37.261	38.881	42.493
Freundlich	K_F [(mg g^{-1})(L mg^{-1})$^{1/n}$]	22.233	21.390	22.443
	n	0.410	0.607	0.674
	R^2_{Adj}	0.854	0.932	0.927
	χ^2_{Red}	18.728	17.106	24.819
	AIC_C	35.733	34.828	38.550
BET	q_B (mmol g^{-1})	0.104	0.105	0.101
	q_B (mg g^{-1})	30.703	31.241	29.973
	K_B (L mg^{-1})	2.054	1.619	1.957
	K_U (L mg^{-1})	0.065	0.098	0.120
	R^2_{Adj}	0.923	0.971	0.978
	χ^2_{Red}	15.613	9.561	9.158
	AIC_C	39.914	35.010	34.580

Isotherms profiles shown in Figure 4.12 indicate that the material is not completely saturated with the decrease in nanoadsorbent mass, suggesting that the

adsorbate is deposited in multilayers. The difference between q_{Max} values proposed by Langmuir model and experimental ones corroborates with this statement, since this model considers homogeneous surface and monolayer adsorption (Song et al., 2013). Although the values of R^2_{Adj} for Langmuir and Freundlich model are similar, the lower values of χ^2_{Red} and AIC_C for Freundlich model are indicative of multilayer physisorption on a heterogeneous surface (Oliveira et al., 2019). Values of n less than 1 indicate low energy interactions between the adsorbate and the adsorbent, which are also characteristic of physical interactions (Site, 2001). The experimental behavior was better represented by the BET model, implying more satisfactory values of R^2_{Adj} e χ^2_{Red}. Despite better representing experimental data, the corrected Akaike criterion for BET model presents a slightly higher value at some temperatures because the model presents one more adjustment parameter than Langmuir and Freundlich models. The maximum monolayer adsorption capacity, represented by q_B, was about 30 mg g^{-1}. However, this value differs from maximum adsorption capacity that tends to grow with formation of multilayers (Ebadi et al., 2009; Piccin et al., 2017). The simultaneous occurrence of chemical and physical interactions in EE2 removal by GO/mCS/OC is supported by kinetic tests and by favoring adsorption with increasing temperature (chemical interactions), as well as by the evidence presented in Freundlich and BET models (physical interactions).

Table 4.4 summarizes and compares the maximum adsorption capacity observed for GO/mCS/OC with other adsorbents reported in literature. GO/mCS/OC showed superior performance to several advanced adsorbents such as carbon nanotubes, polyamides and reduced graphene oxide, indicating that it is a promising material for the removal of EE2 from aqueous media.

Table 4.4 – Maximum adsorption capacity of EE2 adsorption for different adsorbents.

Adsorbent	$q_{Máx}$ **(mg g^{-1})**	**Reference**
GO/mCS/OC	50.47 (30 °C)	This study
GO/mCS/OC	64.55 (40 °C)	This study
GO/mCS/OC	73.29 (50 °C)	This study
Polyamide 612	25.4 (25 °C)	(Han et al., 2013)
Nano-copper Sulfide	147.06 (25 °C)	(Zhang et al., 2020)
Metal-organic Framework	200.4 (40 °C)	(Jun et al., 2019)
Reduced graphene oxide magnetic composite	37.33 (45 °C)	(Luo et al., 2017)
Multi-walled carbon nanotubes	0.472 (25 °C)	(Al-Khateeb et al., 2014)
Molecular imprinted polymer	34.2*	(Zhongbo and Hu, 2008)
Champignon Stalk	18.95 (25 °C)	(Menk et al., 2019)
$CeO_2/CuFe_2O_4$ nanofibers	179 (25 °C)	(Sobhanardakani and Zandipak, 2018)
Electrospun microfibers (PBAT)	2.23 (25 °C)	(Westrup et al., 2021)

* The study does not mention the temperature of the experiment.

3.5. Adsorption thermodynamics

The thermodynamic parameters of EE2 adsorption in GO/mCS/OC were evaluated and are summarized in Table 4.5. Henry's law was applied in the infinite dilution region and parameters were calculated from the graph of $ln(K_D)$ vs $1/T$.

Table 4.5 – Thermodynamic parameters of EE2 adsorption on GO/mCS/OC in different temperatures (30, 40 and 50 °C).

T (°C)	ΔH^0 (kJ mol^{-1})	ΔS^0 (kJ mol^{-1}K^{-1})	ΔG^0 (kJ mol^{-1})	$T\Delta S^0$ (kJ mol^{-1})	E_a (kJ mol^{-1})
30			–21.674	54.017	34.863
40	32.343	0.178	–23.456	55.798	34.946
50			–25.278	57.580	35.029

The positive value of enthalpy variation (ΔH^0) indicates that EE2 adsorption on GO/mCS/OC has an endothermic nature, therefore, it is favored by temperature. The increase in activation energy with increasing temperature also indicates the endothermic profile of the system. Values of ΔH^0 in the range between 2 – 21 kJ mol^{-1} are related to systems governed by physical adsorption, while values between 80 – 200 kJ mol^{-1} are related to chemical adsorption processes (Saha and Chowdhury, 2011). Intermediate values are related to systems wherein both interactions take place. However, the proximity between 21 e 32 kJ mol^{-1} indicates predominance of physisorption. The occurrence of physisorption corroborates the presence of π – π interactions between the aromatics of nanoadsorbent and adsorbate (Pérez-Guardiola et al., 2017). Positive values of entropy variation (ΔS^0) indicate an increase in system disorder and the presence of dissociative mechanisms in the adsorption process (Saha and Chowdhury, 2011). Negative values of variation of Gibbs energy and its decrease with increasing temperature suggest that the process is spontaneous and favored by the increase in temperature (Mansouriieh et al., 2016).

The proposed adsorbate-adsorbent system is controlled by entropy changes, because for all temperatures $T\Delta S^0 > \Delta H^0$, revealing that the system entropy has more influence on the EE2 adsorption process. The endothermic and spontaneous profile as well as the tendency for physical adsorption of EE2 were reported in the literature for some materials such as metal-organic framework and reduced graphene oxide magnetic composite (Jun et al., 2019; Luo et al., 2017). The adsorption of EE2 on nano-copper sulfide showed evidence of chemical interactions, while its adsorption on carbon nanotubes showed an exothermic nature (Al-Khateeb et al., 2014; Zhang et al., 2020).

3.6. Designing a simplified bath adsorption system

The simplified batch design for GO/mCS/OC – EE2 system estimated the amount of nanocomposite needed to remove 50, 70 and 90 % of the microcontaminant from the aqueous medium (Figure 4.13) with an initial concentration of 0.03 mmol L^{-1}. The BET model was used due to its better fit to equilibrium data to estimate the values of q_e in a simplified batch system.

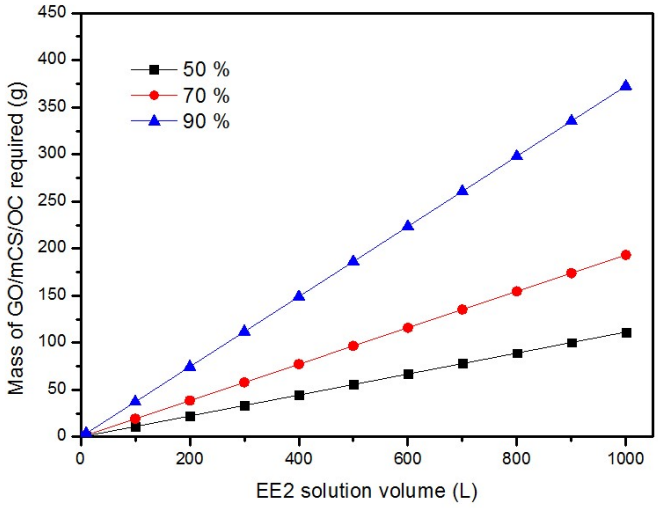

Figure 4.13 – Estimate of the mass of nanoadsorbent (g) needed to remove 50, 70 and 90% of EE2 from 1000 L of solution of 0.03 mmol L^{-1}.

There is a linear relationship between effluent volume and nanocomposite mass for all evaluated efficiencies. For 1000 L of effluent with an initial concentration of 0.03 mmol L^{-1}, 112, 194 and 373 g of nanocomposite are needed to remove 50, 70 and 90 % of EE2, respectively. Farias *et* al. (2022) proposed a similar batch system for removing bisphenol A, another emerging contaminant, and a considerably superior performance was observed for GO/mCS/OC nanocomposite. The study used the same organoclay applied in nanocomposite synthesis, however, to remove 90 % of BPA in 1000 L of solution with 1 mmol L^{-1}, a mass 20 times greater was required than those calculated in the work (Farias et al., 2022). Coelho *et* al. (2020) also proposed a batch system using a bioadsorbent obtained from residual algae to remove propranolol hydrochloride, another drug considered an emerging contaminant. The system presented required 18.4 g of bioadsorbent to remove 90 % of the contaminant from only 10 L of solutions with 1 mmol L^{-1} (Coelho et al., 2020). A direct comparison of these systems reported for BPA and propranolol with the present study is not possible, as they are different adsorbates and the studies were carried out at different concentrations.

3.7. Isosteric heat of adsorption

The isosteres obtained for different values of constant surface coverage (q_e) were illustrated in Figure 4.14. The values of q_e chosen for the evaluation of isosteric heat of adsorption were 16.3, 32.4, 39 and 49.5 mg g^{-1} and their values are shown in Table 4.6.

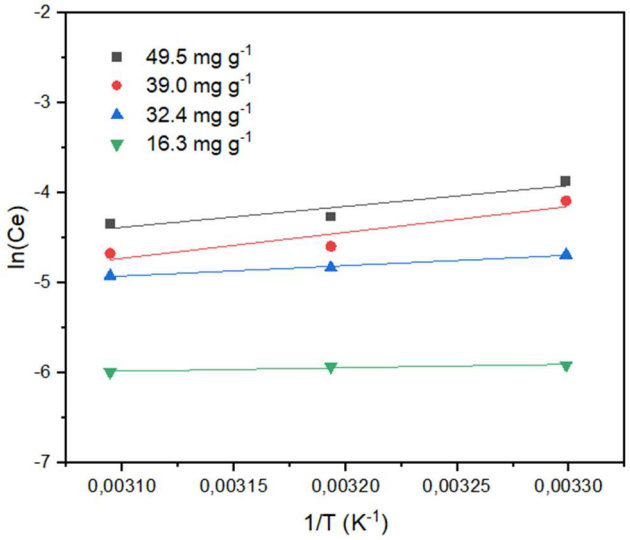

Figure 4.14 – Adsorption isosteres of EE2 adsorption on GO/mCS/OC applied for different fixed adsorption capacities (q_e) (16.3; 32.4; 39 and 49.5 mg g^{-1}).

Table 4.6 – Isosteric heat values of EE2 adsorption on GO/mCS/OC applied for different fixed adsorption capacities (q_e) (16.3; 32.4; 39 and 49.5 mg g^{-1}).

q_e (mg g^{-1})	ΔH_{Iso} (kJ mol^{-1})	R^2
49.5	19.33	0.88
39	23.95	0.86
32.4	9.62	0.99
16.3	3.15	0.91

The ΔH_{Iso} values obtained were 19.33, 23.95, 9.62 and 3.15 kJ mol^{-1} for q and 49.5, 39, 32.4 and 16.3 mg g^{-1}. The variation of isosteric heat values indicates that the nanocomposite surface is energetically heterogeneous (Silva et al., 2021). Furthermore, its values below 80 kJ mol^{-1} indicate that the adsorption process is governed by physical mechanisms (Silva et al., 2021). The results corroborate with experimental data that were better represented (Freundlich and BET models), also denoting the heterogeneous characteristic and the energetic non-uniformity of the active sites.

3.8. Regeneration cycles in bath

The reuse of GO/mCS/OC was investigated for five cycles to remove EE2, evaluating acetonitrile and ethanol as eluents (Figure 4.15). Removal efficiency and adsorption capacity using acetonitrile as eluent decreased from 74.9 % and 36.5 mg g^{-1} to 46.7 % and 20 mg g^{-1} in the fifth adsorptive cycle. In its turn, using ethanol as eluent, the same response variables decreased from 68.9 % and 30.8 mg g^{-1} to 32.1 % and 14.4 mg g^{-1} in the fifth adsorptive cycle, respectively. In comparison with the results obtained under the same conditions in the equilibrium tests (69.3 % and 30.8 mg g^{-1}), the regeneration of GO/mCS/OC using acetonitrile as eluent presented a satisfactory performance compared to the initial for the first two cycles, decreasing only from the third adsorptive cycle. The regeneration of GO/mCS/OC using ethanol showed a lower performance compared to acetonitrile and a significant decrease from the second cycle. The decrease in GO/mCS/OC regenerability may be related to the shear force, which alters the structure and reduces the number of active sites, and to the loss of mass of the nanocomposite due to its reuse for five consecutive cycles. The results indicated that the synthesized nanocomposite is a potential adsorbent for EE2 removal in up to two cycles, losing up to about 40% of its EE2 adsorptive capacity thereafter.

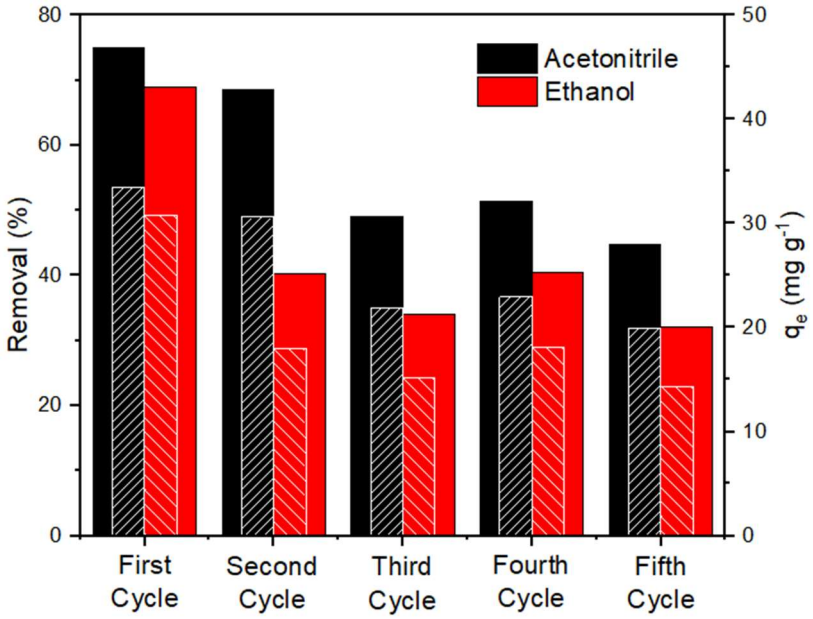

Figure 4.15 – Removal percentages and adsorption capacities of EE2 on GO/mCS/OC by consecutive regeneration cycles. Solid bars indicate percent removal efficiency (%) and hatched bars refer to adsorption capacity (q_e).

3.9. Selectivity evaluation

The selectivity of the nanocomposite was evaluated for three different initial concentration conditions in binary solutions of EE2 and BPA (Figure 4.16). In the condition with the highest amount of EE2 the tests showed removal percentages of 84.9 and 67.5 % for EE2 and BPA, as well as adsorption capacities of 0.069 and 0.030 mmol L^{-1} (20.5 and 6.9 mg g^{-1}) respectively. In the solution with the highest amount of BPA, a removal percentage of 82.4 and 64.7 % for EE2 and BPA, as well as adsorption capacities of 0.044 and 0.055 mmol L^{-1} (13.1 and 12.7 mg g^{-1}) were observed, respectively. In the equimolar solution, a removal percentage of 89.3 and 73.2 % for EE2 and BPA, as well as adsorption capacities of 0.048 and 0.039 mmol L^{-1} (14.2 and 8.8 mg g^{-1}) were obtained, respectively. All conditions evaluated showed satisfactory removal percentages and adsorption capacities for both emerging contaminants.

Removal percentages and adsorption capacities for EE2 were higher than for BPA in all evaluated conditions, except in the condition where BPA was predominant. Under these conditions, although the percentage of removal of EE2 is higher, its adsorption capacity was lower than BPA adsorption capacity due to the excess of this contaminant in the medium, implying a greater adsorbed amount. Selectivity assays demonstrated that GO/mCS/OC interacts better with EE2 than with BPA.

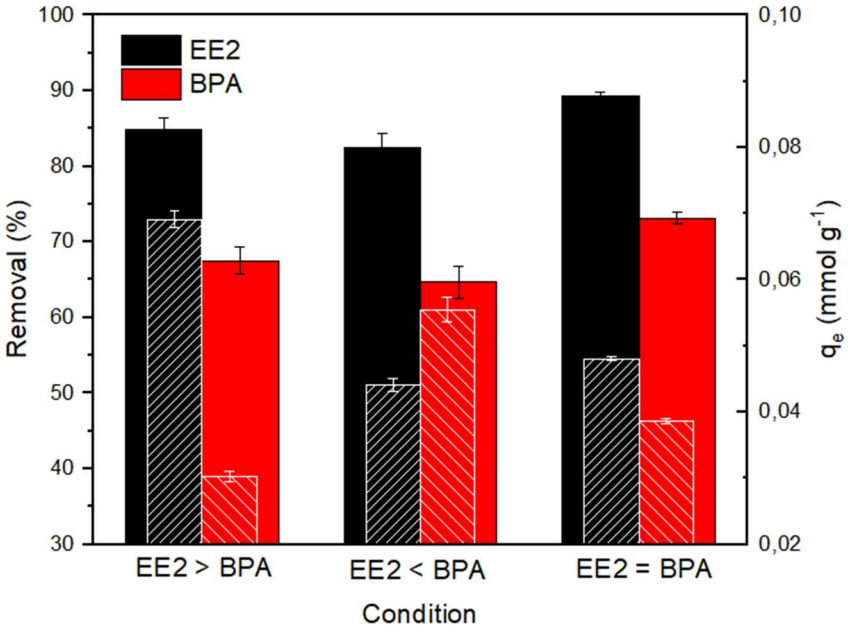

Figure 4.16 – Selectivity tests for 5 mL of binary solutions of BPA and EE2 for three different initial concentrations (EE2/BPA: 0.016/0.009 mmol L^{-1}, 0.010/0.017 mmol L^{-1} and 0.010/0.010 mmol L^{-1}). Solid bars indicate percent removal efficiency (%) and hatched bars refer to adsorption capacity (q_e).

The distribution coefficient (K_{EE2} and K_{BPA}) and selectivity coefficient ($K_{EE2/BPA}$) are shown in Table 4.7. $K_{EE2/BPA}$ values greater than 1 indicate more selective adsorption for EE2 than BPA. $K_{EE2/BPA}$ values greater than 1 and close to unity, even in the condition where BPA was more abundant, suggest that the surface of GO/mCS/OC presents higher affinity with EE2.

Table 4.7 – Distribution and selectivity coefficients of tests in binary solutions of BPA and EE2 for three different concentrations (EE2/BPA: 0.016/0.009 mmol L^{-1}, 0.01/0.017 mmol L^{-1} and 0.01/0.01 mmol L^{-1}).

Condition	K_{EE2} (L g^{-1})	K_{BPA} (L g^{-1})	$K_{EE2/BPA}$
EE2 > BPA	24.13	10.23	2.36
EE2 < BPA	15.87	19.58	0.81
EE2 = BPA	15.94	12.04	1.32

BPA and EE2 molecules (Figure 4.17) have the same number of ionizable hydroxyls that theoretically are involved in hydrogen bonds. On the other hand, the BPA molecule has one more aromatic than the EE2 molecule, which should cause a greater possibility of π–π interactions. Although there are satisfactory affinities of the material for adsorption of both EE2 and BPA, its preference for EE2 is notable. A possible explanation for this may be related to the angular conformation of the BPA molecule, which can impair its physisorption in multilayers. Even though the EE2 molecule is bigger than that of BPA, its flatter conformation seems to favor its deposition onto the GO/mCS/OC surface.

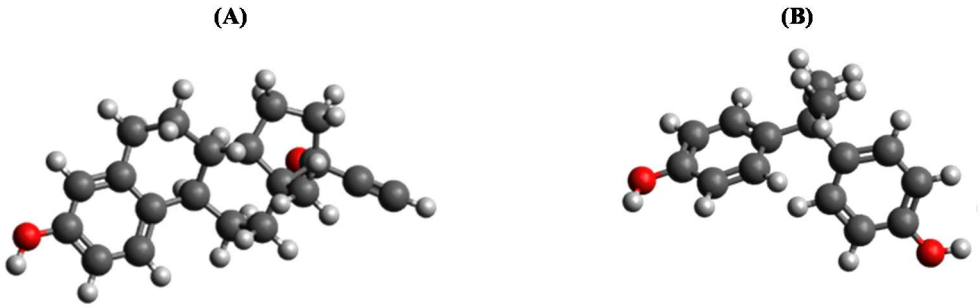

Figure 4.17 – Molecule structure of EE2 (A) and BPA (B), such that gray spheres represent carbon, red spheres represent oxygen, and white spheres represent hydrogen.

4. CONCLUSIONS

The synthesized nanocomposite (GO/mCS/OC) showed satisfactory performance in removing EE2 from the aqueous medium. The large adsorption capacity reached even with a small dose of adsorbent and low concentration of adsorbate suggest GO/mCS/OC as a promising material for environmental application. The nitrogen physisorption isotherms obtained were type II and are typical of meso and macroporous materials. The original material had a surface area of 17.8 m^2 g^{-1}, which was partially reduced after the adsorption process (13.2 m^2 g^{-1}). XRD spectra and SEM micrographs showed a heterogeneous structure of the prepared nanocomposite. Raman analysis showed the structural changes of GO and of the raw and contaminated GO/mCS/OC, indicating an increase in imperfections in the nanocomposite structure after the contamination process. XPS and FTIR analyses provided information on predominant functional groups and bonds in nanocomposite structure, revealing that oxygenated and nitrogenated groups, as well as aromatic structure, participate in the EE2 capture through hydrogen bonds and π–π interactions. The models fitted to kinetic data indicated that chemisorption was present, corroborating hydrogen bonds, and that external mass transfer was the main step in the adsorption process. Equilibrium isotherms showed an endothermic profile for the system, being also indicative of the presence of chemisorption. BET and Freundlich models fitted the equilibrium data well, suggesting that the material has heterogeneous characteristics and that there is formation of multilayers through physisorption, corroborating π–π interactions highlighted in the process. The maximum experimental adsorption capacity obtained for GO/mCS/OC at 30 °C was 50.5 mg g^{-1}, while the BET model predicted a maximum monolayer adsorption capacity of 30.7 mg g^{-1}. This difference in the maximum adsorbed amount also corroborates the coexistence of chemisorption and physisorption. Although both types of interactions are present in EE2 adsorption process in GO/mCS/OC, the values of Freundlich's *n* factor, enthalpy variation and isosteric heat suggest a predominance of physical interactions. The design of the simplified batch system showed the possibility of treating large volumes of effluent with a small amount of nanocomposite. GO/mCS/OC nanocomposite showed satisfactory regeneration performance using acetonitrile as eluent through two successive adsorptions, reducing up to 40% of its capacity until the fifth cycle. The selectivity tests displayed the best performance of EE2 against BPA, in addition to an ability to remove a large percentage of both even in a binary system. The set of results indicates the GO/mCS/OC as a

promising adsorbent technology for removal of emerging contaminants, with impactful benefits for the environment and suggests the evaluation of this material in more complex real aqueous matrices.

CREDIT AUTHORSHIP CONTRIBUTION STATEMENT

Arthur da Silva Vasconcelos de Almeida: Methodology, Writing - original draft, Investigation, Data curation. **Valmor Roberto Mastelaro:** Data curation. **Meuris Gurgel Carlos da Silva:** Writing – review & editing, Resources, Validation, Supervision. **Patrícia Prediger:** Methodology, Writing – review & editing, Resources, Supervision. **Melissa Gurgel Adeodato Vieira:** Conceptualization, Writing – review & editing, Resources, Validation, Supervision.

DECLARATION OF COMPETING INTERESTS

The authors declare that they have no known competing financial interests or personal relationships that could have appeared to influence the work reported in this paper.

ACKNOWLEDGMENT

The authors are grateful for the funding for this research provided by Research Supporting Foundation of the State of São Paulo (FAPESP, grants no. 2020/16004-9 and 2019/07822-2), the Brazilian National Research Council (CNPq, grants no. 406193/2018-5 and 308046/2019-6), and the Coordination for the Improvement of Higher Education Personnel (CAPES, financial code – 001). We also thank the SpectroChem Company for donating the organoclay.

APPENDIX 4.A. SUPPLEMENTARY DATA

The development of GO/mCS/OC nanocomposite comprised the synthesis of graphene oxide and magnetized chitosan, as well as its preparation with the commercial organophilic clay Spectrogel® - type C. The graphene oxide was synthesized using modified Hummers method (Hummers and Offeman, 1958), which consisted in the pre-oxidation of graphite, oxidation, washing and salts removal as illustrated in Figure 4.S1.

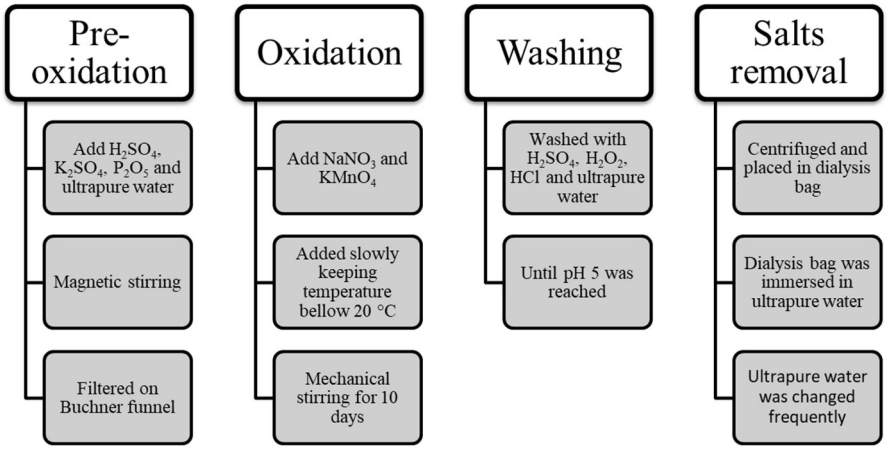

Figure 4.S1 – Graphene oxide synthesis scheme.

The synthesis of magnetic chitosan (Figure 4.S2) consisted of the preparation of iron nanoparticles, their reaction with chitosan and the washing of the material as suggested by Silva et al. (2013) and Wang et al. (2016).

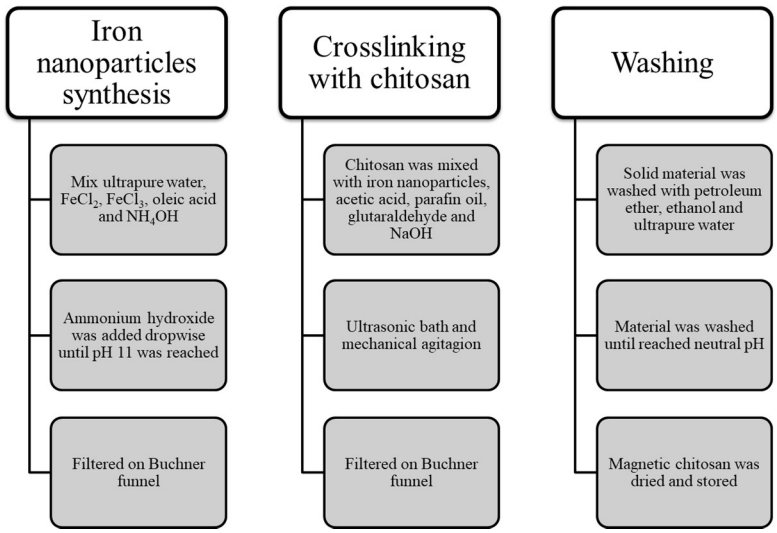

Figure 4.S2 – Magnetic chitosan synthesis scheme.

The GO/mCS/OC preparation (Figure 4.S3) involved the incorporation of magnetic chitosan in GO structure, washing to remove the non-adhered material and mixing with the Spectrogel® type C organoclay. The incorporation of magnetic chitosan in GO structure was based on Maleki and Paydar (2015). The size of the organoclay particles was classified between 200 – 400 mesh. The added organoclay mass was similar to the GO/mCS mass present in the system, resulting in a nanocomposite composed of 50% of each base material.

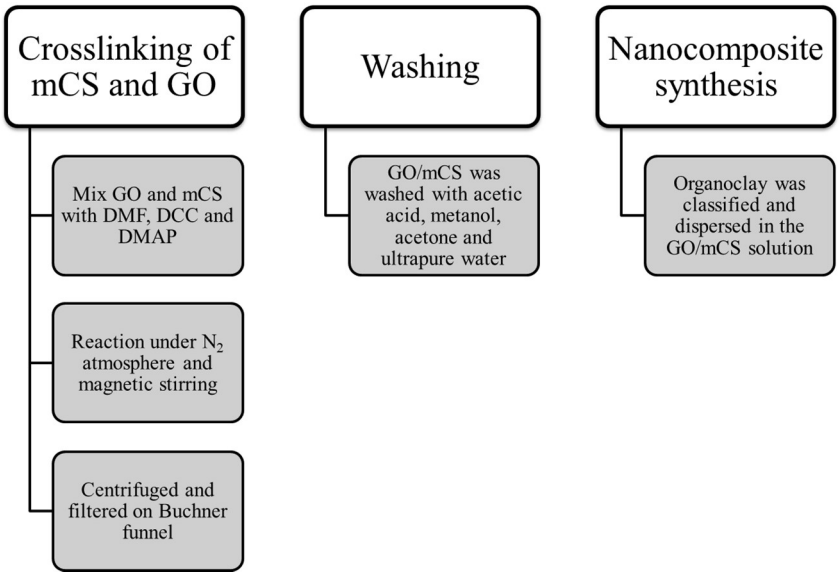

Figure 4.S3 – GO/mCS/OC synthesis scheme.

REFERENCES

Akhavan, O., 2015. Bacteriorhodopsin as a superior substitute for hydrazine in chemical reduction of single-layer graphene oxide sheets. Carbon 81, 158–166.

Al-Gaashani, R., Najjar, A., Zakaria, Y., Mansour, S., Atieh, M.A., 2019. XPS and structural studies of high quality graphene oxide and reduced graphene oxide prepared by different chemical oxidation methods. Ceramics International 45, 14439–14448. https://doi.org/10.1016/j.ceramint.2019.04.165

Al-Khateeb, L.A., Obaid, A.Y., Asiri, N.A., Abdel Salam, M., 2014. Adsorption behavior of estrogenic compounds on carbon nanotubes from aqueous solutions: Kinetic and thermodynamic studies. Journal of Industrial and Engineering Chemistry 20, 916–924. https://doi.org/10.1016/j.jiec.2013.06.023

Almeida, A. da S.V., Neves, T. de F., Silva, M.G.C., Prediger, P., Vieira, M.G.A., 2022. Synthesis of a novel magnetic composite based on graphene oxide, chitosan and organoclay and its application in the removal of bisphenol A, 17α-ethinylestradiol and triclosan. Journal of Environmental Chemical Engineering 10, 107071.

Alqadami, A.A., Naushad, Mu., Abdalla, M.A., Khan, M.R., Alothman, Z.A., 2016. Adsorptive Removal of Toxic Dye Using Fe3O4−TSC Nanocomposite: Equilibrium, Kinetic, and Thermodynamic Studies. Journal of Chemical and Engineering Data 61, 3806–3813.

Alqadami, A.A., Naushad, Mu., Alothman, Z.A., Ahamad, T., 2018. Adsorptive performance of MOF nanocomposite for methylene blue and malachite green dyes: Kinetics, isotherm and mechanism. Journal of Environmental Management 223, 29–36.

Álvarez-Torrellas, S., Sotelo, J.L., Rodríguez, A., Ovejero, G., García, J., 2017. Influence of the natural organic matter in the removal of caffeine from water by fixed-bed column adsorption. International Journal of Environmental Science and Technology 14, 833–840. https://doi.org/10.1007/s13762-016-1189-7

Antonelli, R., Malpass, G.R.P., da Silva, M.G.C., Vieira, M.G.A., 2021. Fixed-bed adsorption of ciprofloxacin onto bentonite clay: Characterization, mathematical modeling, and DFT-based calculations. Industrial and Engineering Chemistry Research 60, 4030–4040. https://doi.org/10.1021/acs.iecr.0c05700

Astrahan, P., Korzen, L., Khanin, M., Sharoni, Y., Israel, Á., 2021. Seaweeds fast EDC bioremediation: Supporting evidence of EE2 and BPA degradation by the red seaweed

Gracilaria sp., and a proposed model for the remedy of marine-borne phenol pollutants. Environmental Pollution 278. https://doi.org/10.1016/j.envpol.2021.116853

Bavasso, I., Poggi, C., Petrucci, E., 2020. Enhanced degradation of paracetamol by combining UV with electrogenerated hydrogen peroxide and ozone. Journal of Water Process Engineering 34. https://doi.org/10.1016/j.jwpe.2019.101102

Bediako, J.K., Lin, S., Sarkar, A.K., Zhao, Y., Choi, J.W., Song, M.H., Cho, C.W., Yun, Y.S., 2019. Evaluation of orange peel-derived activated carbons for treatment of dye-contaminated wastewater tailings. Environmental Science and Pollution Research 27, 1053–1068. https://doi.org/10.1007/s11356-019-07031-8

Bonate, P.L., 2011. Pharmacokinetic-Pharmacodynamic Modeling and Simulation, 2nd ed. Springer.

Boyd, G.E., Adamson, A.W., Myers Jr, L.S., 1947. The Exchange Adsorption of Ions from Aqueous Solutions by Organic Zeolites. II. Kinetics.

Brazovskaya, E.Y., Golubeva, O.Y., 2020. Development of Magnetic Nanocomposites Based on Beta Zeolites and Study of Their Sorption Properties. Petroleum Chemistry 60, 957–963. https://doi.org/10.1134/S0965544120080046

Briao, G.V., Silva, M.G.C., Vieira, M.G.A., Chu, K.H., 2022. Correlation of type II adsorption isotherms of water contaminants using modified BET equations. Colloid And Interface Science Communications 46, 100557. https://doi.org/10.1016/j.colcom.2021.100557

Cheng, N., Wang, B., Wu, P., Lee, X., Xing, Y., Chen, M., Gao, B., 2021. Adsorption of emerging contaminants from water and wastewater by modified biochar: A review. Environmental Pollution. https://doi.org/10.1016/j.envpol.2021.116448

Cobos, M., González, B., Fernández, M.J., Fernández, M.D., 2018. Study on the effect of graphene and glycerol plasticizer on the properties of chitosan-graphene nanocomposites via in situ green chemical reduction of graphene oxide. International Journal of Biological Macromolecules 114, 599–613. https://doi.org/10.1016/j.ijbiomac.2018.03.129

Coelho, C.M., de Andrade, J.R., da Silva, M.G.C., Vieira, M.G.A., 2020. Removal of propranolol hydrochloride by batch biosorption using remaining biomass of alginate extraction from Sargassum filipendula algae. Environmental Science and Pollution Research 27, 16599–16611. https://doi.org/10.1007/s11356-020-08109-4

Cychosz, K.A., Guillet-Nicolas, R., García-Martínez, J., Thommes, M., 2017. Recent advances in the textural characterization of hierarchically structured nanoporous materials. Chemical Society Reviews. https://doi.org/10.1039/c6cs00391e

Dai, J., Meng, X., Zhang, Y., Huang, Y., 2020. Effects of modification and magnetization of rice straw derived biochar on adsorption of tetracycline from water. Bioresource Technology 311. https://doi.org/10.1016/j.biortech.2020.123455

de Andrade, J.R., da Silva, M.G.C., Gimenes, M.L., Vieira, M.G.A., 2020. Performance of organoclay in adsorptive uptake of antihypertensive losartan potassium: A comparative batch study using micro-grain activated carbon. Journal of Environmental Chemical Engineering 8, 103562. https://doi.org/10.1016/j.jece.2019.103562

de Farias, M.B., Spaolonzi, M.P., Silva, M.G.C., Vieira, M.G.A., 2021. Fixed-bed adsorption of bisphenol A onto organoclay: Characterisation, mathematical modelling and theoretical calculation of DFT-based chemical descriptors. Journal of Environmental Chemical Engineering 9. https://doi.org/10.1016/j.jece.2021.106103

de Figueiredo Neves, T., Barticiotto Dalarme, N., da Silva, P.M.M., Landers, R., Siqueira Franco Picone, C., Prediger, P., 2020. Novel magnetic chitosan/quaternary ammonium salt graphene oxide composite applied to dye removal. Journal of Environmental Chemical Engineering 8, 103820. https://doi.org/10.1016/j.jece.2020.103820

do Nascimento, D.C., da Silva, M.G.C., Vieira, M.G.A., 2021. Adsorption of propranolol hydrochloride from aqueous solutions onto thermally treated bentonite clay: A complete batch system evaluation. Journal of Molecular Liquids 337. https://doi.org/10.1016/j.molliq.2021.116442

Ebadi, A., Soltan Mohammadzadeh, J.S., Khudiev, A., 2009. What is the correct form of BET isotherm for modeling liquid phase adsorption? Adsorption 15, 65–73. https://doi.org/10.1007/s10450-009-9151-3

Ederer, J., Janos, P., Ecorchard, P., Tolasz, J., Stengl, V., Benes, H., Perchacz, M., Pop-Georgievski, O., 2017. Determination of amino groups on functionalized graphene oxide for polyurethane nanomaterial. RSC Advances.

Egea-Corbacho, A., Gutiérrez Ruiz, S., Quiroga Alonso, J.M., 2019. Removal of emerging contaminants from wastewater using nanofiltration for its subsequent reuse: Full–scale pilot plant. Journal of Cleaner Production 214, 514–523. https://doi.org/10.1016/j.jclepro.2018.12.297

Erim, B., Ciğeroğlu, Z., Bayramoğlu, M., 2021. Green synthesis of TiO2/GO/chitosan by using leaf extract of Olea europaea as a highly efficient photocatalyst for the degradation of cefixime trihydrate under UV-A radiation exposure: An optimization study with D-optimal design. Journal of Molecular Structure 1234. https://doi.org/10.1016/j.molstruc.2021.130194

Fagerlund, G., 1973. Determination of specific surface by the BET method. Matériaux et Construction 239–245.

Farias, M.B. de, Silva, M.G.C., Vieira, M.G.A., 2022. Adsorption of bisphenol A from aqueous solution onto organoclay: Experimental design, kinetic, equilibrium and thermodynamic study. Powder Technology 395, 695–707. https://doi.org/10.1016/j.powtec.2021.10.021

Freitas, E.D., de Almeida, H.J., Vieira, M.G.A., 2017. Binary adsorption of zinc and copper on expanded vermiculite using a fixed bed column. Applied Clay Science 146, 503–509. https://doi.org/10.1016/j.clay.2017.07.004

Freundlich, H., 1906. Über die Adsorption in Lösungen (Concerning adsorption in solutions). Chemie–Stochiometrie, Zeitschrift Fur Physikalische.

Ghosh, A., Ghosh, S., Seshadhri, G.M., Ramaprabhu, S., 2019. Green synthesis of nitrogen-doped self-assembled porous carbon-metal oxide composite towards energy and environmental applications. Scientific Reports 9. https://doi.org/10.1038/s41598-019-41700-5

Gong, Y., Yu, Y., Kang, H., Chen, X., Liu, H., Zhang, Y., Sun, Y., Song, H., 2019. Synthesis and Characterization of Graphene Oxide Chitosan Composite Aerogels. Polymers.

Han, J., Qiu, W., Cao, Z., Hu, J., Gao, W., 2013. Adsorption of ethinylestradiol (EE2) on polyamide 612: Molecular modeling and effects of water chemistry. Water Research 47, 2273–2284. https://doi.org/10.1016/j.watres.2013.01.046

Hasijaa, V., Sudhaika, A., Raizadaa, P., Hosseini-Bandegharaeib, A., Singh, P., 2019. Carbon quantum dots supported AgI/ZnO/phosphorus doped graphitic carbon nitride as Z-scheme photocatalyst for efficient photodegradation of 2,4-dinitrophenol graphitic. Journal of Environmental Chemical Engineering 7, 103272.

Ho, Y.S., McKay, G., 1998. A Comparison of chemisorption kinetic models applied to pollutant removal on various sorbents. Process Safety and Environmental Protection 76, 332–340. https://doi.org/10.1205/095758298529696

Hosseini, Y., Najafi, M., Khalili, S., Jahanshahi, M., Peyravi, M., 2021. Assembly of amine-functionalized graphene oxide for efficient and selective adsorption of CO2. Materials Chemistry and Physics 270. https://doi.org/10.1016/j.matchemphys.2021.124788

Hu, D., Lian, Z., Xian, H., Jiang, R., Wang, N., Weng, Y., Peng, X., Wang, S., Ouyang, X. – K, 2020. Adsorption of Pb(II) from aqueous solution by polyacrylic acid grafted magnetic chitosan nanocomposite. International Journal of Biological Macromolecules 154, 1537–1547. https://doi.org/10.1016/j.ijbiomac.2019.11.038

Hu, Y., Zhu, Y., Zhang, Y., Lin, T., Zeng, G., Zhang, S., Wang, Y., He, W., Zhang, M., Long, H., 2019. An efficient adsorbent: Simultaneous activated and magnetic ZnO doped biochar derived from camphor leaves for ciprofloxacin adsorption. Bioresource Technology 288. https://doi.org/10.1016/j.biortech.2019.121511

Huang, Z., Li, Z., Zheng, L., Zhou, L., Chai, Z., Wang, X., Shi, W., 2017. Interaction mechanism of uranium(VI) with three-dimensional graphene oxide-chitosan composite: Insights from batch experiments, IR, XPS, and EXAFS spectroscopy. Chemical Engineering Journal 328, 1066–1074. https://doi.org/10.1016/j.cej.2017.07.067

Ifelebuegu, A.O., Ezenwa, C.P., 2011. Removal of endocrine disrupting chemicals in wastewater treatment by fenton-like oxidation. Water, Air, and Soil Pollution 217, 213–220. https://doi.org/10.1007/s11270-010-0580-0

Im, J.S., Park, S.J., Lee, Y.S., 2007. Preparation and characteristics of electrospun activated carbon materials having meso- and macropores. Journal of Colloid and Interface Science 314, 32–37. https://doi.org/10.1016/j.jcis.2007.05.033

Jawad, A.H., Malek, N.N.A., Abdulhameed, A.S., Razuan, R., 2020. Synthesis of Magnetic Chitosan-Fly Ash/Fe3O4 Composite for Adsorption of Reactive Orange 16 Dye: Optimization by Box–Behnken Design. Journal of Polymers and the Environment 28, 1068–1082. https://doi.org/10.1007/s10924-020-01669-z

Jiang, N., Shang, R., Heijman, S.G.J., Rietveld, L.C., 2020. Adsorption of triclosan, trichlorophenol and phenol by high-silica zeolites: Adsorption efficiencies and mechanisms. Separation and Purification Technology 235. https://doi.org/10.1016/j.seppur.2019.116152

Jiang, T., Liu, W., Mao, Y., Zhang, L., Cheng, J., Gong, M., Zhao, H., Dai, L., Zhang, S., Zhao, Q., 2015. Adsorption behavior of copper ions from aqueous solution onto graphene oxide–CdS composite. Chemical Engineering Journal 259, 603–610.

Jun, B.M., Hwang, H.S., Heo, J., Han, J., Jang, M., Sohn, J., Park, C.M., Yoon, Y., 2019. Removal of selected endocrine-disrupting compounds using Al-based metal organic framework: Performance and mechanism of competitive adsorption. Journal of Industrial and Engineering Chemistry 79, 345–352. https://doi.org/10.1016/j.jiec.2019.07.009

Karimi, F., Ayati, A., Tanhaei, B., Sanati, A.L., Afshar, S., Kardan, A., Dabirifar, Z., Karaman, C., 2022. Removal of metal ions using a new magnetic chitosan nano-bio-adsorbent; A powerful approach in water treatment. Environmental Research 203. https://doi.org/10.1016/j.envres.2021.111753

Kong, Q., Shi, X., Ma, W., Zhang, F., Yu, T., Zhao, F., Zhao, D., Wei, C., 2021. Strategies to improve the adsorption properties of graphene-based adsorbent towards heavy metal ions and their compound pollutants: A review. Journal of Hazardous Materials. https://doi.org/10.1016/j.jhazmat.2021.125690

Ladavos, A.K., Katsoulidis, A.P., Iosifidis, A., Triantafyllidis, K.S., Pinnavaia, T.J., Pomonis, P.J., 2012. The BET equation, the inflection points of N 2 adsorption isotherms and the estimation of specific surface area of porous solids. Microporous and Mesoporous Materials 151, 126–133. https://doi.org/10.1016/j.micromeso.2011.11.005

Lagergren, S., 1898. Zur theorie Der Sogenannten adsorption geloster stoffe, Kungliga Svenska Vetenskapsakademiens.

Lai, C., He, H., Xie, W., Fan, S., Huang, H., Wang, Y., Huang, B., Pan, X., 2022. Adsorption and photochemical capacity on 17α-ethinylestradiol by char produced in the thermo treatment process of plastic waste. Journal of Hazardous Materials 423. https://doi.org/10.1016/j.jhazmat.2021.127066

Langmuir, I., 1918. The adsorption of gases on plane surfaces of glass, mica and platinum. Journal of the American Chemical Society 40, 1361–1403. https://doi.org/10.1021/ja02242a004

Lawrie, G., Keen, I., Drew, B., Chandler-Temple, A., Rintoul, L., Fredericks, P., Grøndahl, L., 2007. Interactions between alginate and chitosan biopolymers characterized using FTIR and XPS. Biomacromolecules 8, 2533–2541. https://doi.org/10.1021/bm070014y

Li, X., Zhou, H., Wu, W., Wei, S., Xu, Y., Kuang, Y., 2015. Studies of heavy metal ion adsorption on Chitosan/Sulfydrylfunctionalized graphene oxide composites. Journal of Colloid and Interface Science 448, 389–397.

Li, Y., Umer, R., Samad, Y.A., Zheng, L., Liao, K., 2013. The effect of the ultrasonication pre-treatment of graphene oxide (GO) on the mechanical properties of GO/polyvinyl alcohol composites. Carbon 55, 321–327. https://doi.org/10.1016/j.carbon.2012.12.071

Lin, Z., Waller, G.H., Liu, Y., Liu, M., Wong, C.P., 2013. Simple preparation of nanoporous few-layer nitrogen-doped graphene for use as an efficient electrocatalyst for oxygen reduction and oxygen evolution reactions. Carbon 53, 130–136. https://doi.org/10.1016/j.carbon.2012.10.039

Liu, F.F., Zhao, J., Wang, S., Du, P., Xing, B., 2014. Effects of solution chemistry on adsorption of selected pharmaceuticals and personal care products (PPCPs) by graphenes and carbon nanotubes. Environmental Science and Technology 48, 13197–13206. https://doi.org/10.1021/es5034684

Liu, S.H., Tang, W.T., 2020. Photodecomposition of ibuprofen over g-C3N4/Bi2WO6/rGO heterostructured composites under visible/solar light. Science of the Total Environment 731. https://doi.org/10.1016/j.scitotenv.2020.139172

Liu, T., Han, X., Wang, Y., Yan, L., Du, B., Wei, Q., Wei, D., 2017. Magnetic chitosan/anaerobic granular sludge composite: Synthesis, characterization and application in heavy metal ions removal. Journal of Colloid and Interface Science 508, 405–414. https://doi.org/10.1016/j.jcis.2017.08.067

Liu, X., Cao, Z., Yuan, Z., Zhang, J., Guo, X., Yang, Y., He, F., Zhao, Y., Xu, J., 2018. Insight into the kinetics and mechanism of removal of aqueous chlorinated nitroaromatic antibiotic chloramphenicol by nanoscale zero-valent iron. Chemical Engineering Journal 334, 508–518. https://doi.org/10.1016/j.cej.2017.10.060

López-Velázquez, K., Guzmán-Mar, J.L., Saldarriaga-Noreña, H.A., Murillo-Tovar, M.A., Hinojosa-Reyes, L., Villanueva-Rodríguez, M., 2021. Occurrence and seasonal distribution of five selected endocrine-disrupting compounds in wastewater treatment plants of the Metropolitan Area of Monterrey, Mexico: The role of water quality parameters. Environmental Pollution 269. https://doi.org/10.1016/j.envpol.2020.116223

Lu, Y., Zhang, S., Yin, J., Bai, C., Zhang, J., Li, Y., Yang, Y., Ge, Z., Zhang, M., Wei, L., Ma, M., Ma, Y., Chen, Y., 2017. Mesoporous activated carbon materials with ultrahigh mesopore volume and effective specific surface area for high performance supercapacitors. Carbon 124, 64–71. https://doi.org/10.1016/j.carbon.2017.08.044

Luo, Z., Li, H., Yang, Y., Lin, H., Yang, Z., 2017. Adsorption of 17α-ethinylestradiol from aqueous solution onto a reduced graphene oxide-magnetic composite. Journal of the Taiwan Institute of Chemical Engineers 80, 797–804. https://doi.org/10.1016/j.jtice.2017.09.028

Ly, Q.V., Maqbool, T., Zhang, Z., van Le, Q., An, X., Hu, Y., Cho, J., Li, J., Hur, J., 2021. Characterization of dissolved organic matter for understanding the adsorption on nanomaterials in aquatic environment: A review. Chemosphere. https://doi.org/10.1016/j.chemosphere.2020.128690

Ma, J.W., Lee, W.J., Bae, J.M., Jeong, K.S., Oh, S.H., Kim, J.H., Kim, S.H., Seo, J.H., Ahn, J.P., Kim, H., Cho, M.H., 2015. Carrier Mobility Enhancement of Tensile Strained Si and SiGe Nanowires via Surface Defect Engineering. Nano Letters 15, 7204–7210. https://doi.org/10.1021/acs.nanolett.5b01634

Maia, G.S., de Andrade, J.R., da Silva, M.G.C., Vieira, M.G.A., 2019. Adsorption of diclofenac sodium onto commercial organoclay: Kinetic, equilibrium and thermodynamic study. Powder Technology 345, 140–150. https://doi.org/10.1016/j.powtec.2018.12.097

Malwal, D., Gopinath, P., 2017. Silica Stabilized Magnetic-Chitosan Beads for Removal of Arsenic from Water. Colloids and Interface Science Communications 19, 14–19. https://doi.org/10.1016/j.colcom.2017.06.003

Mansouriieh, N., Sohrabi, M.R., Khosravi, M., 2016. Adsorption kinetics and thermodynamics of organophosphorus profenofos pesticide onto Fe/Ni bimetallic nanoparticles. International Journal of Environmental Science and Technology 13, 1393–1404. https://doi.org/10.1007/s13762-016-0960-0

Meidanchi, A., Akhavan, O., 2014. Superparamagnetic zinc ferrite spinel–graphene nanostructures for fast wastewater purification. Carbon 69, 230–238.

Menk, J. de J., do Nascimento, A.I.S., Leite, F.G., de Oliveira, R.A., Jozala, A.F., de Oliveira Junior, J.M., Chaud, M.V., Grotto, D., 2019. Biosorption of pharmaceutical products by mushroom stem waste. Chemosphere 237. https://doi.org/10.1016/j.chemosphere.2019.124515

Milonjić, S.K., 2007. A consideration of the correct calculation of thermodynamic parameters of adsorption. Journal of the Serbian Chemical Society 72, 1363–1367. https://doi.org/10.2298/JSC0712363M

Mohseni Kafshgari, M., Tahermansouri, H., 2017. Development of a graphene oxide/chitosan nanocomposite for the removal of picric acid from aqueous solutions: Study of sorption parameters. Colloids and Surfaces B: Biointerfaces 160, 671–681. https://doi.org/10.1016/j.colsurfb.2017.10.019

Morin-Crini, N., Lichtfouse, E., Fourmentin, M., Ribeiro, A.R.L., Noutsopoulos, C., Mapelli, F., Fenyvesi, É., Vieira, M.G.A.V., Picos-Corrales, L.A., Moreno-Piraján, J.C., Giraldo, L., Sohajda, T., Huq, M.M., Soltan, J., Torri, G., Magureanu, M., Bradu, C., Crini, G., 2022. Removal of emerging contaminants from wastewater using advanced treatments. A review. Environmental Chemistry Letters. https://doi.org/10.1007/s10311-021-01379-5

Narayanan, D.P., Gopalakrishnan, A., Yaakob, Z., Sugunan, S., Narayanan, B.N., 2020. A facile synthesis of clay – graphene oxide nanocomposite catalysts for solvent free multicomponent Biginelli reaction. Arabian Journal of Chemistry 13, 318–334. https://doi.org/10.1016/j.arabjc.2017.04.011

Nasri, A., Mezni, A., Lafon, P.-A., Wahbi, A., Cubedo, N., Clair, P., Harrath, A.H., Beyrem, H., Rossel, M., Perrier, V., 2021. Ethinylestradiol (EE2) residues from birth control pills impair nervous system development and swimming behavior of zebrafish larvae. Science of the Total Environment. https://doi.org/10.1016/j.scitotenv.2021.145272

Naushada, M., Alqadamia, A.A., Al-Kahtania, A.A., Ahamada, T., Awualb, Md.R., Tatarchuk, T., 2019. Adsorption of textile dye using para-aminobenzoic acid modifiedactivated carbon: Kinetic and equilibrium studies. Journal of Molecular Liquids 296, 112075. https://doi.org/10.1016/j.molliq.2019.112075

Nazraz, M., Yamini, Y., Asiabi, H., 2019. Chitosan-based sorbent for efficient removal and extraction of ciprofloxacin and norfloxacin from aqueous solutions. Microchimica Acta 186. https://doi.org/10.1007/s00604-019-3563-x

Neves, T. de F., Assano, P.K., Sabino, L.R., Nunes, W.B., Prediger, P., 2020. Influence of Adsorbent/Adsorbate Interactions on the Removal of Cationic Surfactants from Water by Graphene Oxide. Water, Air, and Soil Pollution 231. https://doi.org/10.1007/s11270-020-04669-w

Nowak, S., Lafon, S., Caquineau, S., Journet, E., Laurent, B., 2018. Quantitative study of the mineralogical composition of mineral dust aerosols by X-ray diffraction. Talanta 186, 133–139. https://doi.org/10.1016/j.talanta.2018.03.059

Oliveira, L.C.A., Rios, R.V.R.A., Fabris, J.D., Sapag, K., Garg, V.K., Lago, R.M., 2003. Clay-iron oxide magnetic composites for the adsorption of contaminants in water. Applied Clay Science 22, 169–177. https://doi.org/10.1016/S0169-1317(02)00156-4

Oliveira, M.F., da Silva, M.G.C., Vieira, M.G.A., 2019. Equilibrium and kinetic studies of caffeine adsorption from aqueous solutions on thermally modified Verde-lodo bentonite. Applied Clay Science 168, 366–373. https://doi.org/10.1016/j.clay.2018.12.011

Parladé, E., Hom-Diaz, A., Blánquez, P., Martínez-Alonso, M., Vicent, T., Gaju, N., 2018. Effect of cultivation conditions on B-estradiol removal in laboratory and pilot-plant photobioreactors by an algal-bacterial consortium treating urban wastewater. Water Research 137, 86–96. https://doi.org/10.1016/j.watres.2018.02.060

Pérez-Guardiola, A., Pérez-Jiménez, A.J., Sancho-García, J.C., 2017. Studying physisorption processes and molecular friction of cycloparaphenylene molecules on graphene nano-sized flakes: Role of π···π and CH···π interactions. Molecular Systems Design and Engineering 2, 253–262. https://doi.org/10.1039/c7me00024c

Piccin, J.S., Cadaval, T.R.S.A., de Pinto, L.A.A., Dotto, G.L., 2017. Adsorption isotherms in liquid phase: Experimental, modeling, and interpretations, in: Adsorption Processes for

Water Treatment and Purification. Springer International Publishing, pp. 19–51. https://doi.org/10.1007/978-3-319-58136-1_2

Racar, M., Dolar, D., Karadakić, K., Čavarović, N., Glumac, N., Ašperger, D., Košutić, K., 2020. Challenges of municipal wastewater reclamation for irrigation by MBR and NF/RO: Physico-chemical and microbiological parameters, and emerging contaminants. Science of the Total Environment 722. https://doi.org/10.1016/j.scitotenv.2020.137959

Rad, L.R., Anbia, M., 2021. Zeolite-based composites for the adsorption of toxic matters from water: A review. Journal of Environmental Chemical Engineering 9. https://doi.org/10.1016/j.jece.2021.106088

Reichenberg, D., 1953. Properties of Ion-Exchange Resins in Relation to their Structure. III. Kinetics of Exchange. Journal of the American Chemical Society 75, 589–597. https://doi.org/10.1021/ja01099a022

Rojas, S., Navarro, J.A.R., Horcajada, P., 2021. Metal-organic frameworks for the removal of the emerging contaminant atenolol under real conditions. Dalton Transactions 50, 2493–2500. https://doi.org/10.1039/d0dt03637d

Ruiz, B., Cabrita, I., Mestre, A.S., Parra, J.B., Pires, J., Carvalho, A.P., Ania, C.O., 2010. Surface heterogeneity effects of activated carbons on the kinetics of paracetamol removal from aqueous solution. Applied Surface Science 256, 5171–5175. https://doi.org/10.1016/j.apsusc.2009.12.086

Sáaedi, A., Yousefi, R., Jamali-Sheini, F., Zak, A.K., Cheraghizade, M., Mahmoudian, M.R., Baghchesara, M.A., Dezaki, A.S., 2016. XPS studies and photocurrent applications of alkali-metals-doped ZnO nanoparticles under visible illumination conditions. Physica E: Low-Dimensional Systems and Nanostructures 79, 113–118. https://doi.org/10.1016/j.physe.2015.12.002

Saha, P., Chowdhury, S., 2011. Insight Into Adsorption Thermodynamics, in: Thermodynamics. pp. 349–363.

Saheed, I.O., Oh, W. da, Suah, F.B.M., 2021. Chitosan modifications for adsorption of pollutants – A review. Journal of Hazardous Materials. https://doi.org/10.1016/j.jhazmat.2020.124889

Sahoo, G., Sarkar, N., Swain, S.K., 2018. The effect of reduced graphene oxide intercalated hybrid organoclay on the dielectric properties of polyvinylidene fluoride nanocomposite films. Applied Clay Science 162, 69–82. https://doi.org/10.1016/j.clay.2018.05.008

Sahu, S., Pahi, S., Tripathy, S., Singh, S.K., Behera, A., Sahu, U.K., Patel, R.K., 2020. Adsorption of methylene blue on chemically modified lychee seed biochar: Dynamic,

equilibrium, and thermodynamic study. Journal of Molecular Liquids 315. https://doi.org/10.1016/j.molliq.2020.113743

Salahuddin, N.A., EL-Daly, H.A., el Sharkawy, R.G., Nasr, B.T., 2018. Synthesis and efficacy of PPy/CS/GO nanocomposites for adsorption of ponceau 4R dye, Polymer. Elsevier Ltd. https://doi.org/10.1016/j.polymer.2018.04.053

Sauvé, S., Desrosiers, M., 2014. A review of what is an emerging contaminant, Chemistry Central Journal.

Sekulic, M.T., Boskovic, N., Slavkovic, A., Garunovic, J., Kolakovic, S., Pap, S., 2019. Surface functionalised adsorbent for emerging pharmaceutical removal: Adsorption performance and mechanisms. Process Safety and Environmental Protection 125, 50–63. https://doi.org/10.1016/j.psep.2019.03.007

Shahid, M.K., Kashif, A., Fuwad, A., Choi, Y., 2021. Current advances in treatment technologies for removal of emerging contaminants from water – A critical review. Coordination Chemistry Reviews. https://doi.org/10.1016/j.ccr.2021.213993

Shang, J., Guo, Y., He, D., Qu, W., Tang, Y., Zhou, L., Zhu, R., 2021. A novel graphene oxide-dicationic ionic liquid composite for Cr(VI) adsorption from aqueous solutions. Journal of Hazardous Materials 416. https://doi.org/10.1016/j.jhazmat.2021.125706

Sharma, G., Sharma, S., Kumar, A., Naushad, Mu., Du, B., Ahamad, T., Ghfar, A.A., Alqadami, A.A., Stadler, F.J., 2019. Honeycomb structured activated carbon synthesized from Pinus roxburghii cone as effective bioadsorbent for toxic malachite green dye. Journal of Water Process Engineering 32, 100931.

Siebdrath, N., Skibinski, B., Abraham, S., Bernstein, R., Berger, R., Stein, N., Kaufman, Y., Lerch, A., Herzberg, M., 2021. Impact of pretreatment on RO membrane organic fouling: composition and adhesion of tertiary wastewater effluent organic matter. Environmental Science Water Research & Technology 7, 775.

Silva, T.L. da, Silva, M.G.C. da, Vieira, M.G.A., 2021. Palladium adsorption on natural polymeric sericin-alginate particles crosslinked by polyethylene glycol diglycidyl ether. Journal of Environmental Chemical Engineering 9. https://doi.org/10.1016/j.jece.2021.105617

Site, A.D., 2001. Factors Affecting Sorption of Organic Compounds in Natural Sorbent/Water Systems and Sorption Coefficients for Selected Pollutants. A Review. Journal of Physical and Chemical Reference Data 187.

Sivaranjanee, R., Kumar, P.S., 2021. A review on remedial measures for effective separation of emerging contaminants from wastewater. Environmental Technology and Innovation. https://doi.org/10.1016/j.eti.2021.101741

Sobhanardakani, S., Zandipak, R., 2018. Cerium dioxide nanoparticles decorated on CuFe2O4 nanofibers as an effective adsorbent for removal of estrogenic contaminants (bisphenol A and 17-α ethinylestradiol) from water. Separation Science and Technology (Philadelphia) 53, 2339–2351. https://doi.org/10.1080/01496395.2018.1457053

Soboleva, T., Zhao, X., Malek, K., Xie, Z., Navessin, T., Holdcroft, S., 2010. On the micro-, meso-, and macroporous structures of polymer electrolyte membrane fuel cell catalyst layers. ACS Applied Materials and Interfaces 2, 375–384. https://doi.org/10.1021/am900600y

Song, X., Zhang, Y., Yan, C., Jiang, W., Chang, C., 2013. The Langmuir monolayer adsorption model of organic matter into effective pores in activated carbon. Journal of Colloid and Interface Science 389, 213–219. https://doi.org/10.1016/j.jcis.2012.08.060

Sonu, Dutta, V., Sharma, S., Raizada, P., Hosseini-Bandegharaei, A., Gupta, V.K., Singh, P., 2019. Review on augmentation in photocatalytic activity of CoFe2O4 via heterojunction formation for photocatalysis of organic pollutants in water. Journal of Saudi Chemical Society 23, 1119–1136

Spaolonzi, M.P., da Silva, M.G.C., Vieira, M.G.A., 2022. Adsorption of antibiotic cefazolin in organoclay fixed-bed column: characterization, mathematical modeling, and DFT-based calculations. Environmental Science and Pollution Research. https://doi.org/10.1007/s11356-022-18568-6

Speridião, D.D.C.A., dos Santos, O.A.A., de Almeida Neto, A.F., Vieira, M.G.A., 2014. Characterization of spectrogel organoclay used to adsorption of petroleum derivatives. Materials Science Forum 798–799, 558–563. https://doi.org/10.4028/www.scientific.net/MSF.798-799.558

Tang, Z., Liu, Z. hua, Wang, H., Dang, Z., Liu, Y., 2021a. Occurrence and removal of 17α-ethynylestradiol (EE2) in municipal wastewater treatment plants: Current status and challenges. Chemosphere. https://doi.org/10.1016/j.chemosphere.2021.129551

Tang, Z., Liu, Z. hua, Wang, H., Dang, Z., Liu, Y., 2021b. A review of 17α-ethynylestradiol (EE2) in surface water across 32 countries: Sources, concentrations, and potential estrogenic effects. Journal of Environmental Management 292. https://doi.org/10.1016/j.jenvman.2021.112804

Tran, H.N., You, S.J., Chao, H.P., 2016. Thermodynamic parameters of cadmium adsorption onto orange peel calculated from various methods: A comparison study. Journal of Environmental Chemical Engineering 4, 2671–2682. https://doi.org/10.1016/j.jece.2016.05.009

Vieira, W.T., Bispo, M.D., Farias, S.M., de Almeida, A.D.S.V., da Silva, T.L., Vieira, M.G.A., Soletti, J.I., Balliano, T.L., 2021. Activated carbon from macauba endocarp (Acrocomia aculeate) for removal of atrazine: Experimental and theoretical investigation using descriptors based on DFT. Journal of Environmental Chemical Engineering 9. https://doi.org/10.1016/j.jece.2021.105155

Vieira, W.T., Farias, M.B., Spaolonzi, M.P., Silva, M.G.C., Vieira, M.G.A., 2021. Latest advanced oxidative processes applied for the removal of endocrine of endocrine disruptors from aqueous media – A critical report. Journal of Environmental Chemical Engineering 9, 105748. https://doi.org/10.1016/j.jece.2021.105748

Vieira, W.T., Farias, M.B., Spaolonzi, M.P., Silva, M.G.C., Vieira, M.G.A., 2020. Removal of endocrine disruptors in waters by adsorption, membrane filtration and biodegradation. A review. Environmental Chemistry Letters 18, 1113–1143. https://doi.org/10.1007/s10311-020-01000-1

Wang, W., Zhu, Z., Zhang, M., Wang, S., Qu, C., 2020. Synthesis of a novel magnetic multi-amine decorated resin for the adsorption of tetracycline and copper. Journal of the Taiwan Institute of Chemical Engineers 106, 130–137. https://doi.org/10.1016/j.jtice.2019.10.017

Wang, X., Song, L., Yang, H., Xing, W., Kandola, B., Hu, Y., 2012. Simultaneous reduction and surface functionalization of graphene oxide with POSS for reducing fire hazards in epoxy composites. Journal of Materials Chemistry 22, 22037–22043. https://doi.org/10.1039/c2jm35479a

Wang, Y., Yang, Q., Dong, J., Huang, H., 2018. Competitive adsorption of PPCP and humic substances by carbon nanotube membranes: Effects of coagulation and PPCP properties. Science of the Total Environment 619–620, 352–359. https://doi.org/10.1016/j.scitotenv.2017.11.117

Weber, W., Morris, J., 1963. Kinetics of adsorption on carbon from solution. Journal of the Sanitary Engineering Division 89, 31–60.

Westrup, J.L., Bertoldi, C., Cercena, R., Dal-Bó, A.G., Soares, R.M.D., Fernandes, A.N., 2021. Adsorption of endocrine disrupting compounds from aqueous solution in poly(butyleneadipate-co-terephthalate) electrospun microfibers. Colloids and Surfaces A:

Physicochemical and Engineering Aspects 611. https://doi.org/10.1016/j.colsurfa.2020.125800

Wong, S., Lim, Y., Ngadi, N., Mat, R., Hassan, O., Inuwa, I.M., Mohamed, N.B., Low, J.H., 2018. Removal of acetaminophen by activated carbon synthesized from spent tea leaves: equilibrium, kinetics and thermodynamics studies. Powder Technology 338, 878–886. https://doi.org/10.1016/j.powtec.2018.07.075

Wu, F.C., Tseng, R.L., Juang, R.S., 2009. Initial behavior of intraparticle diffusion model used in the description of adsorption kinetics. Chemical Engineering Journal 153, 1–8. https://doi.org/10.1016/j.cej.2009.04.042

Wu, S.-T., 1975. A Rigorous Justification of the Point B Method for Determination of Monolayer Capacity from a Type II Adsorption Isotherm, Progress of Theoretical Physics. https://doi.org/10.1143/PTP.53.21

Wu, Z., Huang, W., Shan, X., Li, Z., 2020. Preparation of a porous graphene oxide/alkali lignin aerogel composite and its adsorption properties for methylene blue. International Journal of Biological Macromolecules 143, 325–333.

Xiong, J.Q., Kurade, M.B., Patil, D. v., Jang, M., Paeng, K.J., Jeon, B.H., 2017. Biodegradation and metabolic fate of levofloxacin via a freshwater green alga, Scenedesmus obliquus in synthetic saline wastewater. Algal Research 25, 54–61. https://doi.org/10.1016/j.algal.2017.04.012

Xu, L., Teng, J., Li, L., Huang, H.D., Xu, J.Z., Li, Y., Ren, P.G., Zhong, G.J., Li, Z.M., 2019. Hydrophobic Graphene Oxide as a Promising Barrier of Water Vapor for Regenerated Cellulose Nanocomposite Films. ACS Omega 4, 509–517. https://doi.org/10.1021/acsomega.8b02866

Yang, C., Wu, S., Cheng, J., Chen, Y., 2016. Indium-based metal-organic framework/graphite oxide composite as an efficient adsorbent in the adsorption of rhodamine B from aqueous solution. Journal of Alloys and Compounds 687, 804–812. https://doi.org/10.1016/j.jallcom.2016.06.173

Yang, W., Pan, M., Huang, C., Zhao, Z., Wang, J., Zeng, H., 2021. Graphene oxide-based noble-metal nanoparticles composites for environmental application. Composites Communications 24. https://doi.org/10.1016/j.coco.2021.100645

Yankovych, H., Melnyk, I., Václavíková, M., 2021. Understanding of mechanisms of organohalogens removal onto mesoporous granular activated carbon with acid-base properties. Microporous and Mesoporous Materials 317. https://doi.org/10.1016/j.micromeso.2021.110974

Zambianchi, M., Durso, M., Liscio, A., Treossi, E., Bettini, C., Capobianco, M.L., Aluigi, A., Kovtun, A., Ruani, G., Corticelli, F., Brucale, M., Palermo, V., Navacchia, M.L., Melucci, M., 2017. Graphene oxide doped polysulfone membrane adsorbers for the removal of organic contaminants from water. Chemical Engineering Journal 326, 130–140. https://doi.org/10.1016/j.cej.2017.05.143

Zhang, L., Zhang, B., Wu, T., Sun, D., Li, Y., 2015. Adsorption behavior and mechanism of chlorophenols onto organoclays in aqueous solution. Colloids and Surfaces A: Physicochemical and Engineering Aspects 484, 118–129. https://doi.org/10.1016/j.colsurfa.2015.07.055

Zhang, S., Meng, W., Wang, L., Li, L., Long, Y., Hei, Y., Zhou, L., Wu, S., 2020. Preparation of Nano-Copper Sulfide and Its Adsorption Properties for 17 α -Ethynyl Estradiol. https://doi.org/10.1186/s11671-020-3274-6

Zhang, Y.-L., Zhang, J., Dai, C.-M., Zhou, X.-F., Liu, S.-G., 2013. Sorption of carbamazepine from water by magnetic molecularly imprinted polymers based on chitosan-Fe3O4. Carbohydrate Polymers 97, 809–816. https://doi.org/10.1016/j.carbpol.2013.05.072

Zhao, B., Ji, Y., Wang, F., Lei, H., Gu, Z., 2016. Adsorption of tetracycline onto alumina: experimental research and molecular dynamics simulation. Desalination and Water Treatment 57, 5174–5182. https://doi.org/10.1080/19443994.2015.1004595

Zhongbo, Z., Hu, J., 2008. Selective removal of estrogenic compounds by molecular imprinted polymer. Water Research 42, 4101–4108.https://doi.org/10.1016/j.watres.2008.07.006

Zhuang, S., Wang, J., 2021. Adsorptive removal of pharmaceutical pollutants by defective metal organic framework UiO-66: Insight into the contribution of defects. Chemosphere 281. https://doi.org/10.1016/j.chemosphere.2021.130997

CAPÍTULO 5. DISCUSSÃO GERAL

A presença de contaminantes emergentes em matrizes aquáticas, mesmo em baixas concentrações, vem provocando diversos danos à saúde humana e ao ecossistema. A grande diversidade dessa classe de contaminantes implica em moléculas com propriedades físico-químicas distintas que são dificilmente removidas com eficiência das estações de tratamento de água e esgoto pelo procedimento convencional. A falta de monitoramento dos poluentes emergentes no mundo também contribui para a problemática, que vem atraindo cada vez mais atenção para procedimentos alternativos que removam com eficiência esses contaminantes. A adsorção vem se destacando para esta finalidade devido à sua simplicidade, alta eficiência, baixo custo e grande variedade de materiais adsorventes. Nos últimos anos, nanocompósitos vêm sendo amplamente investigados para remoção de contaminantes emergentes de soluções aquosas, aproveitando da sua heterogeneidade para remover diferentes contaminantes emergentes da água, diminuindo seu impacto ambiental e à saúde humana. Desta forma, o presente trabalho de mestrado foi desenvolvido com o intuito de sintetizar um nanocompósito magnético baseado em óxido de grafeno, quitosana e argila organofílica e investigar seu uso para remoção de diferentes contaminantes emergentes em meio aquoso.

Na Revisão Bibliográfica discorreu-se sobre a presença de contaminantes emergentes em efluentes e a importância da aplicação de tratamentos avançados para resolução da problemática. Dentre os contaminantes emergentes foram destacados o BPA, o EE2 e o TCS, abordando suas propriedades moleculares, danos, principais fontes de contaminação e concentrações de ocorrência. Dentre os métodos de remoção avançados foram abordados a aplicação de processos oxidativos avançados, membrana e com destaque para a adsorção, que se apresenta como uma tecnologia que não propaga subprodutos, de fácil aplicação e menos onerosa. Diferentes materiais adsorventes foram detalhados, destacando-se suas características e desempenho na remoção de contaminantes emergentes. A síntese de nanocompósitos também foi discutida, mostrando os aspectos positivos de combinar adsorventes com diferentes características estruturais almejando obter melhores taxas de adsorção. O nanocompósito desenvolvido (GO/mCS/OC) foi sintetizado à base de óxido de grafeno, quitosana e argila organofílica, assim como o teste preliminar de afinidade adsortiva. Os ensaios de afinidade em batelada avaliaram o desempenho do GO/mCS/OC e de sua argila precursora na remoção de BPA, EE2 e TCS de matrizes aquosas. Os resultados mostraram desempenho satisfatório do

nanocompósito na remoção dos contaminantes emergentes avaliados e similares à argila precursora. Os percentuais de remoção obtidos para o TCS, EE2 e BPA foram de 98, 72 e 58 % e as capacidades de adsorção foram de 40, 30 e 20 mg g^{-1}, respectivamente, quando utilizado o nanocompósito. Os descritores químicos moleculares e o mapa de potencial eletrostático dos três contaminantes emergentes foram avaliados pela teoria da densidade funcional (DFT), obtendo informações sobre a reatividade química a nível molecular que corroboraram com os ensaios de afinidade.

Embora a capacidade adsortiva da argila organofílica tenha sido similar à do nanocompósito na remoção dos poluentes emergentes avaliados, o perfil magnético do nanoadsorvente desenvolvido foi um fator decisivo para sua seleção para estudos complementares, devido à sua facilidade de remoção do sistema pós adsorção do meio aquoso. O GO/mCS/OC foi então selecionado para o estudo de adsorção com o EE2, que como foi destacado anteriormente, é uma substância amplamente utilizada em sociedade atualmente, através dos contraceptivos orais, e que aparece cada vez mais concentrado nas matrizes aquáticas contribuindo com danos irreparáveis ao ecossistema e à saúde humana. Portanto, seguiu-se com o estudo do desempenho do nanocompósito na remoção de EE2 através de estudos de adsorção em batelada.

O sistema GO/mCS/OC – EE2 foi investigado, avaliando alguns parâmetros operacionais assim como sua cinética, equilíbrio e termodinâmica, buscando compreender o processo adsortivo proposto. Os parâmetros operacionais investigados foram a dose de nanoadsorvente, o pH inicial e o tempo de ultrassom, buscando obter a condição otimizada para realizar os ensaios posteriores. A dosagem foi avaliada na faixa entre 0,05 – 0,35 mg mL^{-1} avaliando o percentual de remoção e a capacidade adsorvente do nanocompósito. O efeito positivo da dosagem em relação ao percentual de remoção e negativo em relação a capacidade adsorvente foram evidentes, de forma que seu valor máximo foi de 89,8 % na maior dosagem e 50,5 mg g^{-1} na menor. O pH inicial do sistema foi avaliado na faixa entre 3 – 8 mostrando que esse fator não implicava em mudanças significativas no percentual de remoção. A variável "tempo no ultrassom", que foi avaliada desde a ausência de banho até 30 min, mostrou um efeito negativo em relação ao tempo de aplicação, apresentando melhor desempenho quando o sistema não era submetido ao procedimento. As capacidades máximas de adsorção no equilíbrio de EE2 foram obtidas sem alteração no pH da água ultrapura (pH 6 – 7) e sem aplicação de banho de ultrassom. As cinéticas de adsorção de EE2 foram obtidas nas mesmas condições e

com dosagem de 0,1 mg mL^{-1}, diferentemente dos ensaios de equilíbrio que foram avaliados através da variação de dosagem de nanoadsorvente.

As medições das cinéticas de adsorção em batelada foram avaliadas em três concentrações (0,01, 0,02 e 0,03 mmol L^{-1}) e apresentaram um aumento da capacidade de adsorção com o aumento da concentração inicial. O EE2 foi removido rapidamente nos primeiros 30 min e alcançou o equilíbrio com 120 min. Os dados experimentais foram melhor descritas pelo modelo de pseudossegunda ordem para todas as condições avaliadas. O comportamento observado para os modelos de difusão interna e Boyd, além do baixo ajuste, indica que a etapa de difusão não é a que limita o processo, indicando que a etapa de transferência externa assuma esse papel. Os baixos valores de área superficial antes e depois da adsorção corroboram com o indicativo que a difusão não controla o processo, de forma que o processo ocorre majoritariamente na superfície do nanocompósito, e não no seu interior. Os ensaios de equilíbrio foram realizados nas temperaturas de 30, 40 e 50 °C e apresentaram capacidade máxima de adsorção de 50,5, 64,6 e 73,3 mg g^{-1}, respectivamente. O perfil das isotermas de equilíbrio demonstrou que o material não foi completamente saturado com a diminuição da dosagem, sugerindo que o EE2 é adsorvido em multicamadas. O efeito positivo da temperatura nas isotermas também revelou seu caráter endotérmico e sugere que interações químicas (quimissorção) estejam presentes na adsorção do EE2 no GO/mCS/OC. Os dados experimentais foram melhor representados pelos modelos de Freundlich e BET, corroborando com a superfície heterogênea do nanocompósito e formação de multicamada por fisissorção. Apesar dos indicativos da presença de ambos os tipos de interações (química e física) na adsorção do EE2 pelo GO/mCS/OC, o valor da constante *n* menor que 1 está associado à baixa energia com predominância da fisissorção. As análises de FTIR e XPS sugeriram um papel importante de grupos funcionais oxigenados e nitrogenados, como hidroxilas e aminas, assim como da estrutura aromática na interação entre adsorvente e adsorbato. Esses grupos funcionais promoveram ligações de hidrogênio e interações $\pi - \pi$ que demonstraram ser os mecanismos preponderantes no processo e que representam as interações químicas e físicas, respectivamente.

A estimativa dos parâmetros termodinâmicos no processo de adsorção do EE2 no GO/mCS/OC revela a espontaneidade e o caráter endotérmico do mesmo. O valor da variação de entalpia sugeriu a predominância da fisissorção, indicando que as interações $\pi - \pi$ entre os aromáticos do adsorvente e do adsorbato tem papel importante no processo de adsorção. A variação encontrada nos valores do calor isostérico indica que a superfície

do nanocompósito é energeticamente heterogênea, corroborando com o melhor ajuste ao modelo de Freundlich para o equilíbrio. O reuso do nanocompósito foi avaliado por cinco ciclos de adsorção consecutivos, mostrando melhor desempenho utilizando a acetonitrila como eluente. O sistema desempenhou boa remoção do EE2 nos dois primeiros ciclos e apresentou na sequencia diminuição da sua eficiência, variando de 75 a 47 %. A seletividade do GO/mCS/OC em relação ao EE2 e BPA foi avaliada em três concentrações iniciais diferentes, sendo elas com predominância de um dos contaminantes emergentes ou equimolar. O BPA foi selecionado e incluído no sistema para avaliar a seletividade do nanocompósito devido à sua característica energética similar ao EE2, como observado no Capítulo 3 pela modelagem DFT, e por ser um contaminante emergente que também é usualmente encontrado em estações de tratamento de água e esgoto. O nanocompósito mostrou remoção satisfatória de ambos os contaminantes em todas as condições avaliadas e os coeficientes de seletividade sugeriram que sua superfície interage melhor com o EE2. Apesar da molécula de BPA apresentar mais anéis aromáticos que a molécula de EE2 e o mesmo número de hidroxilas ionizáveis, sua conformação angular pode dificultar a sua fisissorção em multicamadas.

Portanto, os resultados obtidos nesta dissertação de mestrado demonstraram o potencial do nanocompósito desenvolvido (GO/mCS/OC) como adsorvente promissor na remoção do 17α–etinilestradiol, podendo ser utilizado no tratamento de águas residuárias, reduzindo o seu impacto no ecossistema.

CAPÍTULO 6. CONCLUSÕES E PERSPECTIVAS FUTURAS

A presente dissertação de mestrado apresentou um nanocompósito adsorvente (GO/mCS/OC) promissor para remoção do 17α–etinilestradiol de soluções aquosas. Através dos ensaios experimentais, modelagens moleculares e das caracterizações foi possível verificar as principais características do adsorvente sintetizado e os mecanismos de adsorção mais prováveis na captura do EE2. Além disso, os principais desafios e limitações da sua síntese e metodologia empregada com relação à eficiência do processo foram avaliados. Portanto, esta pesquisa pode contribuir com trabalhos futuros acerca da remoção de contaminantes emergentes por nanocompósitos adsorventes. Nesse capítulo são apresentadas as principais conclusões e considerações deste trabalho, assim como sugestões para trabalhos futuros.

Dentre as principais conclusões, destacam-se:

- As caracterizações demonstraram o sucesso na síntese do nanocompósito, conferindo ao material sua característica heterogênea, capacidade magnética e estabilidade térmica;
- O nanocompósito sintetizado apresentou área específica de 17,8 m^2 g^{-1} e diâmetro médio de 9,8 nm, e após o processo de adsorção sua área diminuiu para 13,2 m^2 g^{-1} e seu diâmetro médio aumentou para 13,2 nm;
- O GO/mCS/OC apresentou também composição heterogênea, predominância de meso e macroporos e distância interplanar de cerca de 1,3 nm;
- Os testes de afinidade adsortiva mostraram que o nanocompósito desempenhou remoção satisfatória dos três contaminantes emergentes avaliados, com destaque para o TCS e EE2 que obtiveram percentuais de remoção acima de 70 %;
- A modelagem molecular dos contaminantes emergentes avaliados indicou maior reatividade química do TCS frente ao BPA ou EE2, corroborando com os ensaios de afinidade, e trouxe informações relevantes sobre suas conformações geométricas, regiões de densidade eletrostática e descritores químicos moleculares;
- A dosagem de nanoadsorvente ótima selecionada para os ensaios cinéticos foi de 0,1 mg mL^{-1} devido aos resultados satisfatórios de capacidade de adsorção e percentual de remoção do EE2 do sistema;

- O pH inicial da solução não demonstrou influência significativa no percentual de remoção na faixa entre o pH 3 – 8;
- O tempo que o sistema era submetido no ultrassom não impactou significativamente no percentual de remoção, entretanto a ausência desse tratamento promoveu melhores resultados;
- Os ensaios cinéticos apresentaram tempo de equilíbrio de 120 min e as capacidades de adsorção aumentaram progressivamente (0,06, 0,10 e 0,13 mmol g^{-1}) à medida que a concentração inicial cresceu (0,01, 0,02 e 0,03 mmol L^{-1});
- Os perfis cinéticos foram melhor representados pelo modelo de pseudossegunda ordem e a difusão externa foi indicada como mecanismo de transferência de massa limitante do processo;
- Os ensaios de equilíbrio de adsorção mostraram que a capacidade máxima de adsorção pelo nanocompósito tiveram efeito positivo em relação à temperatura e alcançaram 0,25 mmol g^{-1} a 50 °C;
- As isotermas obtidas foram melhor representadas pelos modelos de Freundlich e BET, sugerindo que o nanocompósito possui superfície heterogênea e que as interações químicas e físicas estão envolvidas na adsorção do EE2 pelo GO/mCS/OC, entretanto com predominância da fisissorção em multicamada;
- As análises de FTIR e XPS corroboraram com presença de ambos os tipos de interação, mostrando que tanto as ligações de hidrogênio promovidas pelos grupos funcionais oxigenados e nitrogenados, quanto os grupos aromáticos presentes no nanocompósito participam do mecanismo de captura do EE2;
- As grandezas termodinâmicas indicaram que o processo de adsorção do EE2 pelo nanocompósito é endotérmico e espontâneo, assim como corroboraram com a predominância da fisissorção;
- O nanocompósito demonstrou sua capacidade de reuso para a remoção do EE2, utilizando acetonitrila como eluente.
- O nanocompósito desenvolvido apresentou boa seletividade para o EE2 em sistemas bicomposto com BPA;
- O nanocompósito sintetizado mostrou ser uma boa alternativa para o tratamento da água visando à remoção de contaminantes emergentes do meio.

Para pesquisas futuras relacionadas à remoção de EE2 de matrizes aquosas, sugere-se:

- Avaliação do nanocompósito em sistemas multicomponentes mais complexos, contendo maior quantidade de contaminantes emergentes;
- Avaliação do desempenho do nanocompósito em efluentes reais, como por exemplo, efluente de ETEs;
- Realização de testes em reatores de leito fluidizado, visando avaliar o desempenho do nanocompósito em regime contínuo;
- Estudo da aplicação em maior escala buscando se aproximar da aplicação em escala industrial.

CAPÍTULO 7. PRODUÇÃO CIENTÍFICA GERADA

Publicações em periódicos internacionais indexados

Synthesis of a novel magnetic composite based on graphene oxide, chitosan and organoclay and its application in the removal of bisphenol A, 17α-ethinylestradiol and triclosan
Autores: Arthur da Silva Vasconcelos de Almeida, Tauany de Figueiredo Neves, Meuris Gurgel Carlos da Silva, Patricia Prediger and Melissa Gurgel Adeodato Vieira
Journal of Environmental Chemical Engineering, v. 10, p. 107071, 2022.
DOI: https://doi.org/10.1016/j.jece.2021.107071

Adsorption of 17α-ethinylestradiol onto a novel nanocomposite based on graphene oxide, magnetic chitosan and organoclay (GO/mCS/OC): Kinetic, equilibrium, thermodynamic and selectivity studies
Autores: Arthur da Silva Vasconcelos de Almeida, Valmor Roberto Mastelaro, Meuris Gurgel Carlos da Silva, Patricia Prediger and Melissa Gurgel Adeodato Vieira
Journal of Water Process and Engineering, v. 47, p. 102729, 2022.
DOI: https://doi.org/10.1016/j.jwpe.2022.102729

Capítulo de livro

Biomass-derived adsorbents for caffeine removal from aqueous medium
Autores: Tauany de Figueiredo Neves, Natália Gabriele Camparotto, Arthur da Silva Vasconcelos de Almeida, Meuris Gurgel Carlos da Silva, Patrícia Prediger, Melissa Gurgel Adeodato Vieira
In: Ioannis Anastopoulos, Eder Lima, Lucas Meili, Dimitrios Giannakoudakis. (Org.). Biomass-Derived Materials for Environmental Applications. Elsevier.
ISBN: 9780323919142
ISBN-10: 0323919146

CAPÍTULO 8. REFERÊNCIAS

Abdolmaleki, A., Mallakpour, S., Karshenas, A., 2017. Synthesis and characterization of new nanocomposites films using alanine-Cu-functionalized graphene oxide as nanofiller and PVA as polymeric matrix for improving of their properties. Journal of Solid State Chemistry 253, 398–405. https://doi.org/10.1016/j.jssc.2017.06.014

Adolfsson-Erici, M., Pettersson, M., Parkkonen, J., Sturve, J., 2002. Triclosan, a commonly used bactericide found in human milk and in the aquatic environment in Sweden. Chemosphere 46, 1485–1489. https://doi.org/10.1016/S0045-6535(01)00255-7

Agboola, O., Fayomi, O.S.I., Ayodeji, A., Ayeni, A.O., Alagbe, E.E., Sanni, S.E., Okoro, E.E., Moropeng, L., Sadiku, R., Kupolati, K.W., Oni, B.A., 2021. A review on polymer nanocomposites and their effective applications in membranes and adsorbents for water treatment and gas separation. Membranes 11, 1–33. https://doi.org/10.3390/membranes11020139

Ahmat, A.M., Thiebault, T., Guégan, R., 2019. Phenolic acids interactions with clay minerals: A spotlight on the adsorption mechanisms of Gallic Acid onto montmorillonite. Applied Clay Science. https://doi.org/10.1016/j.clay.2019.105188

Alam, S.N., Sharma, N., Kumar, L., 2017. Synthesis of Graphene Oxide (GO) by Modified Hummers Method and Its Thermal Reduction to Obtain Reduced Graphene Oxide (rGO)*. Graphene 06, 1–18. https://doi.org/10.4236/graphene.2017.61001

Al-Gaashani, R., Najjar, A., Zakaria, Y., Mansour, S., Atieh, M.A., 2019. XPS and structural studies of high quality graphene oxide and reduced graphene oxide prepared by different chemical oxidation methods. Ceramics International 45, 14439–14448. https://doi.org/10.1016/j.ceramint.2019.04.165

Al-Ghouti, M.A., Da'ana, D.A., 2020. Guidelines for the use and interpretation of adsorption isotherm models: A review. Journal of Hazardous Materials 393, 122383. https://doi.org/10.1016/j.jhazmat.2020.122383

Alizadeh Fard, M., Barkdoll, B., 2019. Magnetic activated carbon as a sustainable solution for removal of micropollutants from water. International Journal of Environmental Science and Technology 16, 1625–1636. https://doi.org/10.1007/s13762-018-1809-5

Al-Khateeb, L.A., Obaid, A.Y., Asiri, N.A., Abdel Salam, M., 2014. Adsorption behavior of estrogenic compounds on carbon nanotubes from aqueous solutions: Kinetic and thermodynamic studies. Journal of Industrial and Engineering Chemistry 20, 916–924. https://doi.org/10.1016/j.jiec.2013.06.023

Almeida, A.S. V, Vieira, W.T., Bispo, M.D., Melo, S.F., Silva, T.L., Balliano, T.L., Vieira, M.G.A., Soletti, J.I., 2021a. Journal of Environmental Chemical Engineering Caffeine removal using activated biochar from açaí seed (Euterpe oleracea Mart): Experimental study and description of adsorbate properties using Density Functional Theory (DFT). Journal of Environmental Chemical Engineering 9, 104891. https://doi.org/10.1016/j.jece.2020.104891

Almeida, A.S. V, Vieira, W.T., Bispo, M.D., Melo, S.F., Silva, T.L., Balliano, T.L., Vieira, M.G.A., Soletti, J.I., 2021b. Caffeine removal using activated biochar from açaí seed (Euterpe oleracea Mart): Experimental study and description of adsorbate properties using Density Functional Theory (DFT). Journal of Environmental Chemical Engineering 9.

Álvarez-Torrellas, S., Sotelo, J.L., Rodríguez, A., Ovejero, G., García, J., 2017. Influence of the natural organic matter in the removal of caffeine from water by fixed-bed column adsorption. International Journal of Environmental Science and Technology 14, 833–840. https://doi.org/10.1007/s13762-016-1189-7

Amjad, S., Rahman, M.S., Pang, M.G., 2020. Role of antioxidants in alleviating bisphenol a toxicity. Biomolecules 10, 1–26. https://doi.org/10.3390/biom10081105

Andrade, Júlia Resende, Oliveira, M.F., Canevesi, R.L.S., Landers, R., da Silva, M.G.C., Vieira, M.G.A., 2020. Comparative adsorption of diclofenac sodium and losartan potassium in organophilic clay-packed fixed-bed: X-ray photoelectron spectroscopy characterization, experimental tests and theoretical study on DFT-based chemical descriptors. Journal of Molecular Liquids 312. https://doi.org/10.1016/j.molliq.2020.113427

Andrade, J R, Oliveira, M.F., Canevesi, R.L.S., Landers, R., Silva, M.G.C., Vieira, M.G.A., 2020. Comparative adsorption of diclofenac sodium and losartan potassium in organophilic clay-packed fi xed-bed : X-ray photoelectron spectroscopy characterization , experimental tests and theoretical study on DFT-based chemical descriptors. Journal of Molecular Liquids 312, 113427. https://doi.org/10.1016/j.molliq.2020.113427

Antonelli, R., Malpass, G.R.P., da Silva, M.G.C., Vieira, M.G.A., 2021. Fixed-bed adsorption of ciprofloxacin onto bentonite clay: Characterization, mathematical modeling, and DFT-based calculations. Industrial and Engineering Chemistry Research 60, 4030–4040. https://doi.org/10.1021/acs.iecr.0c05700

Antonelli, R., Malpass, G.R.P., da Silva, M.G.C., Vieira, M.G.A., 2020a. Adsorption of ciprofloxacin onto thermally modified bentonite clay: Experimental design, characterization, and adsorbent regeneration. Journal of Environmental Chemical Engineering 8. https://doi.org/10.1016/j.jece.2020.104553

Antonelli, R., Martins, F.R., Malpass, G.R.P., da Silva, M.G.C., Vieira, M.G.A., 2020b. Ofloxacin adsorption by calcined Verde-lodo bentonite clay: Batch and fixed bed system evaluation. Journal of Molecular Liquids 315, 113718. https://doi.org/10.1016/j.molliq.2020.113718

Anwar, J., Shafique, U., Waheed-uz-Zaman, Salman, M., Dar, A., Anwar, S., 2010. Removal of Pb(II) and Cd(II) from water by adsorption on peels of banana. Bioresource Technology 101, 1752–1755. https://doi.org/10.1016/j.biortech.2009.10.021

Appel, C., Ma, L.Q., Rhue, R.D., Kennelley, E., 2003. Point of zero charge determination in soils and minerals via traditional methods and detection of electroacoustic mobility. Geoderma 113, 77–93. https://doi.org/10.1016/S0016-7061(02)00316-6

Aris, A.Z., Shamsuddin, A.S., Praveena, S.M., 2014. Occurrence of 17α-ethynylestradiol (EE2) in the environment and effect on exposed biota: A review. Environment International 69, 104–119. https://doi.org/10.1016/j.envint.2014.04.011

ASTM, 1985. Zeta potential of colloids in water and waste water. ASTM Standard D 4187–82.

Astrahan, P., Korzen, L., Khanin, M., Sharoni, Y., Israel, Á., 2021. Seaweeds fast EDC bioremediation: Supporting evidence of EE2 and BPA degradation by the red seaweed Gracilaria sp., and a proposed model for the remedy of marine-borne phenol pollutants. Environmental Pollution 278. https://doi.org/10.1016/j.envpol.2021.116853

Aydin, E., Talinli, I., 2013. Analysis, occurrence and fate of commonly used pharmaceuticals and hormones in the Buyukcekmece Watershed, Turkey. Chemosphere 90, 2004–2012. https://doi.org/10.1016/j.chemosphere.2012.10.074

Basheer, C., Lee, H.K., 2004. Analysis of endocrine disrupting alkylphenols, chlorophenols and bisphenol-A using hollow fiber-protected liquid-phase

microextraction coupled with injection port-derivatization gas chromatography-mass spectrometry. Journal of Chromatography A 1057, 163–169. https://doi.org/10.1016/j.chroma.2004.09.083

Bavasso, I., Poggi, C., Petrucci, E., 2020. Enhanced degradation of paracetamol by combining UV with electrogenerated hydrogen peroxide and ozone. Journal of Water Process Engineering 34. https://doi.org/10.1016/j.jwpe.2019.101102

Becke, A.D., 1993. Density-functional thermochemistry. III. The role of exact exchange. The Journal of Chemical Physics 98, 5648–5652. https://doi.org/10.1063/1.464913

Bediako, J.K., Lin, S., Sarkar, A.K., Zhao, Y., Choi, J.W., Song, M.H., Cho, C.W., Yun, Y.S., 2019. Evaluation of orange peel-derived activated carbons for treatment of dye-contaminated wastewater tailings. Environmental Science and Pollution Research 27, 1053–1068. https://doi.org/10.1007/s11356-019-07031-8

Bedoux, G., Roig, B., Thomas, O., Dupont, V., Le Bot, B., 2012. Occurrence and toxicity of antimicrobial triclosan and by-products in the environment. Environmental Science and Pollution Research 19, 1044–1065. https://doi.org/10.1007/s11356-011-0632-z

Behera, S.K., Oh, S.Y., Park, H.S., 2010. Sorption of triclosan onto activated carbon, kaolinite and montmorillonite: Effects of pH, ionic strength, and humic acid. Journal of Hazardous Materials 179, 684–691. https://doi.org/10.1016/j.jhazmat.2010.03.056

Bele, S., Samanidou, V., Deliyanni, E., 2016. Effect of the reduction degree of graphene oxide on the adsorption of Bisphenol A. Chemical Engineering Research and Design. https://doi.org/10.1016/j.cherd.2016.03.002

Belfroid, A., Van Velzen, M., Van der Horst, B., Vethaak, D., 2002. Occurrence of bisphenol A in surface water and uptake in fish: Evaluation of field measurements. Chemosphere 49, 97–103. https://doi.org/10.1016/S0045-6535(02)00157-1

Bester, K., 2005. Fate of triclosan and triclosan-methyl in sewage treatment plants and surface waters. Archives of Environmental Contamination and Toxicology 49, 9–17. https://doi.org/10.1007/s00244-004-0155-4

Bhandari, R.K., Deem, S.L., Holliday, D.K., Jandegian, C.M., Kassotis, C.D., Nagel, S.C., Tillitt, D.E., vom Saal, F.S., Rosenfeld, C.S., 2015. Effects of the environmental estrogenic contaminants bisphenol A and 17α-ethinyl estradiol on sexual development and adult behaviors in aquatic wildlife species. General and

Comparative Endocrinology 214, 195–219. https://doi.org/10.1016/j.ygcen.2014.09.014

Bhattacharya, P., Mukherjee, D., Deb, N., Swarnakar, S., Banerjee, S., 2021. Indigenously developed CuO/TiO2 coated ceramic ultrafiltration membrane for removal of emerging contaminantes like phtalates and parabens: Toxicity evaluation in PA-1 cell line. Materials Chemistry and Physics.

Bögi, C., Schwaiger, J., Ferling, H., Mallow, U., Steineck, C., Sinowatz, F., Kalbfus, W., Negele, R.D., Lutz, I., Kloas, W., 2003. Endocrine effects of environmental pollution on Xenopus laevis and Rana temporaria. Environmental Research 93, 195–201. https://doi.org/10.1016/S0013-9351(03)00082-3

Bolong, N., Ismail, A.F., Salim, M.R., Matsuura, T., 2009. A review of the effects of emerging contaminants in wastewater and options for their removal. Desalination 239, 229–246. https://doi.org/10.1016/j.desal.2008.03.020

Bonate, P.L., 2011. Pharmacokinetic-Pharmacodynamic Modeling and Simulation, 2nd ed. Springer.

Boyd, G.E., Adamson, A.W., Myers Jr, L.S., 1947. The Exchange Adsorption of Ions from Aqueous Solutions by Organic Zeolites. II. Kinetics.

Brandt, E.M.F., 2012. Avaliação da remoção de fármacos e desreguladores endócrinos em sistemas simplificados de tratamento de esgoto (reatores uasb seguidos de pós-tratamento). Dissertação de Mestrado em Saneamento do Programa de Pós-Graduação em Saneamento, Meio Ambiente e Recursos Hídricos da Universidade Federal de Minas Gerais.

Brazovskaya, E.Y., Golubeva, O.Y., 2020. Development of Magnetic Nanocomposites Based on Beta Zeolites and Study of Their Sorption Properties. Petroleum Chemistry 60, 957–963. https://doi.org/10.1134/S0965544120080046

Cao, Y., Li, X., 2014. Adsorption of graphene for the removal of inorganic pollutants in water purification: A review. Adsorption 20, 713–727. https://doi.org/10.1007/s10450-014-9615-y

Caon, N.B., Cardoso, C., Faita, F.L., Vitali, L., Parize, A.L., 2020. Magnetic solid-phase extraction of triclosan from water using n -octadecyl modi fi ed silica-coated magnetic nanoparticles. Journal of Environmental Chemical Engineering 8. https://doi.org/10.1016/j.jece.2020.104003

Cargouët, M., Perdiz, D., Mouatassim-Souali, A., Tamisier-Karolak, S., Levi, Y., 2004. Assessment of river contamination by estrogenic compounds in Paris area (France).

Science of the Total Environment 324, 55–66. https://doi.org/10.1016/j.scitotenv.2003.10.035

Catherine, H.N., Ou, M.H., Manu, B., Shih, Y. hsin, 2018. Adsorption mechanism of emerging and conventional phenolic compounds on graphene oxide nanoflakes in water. Science of the Total Environment. https://doi.org/10.1016/j.scitotenv.2018.03.389

Chabot, V., Higgins, D., Yu, A., Xiao, X., Chen, Z., Zhang, J., 2014. A review of graphene and graphene oxide sponge: Material synthesis and applications to energy and the environment. Energy and Environmental Science 7, 1564–1596. https://doi.org/10.1039/c3ee43385d

Chang, K., Hsieh, J., Ou, B., Chang, M., Hseih, W., Lin, J.-H., Huang, P.-J., Wong, K.-F., Chen, S.-T., 2012. Adsorption Studies on the Removal of an Endocrine-Disrupting Compound (Bisphenol A) using Activated Carbon from Rice Straw Agricultural Waste Adsorption Studies on the Removal of an Endocrine-Disrupting Compound (Bisphenol A) using Activated Carbon f. Separation Science and Technology 37–41. https://doi.org/10.1080/01496395.2011.647212

Cheminski, T., De Figueiredo Neves, T., Silva, P.M., Guimarães, C.H., Prediger, P., 2019. Insertion of phenyl ethyleneglycol units on graphene oxide as stabilizers and its application for surfactant removal. Journal of Environmental Chemical Engineering 7, 102976. https://doi.org/10.1016/j.jece.2019.102976

Chen, C.Y., Wen, T.Y., Wang, G.S., Cheng, H.W., Lin, Y.H., Lien, G.W., 2007. Determining estrogenic steroids in Taipei waters and removal in drinking water treatment using high-flow solid-phase extraction and liquid chromatography/tandem mass spectrometry. Science of the Total Environment 378, 352–365. https://doi.org/10.1016/j.scitotenv.2007.02.038

Chen, J., Wang, X., Dai, C., Chen, S., Tu, Y., 2014. Adsorption of GA module onto graphene and graphene oxide: A molecular dynamics simulation study. Physica E: Low-Dimensional Systems and Nanostructures 62, 59–63. https://doi.org/10.1016/j.physe.2014.04.021

Cheng, N., Wang, B., Wu, P., Lee, X., Xing, Y., Chen, M., Gao, B., 2021. Adsorption of emerging contaminants from water and wastewater by modified biochar: A review. Environmental Pollution. https://doi.org/10.1016/j.envpol.2021.116448

Cherednichenko, G., Zhang, R., Bannister, R.A., Timofeyev, V., Li, N., Fritsch, E.B., Feng, W., Barrientos, G.C., Schebb, N.H., Hammock, B.D., Beam, K.G.,

Chiamvimonvat, N., Pessah, I.N., 2012. Triclosan impairs excitation-contraction coupling and Ca2+ dynamics in striated muscle (Proceedings of the National Academy of Sciences of the United States of America (2012) 109, 35, (14158 - 14163) DOI:10.1073/pnas. 1211314109). Proceedings of the National Academy of Sciences of the United States of America 109, 16393. https://doi.org/10.1073/pnas.1215071109

Cobos, M., González, B., Fernández, M.J., Fernández, M.D., 2018. Study on the effect of graphene and glycerol plasticizer on the properties of chitosan-graphene nanocomposites via in situ green chemical reduction of graphene oxide. International Journal of Biological Macromolecules 114, 599–613. https://doi.org/10.1016/j.ijbiomac.2018.03.129

Coelho, C.M., de Andrade, J.R., da Silva, M.G.C., Vieira, M.G.A., 2020. Removal of propranolol hydrochloride by batch biosorption using remaining biomass of alginate extraction from Sargassum filipendula algae. Environmental Science and Pollution Research 27, 16599–16611. https://doi.org/10.1007/s11356-020-08109-4

Cristina do Nascimento, D., Gurgel Carlos da Silva, M., Gurgel Adeodato Vieira, M., 2021. Adsorption of propranolol hydrochloride from aqueous solutions onto thermally treated bentonite clay: A complete batch system evaluation. Journal of Molecular Liquids 337. https://doi.org/10.1016/j.molliq.2021.116442

Crouse, B.A., Ghoshdastidar, A.J., Tong, A.Z., 2012. The presence of acidic and neutral drugs in treated sewage effluents and receiving waters in the Cornwallis and Annapolis River watersheds and the Mill CoveSewage Treatment Plant in Nova Scotia, Canada. Environmental Research 112, 92–99. https://doi.org/10.1016/j.envres.2011.11.011

Cychosz, K.A., Guillet-Nicolas, R., García-Martínez, J., Thommes, M., 2017. Recent advances in the textural characterization of hierarchically structured nanoporous materials. Chemical Society Reviews. https://doi.org/10.1039/c6cs00391e

Dąbrowski, A., 2001. Adsorption - From theory to practice. Advances in Colloid and Interface Science 93, 135–224. https://doi.org/10.1016/S0001-8686(00)00082-8

Dąbrowski, A., Podkościelny, P., Hubicki, Z., Barczak, M., 2005. Adsorption of phenolic compounds by activated carbon - A critical review. Chemosphere 58, 1049–1070. https://doi.org/10.1016/j.chemosphere.2004.09.067

Dai, J., Meng, X., Zhang, Y., Huang, Y., 2020. Effects of modification and magnetization of rice straw derived biochar on adsorption of tetracycline from water. Bioresource Technology 311. https://doi.org/10.1016/j.biortech.2020.123455

Daniel, I.M., Ishai, O., 2006. Engineering mechanics of composite materials, Oxford University Press. https://doi.org/10.1016/s0261-3069(97)87195-6

de Almeida, A. da S.V., de Figueiredo Neves, T., da Silva, M.G.C., Prediger, P., Vieira, M.G.A., 2022. Synthesis of a novel magnetic composite based on graphene oxide, chitosan and organoclay and its application in the removal of bisphenol A, 17α-ethinylestradiol and triclosan. Journal of Environmental Chemical Engineering 10, 107071. https://doi.org/10.1016/j.jece.2021.107071

de Andrade, J. R., da Silva, M.G.C., Gimenes, M.L., Vieira, M.G.A., 2020. Performance of organoclay in adsorptive uptake of antihypertensive losartan potassium: A comparative batch study using micro-grain activated carbon. Journal of Environmental Chemical Engineering 8, 103562. https://doi.org/10.1016/j.jece.2019.103562

De Andrade, J.R., Da Silva, M.G.C., Gimenes, M.L., Vieira, M.G.A., 2020. Performance of organoclay in adsorptive uptake of antihypertensive losartan potassium: A comparative batch study using micro-grain activated carbon. Journal of Environmental Chemical Engineering 8, 103562. https://doi.org/10.1016/j.jece.2019.103562

de Andrade, Júlia Resende, Oliveira, M.F., Canevesi, R.L.S., Landers, R., da Silva, M.G.C., Vieira, M.G.A., 2020. Comparative adsorption of diclofenac sodium and losartan potassium in organophilic clay-packed fixed-bed: X-ray photoelectron spectroscopy characterization, experimental tests and theoretical study on DFT-based chemical descriptors. Journal of Molecular Liquids 312, 113427. https://doi.org/10.1016/j.molliq.2020.113427

de Aquino, S.F., Brandt, E.M.F., Chernicharo, C.A. de L., 2013. Remoção de fármacos e desreguladores endócrinos em estações de tratamento de esgoto: Revisão da literatura. Engenharia Sanitaria e Ambiental 18, 187–204. https://doi.org/10.1590/S1413-41522013000300002

De Assis Gonsalves, A., Araujo, C.R.M., Soares, N.A., Goulart, M.O.F., De Abreu, F.C., 2011. Diferentes Estrategias Para A Reticulaqao De Quitosana. Quimica Nova 34, 1215–1223. https://doi.org/10.1590/S0100-40422011000700021

de Farias, M.B., Spaolonzi, M.P., Silva, M.G.C., Vieira, M.G.A., 2021. Fixed-bed adsorption of bisphenol A onto organoclay: Characterisation, mathematical modelling and theoretical calculation of DFT-based chemical descriptors. Journal of Environmental Chemical Engineering 9. https://doi.org/10.1016/j.jece.2021.106103

de Figueiredo Neves, T., Barticiotto Dalarme, N., da Silva, P.M.M., Landers, R., Siqueira Franco Picone, C., Prediger, P., 2020a. Novel magnetic chitosan/quaternary ammonium salt graphene oxide composite applied to dye removal. Journal of Environmental Chemical Engineering 8, 103820. https://doi.org/10.1016/j.jece.2020.103820

de Figueiredo Neves, T., Barticiotto Dalarme, N., da Silva, P.M.M., Landers, R., Siqueira Franco Picone, C., Prediger, P., 2020b. Novel magnetic chitosan/quaternary ammonium salt graphene oxide composite applied to dye removal. Journal of Environmental Chemical Engineering 8, 103820. https://doi.org/10.1016/j.jece.2020.103820

de Souza, F.M., dos Santos, O.A.A., Vieira, M.G.A., 2019. Adsorption of herbicide 2,4-D from aqueous solution using organo-modified bentonite clay. Environmental Science and Pollution Research 26, 18329–18342. https://doi.org/10.1007/s11356-019-05196-w

de Souza, T.N.V., de Carvalho, S.M.L., Vieira, M.G.A., da Silva, M.G.C., Brasil, D. do S.B., 2018. Adsorption of basic dyes onto activated carbon: Experimental and theoretical investigation of chemical reactivity of basic dyes using DFT-based descriptors. Applied Surface Science 448, 662–670. https://doi.org/10.1016/j.apsusc.2018.04.087

Dehghani, M.H., Ghadermazi, M., Bhatnagar, A., Sadighara, P., Jahed-khaniki, G., Heibati, B., Mckay, G., 2016. Adsorptive removal of endocrine disrupting bisphenol A from aqueous solution using chitosan. Biochemical Pharmacology. https://doi.org/10.1016/j.jece.2016.05.011

Delgado-Moreno, L., Bazhari, S., Nogales, R., Romero, E., 2019. Innovative application of biobed bioremediation systems to remove emerging contaminants: Adsorption, degradation and bioaccesibility. Science of the Total Environment 651, 990–997. https://doi.org/10.1016/j.scitotenv.2018.09.268

Delhiraja, K., Vellingiri, K., Boukhvalov, D.W., Philip, L., 2019. Development of Highly Water Stable Graphene Oxide-Based Composites for the Removal of

Pharmaceuticals and Personal Care Products. Industrial and Engineering Chemistry Research 58, 2899–2913. https://doi.org/10.1021/acs.iecr.8b02668

Dhillon, G.S., Kaur, S., Pulicharla, R., Brar, S.K., Cledón, M., Verma, M., Surampalli, R.Y., 2015. Triclosan: Current status, occurrence, environmental risks and bioaccumulation potential. International Journal of Environmental Research and Public Health 12, 5657–5684. https://doi.org/10.3390/ijerph120505657

Dias, J.M., Alvim-Ferraz, M.C.M., Almeida, M.F., Rivera-Utrilla, J., Sánchez-Polo, M., 2007. Waste materials for activated carbon preparation and its use in aqueous-phase treatment: A review. Journal of Environmental Management 85, 833–846. https://doi.org/10.1016/j.jenvman.2007.07.031

Ding, W.H., Wu, C.Y., 2000. Determination of estrogenic nonylphenol and bisphenol A in river water by solid-phase extraction and gas chromatography-mass spectrometry. Journal of the Chinese Chemical Society 47, 1155–1160. https://doi.org/10.1002/jccs.200000155

Dinwiddie, M.T., Terry, P.D., Chen, J., 2014. Recent evidence regarding triclosan and cancer risk. International Journal of Environmental Research and Public Health 11, 2209–2217. https://doi.org/10.3390/ijerph110202209

Doğan, M., Alkan, M., Demirbaş, Ö., Özdemir, Y., Özmetin, C., 2006. Adsorption kinetics of maxilon blue GRL onto sepiolite from aqueous solutions. Chemical Engineering Journal 124, 89–101. https://doi.org/10.1016/j.cej.2006.08.016

Dordio, A. V., Miranda, S., Prates Ramalho, J.P., Carvalho, A.J.P., 2017. Mechanisms of removal of three widespread pharmaceuticals by two clay materials. Journal of Hazardous Materials 323, 575–583. https://doi.org/10.1016/j.jhazmat.2016.05.091

dos Santos Cardoso, C., Vitali, L., 2021. Chitosan Versus Chitosan-Vanillin Modified: An Evaluation of the Competitive Adsorption of Five Emerging Contaminants. Water, Air, and Soil Pollution 232. https://doi.org/10.1007/s11270-021-05118-y

Drewes, J.E., Hemming, J., Ladenburger, S.J., Schauer, J., Sonzogni, W., 2012. an Assessment of Endocrine Disrupting Activity Changes in Water Reclamation Systems Through the Use of Bioassays and Chemical Measurements. Proceedings of the Water Environment Federation 2004, 47–65. https://doi.org/10.2175/193864704784147476

Ebadi, A., Soltan Mohammadzadeh, J.S., Khudiev, A., 2009. What is the correct form of BET isotherm for modeling liquid phase adsorption? Adsorption 15, 65–73. https://doi.org/10.1007/s10450-009-9151-3

Ederer, J., Janos, P., Ecorchard, P., Tolasz, J., Stengl, V., Benes, H., Perchacz, M., Pop-Georgievski, O., 2017. Determination of amino groups on functionalized graphene oxide for polyurethane nanomaterial. RSC Advances.

Egea-Corbacho, A., Gutiérrez Ruiz, S., Quiroga Alonso, J.M., 2019. Removal of emerging contaminants from wastewater using nanofiltration for its subsequent reuse: Full–scale pilot plant. Journal of Cleaner Production 214, 514–523. https://doi.org/10.1016/j.jclepro.2018.12.297

Erim, B., Ciğeroğlu, Z., Bayramoğlu, M., 2021. Green synthesis of TiO2/GO/chitosan by using leaf extract of Olea europaea as a highly efficient photocatalyst for the degradation of cefixime trihydrate under UV-A radiation exposure: An optimization study with D-optimal design. Journal of Molecular Structure 1234. https://doi.org/10.1016/j.molstruc.2021.130194

Erler, C., Novak, J., 2010. Bisphenol a exposure: Human risk and health policy. Journal of Pediatric Nursing 25, 400–407. https://doi.org/10.1016/j.pedn.2009.05.006

Esmaeili, H., Tamjidi, S., 2020. Ultrasonic-assisted synthesis of natural clay/Fe3O4/graphene oxide for enhance removal of Cr (VI) from aqueous media. Environmental Science and Pollution Research 27, 31652–31664. https://doi.org/10.1007/s11356-020-09448-y

Fagerlund, G., 1973. Determination of specific surface by the BET method. Matériaux et Construction 239–245.

Farias, M.B. de, Silva, M.G.C., Vieira, M.G.A., 2022. Adsorption of bisphenol A from aqueous solution onto organoclay: Experimental design, kinetic, equilibrium and thermodynamic study. Powder Technology 395, 695–707. https://doi.org/10.1016/j.powtec.2021.10.021

Farrah, H., Pickering, W.F., 1979. pH effects in the adsorption of heavy metal ions by clays. Chemical Geology 25, 317–326. https://doi.org/10.1016/0009-2541(79)90063-9

Fazilath Basha A, Liakath Ali Khan, F., Muthu, S., Raja, M., 2021. Computational evaluation on molecular structure (Monomer, Dimer), RDG, ELF, electronic (HOMO-LUMO, MEP) properties, and spectroscopic profiling of 8-Quinolinesulfonamide with molecular docking studies. Computational and Theoretical Chemistry 1198, 113169. https://doi.org/10.1016/j.comptc.2021.113169

Feng, Y., Zhang, Z., Gao, P., Su, H., Yu, Y., Ren, N., 2010. Adsorption behavior of EE2 (17α-ethinylestradiol) onto the inactivated sewage sludge: Kinetics,

thermodynamics and influence factors. Journal of Hazardous Materials 175, 970–976. https://doi.org/10.1016/j.jhazmat.2009.10.105

Fernandes, A.N., Giovanela, M., Esteves, V.I., Grassi, M.T., Almeida, C.A., Sierra, M.M.D., 2011. Remoção dos hormônios E2 e EE2 de soluções aquosas empregando turfa decomposta como material adsorvente 34, 1526–1533.

Flint, S., Markle, T., Thompson, S., Wallace, E., 2012. Bisphenol A exposure, effects, and policy: A wildlife perspective. Journal of Environmental Management 104, 19–34. https://doi.org/10.1016/j.jenvman.2012.03.021

Forder, T.R., Jones, M.D., 2015. Synthesis and characterisation of aluminium(III) imine bis(phenolate) complexes with application for the polymerisation of rac-LA. New Journal of Chemistry 39, 1974–1978. https://doi.org/10.1039/c4nj02228a

Freitas, M.B., Freitas, C.M. de, 2005. A vigilância da qualidade da água para consumo humano: desafios e perspectivas para o Sistema Único de Saúde. Ciência & Saúde Coletiva 10, 993–1004. https://doi.org/10.1590/s1413-81232005000400022

Freundlich, H., 1906. Über die Adsorption in Lösungen (Concerning adsorption in solutions). Chemie–Stochiometrie, Zeitschrift Fur Physikalische.

Frisch, Æ., Hratchian, H.P., Dennington, R.D., Keith, T.A., Millam, J., 2016. Gaussview 6.

Frisch, M.J., Pople, J.A., Binkley, J.S., 1984. Self-consistent molecular orbital methods 25. Supplementary functions for Gaussian basis sets. The Journal of Chemical Physics 80, 3265–3269. https://doi.org/10.1063/1.447079

Frisch, M.J., Trucks, G.W., Schlegel, H.B., Scuseria, G.E., Robb, M.A., Cheeseman, J.R., Scalmani, G., Barone, V., Mennucci, B., Petersson, G.A., Nakatsuji, H., Caricato, M., Li, X., Hratchian, H.P., Izmaylov, A.F., Bloino, J., Zheng, G., Sonnenberg, J.L., Hada, M., Ehar, M., Fox, D.J., 2009. Gaussian 09. Gaussian, Inc., Wallingford.

Fuchsman, P., Lyndall, J., Bock, M., Lauren, D., Barber, T., Leigh, K., Perruchon, E., Capdevielle, M., 2010. Terrestrial ecological risk evaluation for triclosan in land-applied biosolids. Integrated Environmental Assessment and Management 6, 405–418. https://doi.org/10.1897/ieam_2009-071.1

Ge, Y., Zhang, Y., Xia, J., Ma, M., He, S., Nie, F., Gu, N., 2009. Effect of surface charge and agglomerate degree of magnetic iron oxide nanoparticles on KB cellular uptake in vitro. Colloids and Surfaces B: Biointerfaces 73, 294–301. https://doi.org/10.1016/j.colsurfb.2009.05.031

Ghosh, A., Ghosh, S., Seshadhri, G.M., Ramaprabhu, S., 2019. Green synthesis of nitrogen-doped self-assembled porous carbon-metal oxide composite towards energy and environmental applications. Scientific Reports 9. https://doi.org/10.1038/s41598-019-41700-5

Gong, J., Ran, Y., Chen, D., Yang, Y., Ma, X., 2009. Occurrence and environmental risk of endocrine-disrupting chemicals in surface waters of the Pearl River, South China. Environmental Monitoring and Assessment 156, 199–210. https://doi.org/10.1007/s10661-008-0474-4

Gong, Y., Yu, Y., Kang, H., Chen, X., Liu, H., Zhang, Y., Sun, Y., Song, H., 2019. Synthesis and Characterization of Graphene Oxide Chitosan Composite Aerogels. Polymers.

Goyal, N., Bulasara, V.K., Barman, S., 2018. Removal of emerging contaminants daidzein and coumestrol from water by nanozeolite beta modified with tetrasubstituted ammonium cation. Journal of Hazardous Materials 344, 417–430. https://doi.org/10.1016/j.jhazmat.2017.10.051

Gregorio-Jauregui, K.M., Pineda, M.G., Rivera-Salinas, J.E., Hurtado, G., Saade, H., Martinez, J.L., Ilyina, A., López, R.G., 2012. One-step method for preparation of magnetic nanoparticles coated with chitosan. Journal of Nanomaterials 2012. https://doi.org/10.1155/2012/813958

Guerra, A.C.S., de Andrade, M.B., Tonial dos Santos, T.R., Bergamasco, R., 2021. Adsorption of sodium diclofenac in aqueous medium using graphene oxide nanosheets. Environmental Technology (United Kingdom) 42, 2599–2609. https://doi.org/10.1080/09593330.2019.1707882

Guerra, P., Kim, M., Teslic, S., Alaee, M., Smyth, S.A., 2015. Bisphenol-A removal in various wastewater treatment processes: Operational conditions, mass balance, and optimization. Journal of Environmental Management 152, 192–200. https://doi.org/10.1016/j.jenvman.2015.01.044

Han, J., Qiu, W., Cao, Z., Hu, J., Gao, W., 2013. Adsorption of ethinylestradiol (EE2) on polyamide 612: Molecular modeling and effects of water chemistry. Water Research 47, 2273–2284. https://doi.org/10.1016/j.watres.2013.01.046

Han, J., Qiu, W., Meng, S., Gao, W., 2012. Removal of ethinylestradiol (EE2) from water via adsorption on aliphatic polyamides. Water Research 46, 5715–5724. https://doi.org/10.1016/j.watres.2012.08.001

Hanwell, M.D., Curtis, D.E., Lonie, D.C., Vandermeerschd, T., Zurek, E., Hutchison, G.R., 2012. Avogadro: An advanced semantic chemical editor, visualization, and analysis platform. Journal of Cheminformatics 4. https://doi.org/10.1186/1758-2946-4-17

He, H., Ma, L., Zhu, J., Frost, R.L., Theng, B.K.G., Bergaya, F., 2014. Synthesis of organoclays: A critical review and some unresolved issues. Applied Clay Science 100, 22–28. https://doi.org/10.1016/j.clay.2014.02.008

Hemidouche, S., Assoumani, A., Favier, L., Simion, A.I., Grigoras, C.G., Wolbert, D., Gavrila, L., Nationale, E., Chimie, S. De, 2017. Removal of some Endocrine Disruptors via Adsorption on Activated Carbon 410–413.

Ho, Y.S., McKay, G., 2000. The kinetics of sorption of divalent metal ions onto sphagnum moss peat. Water Research 34, 735–742. https://doi.org/10.1016/S0043-1354(99)00232-8

HO, Y.S., MCKAY, G., 1999. Pseudo-second order model for sorption processes. Process Biochemistry 34, 451–465. https://doi.org/10.1021/acs.oprd.7b00090

Ho, Y.S., McKay, G., 1998. A Comparison of chemisorption kinetic models applied to pollutant removal on various sorbents. Process Safety and Environmental Protection 76, 332–340. https://doi.org/10.1205/095758298529696

Honório, K.M., Silva, A.B.F., 2003. An AM1 Study on the Electron-Donating and Electron-Accepting Character of Biomolecules 95, 126–132. https://doi.org/10.1002/qua.10661

Hosseini, Y., Najafi, M., Khalili, S., Jahanshahi, M., Peyravi, M., 2021. Assembly of amine-functionalized graphene oxide for efficient and selective adsorption of CO2. Materials Chemistry and Physics 270. https://doi.org/10.1016/j.matchemphys.2021.124788

Hu, D., Lian, Z., Xian, H., Jiang, R., Wang, N., Weng, Y., Peng, X., Wang, S., Ouyang, X. –K, 2020. Adsorption of Pb(II) from aqueous solution by polyacrylic acid grafted magnetic chitosan nanocomposite. International Journal of Biological Macromolecules 154, 1537–1547. https://doi.org/10.1016/j.ijbiomac.2019.11.038

Hu, Y., Zhu, Y., Zhang, Y., Lin, T., Zeng, G., Zhang, S., Wang, Y., He, W., Zhang, M., Long, H., 2019. An efficient adsorbent: Simultaneous activated and magnetic ZnO doped biochar derived from camphor leaves for ciprofloxacin adsorption. Bioresource Technology 288. https://doi.org/10.1016/j.biortech.2019.121511

Hua, W., Bennett, E.R., Letcher, R.J., 2005. Triclosan in waste and surface waters from the upper Detroit River by liquid chromatography-electrospray-tandem quadrupole mass spectrometry. Environment International 31, 621–630. https://doi.org/10.1016/j.envint.2004.10.019

Huang, Y., Liu, Y., Kong, M., Xu, E.G., Coffin, S., Schlenk, D., Dionysiou, D.D., 2018. Efficient degradation of cytotoxic contaminants of emerging concern by UV/H2O2. Environmental Science: Water Research and Technology 4, 1272–1281. https://doi.org/10.1039/c8ew00290h

Huang, Y.Q., Wong, C.K.C., Zheng, J.S., Bouwman, H., Barra, R., Wahlström, B., Neretin, L., Wong, M.H., 2012. Bisphenol A (BPA) in China: A review of sources, environmental levels, and potential human health impacts. Environment International 42, 91–99. https://doi.org/10.1016/j.envint.2011.04.010

Huang, Z., Li, Z., Zheng, L., Zhou, L., Chai, Z., Wang, X., Shi, W., 2017. Interaction mechanism of uranium(VI) with three-dimensional graphene oxide-chitosan composite: Insights from batch experiments, IR, XPS, and EXAFS spectroscopy. Chemical Engineering Journal 328, 1066–1074. https://doi.org/10.1016/j.cej.2017.07.067

Hummers, W.S., Offeman, R.E., 1958. Preparation of Graphitic Oxide. Journal of the American Chemical Society 80, 1339. https://doi.org/10.1021/ja01539a017

Ifelebuegu, A.O., Ezenwa, C.P., 2011. Removal of endocrine disrupting chemicals in wastewater treatment by fenton-like oxidation. Water, Air, and Soil Pollution 217, 213–220. https://doi.org/10.1007/s11270-010-0580-0

Im, J.S., Park, S.J., Lee, Y.S., 2007. Preparation and characteristics of electrospun activated carbon materials having meso- and macropores. Journal of Colloid and Interface Science 314, 32–37. https://doi.org/10.1016/j.jcis.2007.05.033

Jawad, A.H., Malek, N.N.A., Abdulhameed, A.S., Razuan, R., 2020a. Synthesis of Magnetic Chitosan-Fly Ash/Fe3O4 Composite for Adsorption of Reactive Orange 16 Dye: Optimization by Box–Behnken Design. Journal of Polymers and the Environment 28, 1068–1082. https://doi.org/10.1007/s10924-020-01669-z

Jawad, A.H., Malek, N.N.A., Abdulhameed, A.S., Razuan, R., 2020b. Synthesis of Magnetic Chitosan-Fly Ash/Fe3O4 Composite for Adsorption of Reactive Orange 16 Dye: Optimization by Box–Behnken Design. Journal of Polymers and the Environment 28, 1068–1082. https://doi.org/10.1007/s10924-020-01669-z

Jiang, N., Shang, R., Heijman, S.G.J., Rietveld, L.C., 2020. Adsorption of triclosan, trichlorophenol and phenol by high-silica zeolites: Adsorption efficiencies and mechanisms. Separation and Purification Technology 235. https://doi.org/10.1016/j.seppur.2019.116152

Jun, B.M., Hwang, H.S., Heo, J., Han, J., Jang, M., Sohn, J., Park, C.M., Yoon, Y., 2019. Removal of selected endocrine-disrupting compounds using Al-based metal organic framework: Performance and mechanism of competitive adsorption. Journal of Industrial and Engineering Chemistry 79, 345–352. https://doi.org/10.1016/j.jiec.2019.07.009

Kang, J.H., Kondo, F., 2006. Bisphenol A in the surface water and freshwater snail collected from rivers around a secure landfill. Bulletin of Environmental Contamination and Toxicology 76, 113–118. https://doi.org/10.1007/s00128-005-0896-4

Kang, J.H., Kondo, F., 2002. Effects of bacterial counts and temperature on the biodegradation of bisphenol A in river water. Chemosphere 49, 493–498. https://doi.org/10.1016/S0045-6535(02)00315-6

Karau, A., Benken, C., Thömmes, J., Kula, M.R., 1997. The influence of particle size distribution and operating conditions on the adsorption performance in fluidized beds. Biotechnology and Bioengineering 55, 54–64. https://doi.org/10.1002/(SICI)1097-0290(19970705)55:1<54::AID-BIT7>3.0.CO;2-W

Karimi, F., Ayati, A., Tanhaei, B., Sanati, A.L., Afshar, S., Kardan, A., Dabirifar, Z., Karaman, C., 2022. Removal of metal ions using a new magnetic chitosan nano-bio-adsorbent; A powerful approach in water treatment. Environmental Research 203. https://doi.org/10.1016/j.envres.2021.111753

Karimi-Maleh, H., Ayati, A., Davoodi, R., Tanhaei, B., Karimi, F., Malekmohammadi, S., Orooji, Y., Fu, L., Sillanpää, M., 2021. Recent advances in using of chitosan-based adsorbents for removal of pharmaceutical contaminants: A review. Journal of Cleaner Production 291. https://doi.org/10.1016/j.jclepro.2021.125880

Kim, S., Chu, K.H., Al-Hamadani, Y.A.J., Park, C.M., Jang, M., Kim, D.H., Yu, M., Heo, J., Yoon, Y., 2018. Removal of contaminants of emerging concern by membranes in water and wastewater: A review. Chemical Engineering Journal 335, 896–914. https://doi.org/10.1016/j.cej.2017.11.044

Kong, Q., Shi, X., Ma, W., Zhang, F., Yu, T., Zhao, F., Zhao, D., Wei, C., 2021. Strategies to improve the adsorption properties of graphene-based adsorbent towards heavy metal ions and their compound pollutants: A review. Journal of Hazardous Materials. https://doi.org/10.1016/j.jhazmat.2021.125690

Kozyatnyk, I., Oesterle, P., Wurzer, C., Mašek, O., Jansson, S., 2021. Removal of contaminants of emerging concern from multicomponent systems using carbon dioxide activated biochar from lignocellulosic feedstocks. Bioresource Technology 340, 125561. https://doi.org/10.1016/j.biortech.2021.125561

Kuo, C.Y., Wu, C.H., Wu, J.Y., 2008. Adsorption of direct dyes from aqueous solutions by carbon nanotubes: Determination of equilibrium, kinetics and thermodynamics parameters. Journal of Colloid and Interface Science 327, 308–315. https://doi.org/10.1016/j.jcis.2008.08.038

Kuśmierek, K., ̄wia ̨tkowski, A., 2015. The influence of different agitation techniques on the adsorption kinetics of 4-chlorophenol on granular activated carbon. Reaction Kinetics, Mechanisms and Catalysis 116, 261–271. https://doi.org/10.1007/s11144-015-0889-1

Kyzas, G.Z., Bikiaris, D.N., Mitropoulos, A.C., 2017. Chitosan adsorbents for dye removal: a review. Polymer International 66, 1800–1811. https://doi.org/10.1002/pi.5467

Kyzas, G.Z., Bikiaris, D.N., Seredych, M., Bandosz, T.J., Deliyanni, E.A., 2014. Removal of dorzolamide from biomedical wastewaters with adsorption onto graphite oxide/poly(acrylic acid) grafted chitosan nanocomposite. Bioresource Technology 152, 399–406. https://doi.org/10.1016/j.biortech.2013.11.046

Kyzas, G.Z., Matis, K.A., 2015. Nanoadsorbents for pollutants removal: A review. Journal of Molecular Liquids 203, 159–168. https://doi.org/10.1016/j.molliq.2015.01.004

Ladavos, A.K., Katsoulidis, A.P., Iosifidis, A., Triantafyllidis, K.S., Pinnavaia, T.J., Pomonis, P.J., 2012. The BET equation, the inflection points of N 2 adsorption isotherms and the estimation of specific surface area of porous solids. Microporous and Mesoporous Materials 151, 126–133. https://doi.org/10.1016/j.micromeso.2011.11.005

Lagaly, G., Ogawa, M., Dékány, I., 2006. Chapter 7.3 Clay Mineral Organic Interactions. Developments in Clay Science 1, 309–377. https://doi.org/10.1016/S1572-4352(05)01010-X

Lagergren, S., 1898. Zur theorie Der Sogenannten adsorption geloster stoffe, Kungliga Svenska Vetenskapsakademiens.

Lai, C., He, H., Xie, W., Fan, S., Huang, H., Wang, Y., Huang, B., Pan, X., 2022. Adsorption and photochemical capacity on 17α-ethinylestradiol by char produced in the thermo treatment process of plastic waste. Journal of Hazardous Materials 423. https://doi.org/10.1016/j.jhazmat.2021.127066

Langdon, K.A., Warne, M.S.J., Smernik, R.J., Shareef, A., Kookana, R.S., 2011. Selected personal care products and endocrine disruptors in biosolids: An Australia-wide survey. Science of the Total Environment 409, 1075–1081. https://doi.org/10.1016/j.scitotenv.2010.12.013

Langmuir, I, 1918. The Adsorption of Gases on Plane Surfaces of Glass, Mica and Platinum. Journal of the American Chemical Society 40, 1361–1403. https://doi.org/10.1021/ja01269a066

Langmuir, Irving, 1918. The adsorption of gases on plane surfaces of glass, mica and platinum. Journal of the American Chemical Society 40, 1361–1403. https://doi.org/10.1021/ja02242a004

Lawrie, G., Keen, I., Drew, B., Chandler-Temple, A., Rintoul, L., Fredericks, P., Grøndahl, L., 2007. Interactions between alginate and chitosan biopolymers characterized using FTIR and XPS. Biomacromolecules 8, 2533–2541. https://doi.org/10.1021/bm070014y

Lei, C., Hu, Y., He, M., 2013. Adsorption characteristics of triclosan from aqueous solution onto cetylpyridinium bromide (CPB) modified zeolites. CHEMICAL ENGINEERING JOURNAL 219, 361–370. https://doi.org/10.1016/j.cej.2012.12.099

Leudjo Taka, A., Klink, M.J., Yangkou Mbianda, X., Naidoo, E.B., 2021. Chitosan nanocomposites for water treatment by fixed-bed continuous flow column adsorption: A review. Carbohydrate Polymers 255, 117398. https://doi.org/10.1016/j.carbpol.2020.117398

Li, Y., Umer, R., Samad, Y.A., Zheng, L., Liao, K., 2013. The effect of the ultrasonication pre-treatment of graphene oxide (GO) on the mechanical properties of GO/polyvinyl alcohol composites. Carbon 55, 321–327. https://doi.org/10.1016/j.carbon.2012.12.071

Limousin, G., Gaudet, J.P., Charlet, L., Szenknect, S., Barthès, V., Krimissa, M., 2007. Sorption isotherms: A review on physical bases, modeling and measurement.

Applied Geochemistry 22, 249–275. https://doi.org/10.1016/j.apgeochem.2006.09.010

Lin, X., Xu, J., Keller, A.A., He, L., Gu, Y., Zheng, W., Sun, D., Lu, Z., Huang, J., Huang, X., Li, G., 2020. Occurrence and risk assessment of emerging contaminants in a water reclamation and ecological reuse project. Science of the Total Environment 744. https://doi.org/10.1016/j.scitotenv.2020.140977

Lin, Z., Waller, G.H., Liu, Y., Liu, M., Wong, C.P., 2013. Simple preparation of nanoporous few-layer nitrogen-doped graphene for use as an efficient electrocatalyst for oxygen reduction and oxygen evolution reactions. Carbon 53, 130–136. https://doi.org/10.1016/j.carbon.2012.10.039

Liu, F.F., Zhao, J., Wang, S., Du, P., Xing, B., 2014. Effects of solution chemistry on adsorption of selected pharmaceuticals and personal care products (PPCPs) by graphenes and carbon nanotubes. Environmental Science and Technology 48, 13197–13206. https://doi.org/10.1021/es5034684

Liu, G., Ma, J., Li, X., Qin, Q., 2009. Adsorption of bisphenol A from aqueous solution onto activated carbons with different modification treatments. Journal of Hazardous Materials 164, 1275–1280. https://doi.org/10.1016/j.jhazmat.2008.09.038

Liu, J., Carr, S.A., 2013. Removal of Estrogenic Compounds from Aqueous Solutions Using Zeolites. Water Environment Research 85, 2157–2163. https://doi.org/10.2175/106143013x13736496909356

Liu, J., Wang, R., Huang, B., Lin, C., Zhou, J., Pan, X., 2012. Biological effects and bioaccumulation of steroidal and phenolic endocrine disrupting chemicals in high-back crucian carp exposed to wastewater treatment plant effluents. Environmental Pollution 162, 325–331. https://doi.org/10.1016/j.envpol.2011.11.036

Liu, S.H., Tang, W.T., 2020. Photodecomposition of ibuprofen over g-C3N4/Bi2WO6/rGO heterostructured composites under visible/solar light. Science of the Total Environment 731. https://doi.org/10.1016/j.scitotenv.2020.139172

Liu, T., Han, X., Wang, Y., Yan, L., Du, B., Wei, Q., Wei, D., 2017. Magnetic chitosan/anaerobic granular sludge composite: Synthesis, characterization and application in heavy metal ions removal. Journal of Colloid and Interface Science 508, 405–414. https://doi.org/10.1016/j.jcis.2017.08.067

Liu, X., Cao, Z., Yuan, Z., Zhang, J., Guo, X., Yang, Y., He, F., Zhao, Y., Xu, J., 2018. Insight into the kinetics and mechanism of removal of aqueous chlorinated

nitroaromatic antibiotic chloramphenicol by nanoscale zero-valent iron. Chemical Engineering Journal 334, 508–518. https://doi.org/10.1016/j.cej.2017.10.060

Loganathan, P., Vigneswaran, S., Kandasamy, J., 2013. Enhanced removal of nitrate from water using surface modification of adsorbents - A review. Journal of Environmental Management 131, 363–374. https://doi.org/10.1016/j.jenvman.2013.09.034

López-Velázquez, K., Guzmán-Mar, J.L., Saldarriaga-Noreña, H.A., Murillo-Tovar, M.A., Hinojosa-Reyes, L., Villanueva-Rodríguez, M., 2021. Occurrence and seasonal distribution of five selected endocrine-disrupting compounds in wastewater treatment plants of the Metropolitan Area of Monterrey, Mexico: The role of water quality parameters. Environmental Pollution 269. https://doi.org/10.1016/j.envpol.2020.116223

Lu, J., Wu, Jie, Wu, Jun, Zhang, C., Luo, Y., 2020. Adsorption and Desorption of Steroid Hormones by Microplastics in Seawater. Bulletin of Environmental Contamination and Toxicology. https://doi.org/10.1007/s00128-020-02784-2

Lu, Y., Jiang, M., Wang, C., Wang, Y., Yang, W., 2014. Impact of molecular size on two antibiotics adsorption by porous resins. Journal of the Taiwan Institute of Chemical Engineers 45, 955–961. https://doi.org/10.1016/j.jtice.2013.09.009

Lu, Y., Zhang, S., Yin, J., Bai, C., Zhang, J., Li, Y., Yang, Y., Ge, Z., Zhang, M., Wei, L., Ma, M., Ma, Y., Chen, Y., 2017. Mesoporous activated carbon materials with ultrahigh mesopore volume and effective specific surface area for high performance supercapacitors. Carbon 124, 64–71. https://doi.org/10.1016/j.carbon.2017.08.044

Luo, Z., Li, H., Yang, Y., Lin, H., Yang, Z., 2017. Adsorption of 17α-ethinylestradiol from aqueous solution onto a reduced graphene oxide-magnetic composite. Journal of the Taiwan Institute of Chemical Engineers 80, 797–804. https://doi.org/10.1016/j.jtice.2017.09.028

Ly, Q.V., Maqbool, T., Zhang, Z., van Le, Q., An, X., Hu, Y., Cho, J., Li, J., Hur, J., 2021. Characterization of dissolved organic matter for understanding the adsorption on nanomaterials in aquatic environment: A review. Chemosphere. https://doi.org/10.1016/j.chemosphere.2020.128690

Ma, J.W., Lee, W.J., Bae, J.M., Jeong, K.S., Oh, S.H., Kim, J.H., Kim, S.H., Seo, J.H., Ahn, J.P., Kim, H., Cho, M.H., 2015. Carrier Mobility Enhancement of Tensile Strained Si and SiGe Nanowires via Surface Defect Engineering. Nano Letters 15, 7204–7210. https://doi.org/10.1021/acs.nanolett.5b01634

Madadrang, C.J., Kim, H.Y., Gao, G., Wang, N., Zhu, J., Feng, H., Gorring, M., Kasner, M.L., Hou, S., 2012. Adsorption behavior of EDTA-graphene oxide for Pb (II) removal. ACS Applied Materials and Interfaces 4, 1186–1193. https://doi.org/10.1021/am201645g

Maia, G.S., de Andrade, J.R., da Silva, M.G.C., Vieira, M.G.A., 2019a. Adsorption of diclofenac sodium onto commercial organoclay: Kinetic, equilibrium and thermodynamic study. Powder Technology 345, 140–150. https://doi.org/10.1016/j.powtec.2018.12.097

Maia, G.S., de Andrade, J.R., da Silva, M.G.C., Vieira, M.G.A., 2019b. Adsorption of diclofenac sodium onto commercial organoclay: Kinetic, equilibrium and thermodynamic study. Powder Technology 345, 140–150. https://doi.org/10.1016/j.powtec.2018.12.097

Maia, G.S., de Andrade, J.R., da Silva, M.G.C., Vieira, M.G.A., 2019c. Adsorption of diclofenac sodium onto commercial organoclay: Kinetic, equilibrium and thermodynamic study. Powder Technology 345, 140–150. https://doi.org/10.1016/j.powtec.2018.12.097

Maleki, A., Paydar, R., 2015. Graphene oxide-chitosan bionanocomposite: a highly efficient nanocatalyst for the one-pot three-component synthesis of trisubstituted imidazoles under solvent-free conditions. RSC Advances 5, 33177–33184. https://doi.org/10.1039/c5ra03355a

Mallakpour, S., Dinari, M., 2011. Preparation and characterization of new organoclays using natural amino acids and Cloisite Na+. Applied Clay Science 51, 353–359. https://doi.org/10.1016/j.clay.2010.12.028

Malwal, D., Gopinath, P., 2017. Silica Stabilized Magnetic-Chitosan Beads for Removal of Arsenic from Water. Colloids and Interface Science Communications 19, 14–19. https://doi.org/10.1016/j.colcom.2017.06.003

Mansouriieh, N., Sohrabi, M.R., Khosravi, M., 2016. Adsorption kinetics and thermodynamics of organophosphorus profenofos pesticide onto Fe/Ni bimetallic nanoparticles. International Journal of Environmental Science and Technology 13, 1393–1404. https://doi.org/10.1007/s13762-016-0960-0

Martins, J.T., Guimarães, C.H., Silva, P.M., Oliveira, R.L., Prediger, P., 2021. Enhanced removal of basic dye using carbon nitride/graphene oxide nanocomposites as adsorbents: high performance, recycling, and mechanism. Environmental Science

and Pollution Research 28, 3386–3405. https://doi.org/10.1007/s11356-020-10779-z

Marysková, M., Schaabová, M., Tománková, H., Novotny, V., Rysová, M., 2020. Wastewater Treatment by Novel Polyamide/Polyethylenimine Nanofibers with Immobilized Laccase. Water 12, 588.

Mathews, B.A.P., Zayas, I., 1989. Particle s i z e and shape e f f e c t s on adsorption r a t e parameters 115, 41–55.

McCusker, L.B., Liebau, F., Engelhardt, G., 2001. Nomenclature of structural and compositional characteristics of ordered microporous and mesoporous materials with inorganic hosts: (IUPAC recommendations 2001). Pure and Applied Chemistry 73, 381–394. https://doi.org/10.1351/pac200173020381

McLauchlin, A.R., Thomas, N.L., 2009. Preparation and thermal characterisation of poly(lactic acid) nanocomposites prepared from organoclays based on an amphoteric surfactant. Polymer Degradation and Stability 94, 868–872. https://doi.org/10.1016/j.polymdegradstab.2009.01.012

Menk, J. de J., do Nascimento, A.I.S., Leite, F.G., de Oliveira, R.A., Jozala, A.F., de Oliveira Junior, J.M., Chaud, M.V., Grotto, D., 2019. Biosorption of pharmaceutical products by mushroom stem waste. Chemosphere 237. https://doi.org/10.1016/j.chemosphere.2019.124515

Milanovic, M., Duric, L., Milosevic, N., Milic, N., 2021. Comprehensive insight into triclosan—from widespread occurrence to health outcomes occurrence. Environmental Science and Pollution Research.

Milonjić, S.K., 2007a. A consideration of the correct calculation of thermodynamic parameters of adsorption. Journal of the Serbian Chemical Society 72, 1363–1367. https://doi.org/10.2298/JSC0712363M

Milonjić, S.K., 2007b. A consideration of the correct calculation of thermodynamic parameters of adsorption. Journal of the Serbian Chemical Society 72, 1363–1367. https://doi.org/10.2298/JSC0712363M

Misaelides, P., 2011. Application of natural zeolites in environmental remediation: A short review. Microporous and Mesoporous Materials 144, 15–18. https://doi.org/10.1016/j.micromeso.2011.03.024

Mohseni Kafshgari, M., Tahermansouri, H., 2017. Development of a graphene oxide/chitosan nanocomposite for the removal of picric acid from aqueous solutions:

Study of sorption parameters. Colloids and Surfaces B: Biointerfaces 160, 671–681. https://doi.org/10.1016/j.colsurfb.2017.10.019

Montagner, C.C., Jardim, W.F., Von der Ohe, P.C., Umbuzeiro, G.A., 2014. Occurrence and potential risk of triclosan in freshwaters of São Paulo, Brazil-the need for regulatory actions. Environmental Science and Pollution Research 21, 1850–1858. https://doi.org/10.1007/s11356-013-2063-5

Montagner, C.C., Vidal, C., Acayaba, R.D., 2017. Contaminantes emergentes em matrizes aquáticas do Brasil: Cenário atual e aspectos analíticos, ecotoxicológicos e regulatórios. Quimica Nova 40, 1094–1110. https://doi.org/10.21577/0100-4042.20170091

Mordor Intelligence, 2021. BISPHENOL A (BPA) MARKET - GROWTH, TRENDS, COVID-19 IMPACT, AND FORECASTS (2022 - 2027).

Morrall, D., McAvoy, D., Schatowitz, B., Inauen, J., Jacob, M., Hauk, A., Eckhoff, W., 2004. A field study of triclosan loss rates in river water (Cibolo Creek, TX). Chemosphere 54, 653–660. https://doi.org/10.1016/j.chemosphere.2003.08.002

Motahharifar, N., Nasrollahzadeh, M., Taheri-Kafrani, A., Varma, R.S., Shokouhimehr, M., 2020. Magnetic chitosan-copper nanocomposite: A plant assembled catalyst for the synthesis of amino- and N-sulfonyl tetrazoles in eco-friendly media. Carbohydrate Polymers 232, 115819. https://doi.org/10.1016/j.carbpol.2019.115819

Mumit, M.A., Pal, T.K., Alam, M.A., Islam, M.A.A.A.A., Paul, S., Sheikh, M.C., 2020. DFT studies on vibrational and electronic spectra, HOMO–LUMO, MEP, HOMA, NBO and molecular docking analysis of benzyl-3-N-(2,4,5-trimethoxyphenylmethylene)hydrazinecarbodithioate. Journal of Molecular Structure 1220, 128715. https://doi.org/10.1016/j.molstruc.2020.128715

Narayanan, D.P., Gopalakrishnan, A., Yaakob, Z., Sugunan, S., Narayanan, B.N., 2020. A facile synthesis of clay – graphene oxide nanocomposite catalysts for solvent free multicomponent Biginelli reaction. Arabian Journal of Chemistry 13, 318–334. https://doi.org/10.1016/j.arabjc.2017.04.011

Nascimento, R.F., Melo, D.Q., Lima, A.C.A., Barros, A.L., Vidal, C.B., Raulino, G.S.C., 2014. Adsorção: Aspectos teóricos e aplicações ambientais, Adsorção aspescyos teóricos e aplicações ambientais.

Nasri, A., Mezni, A., Lafon, P.-A., Wahbi, A., Cubedo, N., Clair, P., Harrath, A.H., Beyrem, H., Rossel, M., Perrier, V., 2021. Ethinylestradiol (EE2) residues from birth

control pills impair nervoussystem development and swimming behavior of zebrafish larvae. Science of the Total Environment.

Nayara, T., Souza, V. De, Maria, S., Carvalho, L. De, Gurgel, Melissa, Vieira, A., Gurgel, Meuris, Barros, S., 2018. Applied Surface Science Adsorption of basic dyes onto activated carbon : Experimental and theoretical investigation of chemical reactivity of basic dyes using DFT-based descriptors. Applied Surface Science 448, 662–670. https://doi.org/10.1016/j.apsusc.2018.04.087

Nazraz, M., Yamini, Y., Asiabi, H., 2019. Chitosan-based sorbent for efficient removal and extraction of ciprofloxacin and norfloxacin from aqueous solutions. Microchimica Acta 186. https://doi.org/10.1007/s00604-019-3563-x

Neves, T. de F., Assano, P.K., Sabino, L.R., Nunes, W.B., Prediger, P., 2020. Influence of Adsorbent/Adsorbate Interactions on the Removal of Cationic Surfactants from Water by Graphene Oxide. Water, Air, and Soil Pollution 231. https://doi.org/10.1007/s11270-020-04669-w

Nishi, I., Kawakami, T., Onodera, S., 2008. Monitoring of triclosan in the surface water of the Tone Canal, Japan. Bulletin of Environmental Contamination and Toxicology 80, 163–166. https://doi.org/10.1007/s00128-007-9338-9

Novoselov, K.S., 2011. Nobel Lecture: Graphene: Materials in the Flatland. Reviews of Modern Physics 83, 837–849. https://doi.org/10.1103/RevModPhys.83.837

Nowak, S., Lafon, S., Caquineau, S., Journet, E., Laurent, B., 2018. Quantitative study of the mineralogical composition of mineral dust aerosols by X-ray diffraction. Talanta 186, 133–139. https://doi.org/10.1016/j.talanta.2018.03.059

Olewnik-Kruszkowska, E., Gierszewska, M., Jakubowska, E., Tarach, I., Sedlarik, V., Pummerova, M., 2019. Antibacterial films based on PVA and PVA-chitosan modified with poly(hexamethylene guanidine). Polymers 11. https://doi.org/10.3390/polym11122093

Oliveira, L.C.A., Rios, R.V.R.A., Fabris, J.D., Sapag, K., Garg, V.K., Lago, R.M., 2003a. Clay-iron oxide magnetic composites for the adsorption of contaminants in water. Applied Clay Science 22, 169–177. https://doi.org/10.1016/S0169-1317(02)00156-4

Oliveira, L.C.A., Rios, R.V.R.A., Fabris, J.D., Sapag, K., Garg, V.K., Lago, R.M., 2003b. Clay-iron oxide magnetic composites for the adsorption of contaminants in water. Applied Clay Science 22, 169–177. https://doi.org/10.1016/S0169-1317(02)00156-4

Oliveira, M.F., da Silva, M.G.C., Vieira, M.G.A., 2019. Equilibrium and kinetic studies of caffeine adsorption from aqueous solutions on thermally modified Verde-lodo bentonite. Applied Clay Science 168, 366–373. https://doi.org/10.1016/j.clay.2018.12.011

Parida, V.K., Saidulu, D., Majumder, A., Srivastava, A., Gupta, B., Gupta, A.K., 2021a. Emerging contaminants in wastewater: A critical review on occurrence, existing legislations, risk assessment, and sustainable treatment alternatives. Journal of Environmental Chemical Engineering. https://doi.org/10.1016/j.jece.2021.105966

Parida, V.K., Saidulu, D., Majumder, A., Srivastava, A., Gupta, B., Gupta, A.K., 2021b. Emerging contaminants in wastewater: A critical review on occurrence, existing legislations, risk assessment, and sustainable treatment alternatives. Journal of Environmental Chemical Engineering 9, 105966. https://doi.org/10.1016/j.jece.2021.105966

Park, Y., Ayoko, G.A., Frost, R.L., 2011. Application of organoclays for the adsorption of recalcitrant organic molecules from aqueous media. Journal of Colloid and Interface Science 354, 292–305. https://doi.org/10.1016/j.jcis.2010.09.068

Park, Y., Sun, Z., Ayoko, G.A., Frost, R.L., 2014. Bisphenol A sorption by organo-montmorillonite: Implications for the removal of organic contaminants from water 107, 249–256.

Parladé, E., Hom-Diaz, A., Blánquez, P., Martínez-Alonso, M., Vicent, T., Gaju, N., 2018. Effect of cultivation conditions on B-estradiol removal in laboratory and pilot-plant photobioreactors by an algal-bacterial consortium treating urban wastewater. Water Research 137, 86–96. https://doi.org/10.1016/j.watres.2018.02.060

Pelekani, C., Snoeyink, V.L., 1999. Competitive adsorption in natural water: Role of activated carbon pore size. Water Research 33, 1209–1219. https://doi.org/10.1016/S0043-1354(98)00329-7

Peng, W., Li, H., Liu, Y., Song, S., 2017. A review on heavy metal ions adsorption from water by graphene oxide and its composites. Journal of Molecular Liquids 230, 496–504. https://doi.org/10.1016/j.molliq.2017.01.064

Pérez-Guardiola, A., Pérez-Jiménez, A.J., Sancho-García, J.C., 2017. Studying physisorption processes and molecular friction of cycloparaphenylene molecules on graphene nano-sized flakes: Role of π···π and CH···π interactions. Molecular Systems Design and Engineering 2, 253–262. https://doi.org/10.1039/c7me00024c

Phuekphong, A.F., Imwiset, K.J., Ogawa, M., 2020. Organically modified bentonite as an efficient and reusable adsorbent for triclosan removal from water. Langmuir. https://doi.org/10.1021/acs.langmuir.0c00407

Piccin, J.S., Cadaval, T.R.S.A., de Pinto, L.A.A., Dotto, G.L., 2017. Adsorption isotherms in liquid phase: Experimental, modeling, and interpretations, in: Adsorption Processes for Water Treatment and Purification. Springer International Publishing, pp. 19–51. https://doi.org/10.1007/978-3-319-58136-1_2

Poirier, J.C., Cahoreau, C., Combarnous, Y., 2006. Cross-Inhibitions of Human Chorionic Gonadotropin (hCG) and Ethynyl-Estradiol (EE2) at Pico-Molar Concentrations on Mouse Leydig Tumor Cells (mLTC) Progesterone Secretion. Epidemiology 17, 376.

Pojana, G., Gomiero, A., Jonkers, N., Marcomini, A., 2007. Natural and synthetic endocrine disrupting compounds (EDCs) in water, sediment and biota of a coastal lagoon. Environment International 33, 929–936. https://doi.org/10.1016/j.envint.2007.05.003

Prediger, P., Cheminski, T., de Figueiredo Neves, T., Nunes, W.B., Sabino, L., Picone, C.S.F., Oliveira, R.L., Correia, C.R.D., 2018. Graphene oxide nanomaterials for the removal of non-ionic surfactant from water. Journal of Environmental Chemical Engineering 6, 1536–1545. https://doi.org/10.1016/j.jece.2018.01.072

Prokić, D., Vukčević, M., Kalijadis, A., Maletić, M., Babić, B., Đurkić, T., 2020. Removal of Estrone, 17β-Estradiol, and 17α-Ethinylestradiol from Water by Adsorption onto Chemically Modified Activated Carbon Cloths. Fibers and Polymers 21, 2263–2274. https://doi.org/10.1007/s12221-020-9758-2

Racar, M, Dolar, D., Karadadic, K., Cavarovic, N., Glumac, N., Asperger, D., Kosutic, K., 2020. Challenges of municipal wastewater reclamation for irrigation by MBR and NF/RO: Physico-chemical and microbiological parameters, and emerging contaminantsirrigation. Science of the Total Environment 722, 137959.

Racar, M., Dolar, D., Karadakić, K., Čavarović, N., Glumac, N., Ašperger, D., Košutić, K., 2020. Challenges of municipal wastewater reclamation for irrigation by MBR and NF/RO: Physico-chemical and microbiological parameters, and emerging contaminants. Science of the Total Environment 722. https://doi.org/10.1016/j.scitotenv.2020.137959

Rad, L.R., Anbia, M., 2021. Zeolite-based composites for the adsorption of toxic matters from water: A review. Journal of Environmental Chemical Engineering 9. https://doi.org/10.1016/j.jece.2021.106088

Ramaswamy, B.R., Shanmugam, G., Velu, G., Rengarajan, B., Larsson, D.G.J., 2011. GC-MS analysis and ecotoxicological risk assessment of triclosan, carbamazepine and parabens in Indian rivers. Journal of Hazardous Materials 186, 1586–1593. https://doi.org/10.1016/j.jhazmat.2010.12.037

Rathi, B.S., Kumar, P.S., 2021. Application of adsorption process for effective removal of emerging contaminants from water and wastewater. Environmental Pollution 280, 116995. https://doi.org/10.1016/j.envpol.2021.116995

Regti, A., Ben, H., Ayouchia, E., Rachid, M., Eddine, S., Anane, H., El, M., 2016. Applied Surface Science Experimental and theoretical study using DFT method for the competitive adsorption of two cationic dyes from wastewaters. Applied Surface Science 390, 311–319. https://doi.org/10.1016/j.apsusc.2016.08.059

Reichenberg, D., 1953. Properties of Ion-Exchange Resins in Relation to their Structure. III. Kinetics of Exchange. Journal of the American Chemical Society 75, 589–597. https://doi.org/10.1021/ja01099a022

Rempel, A., Gutkoski, J.P., Nazari, M.T., Biolchi, G.N., Cavanhi, V.A.F., Treichel, H., Colla, L.M., 2021. Current advances in microalgae-based bioremediation and other technologies for emerging contaminants treatment. Science of the Total Environment 772, 144918. https://doi.org/10.1016/j.scitotenv.2020.144918

Ren, X., Chen, C., Nagatsu, M., Wang, X., 2011. Carbon nanotubes as adsorbents in environmental pollution management: A review. Chemical Engineering Journal 170, 395–410. https://doi.org/10.1016/j.cej.2010.08.045

Resende, J., Andrade, D., Gurgel, Melissa, Vieira, A., Gurgel, Meuris, 2020. Oxidative degradation of pharmaceutical losartan potassium with N-doped hierarchical porous carbon and peroxymonosulfate. Chemical Engineering Journal 382, 122971. https://doi.org/10.1016/j.cej.2019.122971

Rivera-Utrilla, J., Sánchez-Polo, M., Ferro-García, M.Á., Prados-Joya, G., Ocampo-Pérez, R., 2013. Pharmaceuticals as emerging contaminants and their removal from water. A review. Chemosphere 93, 1268–1287. https://doi.org/10.1016/j.chemosphere.2013.07.059

Rivera-utrilla, J., Sánchez-polo, M., Ferro-garcía, M.Á., Prados-joya, G., Ocampo-Pérez, R., 2013. Pharmaceuticals as emerging contaminants and their removal from water . A review. Chemosphere 93, 1268–1287.

Rodriguez-Narvaez, O.M., Peralta-Hernandez, J.M., Goonetilleke, A., Bandala, E.R., 2017. Treatment technologies for emerging contaminants in water: A review. Chemical Engineering Journal 323, 361–380. https://doi.org/10.1016/j.cej.2017.04.106

Rojas, S., Navarro, J.A.R., Horcajada, P., 2021. Metal-organic frameworks for the removal of the emerging contaminant atenolol under real conditions. Dalton Transactions 50, 2493–2500. https://doi.org/10.1039/d0dt03637d

Rosenfeldt, E.J., Chen, P.J., Kullman, S., Linden, K.G., 2007. Destruction of estrogenic activity in water using UV advanced oxidation. Science of the Total Environment 377, 105–113. https://doi.org/10.1016/j.scitotenv.2007.01.096

Rotaru, I., Varvara, S., Gaina, L., Maria, L., 2014. Applied Surface Science Antibacterial drugs as corrosion inhibitors for bronze surfaces in acidic solutions. Applied Surface Science 321, 188–196. https://doi.org/10.1016/j.apsusc.2014.09.201

Rudder, J. De, Wiele, T. Van De, Dhooge, W., Comhaire, F., Verstraete, W., 2004. Advanced water treatment with manganese oxide for the removal of 17 a - ethynylestradiol (EE2) 38, 184–192. https://doi.org/10.1016/j.watres.2003.09.018

Ruiz, B., Cabrita, I., Mestre, A.S., Parra, J.B., Pires, J., Carvalho, A.P., Ania, C.O., 2010. Surface heterogeneity effects of activated carbons on the kinetics of paracetamol removal from aqueous solution. Applied Surface Science 256, 5171–5175. https://doi.org/10.1016/j.apsusc.2009.12.086

Sáaedi, A., Yousefi, R., Jamali-Sheini, F., Zak, A.K., Cheraghizade, M., Mahmoudian, M.R., Baghchesara, M.A., Dezaki, A.S., 2016. XPS studies and photocurrent applications of alkali-metals-doped ZnO nanoparticles under visible illumination conditions. Physica E: Low-Dimensional Systems and Nanostructures 79, 113–118. https://doi.org/10.1016/j.physe.2015.12.002

Saha, P., Chowdhury, S., 2011. Insight Into Adsorption Thermodynamics, in: Thermodynamics. pp. 349–363.

Saheed, I.O., Oh, W. da, Suah, F.B.M., 2021. Chitosan modifications for adsorption of pollutants – A review. Journal of Hazardous Materials. https://doi.org/10.1016/j.jhazmat.2020.124889

Sahoo, G., Sarkar, N., Swain, S.K., 2018. The effect of reduced graphene oxide intercalated hybrid organoclay on the dielectric properties of polyvinylidene fluoride nanocomposite films. Applied Clay Science 162, 69–82. https://doi.org/10.1016/j.clay.2018.05.008

Sahu, S., Pahi, S., Tripathy, S., Singh, S.K., Behera, A., Sahu, U.K., Patel, R.K., 2020. Adsorption of methylene blue on chemically modified lychee seed biochar: Dynamic, equilibrium, and thermodynamic study. Journal of Molecular Liquids 315. https://doi.org/10.1016/j.molliq.2020.113743

Salahuddin, N.A., EL-Daly, H.A., el Sharkawy, R.G., Nasr, B.T., 2018. Synthesis and efficacy of PPy/CS/GO nanocomposites for adsorption of ponceau 4R dye, Polymer. Elsevier Ltd. https://doi.org/10.1016/j.polymer.2018.04.053

Sauvé, S., Desrosiers, M., 2014a. A review of what is an emerging contaminant. Chemistry Central Journal 8, 1–7. https://doi.org/10.1186/1752-153X-8-15

Sauvé, S., Desrosiers, M., 2014b. A review of what is an emerging contaminant, Chemistry Central Journal.

Schirmer, W.N., 2007. Avaliação do desempenho de nanotubos de carbono "cup-stacked" na remoção de compostos orgânicos voláteis (COV) de correntes gasosas 91.

Sekar, M., Sakthi, V., Rengaraj, S., 2004. Kinetics and equilibrium adsorption study of lead(II) onto activated carbon prepared from coconut shell. Journal of Colloid and Interface Science 279, 307–313. https://doi.org/10.1016/j.jcis.2004.06.042

Sekulic, M.T., Boskovic, N., Slavkovic, A., Garunovic, J., Kolakovic, S., Pap, S., 2019. Surface functionalised adsorbent for emerging pharmaceutical removal: Adsorption performance and mechanisms. Process Safety and Environmental Protection 125, 50–63. https://doi.org/10.1016/j.psep.2019.03.007

Shahid, M.K., Kashif, A., Fuwad, A., Choi, Y., 2021. Current advances in treatment technologies for removal of emerging contaminants from water – A critical review. Coordination Chemistry Reviews. https://doi.org/10.1016/j.ccr.2021.213993

Shang, J., Guo, Y., He, D., Qu, W., Tang, Y., Zhou, L., Zhu, R., 2021. A novel graphene oxide-dicationic ionic liquid composite for Cr(VI) adsorption from aqueous solutions. Journal of Hazardous Materials 416. https://doi.org/10.1016/j.jhazmat.2021.125706

Sharma, J., Mishra, I.M., Kumar, V., 2016. Mechanistic study of photo-oxidation of Bisphenol-A (BPA) with hydrogen peroxide (H2O2) and sodium persulfate (SPS).

Journal of Environmental Management 166, 12–22. https://doi.org/10.1016/j.jenvman.2015.09.043

Sheela, N.R., Muthu, S., Sampathkrishnan, S., 2014. Molecular orbital studies (hardness, chemical potential and electrophilicity), vibrational investigation and theoretical NBO analysis of 4-4′-(1H-1,2,4-triazol-1-yl methylene) dibenzonitrile based on abinitio and DFT methods. Spectrochimica Acta - Part A: Molecular and Biomolecular Spectroscopy 120, 237–251. https://doi.org/10.1016/j.saa.2013.10.007

Shen, T., Gao, M., 2019. Gemini surfactant modified organo-clays for removal of organic pollutants from water: A review. Chemical Engineering Journal 375, 121910. https://doi.org/10.1016/j.cej.2019.121910

Silva, T.L. da, Silva, M.G.C. da, Vieira, M.G.A., 2021. Palladium adsorption on natural polymeric sericin-alginate particles crosslinked by polyethylene glycol diglycidyl ether. Journal of Environmental Chemical Engineering 9. https://doi.org/10.1016/j.jece.2021.105617

Silva, A.R. V, Ferreira, H.C., 2008. Esmectitas organofílicas: conceitos, estruturas, propriedades, síntese, usos industriais e produtores/fornecedores nacionais e internacionais. Revista Eletrônica de Materiais e Processos 33, 1–11.

Silva, V.A.J., Andrade, P.L., Silva, M.P.C., Bustamante, A.D., de Los Santos Valladares, L., Albino Aguiar, J., 2013. Synthesis and characterization of Fe3O4 nanoparticles coated with fucan polysaccharides. Journal of Magnetism and Magnetic Materials 343, 138–143. https://doi.org/10.1016/j.jmmm.2013.04.062

Singer, H., Müller, S., Tixier, C., Pillonel, L., 2002. Triclosan: Occurrence and fate of a widely used biocide in the aquatic environment: Field measurements in wastewater treatment plants, surface waters, and lake sediments. Environmental Science and Technology 36, 4998–5004. https://doi.org/10.1021/es025750i

Site, A.D., 2001. Factors Affecting Sorption of Organic Compounds in Natural Sorbent/Water Systems and Sorption Coefficients for Selected Pollutants. A Review. Journal of Physical and Chemical Reference Data 187.

Sivaranjanee, R., Kumar, P.S., 2021. A review on remedial measures for effective separation of emerging contaminants from wastewater. Environmental Technology and Innovation. https://doi.org/10.1016/j.eti.2021.101741

Sobhanardakani, S., Zandipak, R., 2018. Cerium dioxide nanoparticles decorated on CuFe2O4 nanofibers as an effective adsorbent for removal of estrogenic

contaminants (bisphenol A and 17-α ethinylestradiol) from water. Separation Science and Technology (Philadelphia) 53, 2339–2351. https://doi.org/10.1080/01496395.2018.1457053

Soboleva, T., Zhao, X., Malek, K., Xie, Z., Navessin, T., Holdcroft, S., 2010. On the micro-, meso-, and macroporous structures of polymer electrolyte membrane fuel cell catalyst layers. ACS Applied Materials and Interfaces 2, 375–384. https://doi.org/10.1021/am900600y

Sodré, F.F., Montagner, C.C., Locatelli, M.A.F., Jardim, W.F., 2007. Ocorrência de Interferentes Endócrinos e Produtos Farmacêuticos em Águas Superficiais da Região de Campinas (SP, Brasil). Journal of the Brazilian Society of Ecotoxicology 2, 187–196. https://doi.org/10.5132/jbse.2007.02.012

Sodré, F.F., Pescara, I.C., Montagner, C.C., Jardim, W.F., 2010. Assessing selected estrogens and xenoestrogens in Brazilian surface waters by liquid chromatography-tandem mass spectrometry. Microchemical Journal 96, 92–98. https://doi.org/10.1016/j.microc.2010.02.012

Song, T., Tian, W., Qiao, K., Zhao, J., Chu, M., Du, Z., Wang, L., Xie, W., 2021. Adsorption Behaviors of Polycyclic Aromatic Hydrocarbons and Oxygen Derivatives in Wastewater on N-Doped Reduced Graphene Oxide. Separation and Purification Technology 254, 117565. https://doi.org/10.1016/j.seppur.2020.117565

Song, X., Zhang, Y., Yan, C., Jiang, W., Chang, C., 2013. The Langmuir monolayer adsorption model of organic matter into effective pores in activated carbon. Journal of Colloid and Interface Science 389, 213–219. https://doi.org/10.1016/j.jcis.2012.08.060

Sophia A., C., Lima, E.C., 2018. Removal of emerging contaminants from the environment by adsorption. Ecotoxicology and Environmental Safety 150, 1–17. https://doi.org/10.1016/j.ecoenv.2017.12.026

Sophia, C.A., Lima, E.C., 2018. Removal of emerging contaminants from the environment by adsorption. Ecotoxicology and Environmental Safety 150, 1–17.

Speridião, D.D.C.A., dos Santos, O.A.A., de Almeida Neto, A.F., Vieira, M.G.A., 2014. Characterization of spectrogel organoclay used to adsorption of petroleum derivatives. Materials Science Forum 798–799, 558–563. https://doi.org/10.4028/www.scientific.net/MSF.798-799.558

Stachel, B., Ehrhorn, U., Heemken, O.P., Lepom, P., Reincke, H., Sawal, G., Theobald, N., 2003. Xenoestrogens in the River Elbe and its tributaries. Environmental Pollution 124, 497–507. https://doi.org/10.1016/S0269-7491(02)00483-9

Starling, M.C.V.M., Souza, P.P., Le Person, A., Amorim, C.C., Criquet, J., 2019. Intensification of UV-C treatment to remove emerging contaminants by UV-C/H2O2 and UV-C/S2O82−: Susceptibility to photolysis and investigation of acute toxicity. Chemical Engineering Journal 376, 120856. https://doi.org/10.1016/j.cej.2019.01.135

Taher, F.A., Kamal, F.H., Badawy, N.A., Shrshr, A.E., 2018. Hierarchical magnetic chitosan graphene oxide 3D nanostructure as highly effective adsorbent. Materials Research Bulletin 97, 361–368.

Tan, X. fei, Liu, Y. guo, Gu, Y. ling, Xu, Y., Zeng, G. ming, Hu, X. jiang, Liu, Shao bo, Wang, X., Liu, Si mian, Li, J., 2016. Biochar-based nano-composites for the decontamination of wastewater: A review. Bioresource Technology 212, 318–333. https://doi.org/10.1016/j.biortech.2016.04.093

Tang, L., Xie, Z., Dong, H., Fan, C., Zhou, Y., Wang, J., Zeng, G., Deng, Y., Wang, J., Wei, X., 2016. Removal of bisphenol A by iron nanoparticles doped magnetic ordered mesoporous carbon. https://doi.org/10.1039/C5RA27710H

Tang, Z., Liu, Z. hua, Wang, H., Dang, Z., Liu, Y., 2021a. Occurrence and removal of 17α-ethynylestradiol (EE2) in municipal wastewater treatment plants: Current status and challenges. Chemosphere. https://doi.org/10.1016/j.chemosphere.2021.129551

Tang, Z., Liu, Z. hua, Wang, H., Dang, Z., Liu, Y., 2021b. A review of 17α-ethynylestradiol (EE2) in surface water across 32 countries: Sources, concentrations, and potential estrogenic effects. Journal of Environmental Management 292. https://doi.org/10.1016/j.jenvman.2021.112804

Tang, Z., Liu, Z., Wang, H., Dang, Z., Liu, Y., 2021c. Occurrence and removal of 17a-ethynylestradiol (EE2) in municipal wastewater treatment plants: Current status and challenges. Chemosphere 271.

Taylor, P., Ganguly, S., Dana, K., Mukhopadhyay, T.K., Parya, T.K., Ghatak, S., Ganguly, S., Dana, K., Mukhopadhyay, T.K., Parya, T.K., Ghatak, S., 2013. Organophilic Nano Clay : A Comprehensive Review Organophilic Nano Clay : A Comprehensive Review. Transactions of the Indian Ceramic Society 37–41.

Ten Hulscher, T.E.M., Cornelissen, G., 1996. Effect of temperature on sorption equilibrium and sorption kinetics of organic micropollutants - A review. Chemosphere 32, 609–626. https://doi.org/10.1016/0045-6535(95)00345-2

Thakur, K., Kandasubramanian, B., 2019. Graphene and Graphene Oxide-Based Composites for Removal of Organic Pollutants: A Review. Journal of Chemical and Engineering Data 64, 833–867. https://doi.org/10.1021/acs.jced.8b01057

Thommes, M., Kaneko, K., Neimark, A. V., Olivier, J.P., Rodriguez-Reinoso, F., Rouquerol, J., Sing, K.S.W., 2015. Physisorption of gases, with special reference to the evaluation of surface area and pore size distribution (IUPAC Technical Report). Pure and Applied Chemistry 87, 1051–1069. https://doi.org/10.1515/pac-2014-1117

Tong, Y., Mayer, B.K., McNamara, P.J., 2016. Triclosan adsorption using wastewater biosolids-derived biochar. Environmental Science: Water Research & Technology 761–768. https://doi.org/10.1039/C6EW00127K

Tran, H.N., You, S.J., Chao, H.P., 2016. Thermodynamic parameters of cadmium adsorption onto orange peel calculated from various methods: A comparison study. Journal of Environmental Chemical Engineering 4, 2671–2682. https://doi.org/10.1016/j.jece.2016.05.009

Transformation Products of Emerging Contaminants in the Environment, 2014. , Transformation Products of Emerging Contaminants in the Environment.

Treybal, R.E., 1980. Mass - Transfer Operations.

Tsai, W.T., 2006. Human health risk on environmental exposure to bisphenol-A: A review. Journal of Environmental Science and Health - Part C Environmental Carcinogenesis and Ecotoxicology Reviews 24, 225–255. https://doi.org/10.1080/10590500600936482

Vakili, M., Rafatullah, M., Salamatinia, B., Abdullah, A.Z., Ibrahim, M.H., Tan, K.B., Gholami, Z., Amouzgar, P., 2014. Application of chitosan and its derivatives as adsorbents for dye removal from water and wastewater: A review. Carbohydrate Polymers 113, 115–130. https://doi.org/10.1016/j.carbpol.2014.07.007

Varsha, M., Kumar, P.S., Rathi, B.S., 2022. A review on recent trends in the removal of emerging contaminants from aquatic environment using low-cost adsorbents. Chemosphere 287.

Viegas, R.M.C., Campinas, M., Costa, H., Rosa, M.J., 2014. How do the HSDM and Boyd's model compare for estimating intraparticle diffusion coefficients in

adsorption processes. Adsorption 20, 737–746. https://doi.org/10.1007/s10450-014-9617-9

Vieira, W.T., Bispo, M.D., de Melo Farias, S., de Almeida, A.D.S.V., da Silva, T.L., Vieira, M.G.A., Soletti, J.I., Balliano, T.L., 2021. Activated carbon from macauba endocarp (Acrocomia aculeate) for removal of atrazine: Experimental and theoretical investigation using descriptors based on DFT. Journal of Environmental Chemical Engineering 9. https://doi.org/10.1016/j.jece.2021.105155

Vigneresse, J.L., 2018. Variations in chemical descriptors during reactions. Chemical Physics Letters 706, 577–585. https://doi.org/10.1016/j.cplett.2018.05.032

Villaverde-De-Sáa, E., González-Mariño, I., Quintana, J.B., Rodil, R., Rodríguez, I., Cela, R., 2010. In-sample acetylation-non-porous membrane-assisted liquid-liquid extraction for the determination of parabens and triclosan in water samples. Analytical and Bioanalytical Chemistry 397, 2559–2568. https://doi.org/10.1007/s00216-010-3789-2

Wang, F., Zhang, Q., Sha, W., Wang, X., Miao, M., Wang, Z.L., Li, Y., 2021. The adsorption of endocrine-disrupting compounds (EDCs) on carbon nanotubes: effects of algal extracellular organic matter (EOM). Journal of Nanoparticle Research 23. https://doi.org/10.1007/s11051-021-05215-3

Wang, L., Ying, G.G., Zhao, J.L., Liu, S., Yang, B., Zhou, L.J., Tao, R., Su, H.C., 2011. Assessing estrogenic activity in surface water and sediment of the Liao River system in northeast China using combined chemical and biological tools. Environmental Pollution 159, 148–156. https://doi.org/10.1016/j.envpol.2010.09.017

Wang, S., Zhai, Y.Y., Gao, Q., Luo, W.J., Xia, H., Zhou, C.G., 2014. Highly efficient removal of acid red 18 from aqueous solution by magnetically retrievable chitosan/carbon nanotube: Batch study, isotherms, kinetics, and thermodynamics. Journal of Chemical and Engineering Data 59, 39–51. https://doi.org/10.1021/je400700c

Wang, W., Zhu, Z., Zhang, M., Wang, S., Qu, C., 2020. Synthesis of a novel magnetic multi-amine decorated resin for the adsorption of tetracycline and copper. Journal of the Taiwan Institute of Chemical Engineers 106, 130–137. https://doi.org/10.1016/j.jtice.2019.10.017

Wang, X., Huang, P., Ma, X., Du, X., Lu, X., 2018. Magnetic Mesoporous Molecularly Imprinted Polymers Based on Surface Precipitation Polymerization for Selective Enrichment of Triclosan and Triclocarban. Journal ofChromatography A.

Wang, X., Song, L., Yang, H., Xing, W., Kandola, B., Hu, Y., 2012. Simultaneous reduction and surface functionalization of graphene oxide with POSS for reducing fire hazards in epoxy composites. Journal of Materials Chemistry 22, 22037–22043. https://doi.org/10.1039/c2jm35479a

Wang, Y., Li, L.L., Luo, C., Wang, X., Duan, H., 2016. Removal of Pb2+ from water environment using a novel magnetic chitosan/graphene oxide imprinted Pb2+. International Journal of Biological Macromolecules 86, 505–511. https://doi.org/10.1016/j.ijbiomac.2016.01.035

Wang, Y., Liang, W., 2021. Occurrence, Toxicity, and Removal Methods of Triclosan: a Timely Review. Current Pollution Reports. https://doi.org/10.1007/s40726-021-00173-9/Published

Wang, Y., Yang, Q., Dong, J., Huang, H., 2018. Competitive adsorption of PPCP and humic substances by carbon nanotube membranes: Effects of coagulation and PPCP properties. Science of the Total Environment 619–620, 352–359. https://doi.org/10.1016/j.scitotenv.2017.11.117

Weber, W., Morris, J., 1963. Kinetics of adsorption on carbon from solution. Journal of the Sanitary Engineering Division 89, 31–60.

Wells, M.J.M., Morse, A., Bell, K.Y., Pellegrin, M.-L., Fono, L.J., 2009. Emerging Pollutants, Water Environment Research. https://doi.org/10.2175/106143009x12445568400854

Westrup, J.L., Bertoldi, C., Cercena, R., Dal-Bó, A.G., Soares, R.M.D., Fernandes, A.N., 2021. Adsorption of endocrine disrupting compounds from aqueous solution in poly(butyleneadipate-co-terephthalate) electrospun microfibers. Colloids and Surfaces A: Physicochemical and Engineering Aspects 611. https://doi.org/10.1016/j.colsurfa.2020.125800

Williams, M., Kookana, R.S., Mehta, A., Yadav, S.K., Tailor, B.L., Maheshwari, B., 2019. Emerging contaminants in a river receiving untreated wastewater from an Indian urban centre. Science of the Total Environment 647, 1256–1265. https://doi.org/10.1016/j.scitotenv.2018.08.084

Wong, S., Lim, Y., Ngadi, N., Mat, R., Hassan, O., Inuwa, I.M., Mohamed, N.B., Low, J.H., 2018. Removal of acetaminophen by activated carbon synthesized from spent tea leaves: equilibrium, kinetics and thermodynamics studies. Powder Technology 338, 878–886. https://doi.org/10.1016/j.powtec.2018.07.075

Wu, F.C., Tseng, R.L., Juang, R.S., 2009. Initial behavior of intraparticle diffusion model used in the description of adsorption kinetics. Chemical Engineering Journal 153, 1–8. https://doi.org/10.1016/j.cej.2009.04.042

Wu, Q., Lam, J.C.W., Kwok, K.Y., Tsui, M.M.P., Lam, P.K.S., 2017. Occurrence and fate of endogenous steroid hormones, alkylphenol ethoxylates, bisphenol A and phthalates in municipal sewage treatment systems. Journal of Environmental Sciences 61, 49–58.

Wu, S.-T., 1975. A Rigorous Justification of the Point B Method for Determination of Monolayer Capacity from a Type II Adsorption Isotherm, Progress of Theoretical Physics.

Wurzer, C., Mašek, O., 2021. Feedstock doping using iron rich waste increases the pyrolysis gas yield and adsorption performance of magnetic biochar for emerging contaminants. Bioresource Technology 321. https://doi.org/10.1016/j.biortech.2020.124473

Xiong, J.Q., Kurade, M.B., Patil, D. v., Jang, M., Paeng, K.J., Jeon, B.H., 2017. Biodegradation and metabolic fate of levofloxacin via a freshwater green alga, Scenedesmus obliquus in synthetic saline wastewater. Algal Research 25, 54–61. https://doi.org/10.1016/j.algal.2017.04.012

Xiong, Q., Hu, L.X., Liu, Y.S., Zhao, J.L., He, L.Y., Ying, G.G., 2021. Microalgae-based technology for antibiotics removal: From mechanisms to application of innovational hybrid systems. Environment International 155, 106594. https://doi.org/10.1016/j.envint.2021.106594

Xu, J., Wang, L., Zhu, Y., 2012. Decontamination of bisphenol A from aqueous solution by graphene adsorption. Langmuir 28, 8418–8425. https://doi.org/10.1021/la301476p

Xu, L., Teng, J., Li, L., Huang, H.D., Xu, J.Z., Li, Y., Ren, P.G., Zhong, G.J., Li, Z.M., 2019. Hydrophobic Graphene Oxide as a Promising Barrier of Water Vapor for Regenerated Cellulose Nanocomposite Films. ACS Omega 4, 509–517. https://doi.org/10.1021/acsomega.8b02866

Yang, S., Feng, X., Müllen, K., 2011. Sandwich-like, graphene-based titania nanosheets with high surface area for fast lithium storage. Advanced Materials 23, 3575–3579. https://doi.org/10.1002/adma.201101599

Yang, S., Hai, F.I., Nghiem, L.D., Roddick, F., Price, W.E., 2013. Removal of trace organic contaminants by nitrifying activated sludge and whole-cell and crude

enzyme extract of Trametes versicolor. Water Science and Technology 67, 1216–1223. https://doi.org/10.2166/wst.2013.684

Yang, W., Pan, M., Huang, C., Zhao, Z., Wang, J., Zeng, H., 2021. Graphene oxide-based noble-metal nanoparticles composites for environmental application. Composites Communications 24. https://doi.org/10.1016/j.coco.2021.100645

Yang, Y., Li, J., Lu, K., Shi, H., Gao, S., 2017. Transformation of 17A-ethinylestradiol by simultaneous photo-enzymatic process in Humic water. Chemosphere 178, 432–438. https://doi.org/10.1016/j.chemosphere.2017.03.077

Yankovych, H., Melnyk, I., Václavíková, M., 2021. Understanding of mechanisms of organohalogens removal onto mesoporous granular activated carbon with acid-base properties. Microporous and Mesoporous Materials 317. https://doi.org/10.1016/j.micromeso.2021.110974

Yap, H.C., Pang, Y.L., Lim, S., Abdullah, A.Z., Ong, H.C., Wu, C.H., 2019a. A comprehensive review on state-of-the-art photo-, sono-, and sonophotocatalytic treatments to degrade emerging contaminants. International Journal of Environmental Science and Technology 16, 601–628. https://doi.org/10.1007/s13762-018-1961-y

Yap, H.C., Pang, Y.L., Lim, S., Abdullah, A.Z., Ong, H.C., Wu, C.H., 2019b. A comprehensive review on state-of-the-art photo-, sono-, and sonophotocatalytic treatments to degrade emerging contaminants. International Journal of Environmental Science and Technology 16, 601–628. https://doi.org/10.1007/s13762-018-1961-y

Ying, G.G., Kookana, R.S., 2007. Triclosan in wastewaters and biosolids from Australian wastewater treatment plants. Environment International 33, 199–205. https://doi.org/10.1016/j.envint.2006.09.008

Ying, G.G., Kookana, R.S., Kumar, A., Mortimer, M., 2009. Occurrence and implications of estrogens and xenoestrogens in sewage effluents and receiving waters from South East Queensland. Science of the Total Environment 407, 5147–5155. https://doi.org/10.1016/j.scitotenv.2009.06.002

Zafra, A., Del Olmo, M., Suárez, B., Hontoria, E., Navalón, A., Vílchez, J.L., 2003. Gas chromatographic-mass spectrometric method for the determination of bisphenol A and its chlorinated derivatives in urban wastewater. Water Research 37, 735–742. https://doi.org/10.1016/S0043-1354(02)00413-X

Zambianchi, M., Durso, M., Liscio, A., Treossi, E., Bettini, C., Capobianco, M.L., Aluigi, A., Kovtun, A., Ruani, G., Corticelli, F., Brucale, M., Palermo, V., Navacchia, M.L., Melucci, M., 2017. Graphene oxide doped polysulfone membrane adsorbers for the removal of organic contaminants from water. Chemical Engineering Journal 326, 130–140. https://doi.org/10.1016/j.cej.2017.05.143

Zhang, L., Zhang, B., Wu, T., Sun, D., Li, Y., 2015. Adsorption behavior and mechanism of chlorophenols onto organoclays in aqueous solution. Colloids and Surfaces A: Physicochemical and Engineering Aspects 484, 118–129. https://doi.org/10.1016/j.colsurfa.2015.07.055

Zhang, S., Dong, Y., Yang, Z., Yang, W., Wu, J., Dong, C., 2016. Adsorption of pharmaceuticals on chitosan-based magnetic composite particles with core-brush topology. Chemical Engineering Journal 304, 325–334. https://doi.org/10.1016/j.cej.2016.06.087

Zhang, S., Meng, W., Wang, L., Li, L., Long, Y., Hei, Y., Zhou, L., Wu, S., 2020. Preparation of Nano-Copper Sulfide and Its Adsorption Properties for 17 α -Ethynyl Estradiol.

Zhang, X., Gao, Y., Li, Q., Li, G., Guo, Q., Yan, C., 2011. Estrogenic compounds and estrogenicity in surface water, sediments, and organisms from Yundang Lagoon in Xiamen, China. Archives of Environmental Contamination and Toxicology 61, 93–100. https://doi.org/10.1007/s00244-010-9588-0

Zhang, Z.F., Wang, L., Zhang, Xianming, Zhang, Xue, Li, Y.F., Nikolaev, A., Li, W.L., 2021. Fate processes of Parabens, Triclocarban and Triclosan during wastewater treatment: assessment via field measurements and model simulations. Environmental Science and Pollution Research 28, 50602–50610. https://doi.org/10.1007/s11356-021-14141-9

Zhao, B., Ji, Y., Wang, F., Lei, H., Gu, Z., 2016. Adsorption of tetracycline onto alumina: experimental research and molecular dynamics simulation. Desalination and Water Treatment 57, 5174–5182. https://doi.org/10.1080/19443994.2015.1004595

Zhao, C., Xie, H.J., Xu, J., Zhang, J., Liang, S., Hao, J., Ngo, H.H., Guo, W., Xu, X., Wang, Q., Wang, J., 2016. Removal mechanisms and plant species selection by bioaccumulative factors in surface flow constructed wetlands (CWs): In the case of triclosan. Science of the Total Environment 547, 9–16. https://doi.org/10.1016/j.scitotenv.2015.12.119

Zhao, J.L., Ying, G.G., Liu, Y.S., Chen, F., Yang, J.F., Wang, L., 2010. Occurrence and risks of triclosan and triclocarban in the Pearl River system, South China: From source to the receiving environment. Journal of Hazardous Materials 179, 215–222. https://doi.org/10.1016/j.jhazmat.2010.02.082

Zhongbo, Z., Hu, J., 2008. Selective removal of estrogenic compoundsby molecular imprinted polymer. Water Research 42, 4101–4108.

Zhou, A., Chen, W., Liao, L., Xie, P., Zhang, T.C., Wu, X., Feng, X., 2019. Comparative adsorption of emerging contaminants in water by functional designed magnetic poly(N-isopropylacrylamide)/chitosan hydrogels. Science of the Total Environment 671, 377–387. https://doi.org/10.1016/j.scitotenv.2019.03.183

Zhou, S., Shao, Y., Gao, N., Deng, J., Tan, C., Reuse, R., Reuse, R., 2013. Equilibrium , Kinetic , and Thermodynamic Studies on the Adsorption of Triclosan onto Multi-Walled Carbon Nanotubes 41, 539–547. https://doi.org/10.1002/clen.201200082

Zhou, X., Lian, Z., Wang, J., Tan, L., Zhao, Z., 2011. Distribution of estrogens along Licun River in Qingdao, China. Procedia Environmental Sciences 10, 1876–1880. https://doi.org/10.1016/j.proenv.2011.09.293

Zhu, X., Liu, Y., Luo, G., Qian, F., Zhang, S., Chen, J., 2014. Facile Fabrication of Magnetic Carbon Composites from Hydrochar via Simultaneous Activation and Magnetization for Triclosan Adsorption.

Zhuang, G., Zhang, Z., Jaber, M., 2019. Organoclays used as colloidal and rheological additives in oil-based drilling fluids: An overview. Applied Clay Science 177, 63–81. https://doi.org/10.1016/j.clay.2019.05.006

Zhuang, S., Wang, J., 2021. Adsorptive removal of pharmaceutical pollutants by defective metal organic framework UiO-66: Insight into the contribution of defects. Chemosphere 281. https://doi.org/10.1016/j.chemosphere.2021.130997

Zuo, Y., Zhang, K., Deng, Y., 2006. Occurrence and photochemical degradation of 17α-ethinylestradiol in Acushnet River Estuary. Chemosphere 63, 1583–1590. https://doi.org/10.1016/j.chemosphere.2005.08.063

ANEXO A. LICENÇAS DE PUBLICAÇÃO DE ARTIGOS NA DISSERTAÇÃO

07/01/2022 17:41 Rightslink® by Copyright Clearance Center

CCC RightsLink®

Home | Help | Live Chat | Sign in | Create Account

ELSEVIER

Synthesis of a novel magnetic composite based on graphene oxide, chitosan and organoclay and its application in the removal of bisphenol A, 17α-ethinylestradiol and triclosan

Author:
Arthur da Silva Vasconcelos de Almeida,Tauany de Figueiredo Neves,Meuris Gurgel Carlos da Silva,Patricia Prediger,Melissa Gurgel Adeodato Vieira

Publication: Journal of Environmental Chemical Engineering

Publisher: Elsevier

Date: February 2022

© 2021 Elsevier Ltd. All rights reserved.

Journal Author Rights

Please note that, as the author of this Elsevier article, you retain the right to include it in a thesis or dissertation, provided it is not published commercially. Permission is not required, but please ensure that you reference the journal as the original source. For more information on this and on your other retained rights, please visit: https://www.elsevier.com/about/our-business/policies/copyright#Author-rights

BACK CLOSE WINDOW

© 2022 Copyright - All Rights Reserved | Copyright Clearance Center, Inc. | Privacy statement | Terms and Conditions
Comments? We would like to hear from you. E-mail us at customercare@copyright.com

18/03/2022 14:51 Rightslink® by Copyright Clearance Center

CCC RightsLink®

Home | Help | Live Chat | Sign in | Create Account

ELSEVIER

Adsorption of 17α-ethinylestradiol onto a novel nanocomposite based on graphene oxide, magnetic chitosan and organoclay (GO/mCS/OC): Kinetics, equilibrium, thermodynamics and selectivity studies

Author:
Arthur da Silva Vasconcelos de Almeida,Valmor Roberto Mastelaro,Meuris Gurgel Carlos da Silva,Patricia Prediger,Melissa Gurgel Adeodato Vieira

Publication: Journal of Water Process Engineering

Publisher: Elsevier

Date: June 2022

© 2022 Elsevier Ltd. All rights reserved.

Journal Author Rights

Please note that, as the author of this Elsevier article, you retain the right to include it in a thesis or dissertation, provided it is not published commercially. Permission is not required, but please ensure that you reference the journal as the original source. For more information on this and on your other retained rights, please visit: https://www.elsevier.com/about/our-business/policies/copyright#Author-rights

BACK CLOSE WINDOW

© 2022 Copyright - All Rights Reserved | Copyright Clearance Center, Inc. | Privacy statement | Terms and Conditions
Comments? We would like to hear from you. E-mail us at customercare@copyright.com